

UNIVERSIDAD AUTONOMA DE MADRID

FACULTAD DE CIENCIAS

DESIGN AND SYNTHESIS OF NEW GOLD, PALLADIUM AND RHODIUM COMPLEXES WITH CHIRAL LIGANDS BASED ON DIOXOLANE AND PROTON SPONGE BACKBONE. STUDY OF THEIR HETEROGENEIZATION AND CATALYTIC BEHAVIOR.

MEMORIA PARA OPTAR AL GRADO DE DOCTOR EN CIENCIAS QUIMICAS

GONZALO VILLAYERDE CANTIZANO

Directores de Tesis:

Dr. Félix Sánchez Alonso

Dra. Marta Iglesias Hernández

Madrid 2011

Abstract.

In green chemistry, both homogeneous and heterogeneous catalysis have great importance in catalyzed processes that have several advantages with classical organic synthesis such as, shorter processes, high selectivity, less salts formation, milder reaction conditions and the use less hazardous solvents and reagents. Furthermore, in some cases catalytic processes need less steps leading to high productivity.

Working lines in our research group are focus on the design and synthesis of new catalytic systems that can be supported (through modifications in the ligand) on inorganic matrix (mesoporous materials as MCM-41) and to induce chirality.

The creation of an asymmetric environment around a metal center to accommodate the transformation of organic substrates, allows the induction of enantioselectivity in catalytic processes. A classical approach to achieve this goal is the use of enantiomerically pure ligands containing donor atoms (mainly nitrogen), with a defined symmetry.

This project involves the design, preparation and evaluation of new gold (I), palladium (II) and rhodium (I) catalysts as soluble and MCM-41 supported forms, with particular attention on the role of the support on reactivity, enantioselectivity and recyclability in asymmetric hydrogenation reactions of pro-chiral succinates and multi-component reaction for the synthesis of propargylamines.

Thus, the goals of this thesis dissertation involves the synthesis of two families of chiral ligands with high capacity for coordination with transition metals (gold, palladium and rhodium) leading catalysts with high activity, enantioselectivity, and stability in the working conditions of catalytic tests, so they could be heterogenized and reused in successive reactions without loss of properties.

N-heterocyclic carbene palladium (II), rhodium (I) and gold (I) complexes are based on a chiral dioxolane backbone, derived from optically pure tartaric acid (the backbone of the ligand is one of the key aspects to considered in the design of chiral ligands) the chiral dioxolane backbone supports groups that coordinate with the corresponding metal such as *N*-heterocyclic carbene groups or different amines, one of them is functionalized with isopropoxysilane groups for immobilization on MCM-41.

In last years, the NHC's are becoming one of the real alternatives to phosphine-based catalysts with the promise of similar reactivity, greater efficiency, less toxicity, stability to air and more electronic and structural diversity.

On the other hand, we synthesized a family of ligands based on a chiral proton sponge building block obtaining the corresponding palladium (II) and rhodium (I) complexes. The first example of a proton sponge (1,8-bis-(dimethylamino) naphthalene) was reported in 1968 by Alder but until now only one complex derived from diamine naphthalene proton sponge and only an example of chiral proton sponge reported by Mazaleyrat are known.

We obtained two types of catalysts derived from this backbone, imino, and perimidine derivatives. Imine catalysts could be supported on MCM-41 by functionalization of the ligands with triethoxysilane groups.

All systems were tested as catalysts in asymmetric hydrogenation of pro-chiral succinates and multi-component reactions for the synthesis of propargylamines. Taking account activity and enantioselectivity and comparing with other catalysts available in the literature. For heterogenized catalysts we studied the role of the support in the activity and enantioselectivity in each model reactions and the possibility of recycling in successive reactions.

For developed of the project the following stages took place:

- Design and synthesis of ligands: Proton sponge ligands are based on chiral 8-((2*R*,5*R*)-2,5-dimethylpyrrolidin-1-yl)naphthalen-1-amine, in this molecule the two methyl groups of pyrrolidine are in *anti* configuration and they confer the ability to induce chirality. *N*-heterocyclic carbene ligands are based on the backbone of the molecule, (4*R*,5*R*)-4,5-bis (iodomethyl) -2,2-dimethyl-1,3-dioxolane. In this molecule the two iodines found in *anti* position, so if they are replaced by an S_N2 reaction with other substituents these must also be in the same position.
- Synthesis of soluble and silyloxy palladium, rhodium and gold complexes.
- Immobilization on MCM-41.

- Study of activity and enantioselectivity in asymmetric hydrogenation reactions of pro-chiral olefins and multi-component reactions for the synthesis of propargylamines, emphasizing the difference between soluble and heterogenized catalysts and recyclability.

Resumen.

Dentro del marco de la Química Sostenible, tanto la catálisis homogénea como heterogénea son de gran importancia ya que los procesos catalizados presentan una serie de ventajas cuando se comparan con la síntesis orgánica clásica, como es tener procesos más cortos, alta selectividad, menor formación de sales, condiciones de reacción más suaves y disolventes y reactivos menos peligrosos. Además en algunos casos los procesos catalíticos pueden presentar menor número de etapas conduciendo a una alta productividad.

En nuestro grupo de trabajo buscamos nuevos catalizadores que induzcan quiralidad a los procesos y que además puedan ser soportados, por medio de modificaciones en el ligando, en materiales mesoporosos de tipo zeolítico como la MCM-41.

La creación de un entorno asimétrico alrededor de un centro metálico, con el fin de acomodar a los sustratos de una transformación orgánica, permite la inducción de enantioselectividad en los procesos catalíticos. Un enfoque clásico para conseguir este objetivo es el uso de ligandos enantioméricamente puros que contengan átomos donantes (principalmente nitrógeno), con una simetría definida.

Este proyecto consiste en el diseño, preparación y evaluación catalítica de nuevos catalizadores de oro (I), paladio (II) y rodio (I) solubles y sus correspondientes heterogeneizados en soportes inorgánicos mesoporosos estructurados, poniendo especial atención en el papel del soporte sobre la reactividad, enantioselectividad y también en su reciclabilidad en reacciones de hidrogenación asimétrica de succinatos proquirales y reacciones multi-componente.

Así, los objetivos de este proyecto de tesis comprenden la síntesis dos familias de ligandos quirales con alta capacidad de coordinación con estructuras básicas muy diferentes pero con objetivos comunes como son la coordinación a metales de transición (oro, paladio y rodio) obteniendo catalizadores con alta actividad, enantioselectividad, y estabilidad en las condiciones de trabajo de los ensayos catalíticos, de forma que pueden ser heterogeneizados y reutilizados en sucesivas reacciones sin pérdida de propiedades.

Los complejos carbeno *N*-heterocíclicos de paladio (II), rodio (I) y oro (I) están basados en un esqueleto dioxolano quiral, derivado del ácido tartárico ópticamente puro (el esqueleto del ligando es uno de los aspectos clave a tener en cuenta en el diseño de ligandos quirales). El esqueleto dioxolano quiral soporta grupos que se coordinan con el correspondiente metal como son los grupos carbeno *N*-heterocíclicos (NHC) o diferentes aminas, una de ellas funcionalizada con grupos isopropoxisilano para su posterior inmovilización en MCM-41. En los últimos años, los NHC's se están convirtiendo en una de las alternativas reales a los catalizadores basados en fosfinas con la promesa de reactividad similar, mayor eficacia, menor toxicidad, estabilidad al aire y mayor diversidad electrónica y estructural.

Por otro lado, se sintetizó una familia de ligandos con estructura de esponja de protones quiral derivada del 1,8-diaminonaftaleno y se obtuvieron sus correspondientes complejos de paladio (II) y rodio (I). El primer ejemplo de una esponja de protones, (1,8-*bis*-(dimetilamino) naftaleno), se reportó en 1968 por Alder pero hasta la fecha, sólo se conoce un complejo de la esponja de protones derivada del diamino naftaleno y tan solo un ejemplo de esponja de protones quiral reportada por Mazaleyrat.

Se obtuvieron dos tipos de catalizadores derivados de esta familia; los derivados imínicos y los derivados perimidínicos. Los catalizadores derivados de imina pudieron ser soportados en MCM-41 mediante funcionalización de los ligandos correspondientes con grupos trietoxisilano.

Con los complejos preparados de las dos familias se realizaron estudios de su actividad catalítica en hidrogenación asimétrica de succinatos y en reacciones multi-componente para la síntesis de propargilaminas demostrando su utilidad en cuanto a actividad y enantioselectividad en comparación con otros catalizadores disponibles en la bibliografía. En el caso de los catalizadores heterogeneizados se estudió el papel del soporte en la actividad y enantioselectividad, en cada una de las reacciones modelo y la posibilidad de su reciclado en sucesivas reacciones.

Para el desarrollo del proyecto se llevaron a cabo las siguientes etapas:

- Diseño y síntesis de los ligandos: La familia de las esponjas quirales se basa en el 8-((2*R*,5*R*)-2,5-dimetilpirrolidin-1-il)naftalen-1-amina, en esta

molécula los dos metilos de la pirrolidina se encuentran en posición *anti* y son los que confieren la capacidad de inducir quiralidad al compuesto. La familia de los ligandos carbeno *N*-heterocíclicos se basa en la molécula, (4*R*,5*R*)-4,5-bis(iodometil)-2,2-dimetil-1,3-dioxolano que da la quiralidad al ligando, en esta molécula los dos yodos se encuentran en posición *anti*, así, si estos son sustituidos por medio de un mecanismo de SN_2 por otros sustituyentes estos también deben de estar en la misma posición.

- Síntesis de los complejos de de paladio, rodio y oro solubles y heterogeneizables.
- Inmovilización de los complejos funcionalizados con trialcoxisilano en MCM-41.
- Estudio de actividad y enantioselectividad en reacciones de hidrogenación asimétrica de olefinas pro-quirales y reacciones multi-componente para la síntesis de propargilaminas, haciendo hincapié en la diferencia entre catalizadores solubles y heterogeneizados y en estudios de reciclabilidad.

List of abbreviations

Ar	Aryl
Cat	Catalyst
cod	cycloocta-1,5-diene
Conv	Conversion
GC	Gas chromatography
L	Ligand
M	Metal
NHC	<i>N</i> -heterocyclic carbene
IHB	Intramolecular hydrogen bond
ORTEP	Oak Ridge Thermal Ellipsoid Plot
PS	Proton Sponge
THF	Tetrahydrofuran
TOF	<i>turnover frequency</i> (mmol substrate./mmol catalyst time)
TON	<i>turnover number</i> (mmol substrate./mmol catalyst)

CONTENTS.

<u>Chapter I: General introduction</u>	1
1 Green chemistry.....	3
2 Catalysis: General remarks.....	4
2.1 Homogeneous Catalysis.	5
2.2 Heterogeneous Catalysis.	7
2.3 Heterogenized Catalysts.	9
3 Relevance of asymmetric hydrogenation in green chemistry.....	14
4 Relevance of multi-component reaction in green chemistry.	19
<u>Chapter II: General targets</u>	23
<u>Chapter III: Chiral complexes bearing N-heterocyclic carbene moieties at dioxolane backbone. Gold, palladium and rhodium complexes as enantioselective hydrogenation catalysts. Homogeneous vs heterogenized</u>	27
1 Introduction	29
2 State of the art.....	30
2.1 Historical background.	30
2.2 Synthesis of imidazolium precursor salts for NHC ligands.....	33
2.3 General features of N-heterocyclic carbenes.	36
2.4 NHC`s complexes as catalysts in organic synthesis	37
3 Discussion and results	46
3.1 Targets.	46
3.2 Synthesis of ligands.....	47
3.3 Synthesis of complexes.	56
3.3.1 Synthesis of bis N-heterocyclic carbene complexes.....	56
3.3.2 Synthesis of mono N-heterocyclic carbene amine complexes.....	60

3.4	Heterogenization of complexes containing pendant alkoxy silane groups to MCM-41.....	64
3.5	Catalytic activity.....	69
4	Conclusions	85
5	Experimental section	86
5.1	Synthesis of precursors.....	86
5.2	Synthesis of ligands.....	90
5.3	Synthesis of complexes.	102
5.3.1	Synthesis of bis N-heterocyclic carbene complexes.....	102
5.3.2	Synthesis of mono N-heterocyclic carbene amine complexes.....	107
5.4	Heterogenization of complexes containing pendant alkoxy silane groups to MCM-41.....	116
5.5	Catalytic Activity.....	118

Chapter IV: Synthesis of chiral ligands based on “proton sponges-core”.
Homogeneous and heterogenized rhodium and palladium complexes as
enantioselective hydrogenation catalysts.....121

1	Introduction	123
2	State of the art.....	124
2.1	Historical background and general features of proton sponges...	124
2.2	Synthesis of naphthalene proton sponges.....	128
2.3	Chiral proton sponges.....	131
2.4	Proton sponges as ligands for organometallic complexes	133
3	Discussion and results.....	136
3.1	Targets	136

3.2	Synthesis of ligands from 8-((2 <i>R</i> ,5 <i>R</i>)-2,5-dimethylpyrrolidin-1-yl)naphthalen-1-amine.....	136
3.3	Synthesis of rhodium and palladium complexes	150
3.4	Heterogenization of complexes containing pendant alkoxy silane groups to MCM-41	156
3.5	Catalytic activity.....	159
4	Conclusions	165
5	Experimental section	166
5.1	Synthesis of precursors.....	167
5.2	Synthesis of ligands.....	169
5.3	Cyclization scope.....	174
5.4	Synthesis of complexes	178
5.5	Heterogeneization on MCM-41.....	184
5.6	Catalytic Activity.....	185
5.7	Single-Crystal X-ray Diffraction.....	186

Chapter V: Gold complexes catalyzed synthesis of propargylamines via multi-component reaction.....189

1	Introduction.	191
2	State of the art.....	192
2.1	Multi-component reactions. Historical background.	192
2.2	Gold-catalyzed multi-component reactions.....	194
3	Discussion and results	200
3.1	Targets.	200
3.2	Multi-component reaction. Optimal conditions.....	200
4	Conclusions	211
5	Experimental section	212

5.1	General procedure for the three-component coupling reaction	212
5.2	MCR pure products.	213
<u>Chapter VI: General conclusions</u>		217
<u>Chapter VII: Articles</u>		227

Chapter I



General introduction

1 Green chemistry.

Science has developed progressively without stopping, evolving to explore new technologies in different fields. These new technologies give benefits which improves standard living. However, negative aspects such as public pollution and global warming etc., have accompanied them and lead to the destruction of the natural environment in some cases.

Concerns to chemistry, from its origins the industry has produced large quantities of waste that has often released to the environment causing a significant environmental impact even for human live. Cases such as the uncontrolled emission of methyl isocyanate in India (1984) that flooded the city, killing thousands of people or oil spill in several incidents with oil tankers, made essential an environmental legislation that applies not only to the manufacture of chemicals but also to transport, and treatment of waste. This fact has heavy economic cost for chemical industries.

In this context the current chemistry is oriented towards research, design and development of new products and processes inside what is called “Green Chemistry”. “Green Chemistry” concept appeared in 1990s and is defined as efficiently utilizes (preferably renewable) raw materials, eliminates waste and avoids the use of toxic and/or hazardous reagents and solvents in the manufacture and application of chemical products.¹

In 1998 Anastas and Warner formulated the following 12 principles of the green chemistry which can be paraphrased as:

[1] a) P. T. Anastas, J. C. Warner, *Green Chemistry: Theory and Practice*, Oxford University Press, Oxford , **2000**, 135; b) P. T. Anastas, T. C. Williamsom, *Green Chemistry: Frontiers in Chemical Synthesis and Processes*, Oxford University Press, Oxford , **1998**; c) P. T. Anastas, M. M. Kirchoff, *Acc. Chem. Res.*, **2002**, 35, 686; d) P. T. Anastas, L. G. Heine, T. C. Williamsom, *Green Chemical Synthesis and Processes*, American Chemical Society, Washington DC, **2000**.

1. Prevention of waste
2. Atom Economy
3. Less Hazardous Chemical Synthesis
4. Designing Safer Chemicals
5. Safer solvents and auxiliaries
6. Energy efficient
7. Renewable feedstocks
8. Reduce derivatives
- 9. Catalysis**
10. Design for degradation
11. Real time analysis for pollution prevention
12. Safety

Green chemistry is a set of principles to address sustainable development by preventing pollution from the beginning. To carry out this new way in chemistry has to be treated as an interdisciplinary subject where each specialist contribute. In our case we focused on the role of catalysis in green chemistry.

2 Catalysis: General remarks.

Replace stoichiometric process by catalytic routes is one of the key in green chemistry. Catalysis is considered a mainstay since the catalytic reactions reduce energy consumption and decrease the need for separation as a result of increased yields and selectivity in the process.

“A catalyst is a substance that transforms reactants into products, through an uninterrupted and repeated cycle of elementary steps in which the catalyst participates while being regenerated in its original form at the end of each cycle during the life of the catalyst.”²

[2] M. Boudart, J. M. Thomas, K. I. Zamaraev, *Blackwell Scientific Publications*, Oxford, **1992**.

Another definition about the nature of the catalyst is: “A catalyst is a substance that changes the kinetic but not the thermodynamics of a chemical reaction”.³ Both definitions are complementary and show what is a catalyst and how works. The first ideas of catalysis were introduced by Berzelius and Mitscherlich in 1830 that summarized several reactions that took place in presence of a substance that “was not affected by the reaction”. Nowadays, catalytic processes are involved in about 90% of the chemical synthesis routes in the industry and are present in food production, bulk chemicals, fine chemicals and pharmaceuticals. Thus, we can say that catalysis is a major topic in environmental issues. There are many types of catalysis that can be easily divided in heterogeneous and homogeneous. Within each category we found several forms of catalysis as organometallic catalysis, organocatalysis and enzymatic catalysis.

2.1 Homogeneous catalysis.

Homogeneous organometallic catalysis refers to a catalytic system that is in the same phase as the reaction mixture. The main advantage is that the active sites are well separated from another one, have high selectivities and high activity. Furthermore, it is possible to tune the chemo-, regio- and enantioselectivity of the catalyst by modification of the ligand and/or the metal center depending on the requirements of the catalytic process, that can be referred catalysts design.

To design a catalyst is essential the study of the ligand effects, then, it is possible to predict the activity and selectivity in reference to the relationship between catalyst structure and its properties. There are two kinds of ligand effects; the steric effects and the electronic effects

2.1.1 *Steric effects: Ligand size, flexibility and symmetry.*

The ligand size is important because the space around the metal center is limited. If ligands have an important steric hindrance, the substrate can't approach to the metal. Sometimes ligand dissociation happens leading enough space to the

[3] G. Ertl, H. Knözinger, J. Weitkamp, *Vol. 1*, Wiley-VCH, Weinheim, **1997**.

General Introduction

substrate coordination; this step often is the transformation of the catalyst precursor in to active species.

Calculating the size of a ligand is difficult, and normally we need tools as calculated models or X-ray structural data to get a sense of the volume occupied by a particular ligand. In case of phosphorus ligands Chadwick Tolman⁴ in the seventies used a cone that encompasses the ligand, with the metal center in its apex and the P atoms situated 2.28 Å away from it. (**Figure. I. 1 A**).

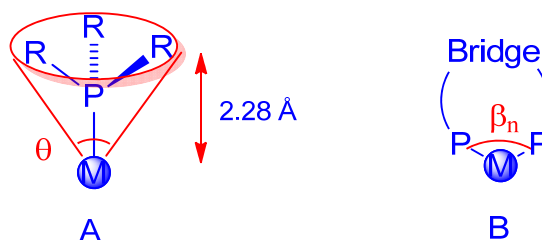


Figure. I. 1. Tolman's cone angle (A) and bite angle (B).

This measure is known as Tolman's cone angle and gives good correlations for symmetric PR_3 ligands. Along the years, other approximations to estimate the volume have been reported. Thus, for bidentate ligands the key parameter is the ligand bite angle α reported by Piet van Leeuwen⁵; in these calculations is important the flexibility of the ligands to change its bite angle and consequently its coordination state in the course of the catalytic cycle for stabilization the reaction intermediates. Thus, is necessary compromise between rigidity and flexibility in the ligand to be effective in the catalytic process.

2.1.2.a Asymmetry and chirality effects of ligands.

The symmetry of the ligand can influence in the selectivity of the final product in the catalytic reaction. Many of bidentate ligands dividing the space around the metal into empty quadrants and full quadrants so the substrate is attached the metal center only into the gaps left by ligand.

[4] C. A. Tolman, *Chem. Rev.*, **1977**, 77, 313.

[5] a) P. W. N. M. van Leeuwen, P. C. J. Kamer, J. N. H. Reek, P. Dierkes, *Chem. Rev.*, **2000**, 100, 2741; b) P. Dierkes, P. W. N. M. van Leeuwen, *J. Chem. Soc., Dalton Trans.*, **1999**, 1519.

The design of a chiral catalyst often starts with an achiral metal complex that exhibits some activity in the desired catalytic reaction. A classical approach⁶ to create a chiral environment around the metal center is the use of enantiomerically pure ligands containing donor atoms (mainly nitrogen or phosphorous) with a defined symmetry.⁷

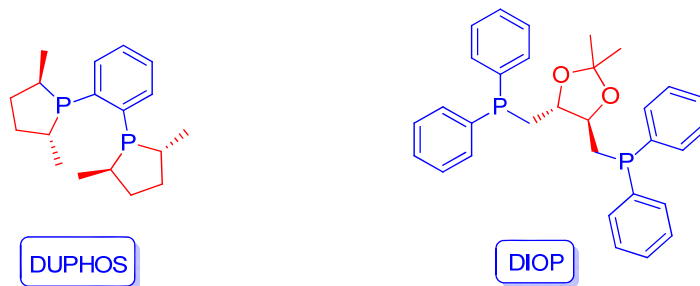


Figure. I. 2. Representative chiral ligands.

To obtain chiral ligands there are two routes:

- The introduction of a chiral backbone (**Figure. I. 2**, DIOP).
- The introduction of chiral substituents in the donor atoms those are coordinated to the metal center (**Figure. I. 2**, DUPHOS).

2.1.2 *Electronic effects of ligand.*

Electronic effects of the ligands are extremely important in the design of catalysts. Species that coordinate to the metal center tune the electron density around of the metal by pushing or pulling electrons. This fact makes easier the transition state of conventional catalysis cycles that frequently involve changes in metal oxidation state such as oxidative addition or reductive elimination steps.

2.2 Heterogeneous catalysis.

Heterogeneous catalysis covers all cases where the catalyst and the substrate are in different phase. Usually, heterogeneous refers when the catalyst is solid and the reactants in most cases are liquids or gases.⁸

[6] a) I. Ojima, *Catalytic Asymmetric Synthesis*, 2nd edn, Wiley-VCH, New York, **2000**; (b) P. J. Walsh, M. C. Kozlowski, *Fundamentals of Asymmetric Catalysis*, University Science Book, Sausalito, **2009**, 191.

[7] E. M. Jacobsen, A. Pfaltz H. Yamamoto, *Comprehensive Asymmetric Catalysis*, Springer-Verlag, Berlin, **1999**.

[8] R. Noyori, *Asymmetric Catalysis in Organic Synthesis*, **1994**, Wiley-Interscience, New York.

General Introduction

Most catalytic processes use solid catalysts. These solid catalysts sometimes have high complex composition (sometimes grow to 10 or more elements in the formula), however, there are three basic components: the active phase, support and promoter.

The active phase is directly responsible for the catalytic activity. The active phase may be a single chemical phase or set of them, however, is characterized by itself can carry out the catalytic reaction. However, this active phase could be very costly, as in the case of noble metals (Pt, Pd, Rh, etc...) .

The matrix is the support which is deposited the active phase and optimizing its catalytic properties. This support can be porous and therefore present a high surface area per gram.

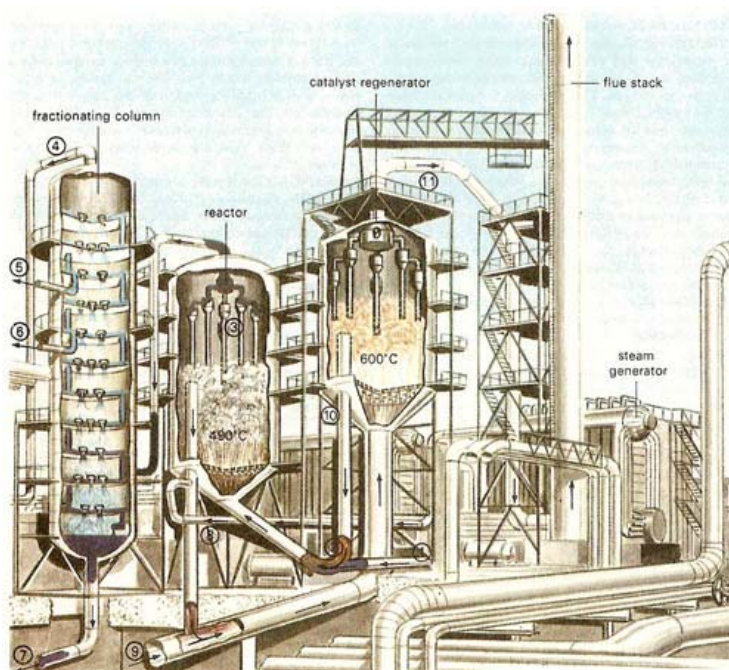


Figure. I. 3. Catalytic petroleum cracker.

Heterogeneous catalysis has a fundamental role in the developed of a suitable industry because its performances in terms of cost reduction for its easy separation from the reaction mixture and the possibility of recycling. Thus, since 90% of the manufacturing processes of chemicals in the world use heterogeneous catalysis. Such

as examples, processes as the production of nitric oxide from ammonia (Rh/Pt catalyst) or petroleum cracking⁹ (nickel aluminous silicate catalyst) take place by heterogeneous catalysts. (**Figure. I. 3**).

However most of the classical heterogeneous processes; usually possess a lower activity and selectivity compared with referable homogeneous catalytic processes this fact makes many processes not viable with these types of catalytic materials. In this way appeared the heterogenized catalysts.

2.3 Heterogenized catalysts.

Many soluble catalysts systems have not been commercialized because of the difficulty in separating the catalyst from the final reaction product. Removal of trace amounts of catalyst from the end product is essential since the metal contamination is highly regulated, especially by the pharmaceutical industry. On the other hand, heterogeneous catalysts present less activity and selectivity than soluble ones.

The need of regio- and enantioselective catalysts but at the same time, easy separation of the reaction medium and reusable for the industrial implementation is the key of heterogenized catalysts that involves the immobilization of a soluble selective and active catalyst on a support that results heterogeneous in the reaction mixture.

The term catalyst immobilization or heterogeneization can be defined as “the transformation of a soluble catalyst into a heterogeneous one, which is able to be separated from the reaction mixture and preferably be reused for multiple times”. Thus, we focused in the goal to combine the positive aspects of soluble catalysts with those the heterogeneous catalysts.

The past two decades have developed several methods in transferring the soluble molecular approach to heterogeneous catalysts, especially for the introduction of chiral induction in these processes.¹⁰

[9] J. H. Gary, G. E. Handwerk, and *Petroleum Refining: Technology and Economics*, **2001**, CRC Press, Boca Raton.

[10] G. J. Hutchings, *Chem. Commun.*, **1999**, 301, 6.

2.3.1 Types of supports.

Supports can be classified according to their nature in organic and inorganic.

2.3.1.a Organic supports.

Organic supports (polymers and dendrimers) are easily functionalized and active and selective centers can be easily incorporated into their structure.

A wide variety of polymers-supported chiral complexes have been prepared and tested over a broad spectrum of synthetic reactions. Some systems have demonstrated catalytic performance (activity and selectivity) rivaling with their homogeneous counterparts in certain model reactions with the additional advantage of easy recovery and reusability.¹¹

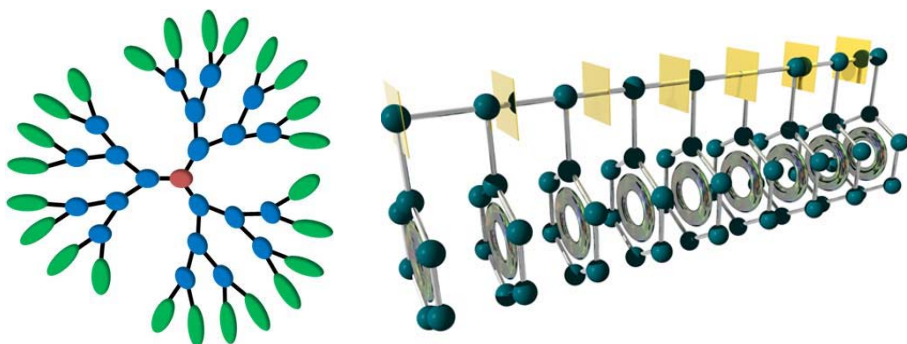


Figure. I. 4. Dendrimer (left) and polymer (right).

Dendrimers are a class of macromolecules with highly branched and well-defined structures and have recently attracted much attention as soluble supports for catalyst immobilization.¹² Dendrimers allow for the precise construction of catalyst structures with uniformly distributed catalytic sites, a feature which is very valuable when performing an analysis of catalytic events and mechanistic studies.¹³

[11] a) S. J. Shuttleworth, S. M. Allin, P. K. Sharma, *Synthesis*, **1997**, 1217; b) D. E. Bergbreiter, *Catal. Today*, **1998**, 42, 389.

[12] D. Astruc, F. Chardac, *Chemical Reviews*, **2001**, 101, 2991.

[13] a) G. R. Newkome, H. He, C. N. Moorefield, *Chem. Rev.*, **1999**, 99, 1689; b) L. J. Twyman, A. S. H. King, I. K. Martin, *Chem. Soc. Rev.*, **2002**, 31, 69; c) R. van Heerbeek, P. C. J. Kamer, P. W. N. M. van Leeuwen, J. N. H. Reek, *Chem. Rev.*, **2002**, 102, 3717; d) G. P. M. van Klink, H. P. Dijkstra, G. C. R. van Koten, *Chim.*, **2003**, 6, 1079; e) Y. Ribourbouille, G. D. Engel, L. H. C. R. Gade, *Chim.*, **2003**, 6, 1087; f) P. A. Chase, R. J. M. KleinGebbink, G. van Koten, *J. Organomet. Chem.*, **2004**, 689, 4016.

As disadvantages, in general, organic supports have low surface area and present low capacity for heat transfer and the phenomenon known as swelling. This phenomenon happens when the organic supports are in contact with the solvent for long time then, the solvent penetrates through the chains of the support causing an increase in volume thus, the active centers become inaccessible for the substrate.

2.3.1.b Inorganic supports.

The most commonly used inorganic support is silica,¹⁴ although there are others that are used less as alumina, zirconite and zinc oxide. These porous materials have high number of advantages such as:

- Conservation of surface area more rigid than in the case of polymers.
- Mechanical and thermal stability.
- Provision of supported catalyst stability by having a large surface area.
- Help to keep catalytic activity because there isn't mass transfer between the liquid phase and solid phase.

Last years, interest in structured porous materials has been increasing for their potential as supports in catalysis, so depending on the pore size can be classified into:

- Microporous (0.2-2.0 nm)
- Mesoporous (2.0-50.0 nm)
- Macroporous (over 50 nm)

In 1990, Kuroda et al¹⁵ reported the first mesoporous silica with uniform pore size. The porous size can be controlled through an organic cation salt that is sandwiched between layers of the polysilicate. These structure directing agents were called *templates*.

Thus depending on the size and shape of *template*, the pore size can be controlled. There are described several types of silica porous supports such as MCM-

[14] D. E. de Vos, I. F. J. Vankelecom, P. A. Jacobs, *Chiral Catalyst Immobilization and Recycling*, **2000**, John Wiley-VCH.

[15] T. Yanagisawa, T. Shimizu, K. Kuroda, C. Kato, *Bull. Chem. Soc. Jpn.*, **1990**, 63, 988.

41,¹⁶ MCM-48, MCM-50, SBA-15 with pores of size that could be adequate for catalysts heterogeneization for organic reactions.

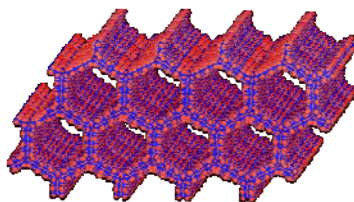


Figure. I. 5. MCM-41 structure.

The regular structure of pores of these materials allows the introduction of molecules or particles that are stabilized and have a particular spatial arrangement as a result of this structure. These materials offer great thermal stability, ability to control the pore size or acidity by synthesis. In the field of catalysis, they are interesting possibilities to immobilize the catalyst on their structure.

2.3.2 Heterogeneization methods.

There are several strategies for heterogenizing soluble catalysts and the formation of covalent bonds or noncovalent interactions (physisorption, electrostatic interactions, H-bonding) have been employed for linking the complexes to solids supports, either onto external surface or into the interior pores. (**Figure. I. 6**). Each of these immobilization strategies has advantages and limitations with respect to the others.

The formation of a covalent bond between the catalyst and the inorganic support is, in principle, the "ideal" method to connect them, because given certain catalytic conditions, will best optimize the high activity and selectivity in the catalytic reactions like homogeneous phase of these catalyst and being the most resistant to extreme conditions minimizing leaching problems.

[16] J. S. Beck, J. C. Vartulli, W. J. Roth, M. E. Leonowicz, C. T. Kresge, K. D. Schmitt, C. T. W. Chu, D. H. Olson, E. W. Sheppard, S. B. McCullen, J. B. Higgins, J. L. Schlenker, *J. Am. Chem. Soc.*, **1992**, *114*, 10834.

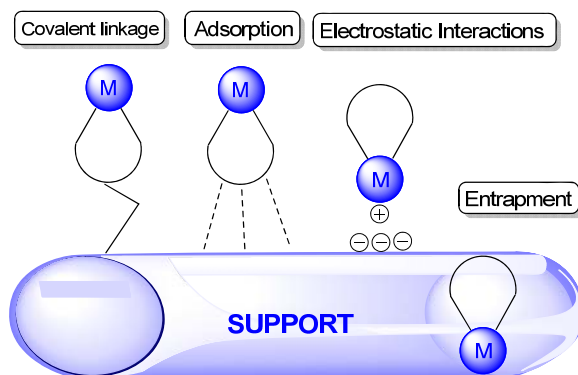


Figure. I. 6. Strategies for immobilizing soluble catalyst on solids.

The immobilization of soluble catalyst via covalent bond can be made for several routes. (**Figure. I. 7**).

Route 1: The most important way is achieved by anchoring the soluble catalyst to an inorganic support via covalent bonds between the solid with silanols groups in the surface and the complex that is appropriate functionalized with a pendant alkoxy-silyl groups.

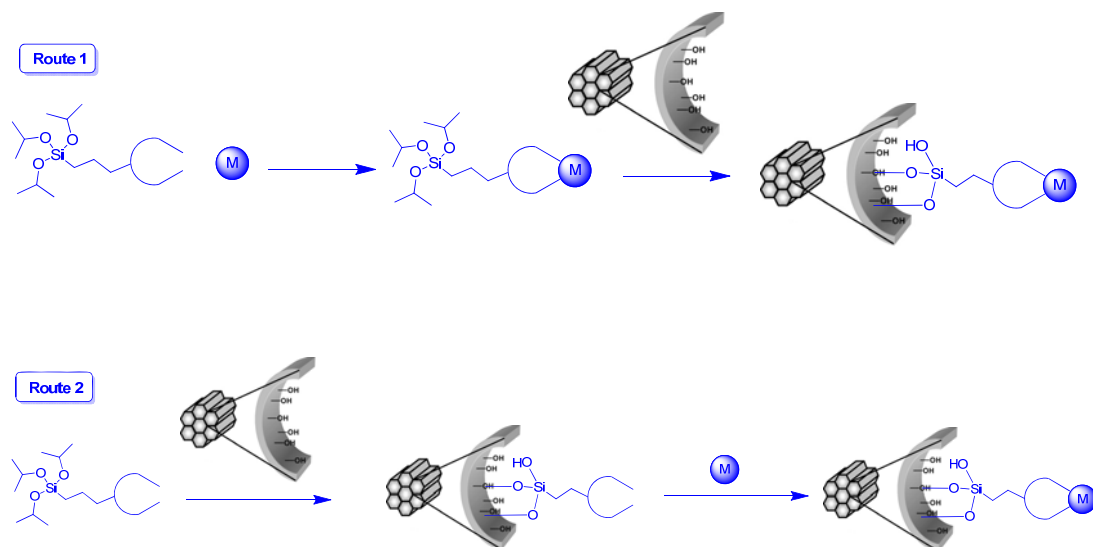


Figure. I. 7. Covalent linkage routes.

Route 2: The supported catalyst is obtained by the anchoring the ligand to the support and reacted with the starting complex to give the respective heterogenized catalyst.

For long time, most examples of supported catalysts tended to have inferior catalytic properties relative to their soluble counterparts. However has been reported that by choosing a suitable support a heterogenized catalyst can provide much better catalytic performances than its soluble analogous.¹⁷

The use of inorganic solids can demonstrate certain advantage over organic supports. In general, the rigid framework can prevent the aggregation of active catalyst which sometimes leads to the formation of inactive multinuclear species. The chemical and thermal stabilities of inorganic supports are also superior, rendering them compatible with a wide range of reagents and relatively harsh reaction conditions.

The advantage of incorporate a chiral catalyst in the several supports in order to obtain chiral and recyclable catalytic materials is one of the best goals in green chemistry because can be very useful in the industry for reducing costs and waste in a large number of chiral processes. One of the key reactions in the industry is the asymmetric hydrogenation that is present in several synthesis routes for pharmaceutical and fine chemicals industry.

3 Relevance of asymmetric hydrogenation in green chemistry.

Enantiopure organic products are very important in several fields in chemistry as, drugs synthesis, or fine chemicals. The challenge is to found efficient methods to obtain optically pure compounds.

Many examples in the literature show the importance of chirality in the chemical industry which is demonstrated in disasters as the administration of thalidomide to pregnant women in racemate form, being the isomer (*R*) desirable sedative while the (*S*) isomer induces fetal malformations. This tragic case led to strict

[17] A. Corma, M. Iglesias, J. R. Obispo, F. Sánchez, *Quiral Reactions in Heterogeneous Catalysis*, Plenum, N. Y. 1995.

regulations on the testing enantiomers and encouraged the scientific community to improve the routes to obtain pure enantiomers.

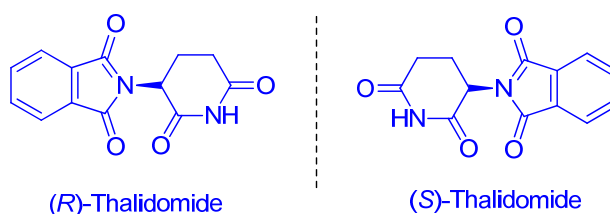


Figure. I. 8. Chemical structures of (R)- and (S)-Thalidomide.

Nevertheless in nineties about the 90% of synthetic chiral drugs were still racemic, which reflects the difficulty in the practical synthesis of enantiomeric pure compounds.

There are three general approaches to obtain pure compounds; (1) use of chiral pool, (2) by the classical resolution of a racemate¹⁸ (through crystallization methods or kinetic resolution using an enzyme) and (3) asymmetric catalysis.

The classical resolution of a racemate leads low yields (50% in the best case) and resulted very expensive. The asymmetric catalysis offers the smartest way to obtain chiral pure products efficiently getting the least amount of secondary products.

In this dissertation, we focused in the asymmetric hydrogenation because is one of the more important key steps in the asymmetric synthesis of enantiomeric pure important products in pharmaceuticals and fine chemicals. Because of its atom economy and operational simplicity, the asymmetric hydrogenation of terminal alkenes could be an alternative sustainable and direct synthetic tool for preparing these compounds.

[18] a) H. B. Kagan, *Tetrahedron*, **2001**, 57, 2449; b) E. Fogassy, M. Nogardi, D. Kozma, G. Egri, E. Palovics, V. Kiss, *Org. Biomol. Chem.*, **2006**, 4, 3011; c) K. Faber, *Chem. Eur. J.*, **2001**, 7, 5004.

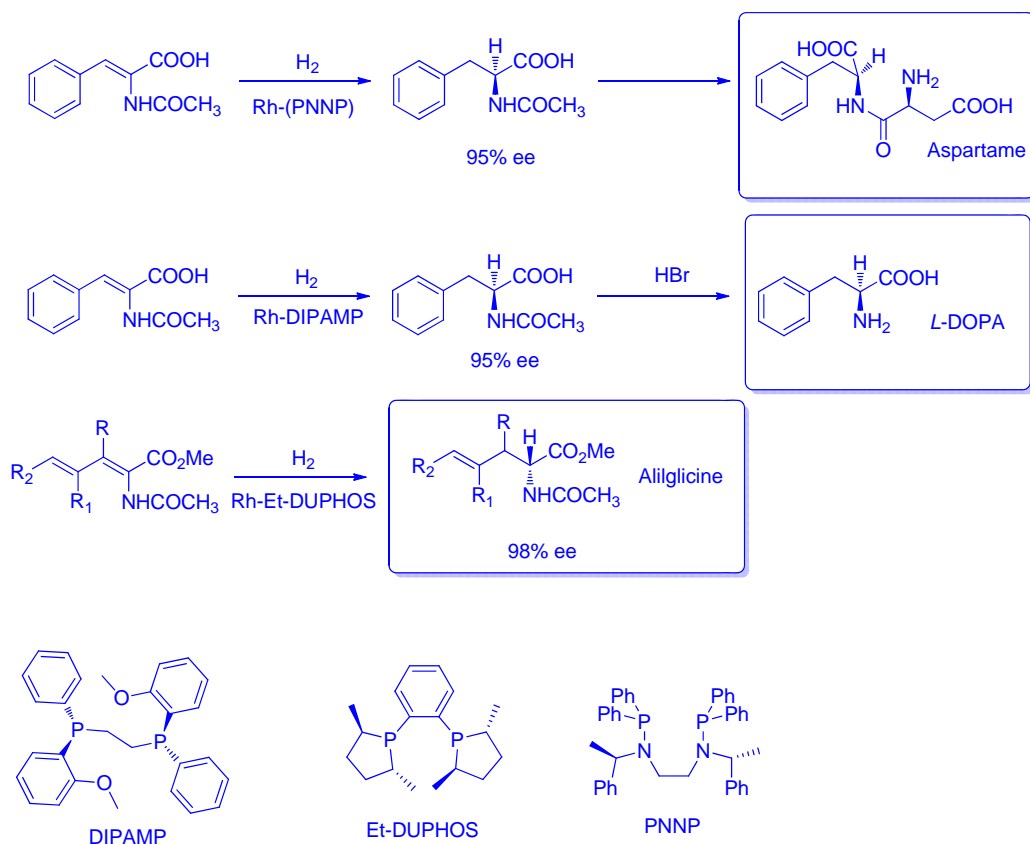


Figure. I. 9. Asymmetric hydrogenation of different aminoacrylates.

There are many examples of the industrial application of the asymmetric hydrogenation. For example the hydrogenation of different aminoacrylates with different ligands as the synthesis of sweeteners such as aspartame, intermediates for the total synthesis of amino acids or even for the synthesis of pharmaceuticals as *L*-Dopha (Knowles). (**Figure. I. 9**).

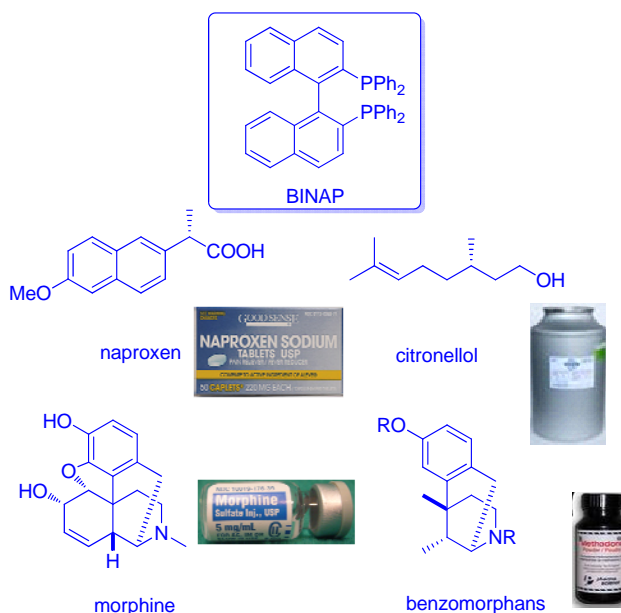


Figure. I. 10. Industrial applications of BINAP-Ru catalyzed hydrogenation of olefins.

In 2001 Ryoji Noyori and William S. Knowles received the Nobel Prize for their contributions in asymmetric catalysis. Knowles thanks to the new industrial synthesis route¹⁹ to obtain *L*-DOPA that is a high active product against the Parkinson's disease and Noyori for the developed of the Ru-BINAP^{20,21} which is an excellent catalyst for the hydrogenation of various functionalized alkenes that are in some cases commercial drugs as naproxen (anti-inflammatory) or citronerol. The asymmetric hydrogenation is a key step also in total synthesis of isoquinoline alkaloids including morphine, benzomorphans and morphinans such as the antitussive dextromethorphan.^{22,23}

[19] a) W. S. Knowles, M. J. Sabacky, B. D. Vineyard, *J. Chem. Soc. Chem. Commun.* **1972**, 10; b) B. D. Vineyard, W. S. Knowles, M. J. Sabacky, G. L. Bachman, D. J. Weinkauff, *J. Am. Chem. Soc.* **1977**, 99, 5946; c) W. S. Knowles, *Acc. Chem. Res.* **1983**, 16, 106; d) J. Crosby, *Chirality in Industry: The Commercial Manufacture and Applications of Optically Active Compounds*, Wiley, **1992**, Chichester, chap. 1.

[20] R. Noyori, M. Ohta, Y. Hsiao, M. Kitamura, T. Ohta, H. Takaya, *J. Am. Chem. Soc.*, **1986**, 108, 711.

[21] a) T. Ohta, H. Takaya, R. Noyori, *Inorg. Chem.* **1988**, 27, 566; b) M. Kitamura, M. Tokunaga, R. Noyori, *J. Org. Chem.*, **1992**, 57, 4053; c) H. Takaya, T. Ohta, S. Inoue, M. Tokunaga, M. Kitamura, R. Noyori, *Org. Synth.*, **1993**, 72, 74.

[22] M. Kitamura, I. Kasahara, K. Manabe, R. Noyori, H. Takaya, *J. Org. Chem.* **1988**, 53, 708.

[23] a) G. M. Ramos Tombo, G. Bellusoe, *Angew. Chem.* **1991**, 103, 1219; *Angew. Chem. Int. Ed. Engl.* **1991**, 30, 1193; b) A. Barner, J. Holz, *Transition Metals for Organic Synthesis*, **1998**, Vol. 2, 3, Wiley-VCH, Weinheim; c) J. M. Brown *Comprehensive Asymmetric Catalysis*, **1999**, Vol. 1, 121, Springer, Berlin; d) T. Ohkuma, M. Kitamura, R. Noyori, *Catalytic Asymmetric Synthesis*, 2nd ed., **2000**, Wiley-VCH, New York.

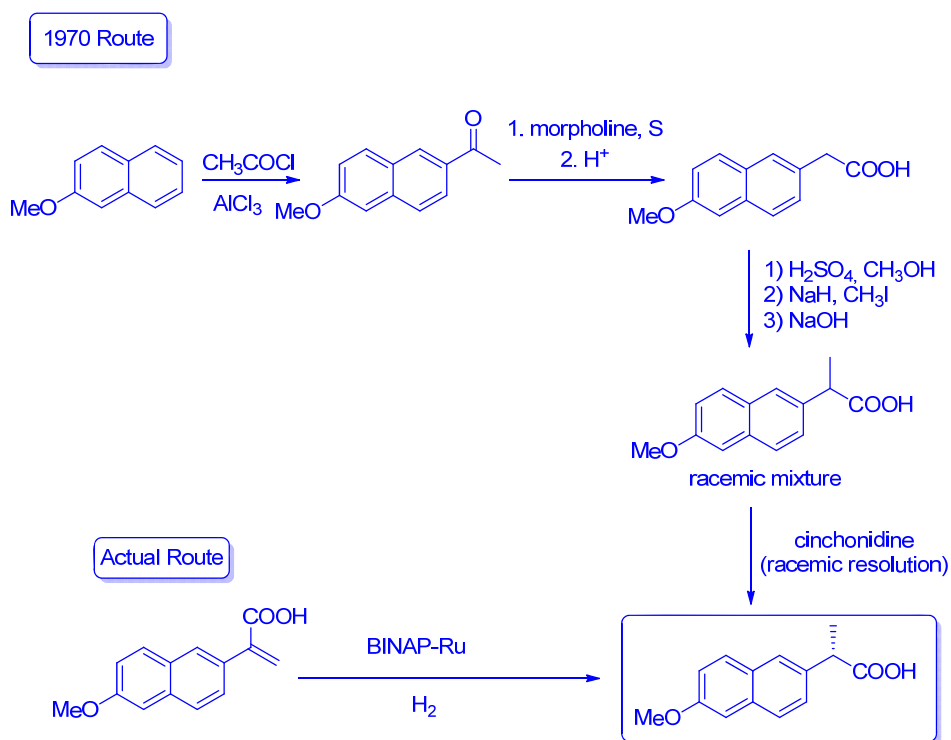


Figure. I. 11. Synthesis of naproxen.

BINAP not only works with olefinic substrates but also is an efficient catalyst in asymmetric ketone hydrogenations.²⁴

The introduction of catalyzed asymmetric hydrogenation in the industry has been a revolution in industrial processes that took place in multiple stages with continuous waste production. With this methodology, processes became simpler and more respect for atom economy. As an example, the well known synthesis of naproxen that has suffered for years a representative evolution.²⁵ (**Figure. I. 11**).

The first large-scale for the synthesis of naproxen produced 500 Kg of material in 1970. That synthesis consisted in four steps which involve Friedel-Craft acylation that wasn't regiospecific, producing also the 1-isomer which can be removed by

[24] a) M. Kitamura, M. Tokunaga, T. Ohkuma, R. Noyori, *Tetrahedron Lett.*, **1991**, 32, 4163; b) M. Kitamura, M. Tokunaga, T. Ohkuma, R. Noyori, *Org. Synth.*, **1993**, 71, 1; c) K. Mashima, K. Kusano, N. Sato, Y. Matsumura, K. Nozaki, H. Kumobayashi, N. Sayo, Y. Hori, T. Ishizaki, S. Akutagawa, H. Takaya, *J. Org. Chem.*, **1994**, 59, 3064.
[25] P. J. Harrington, E. Lodewij, *Organic Process Research and Development*, **1997**, 1, 72.

crystallization methods. Aluminum hydroxide wastes were produced in high quantities and undesirables reagents in the sequence as nitrobenzene, ammonium sulfide, sodium hydride and methyl iodine.

At present, an option to obtain (*S*)-Naproxen is by reducing the naphthacrylic acid using chiral catalysts as BINAP, however this type of catalysts have some drawbacks, such as high cost, low temperature stability and the difficulty of recovery and reuse. Thus the next improvement in this process could be the heterogenized catalyst such as alternative to improve the hydrogenation step.

4 Relevance of multi-component reaction in green chemistry.

A multi-component (MCR) reaction is defined as a reaction in which three or more compounds react in a single operation to form a single product that contains essentially all atoms of the starting materials (with the exception of condensation products, such as, H₂O, HCl or MeOH).²⁶ The product forms either sequentially in a tandem or domino fashion, or all at once.

The concept of multi-component coupling can be found in nature. Many building blocks of life are believed to have resulted from multi-component couplings and involve an economy of steps and, often, atom economy. These processes are emerging as a powerful weapon for reducing operative steps and enhancing synthesis efficiency²⁷ in the synthesis of biologically important compounds. Currently, the major issues concerning the use of MCR's as tools in chemical biology are the limited scaffold diversity, and the poor stereocontrol.

[26] E. Ruijter, R. Scheffelaar, R. V. A. Orru, *Angew. Chem. Int. Ed.*, **2011**, 50, 6234-6246.

[27] For some recent reviews, see: (a) C. Hulme, V. Gore, *Curr. Med. Chem.*, **2003**, 10, 51-80; (b) R. Orru, M. De Greef, *Synthesis*, **2003**, 1471-1499; (c) L. Weber, *Curr. Med. Chem.*, **2002**, 9, 2085-2093.

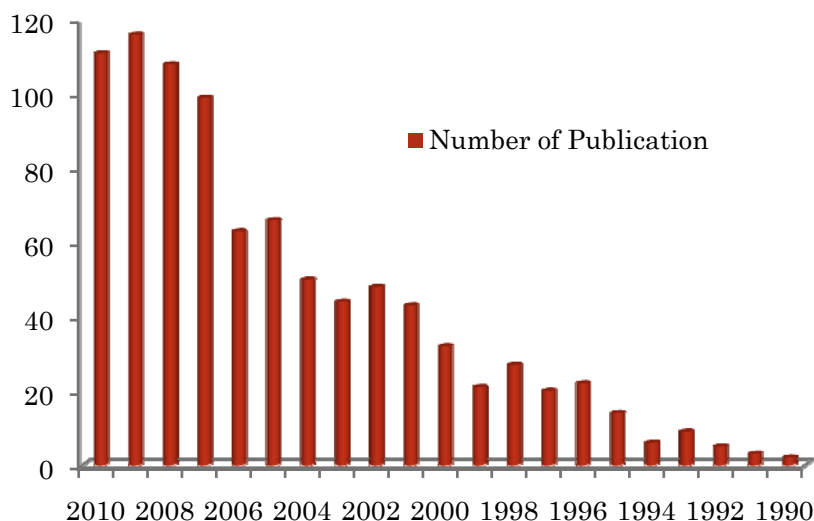


Figure. I. 12. Number of publications dealing with MCR's in last 15 years (results are derived from a Web of Knowledge query "multi-component reaction").

The first one is addressed by the continuous discovery of novel MCR's and the second is in connection with modeling more selective catalyst to perform these processes. Although serendipity has always played an important role in the discovery of new MCR's, the emergence of a more rational design approach in recent years is reflected in the number of scientific publications in the past two decades that deal with MCRs. (**Figure. I. 12**).

The developments of chemical reactions that are atom-efficient and environmentally friendly with enhanced selectivity are attractive for the synthetic chemists. The ideal synthesis should allow the construction of the desired product in as few steps as possible, in good overall yield, and by using environmentally acceptable reagents.

The synthetic variables that have to be optimized are time, cost, overall yield, simplicity of performance, safety, and environmental impact. Most synthetic schemes still use a simple step-by step approach to convert a starting material into a final product, in which intermediate products are isolated and purified for the next conversion step. Such traditional practice has the disadvantages of being time-

consuming, with the likelihood of producing large amounts waste. MCR's convert three or starting materials directly into their products by one-pot operations and therefore are more efficient than multistep syntheses because both the synthetic and work-up procedures need to be done only once. The other attractive features of MCR's are the formation of several new bonds in one pot, the attainment of higher atom economy and chemoselectivity, and the generation of a low level of by-products, compared to classical stepwise syntheses.

One of the fundamental aspects in green chemistry is linked to the minimization of the number of steps required in organic synthesis, as well as, to achieve the maximum atom economy. From this point of view, multi-component reactions (MCR's) are thus becoming an increasingly important class of reactions as they allow several starting materials to be combined to, usually, form a single compound, in a one-pot operation.



General targets

1 Targets.

This PhD dissertation is focused on the design and synthesis of new chiral gold, palladium and rhodium complexes with ligands based on two different structures:

- a) Ligands based on a dioxolane backbone bearing *N*-heterocyclic carbene moieties.
- b) Ligands based on proton sponges as building block.

For heterogeneization proposes, both families of ligands have been functionalized and supported on MCM-41. Thus, the project involves the design, preparation and evaluation of new soluble catalysts and the corresponding heterogenized on a mesoporous inorganic support, paying particular attention to the role of the support on reactivity, enantioselectivity and recyclability in successive reactions. Within these general targets, the following steps are included:

1) Design and synthesis of ligands

The development of new easy strategies for synthesis of the two classes of chiral ligands, that result inexpensive and from accessible materials. Each family has its particular objectives:

- a. *N*-heterocyclic carbenes: Study the behavior of NHC's compared with the analogous phosphine complexes.
- b. Proton sponges: Study the effects of "proton sponge-core ligands" compared with other Schiff base ligands.

In both types of structures we have developed synthesis strategies for obtaining:

- a) New soluble ligands with new chiral structures.
- b) New chiral referable functionalized ligands for further heterogeneization.

2) Synthesis of of palladium, rhodium and gold complexes

Preparation and characterization of transition metal complexes (Pd, Rh, Au) for each family of ligands.

3) Heterogeneization on inorganic support

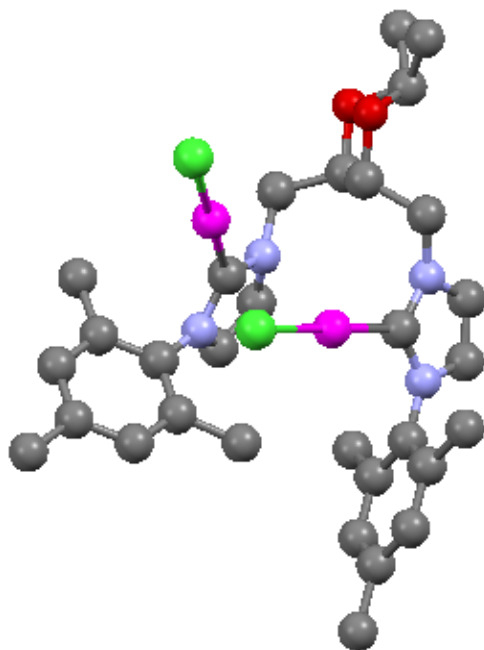
The development of catalyst-immobilization strategy should allow the design of many highly active, reusable and enantioselective heterogeneous asymmetric catalysis.

4) Study of new catalysts in homogeneous and heterogeneous reaction conditions in enantioselective hydrogenations

The development of new transformations focusing on asymmetric hydrogenation of prochiral succinates in order to study the influence of the ligand substituents, steric bulkiness of the substrates and support.

5) Application of gold catalysts in multi-component reaction

Study of the performances of the gold catalysts obtained in multi-component reactions comparing soluble and heterogenized catalysts in terms of activity and with several starting materials.



Chiral complexes bearing N-heterocyclic carbene
moieties at a dioxolane backbone.
Gold, palladium and rhodium complexes as
enantioselective hydrogenation catalysts.
Homogeneous Vs heterogenized.

1 Introduction.

The chemistry of *N*-heterocyclic carbenes (NHC's) has developed significantly over recent years encompassing their synthesis, reactivity, coordination chemistry and application.^{1,2} Because of their modular structures, many modifications of the basic imidazole-based motif have been produced. While one area of these studies has been directed towards the elucidation of the factors determining the stability of the free carbenes in terms of electronic and steric effects,³ another part of the investigations has focused on potential applications of NHC's, mainly as ligands for transition-metal-catalyzed reactions.⁴

In the latter context, significant recent developments include, for example, the incorporation of NHC moieties into multidentate chelate ligands⁵ and the chiral modification of NHC's with implications for their use in asymmetric catalysis.⁶ Arguably, the most significant stimulus for continued interest is the catalytic application to organo- and metal-mediated catalysis and there is now ample evidence demonstrating that NHC systems can lead to new reactivity and improved catalytic

[1] For monographs, see a) F. Glorius, in *N-heterocyclic Carbenes (NHC) in Transition Metal Catalysis (Topics in Organometallic Chemistry)*, SPRINGER-VERLAG, Berlin, **2006**; b) S. P. Nolan, in *N-Heterocyclic Carbenes in Synthesis*, WILEY-VCH, **2006**.

[2] For general reviews on NHCs, see: a) D. Bourissou, O. Guerret, F. P. Gabbaï, G. Bertrand, *Chem. Rev.*, **2000**, *100*, 39-92; b) F. E. Hahn, M. C. Jahnke, *Angew. Chem., Int. Ed.*, **2008**, *47*, 3122-3172; c) V. Nair, S. Bindu, V. Sreekumar, *Angew. Chem., Int. Ed.*, **2004**, *43*, 5130-5135; d) N. Marion, S. Diez-Gonzalez, I. P. Nolan, *Angew. Chem., Int. Ed.*, **2007**, *46*, 2988-3000; e) P. de Fremont, N. Marion, S. P. Nolan, *Coord. Chem. Rev.*, **2009**, *253*, 862-892; f) O. Schuster, L. Yang, H. G. Raubenheimer, M. Albrecht, *Chem. Rev.*, **2009**, *109*, 3445-3478.

[3] L. Cavallo, A. Correa, C. Costabile, H. Jacobsen, *J. Organomet. Chem.*, **2005**, *690*, 5407-5413.

[4] a) W. A. Herrmann, *Angew. Chem.*, **2002**, *114*, 1342-1363; *Angew. Chem. Int. Ed.*, **2002**, *41*, 1290-1309; application of NHCs in olefin metathesis: b) Y. Schrodi, R. L. Pederson, *Aldrichimica Acta*, **2007**, *40*, 45-52.

[5] For phosphine-functionalized NHCs see, for example: a) A. A. Danopoulos, N. Tsoureas, S. A. Macgregor, C. Smith, *Organometallics*, **2007**, *26*, 253-263, and references therein; b) N. Stylianides, A. A. Danopoulos, N. Tsoureas, *J. Organomet. Chem.*, **2005**, *690*, 5948-5958; c) A. A. Danopoulos, S. Winston, T. Gelbrich, M. B. Hursthouse, R. P. Tooe, *Chem. Commun.*, **2002**, 482-483; d) C. C. Lee, W. C. Ke, K. T. Chan, C. L. Lai, C. H. Hu, H. M. Lee, *Chem. Eur. J.*, **2007**, *13*, 582-591, and references therein; e) F. E. Hahn, M. C. Jahnke, T. Pape, *Organometallics*, **2006**, *25*, 5927-5936, and references therein; f) O. Kaufhold, A. Stasch, P. G. Edwards, F. E. Hahn, *Chem. Commun.*, **2007**, 1822-1824; g) S. Nanchen, A. Pfaltz, *Helv. Chim. Acta*, **2006**, *89*, 1559-1573; h) J. Zhong, J. H. Xie, A. E. Wang, W. Zhang, Q. L. Zhou, *Synlett*, **2006**, 1193-1196, and references therein; i) L. D. Field, B. A. Messerle, K. Q. Vuong, P. Turner, *Organometallics*, **2005**, *24*, 4241-4250; j) E. Bappert, G. Helmchen, *Synlett*, **2004**, 1789-1793; k) T. Focken, G. Raabe, C. Bolm, *Tetrahedron: Asymmetry*, **2004**, *15*, 1693-1706; l) H. Lang, J. J. Vittal, P. H. Leung, *J. Chem. Soc. Dalton Trans.*, **1998**, 2109-2110; m) W. A. Herrmann, C. Kçcher, L. J. Gooßen, G. R. J. Artus, *Chem. Eur. J.*, **1996**, *2*, 1627-1636; other donor functions: n) H. V. Huynh, C. H. Yeo, G. K. Tan, *Chem. Commun.*, **2006**, 3833-3835; o) M. Poyatos, A. Maisse-Francois, S. Bellemin-Lapponnaz, L. H. Gade, *Organometallics*, **2006**, *25*, 2634-2641; p) P. L. Arnold, M. Rodden, C. Wilson, *Chem. Commun.*, **2005**, 1743-1745.

[6] a) M. C. Perry, K. Burgess, *Tetrahedron: Asymmetry*, **2003**, *14*, 951-961; b) V. César, S. Bellemin-Lapponnaz, L. H. Gade, *Chem. Soc. Rev.*, **2004**, *33*, 619-636.

rate, lifetime and selectivity. Of the many reactions that have been investigated using NHC's containing catalysts, hydrogenation and transfer hydrogenation have featured prominently, which is in part due to their wide ranging use in synthetic chemistry and continued industrial importance.

In our case we were looking for make these systems more efficient and recyclable by supporting these catalysts on inorganic solids, in order to reduce the costs in catalytic processes. The efficient separation of catalyst from the reaction mixtures is one of the key factors to decrease costs and to make several industrial processes environmentally friendly.

2 State of the art.

2.1 Historical background.

Carbenes are compounds that have a double-coordinated carbon, being deficient in electrons having two unshared electrons. In the ground state, the two electrons are placed in the same orbital with antiparallel spins (in the singlet state) or in two different orbital with parallel spin (triplet state)⁷.

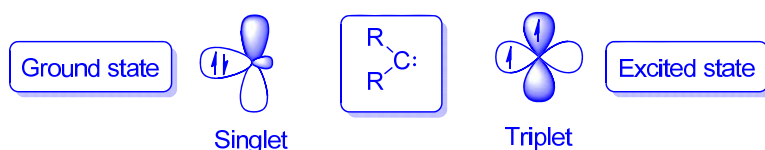


Figure. III. 1. Electronic configuration of carbene compound.

Initially the quest for a stable carbene seemed an unattainable goal until Wanzlick⁸ in 1961 showed that the stability of carbenes could be dramatically increased by vicinal amino substituents. In 1964, Fischer⁹ described the first transition metal complex with a carbene ligand, this new complex was called carbene-Fischer, and the carbenic carbon has electrophilic behavior. This carbene form a metal-carbon

[7] S. Díez-González, S. P. Nolan, *Coord. Chem. Rev.*, **2007**, 251, 874-883.

[8] (a) H. W. Wanzlick, H. J. Kleiner, *Angew. Chem.*, **1961**, 73, 493; (b) H. W. Wanzlick, *Angew. Chem.*, **1962**, 74, 129; (c) H. W. Wanzlick, F. Esser, H. J. Kleiner, *Chem. Ber.*, **1963**, 96, 1208; (d) H. W. Wanzlick, H. J. Kleiner, *Chem. Ber.* **1963**, 96, 3024.

[9] E. O. Fischer, A. Maasböl, *Angew. Chem., Int. Ed. Engl.*, **1964**, 3, 580.

bond constituted by mutual acceptor interaction. These bond it seen as a single bond because the π -back donation is weakly, because the σ -interaction stabilizes enough. Fisher carbene complex is associate with low oxidation state metals.

Ten years later, it was isolated another type carbene complexes by Schrock¹⁰ in these new carbenes, the polarization of metal-carbon bond is inverted and carbenic carbon has nucleophilic behavior. In this case the π -electrons are distributed between the carbon and the metal, thus, it is real metal-carbon double bond. The Schrock carbenes are associate with high oxidation state metals. (**Figure. III. 2**).

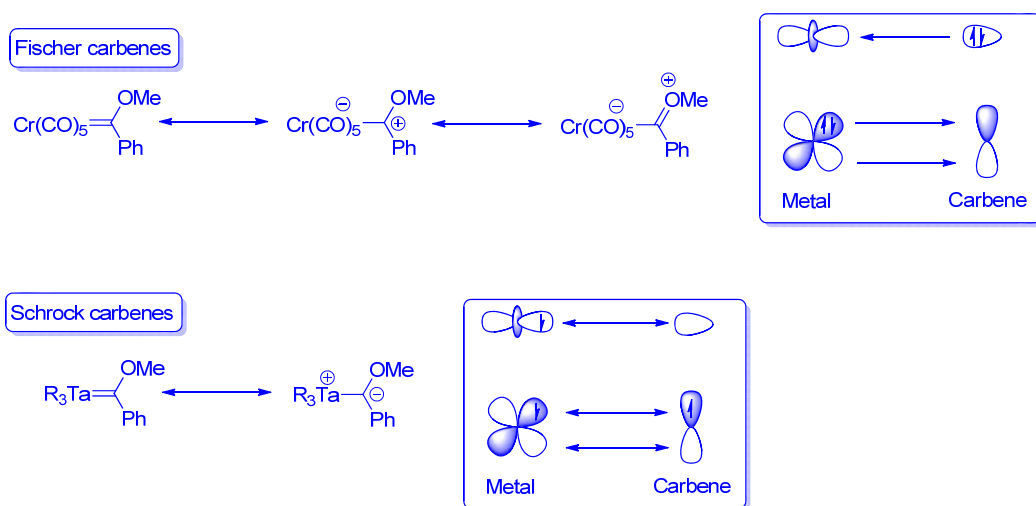


Figure. III. 2. Fischer and Schrock carbene types.

Wanzlick and Ophel¹¹ described the first complexes bearing (NHC) ligands and Arduengo et al¹² in 1991 isolated the very first free stable imidazol carbene. (**Figure. III. 3**). These kind of compounds resulted stable to moisture and air, this fact gave high variety of complexes with several structural possibilities, with the simple complexation of these compounds to a metal.

[10] R. R. Schrock, *J. Am. Chem. Soc.* **1974**, 96, 6796.

[11] H. W. Wanzlick, H. J. Schönherr, *Angew. Chem., Int. Ed. Engl.*, **1968**, 7, 141.

[12] A. J. Arduengo, R. L. Harlow, M. A. Kline, *J. Am. Chem. Soc.*, **1991**, 113, 361.

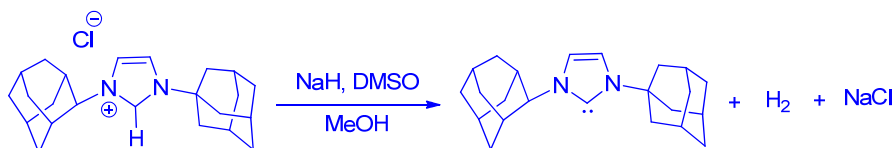


Figure. III. 3. Formation of first stable NHC.

The NHC's belong to the third carbene group and although formally they are Fischer type carbenes, chemically they behave as nucleophiles (Schrock type). Thus in NHC's the carbenic carbon is in singlet state due to two nitrogen mesomeric stabilization. From an electronically point of view, the NHC-Metal bond is mostly σ -donor, but the stabilization is also due to π interactions, as well as, in electron-rich metals through π back-bonding, as in electron-deficient metal through π donation. (**Figure. III. 4**).

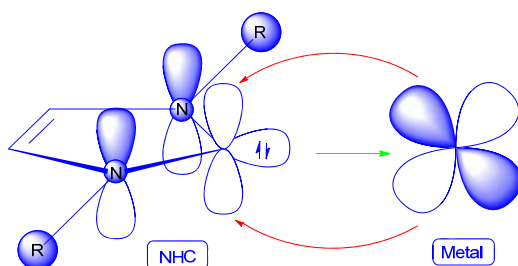


Figure. III. 4. NHC-Metal electronic configuration..

Due to their strong σ -electron donating character properties, NHC ligands form stronger bonds with metal centers than most of classical ligands, such as phosphines. This fact give metal complexes that are generally resistant to decomposition, very useful behavior when the complex is onto a catalytic system that sometimes presents hard reaction conditions. These beneficial features have contributed to the recognition of NHC's, as ubiquitous ligands in organometallic chemistry¹, as evidenced by numerous applications from catalysis¹³ and medicinal sciences¹⁴. These successes have motivated intense efforts toward the design and development of new NHC architectures.

[13] (a) L. Mercs, M. Albrecht, *Chem. Soc. Rev.*, **2010**, 39, 1903; (b) M. L. Teyssot, A. S. Jarrousse, M. Manin, A. Chevy, S. Roche, F. Norre, C. Beaudoin, L. Morel, D. Boyer, R. Mahiou, A. Gautier, *Dalton Trans.*, **2009**, 6894; (c) D. Tapu, D. A. Dixon, C. Roe, *Chem. Rev.*, **2009**, 109, 3385; (d) C. Samojowicz, M. Bieniek, K. Grela, *Chem. Rev.*, **2009**,

2.2 Synthesis of imidazolium precursor salts for NHC ligands.

The deprotonation of the heterocyclic cationic ring precursor is by far, the most common pathway to afford carbene complexes, thus the study of the synthesis of new carbene complexes is focus on the synthesis of cationic heterocycles, which are the typical NHC's ligand precursors. The most used procedure is the quaternization of imidazole moiety previously synthesized but, nowadays there are others protocols that can be easy classified (**Figure. III. 5**) based on the nature of the latest subunit being installed in the final cyclization step:

- Ring closure by final introduction of pre-carbenic unit.
- Ring closure by final linkage of the backbone to the preassembled pre-carbenic and amino units.
- Ring closure by final introduction of the amino moiety.

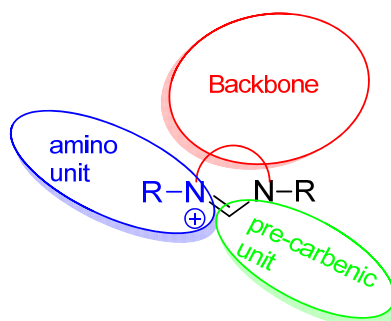


Figure. III. 5. Classification of general pathways to afford NHC precursors.

109, 3708; (e) M. Poyatos, J. A. Mata, E. Peris, *Chem. Rev.*, **2009**, 109, 3677; (f) D. McGuinness, *Dalton Trans.*, **2009**, 6915; (g) J. C. Y. Lin, R. T. W. Huang, C. S. Lee, A. Bhattacharyya, W. S. Hwang, I. J. B. Lin, *Chem. Rev.*, **2009**, 109, 3561; (h) H. Jacobsen, A. Correa, A. Poater, C. Costabile, L. Cavallo, *Coord. Chem. Rev.*, **2009**, 253, 687; (i) K. M. Hindi, M. J. Panzner, C. A. Tessier, C. L. Cannon, W. J. Youngs, *Chem. Rev.*, **2009**, 109, 3859; (j) P. L. Arnold, I. J. Casely, *Chem. Rev.*, **2009**, 109, 3599; (k) N. Marion, S. P. Nolan, *Acc. Chem. Res.*, **2008**, 41, 1440; (l) F. E. Hahn, M. C. Jahnke, *Angew. Chem., Int. Ed.*, **2008**, 47, 3122; (m) S. Díez-Gonzalez, S. P. Nolan, *Acc. Chem. Res.*, **2008**, 41, 349; (n) K. Cavell, *Dalton Trans.*, **2008**, 6676; (o) L. H. Gade, S. Bellemin-Laponnaz, *Coord. Chem. Rev.*, **2007**, 251, 718; (p) E. Kantchev, C. O'Brien, M. Organ, *Angew. Chem., Int. Ed.*, **2007**, 46, 2768; (q) V. César, S. Bellemin-Laponnaz, L. H. Gade, *Chem. Soc. Rev.*, **2004**, 33, 619; (r) W. A. Herrmann, *Angew. Chem., Int. Ed.*, **2002**, 41, 1290. [14] (a) V. Nair, S. Vellalath, B. P. Babu, *Chem. Soc. Rev.*, **2008**, 37, 2691; (b) D. Enders, O. Niemeier, A. Henseler, *Chem. Rev.*, **2007**, 107, 5606; (c) N. Marion, S. Díez-González, S. P. Nolan, *Angew. Chem., Int. Ed.*, **2007**, 46, 2988; (d) D. Enders, T. Balensiefer, *Acc. Chem. Res.*, **2004**, 37, 534.

In the following paragraphs, we will discuss the three kinds of NHC synthesis, with a strong focus on chiral and high functionalized NHC's that could be useful in asymmetric catalytic application through complexation with a transition metal, one of our best goals in this project.

2.2.1 Cyclization by final introduction of precarbenic atom.

The cyclization by introduction of precarbenic atom in the final step is the most used strategy to afford NHC precursors. This pathway consists in to obtain a tuned diamine substrate that treated with different types of reagents leads to the heterocyclic desired salts. As an example Hoveyda and co-workers¹⁵ were able to apply this method to the synthesis of an un-symmetrical and chiral carbene precursor using (*S*)-NOBIN as starting material only in two steps sequence with nice yields. (**Figure. III. 6**).

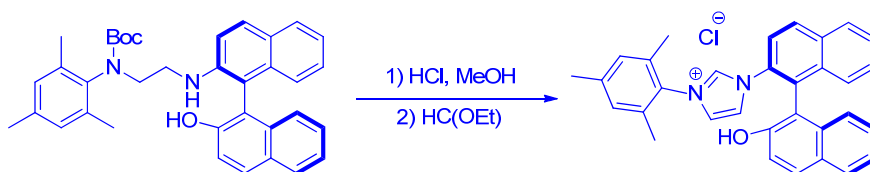


Figure. III. 6. Final step of cyclization according with Hoveyda synthesis of NHC precursors.

The deprotection of the Boc group occurred during the second step forming the dihydrochloride salt of the diamine. This example shows a general and easy methodology to get much functionalized, chiral and asymmetric NHC precursor that could be applied with different chiral diamines.

2.2.2 Cyclization by final introduction of the backbone.

In this case, the method consists of a capping of the precarbenic unit with the desired heterocyclic backbone. One of the routes to carry out this methodology is the

[15] J. J. Van Veldhuizen, S. B. Garber, J. S. Kingsbury, A. H. Hoveyda, *J. Am. Chem. Soc.*, **2002**, 124, 4954.

intramolecular quaternization of imines. As, an example we described the synthesis reported by Bertrand et al.¹⁶ (**Figure. III. 7**).

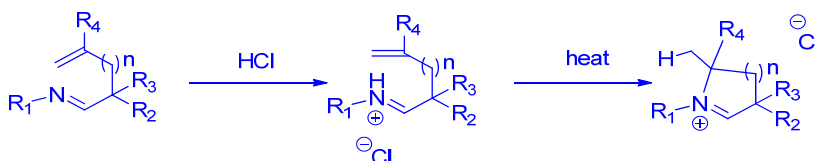


Figure. III. 7. Intramolecular quaternization of imines.

They were encouraged in this way by previous works reporting the hydroamination of weakly basic amine catalyzed by Brönsted acids. Considering imines are less basic than amines the reaction was found to be a powerful cyclization strategy due to the number of variants of the method by simply choosing the desired imine, as well as, high functionalized or chiral imines, even building five and six member heterocyclic rings.

2.2.3 Cyclization by final introduction of amino moiety.

The third alternative could be easily represented by the one-pot synthesis of Isoquinolinium chlorides reported by Lassaletta et al.¹⁷ through Zincke reaction between aromatic pyridine salts and chiral amine to afford chiral precarbenic ligands salts. (**Figure. III. 8**.)

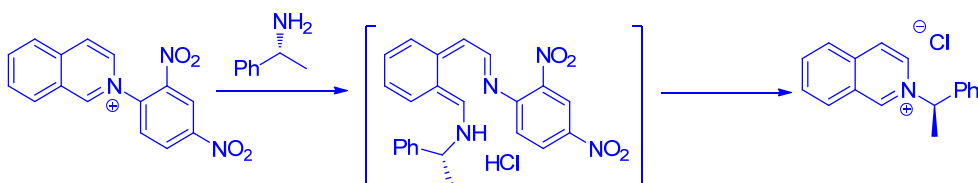


Figure. III. 8. Zincke reaction for synthesis of precarbenic salts.

[16] (a) X. Zeng, G. D. Frey, R. Kinjo, B. Donnadieu, G. Bertrand, *J. Am. Chem. Soc.*, **2009**, *131*, 8690; (b) R. Jazzar, R. D. Dewhurst, J. B. Bourg, B. Donnadieu, Y. Canac, G. Bertrand, *Angew. Chem., Int. Ed.*, **2007**, *46*, 2899.

[17] S. Gomez-Bujedo, M. Alcarazo, C. Pichon, E. Álvarez, R. Fernandez, J. M. Lassaletta, *Chem. Commun.*, **2007**, 1180.

This heterocyclic interconversion takes place by ring opening and ring closing sequence via imino intermediates.

2.3 General features of *N*-heterocyclic carbenes.

In electronic terms NHC's have a close relationship with phosphines. Both have strong σ -donor and low π -donor character but NHC's are stronger σ -donor than phosphines, this fact involves more stability in transition metal complexes and makes the NHC's more useful in catalytic systems. To understand this electronic behavior so many reports have been reflected with various theoretical and empirical studies.

The electron donating property can be quantified by comparison of the stretching frequencies of CO ligands in NHC's complexes. Nolan et al¹⁸ reported the study of the carbonyl stretching frequencies of [(NHC)Ni(CO)₃] complexes that were synthesized and compared with tertiary phosphines Ni complexes. They conclude that *N*-heterocyclic carbenes have very similar levels of electron-donating ability, whereas phosphines span a much wider electronic range going from alkyl to aryl phosphines.

In the other hand, steric protection from the *N*-substituents may enhance the stability of the carbenes. Despite the fact that *N*-heterocyclic carbenes have often been used as phosphine mimics, their shape is very different because phosphine have three substituents on the atom which acts as a ligand, causing it has a conical shape while the NHC's has flat structure in wedge-shaped. In order to quantify the steric requirements of these two kinds of ligands, a new model was designed by Nolan et al¹⁹: the percent of the volume occupied by ligand atoms in a sphere centered on the metal (%V_{Bur}). This model allows for a more realistic comparison with other ligands, particularly tertiary phosphines. The model also takes into account the high asymmetry of these ligands. For [Cp*Ru(L)Cl] complexes, the experimental (and theoretical) bond-dissociation energies (BDE's) plotted versus %V_{Bur} resulted in a linear correlation, indicating that the BDE's are essentially controlled by the steric requirements of the ligand.

[18] (a) R. Dorta, E. D. Stevens, C. D. Hoff, S. P. Nolan, *J. Am. Chem. Soc.*, **2003**, *125*, 10490–10491. (b) R. Dorta, E. D. Stevens, N. M. Scott, C. Costabile, L. Cavallo, C. D. Hoff, S. P. Nolan, *J. Am. Chem. Soc.*, **2003**, *125*, 2485–2495.

[19] A. C. Hillier, W. J. Sommer, B. S. Yong, J. L. Petersen, L. Cavallo, S.P. Nolan, *Organometallics*, **2003**, *22*, 4322.

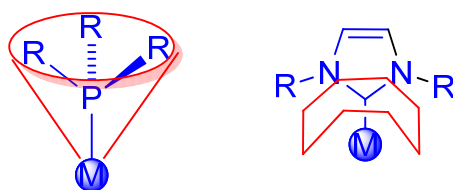


Figure. III. 9. Shape of phosphines and NHC's.

Due to all of these features, during the last years the catalytic properties of different NHC's complexes have been studied and compared with phosphine systems. Herein, we focused on NHC-palladium, -rhodium and -gold complexes and their catalytic behavior.

2.4 NHC's complexes as catalysts in organic synthesis.

Unlike phosphines, the coordination of NHC's to metal centers usually requires the activation of a precursor. There is a variety of methods for forming carbenes, most of them from the corresponding azolium salts. By far the transmetallation from silver NHC's complexes is the more efficient and cleanest pathway to obtain NHC complexes but sometimes for steric or electronics impediments it is impossible to use this method. This, implies the developed of new methods to prepare NHC-metal complexes; witch can be classified according to the nature of the NHC precursor and the activation method employed. In this sense, the most widely used strategies are:

- Insertion of a metal into the C=C bond of *bis*-(imidazolidin-2-ylidene) olefins.
- Use of carbene adducts or “protected” forms of free NHC carbenes.
- Use of preformed, isolated free carbenes.
- Deprotonation of an azolium salt with a base.
- Transmetallation from a Ag-NHC complex prepared from direct reaction of an imidazolium precursor and Ag₂O.
- Oxidative addition via activation of the C-X (X = Me, halogen, H) of an imidazolium cation.

2.4.1 NHC Palladium complexes.

Palladium complexes is one of the most versatile and widely organometallic catalysts used on both industrial and laboratory scales. Tertiary palladium phosphine catalysts have been largely used to control reactivity and selectivity in organometallic chemistry. However, these ligands are often air-sensitive and significant phosphorus–carbon bond degradation occurs when these are subjected to high temperatures, which leads to catalyst deactivation.

In 1995, Herrmann et al.²⁰ reported the first NHC-based soluble catalyst. (Figure. III. 10).

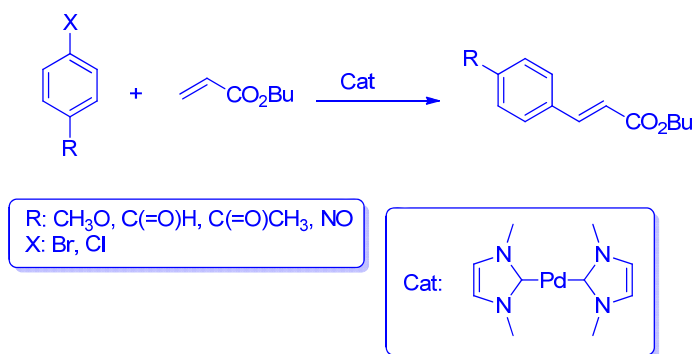


Figure. III. 10. First example of NHC catalytic properties in Heck reaction.

In this work, the authors studied the activity of different NHC-containing palladium catalysts in the Heck reaction. The NHC-Pd(0) derivative shows the best catalytic records, showing no induction time in the catalytic profile. This fact probes the amazing stabilization power of NHC ligands for electron rich metals.

Since then, many research groups have provided a large number of NHC-based catalysts for a wide variety of reactions. Nowadays these NHC-Pd catalysts have become a real alternative to Pd-phosphines and their use has allowed for significant improvements in catalytic performance in many transformations. Indeed, the well known cross-coupling C-C and C-N reactions such as the abovementioned Heck,

[20] W. A. Herrmann, M. Elison, J. Fischer, C. Kocher, G. R. J. Artus, *Angew. Chem. Int. Ed. Engl.*, **1995**, 34, 2371–2374.

Suzuki-Miyaura, Negishi, Kumada-Corriu, Sonogashira, Buchwald-Hartwig reactions, but also polymerization, hydrogenation and oxidation processes have benefited from the development of new NHC-Pd complexes. (**Figure. III. 11**).

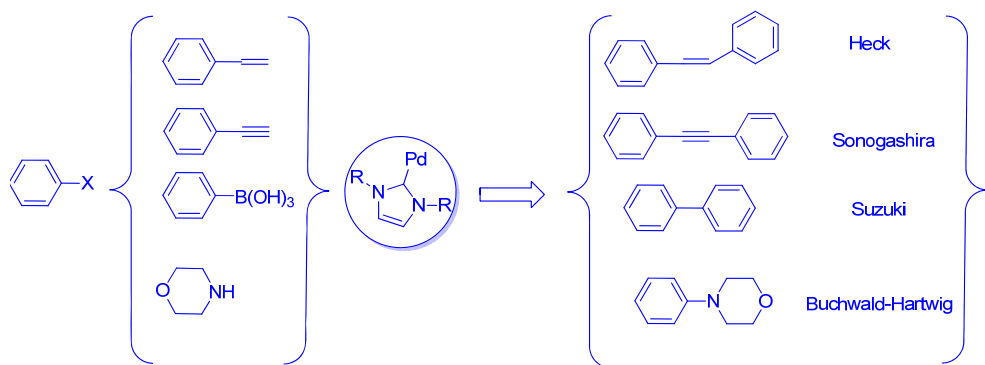


Figure. III. 11. C-C and C-N cross coupling reactions catalyzed by NHC-Pd complexes.

One of the key points to compare the NHC with phosphine systems is the capacity to promote enantioselective transformations. In this way, many reports were recently spending efforts to found efficient asymmetric NHC-Pd catalytic systems.

As we shown above, the synthesis of enantiomeric pure precursor of NHC could be relatively easy, but is difficult to found enantioselective C-C formation catalyzed by NHC-Pd efficient systems in the bibliography. However in 1996, Enders et al²¹ reported the catalytic application of a chiral NHC-Pd complex in asymmetric Heck reaction, but poor chiral induction was observed.

In 2010 Shi et al²² have reported a chiral C_2 -symmetric NHC-Pd catalyst derived from (*R*)-BINAM that could be used as enantioselective catalyst to obtain α -hydroxylation of β -keto esters using oxaziridines as oxidants. These systems resulted effective giving high yields and moderated enantioselectivities. (**Figure. III. 12**, equation A).

[21] D. Enders, H. Gielen, G. Raabe, J. Runsink, J. H. Teles, *Chem. Ber.*, **1996**, 129, 1483–1488.

[22] S. H. Cao, M. Shi, *Tetrahedron: Asymmetry*, **2010**, 21, 2675-2680.

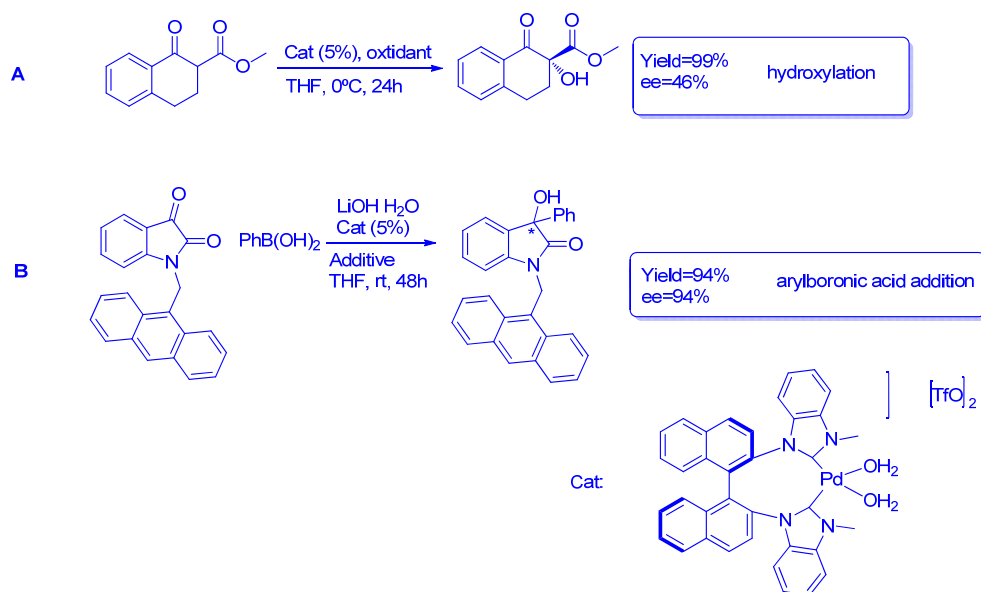


Figure. III. 12. Enantioselective reactions with NHC-Pd catalyst.

The same group²³ reported in 2011 the addition of arylboronic acids to indolines catalyzed by the same catalyst, at this time, excellent yields and enantioselectivities were obtained. (**Figure. III. 12**, equation B). These examples show the interesting effect of a chiral backbone in NHC catalysts.

For asymmetric hydrogenation reactions catalyzed by NHC-Pd only (NHC)CNN-Pincer type afforded moderated enantiomeric excess²⁴ (up to 41% of ee in the hydrogenation of (*E*)-diethyl 2-benzylidenesuccinate) using complexes with NHC and (*S*)-proline moieties.

2.4.2 NHC Rhodium complexes.

NHC-Rh catalyst have a wide scope of applications in organic chemistry and essential transformation takes place with these systems such as, H₂ hydrogenation, transfer hydrogenation, hydrosilylation, hydroamination of alkenes and hydroformylation reactions (**Figure. III. 13**).

[23] Z. Liu, P. Gu, P. McDowell, G. Li, *Organic Letters*, **Published on Web 2011**.

[24] M. Boronat, A. Corma, C. Gonzalez-arellano, M. Iglesias, F. Sánchez, *Organometallics*, **2010**, 29, 134-141.

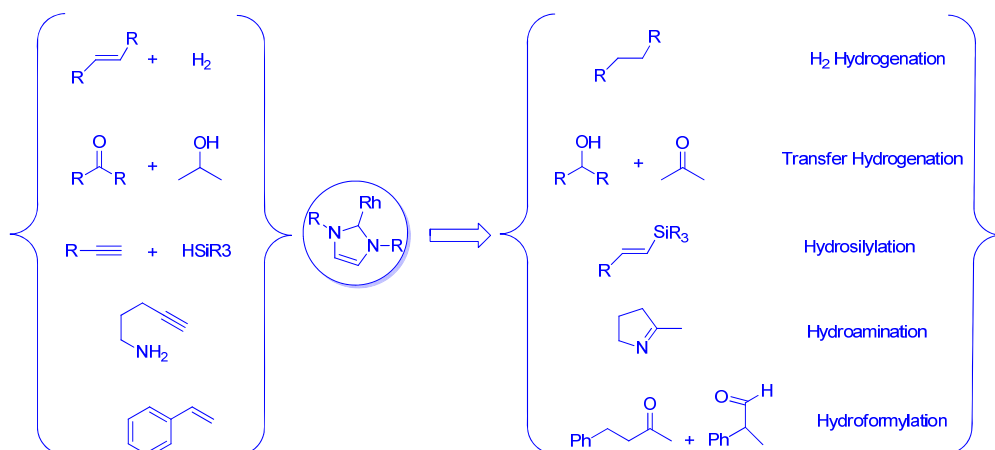


Figure. III. 13. Reactions catalyzed by NHC-Rh complexes.

Appeared in 1996, the first report with chiral inductions by NHC catalysts.²⁵ These amazing results were obtained with a chiral NHC-Rh as **Figure. III. 14** shows. The hydrosilylation of acetophenone in the presence of diphenylsilane and rhodium catalyst produced the corresponding silyl ether in excellent yield and moderated enantiomeric excess (30%); this report validated for first time the possibility of asymmetric synthesis with NHC ligands.

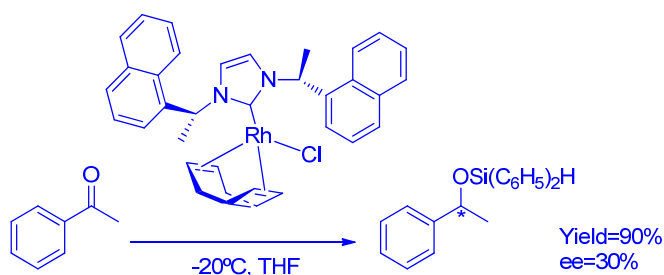


Figure. III. 14. First chiral induction using NHC catalyst.

In recent years the asymmetric induction for catalyzed NHC-Rh processes has been reported. As example, we could mention the efficient asymmetric hydrosilylation

[25] Herrmann, W. A.; Goossen, L. J.; Köcher, C.; Artus, G. R. J. *Angew. Chem., Int. Ed. Engl.*, **1996**, 35, 2805–2807.

reported by Gade and coworkers²⁶ using an oxazoline carbene ligand. In this case, high enantioselectivities in the hydrosilylation of aryl ketones (88–91% ee) and for dialkyl ketones (including ketones lacking α -branching) were achieved. Other asymmetric transformations as oxidative kinetic resolution,²⁷ asymmetric conjugate addition²⁸ and asymmetric arylation²³ give us a notion of the possibilities of these systems.

In terms on hydrogenation reactions, there is to date, only one example of enantioselective alkene hydrogenation has been reported using a chiral rhodium bidentate based on 1,2,4-triazole NHC complexes²⁹ with a chiral diaminocyclohexane backbone. This work was published after we reported the first paper with a chiral dioxolane backbone which is a part of this PhD.³⁰

2.4.3 NHC Gold complexes.

Several years ago, gold has lived in the shadow of other metals in organic chemistry, because it was considered rare, expensive and also chemically inert.

Gold is a rare and expensive metal, but several other precious metals such as, ruthenium, palladium, rhodium, platinum, osmium or iridium are even more expensive, however they are widely used in organic chemistry. This fact makes gold catalysts an attractive alternative for the chemical industry.

Gold is not used in organic chemistry in its elementary state, but as a gold(I) or gold(III) salts complexes. The complexes of both types proved to be active in a large number of transformations using different kinds of ligands. [(PPh₃)AuCl] is the most frequently encountered gold catalyst, this complex requires strong electronic and steric stabilization from its ligand and as we have seen previously, NHC's have been proposed as a more stable alternative than phosphines therefore is not strange that in last times the field of NHC-gold has been extensively investigated.

[26] L. H. Gade, V. César, S. Bellemin-Laponnaz, *Angew Chem Int Ed.*, **2004**, *43*, 1014.

[27] (a) T. Chen, J. J. Jiang, Q. Xu, M. Shi, *Org. Lett.*, **2007**, *9*, 865–868; (b) S. J. Liu, L. J. Liu, M. Shi, *Appl. Organomet. Chem.*, **2009**, *23*, 183–190.

[28] (a) T. Zhang, M. Shi, *Chem.–Eur. J.*, **2008**, *14*, 3759–3764; (b) H. Clavier, J. C. Guillemin, M. Mauduit, *Chirality*, **2007**, *19*, 471–476.

[29] S. K. U. Riederer, B. Bechlars, W. A. Herrmann, F. E. Kühn, *Dalton Trans.*, **2011**, *40*, 41.

[30] A. Arnanz, C. Gonzalez-Arellano, A. Juan, G. Villaverde, A. Corma, M. Iglésias, F. Sánchez, *Chem. Commun.*, **2010**, *17*, 3001–3003.

The unique properties of gold catalysts arise from the special nature of the metal center because, forms stronger gold-ligand bonds compared to other group 11 metals, even can also interact with each other, forming Au-Au interactions of the same intensity as the hydrogen bonds (aurophilicity). Even more important behavior is that gold complexes are excellent Lewis acids reacting preferentially with soft species (such as alkynes and allenes). At the same time gold(I) and gold(III) complexes are poor oxophilic compounds, they have oxygen tolerance and makes their catalytic systems stable to air, water or alcohols, namely have a high stability in multiple reaction conditions. The stability of gold complexes to various oxygenated solvents has been exploited sometimes to develop eco-friendly chemical reactions using water or alcohols as solvents.

Taking account this features, gold carbenes present a widely and amazing reactivity especially with substrates functionalized with double and triple bonds, stabilizing transition states that with other metals, are unstable.

In 2003, Herrmann et al³¹ reported the first NHC-Au catalytic application through addition of water to alkynes previously reported by phosphine gold complexes. This fact validated the utilization of NHC's-Au as substitutes of gold phosphine catalyst.

There are many types of transformations catalyzed by gold complexes, but the majority of them take place through activation of a π -system, so, we can sort the reactions involving gold carbenes based on the type of substrate that is activated for the catalyst. Thus, there are alkene, allene, alkyne activations, inside each class there is a large number of reactions. Herein we will focus on the most modern representing ones, involving enantio- or regio- selective transformations.

Chiral version of cycloisomerization of enyne has been recently reported by Czekelius et al³² using chiral NHC-Au with a tetrahydroisoquinoline backbone affording moderated enantiomeric excess (**Figure. III. 15**, equation A). The results

[31] S. K. Schneider, W. A. Herrmann, E. Herdtweck, *Z. Anorg. Allg. Chem.*, **2003**, 629, 2363–2370.

[32] K. Wilckens, D. Lentz, C. Czekelius, *Organometallics*, **2011**, 30, 1287–1290.

were comparable to those of the best gold phosphine catalysts known for this transformation.

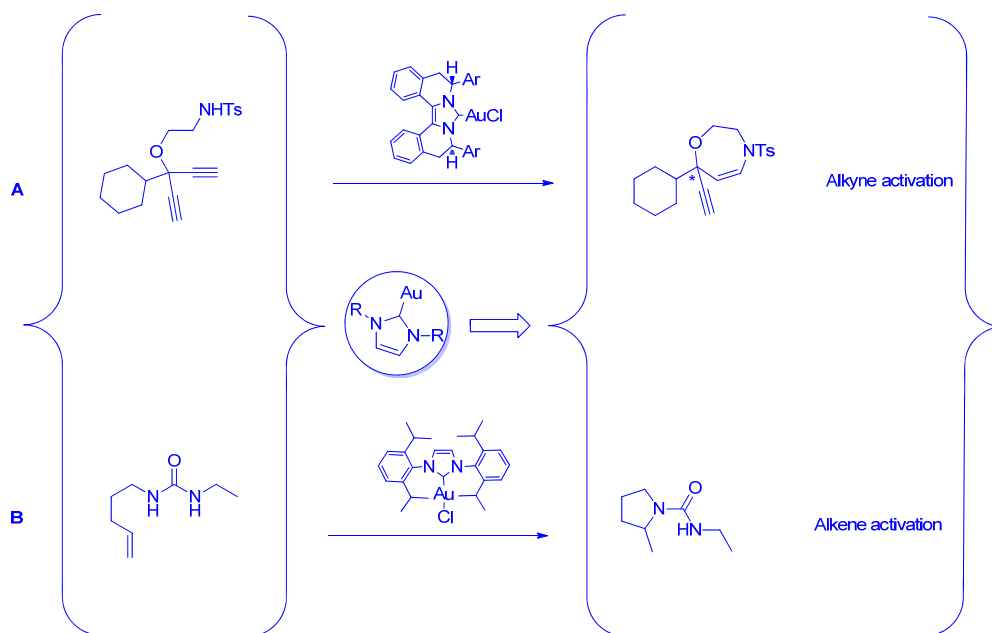


Figure. III. 15. π -activation reactions with NHC-Au.

The alkene activation is less studied reactions for gold catalysis, the first was reported by Peris et al.³³ They showed the efficiency of gold (I) *bis*-carbene catalyst in olefin diboration; but the reaction more studied was the hydroamination reported by Windenhoefer and Bender.³⁴ In this case the authors found a very active catalyst [(IPr)AuCl] (**Figure. III. 15**, equation B) to get *N*-alkenyl ureas with excellent *exo*-selectivity and good diastereoselectivity.

Our research group, reported in 2007³⁵ new applications for NHC-Au(I) as the hydrosilylation of styrene and benzaldehyde with moderates yields. Although the results were not competitive with other catalysts, this fact opened a new door in the gold reactivity and spanned a wide spectrum of organic transformations for Au(I)-NHC's.

[33] R. Corberán, J. Ramirez, M. Poyatos, E. Peris, E. Fernández, *Tetrahedron: Asymmetry*, **2006**, 17, 1759–1762.

[34] C. F. Bender, R. A. Widenhoefer, *Org. Lett.*, **2006**, 8, 5303–5305.

[35] A. Corma, C. González-Arellano, M. Iglesias, F. Sánchez, *Angew. Chem. Int. Ed.*, **2007**, 46, 7820–7822.

Thus, the group has focused on extending the reactivity of these NHC's- Au(I) reporting hydrogenation and cross coupling reactions³⁶ with these catalyst even with its heterogenized form. (**Figure. III. 16**).

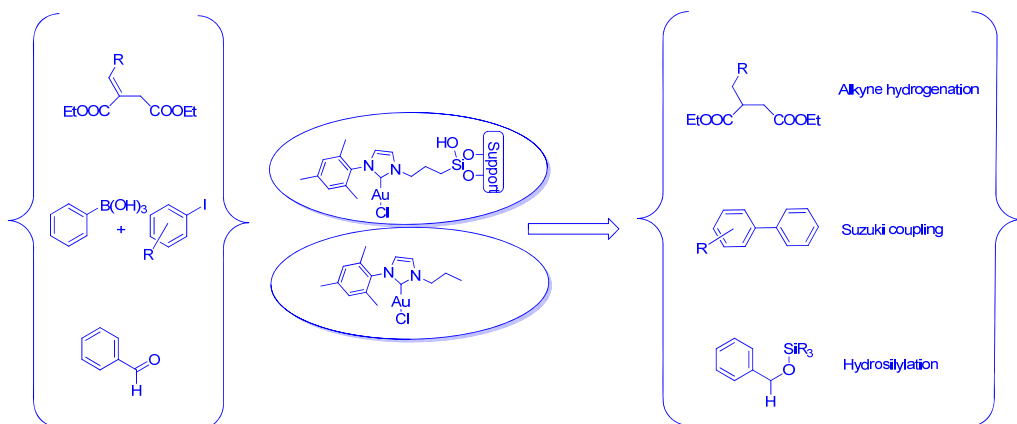


Figure. III. 16. Soluble and heterogenized NHC-Au(I) applications.

For these applications, the NHC's-gold have become alternatives to tertiary phosphines, even more when recently during this PhD dissertation has been reported chiral reactions induced by chiral NHC with both gold (I)³⁰ and gold (III)³⁷.

In last years, the number of catalyzed reactions by the mostly transition metal NHC complexes (such as Ni, Cu, Rh, Ir, Ru, and Pd) has risen. By coordinating an NHC ligand, the stability of the transition metal typically increases and the increased donacity of the NHC ligand helps to enhance the catalytic activity. Of course, the arrival of these NHC's has opened new horizons in the field of transition metal catalysis.

[36] A. Corma, E. Gutiérrez-Puebla, M. Iglesias, A. Monge, S. Pérez-Ferreras, F. Sánchez, *Adv. Synth. Catal.*, **2006**, 25, 2237-2241.

[37] C. del Pozo, A. Corma, M. Iglesias, F. Sánchez, *Organometallics*, **2010**, 29, 4491-4498.

3 Discussion and results.

3.1 Targets.

In this chapter we report the design, synthesis and characterization of a family of chiral compounds based on *N*-heterocyclic *mono*-carbene and *bis*-carbene, which were used as ligands for the formation of the corresponding gold, palladium and rhodium complexes, studying their behavior as chiral catalysts for asymmetric reactions. The attraction of this ligand design³⁸ and catalysis is straightforward; NHC supported complexes have the potential to promote any reaction catalyzed by traditional tertiary phosphine- and phosphite-based catalysts.³⁹ While the promise of similar reactivity is inviting, the hope of increased efficiency, lower toxicity, air stability, and electronic and structural diversity⁴⁰ makes NHC's a logical and smart choice for exploration. We will study the behavior of NHC's confronting with their analogous phosphine complexes not only looking for best records in activity and selectivity but also better stability.

Other way, we expected that these new systems will be stable enough to be supported in inorganic materials as MCM-41 and could be used in catalytic systems without any loss of their performances with the goal to have recycling material, crucial target in our investigation inside the green chemistry.

[38] C. J. O'Brien, E. A. B. Kantchev, G. A. Chass, N. Hadei, A. C. Hopkinson, M. G. Organ, D. H. Setiadi, T. H. Tang and D. C. Fang, *Tetrahedron*, **2005**, *61*, 9723.

[39] R. H. Crabtree, *J. Organomet. Chem.*, **2005**, *690*, 5451.

[40] a) R. Dorta, E. D. Stevens, N. M. Scott, C. Costabile, L. Cavallo, C. D. Hoff and S. P. Nolan, *J. Am. Chem. Soc.*, **2005**, *127*, 2485; b) H. Jacobsen, A. Correa, C. Costabile and L. Cavallo, *J. Organomet. Chem.*, **2006**, *691*, 4350; c) W. A. Herrmann, J. Schutz, G. D. Frey and E. Herdtweck, *Organometallics*, **2006**, *25*, 2437.

3.2 Synthesis of ligands.

3.2.1 Synthesis of soluble bis-*N*-heterocyclic carbene precursor salts.

We have designed and synthesized a new family of chiral *bis*-carbene precursor ligands based in a chiral dioxolane backbone in order to compare their properties with the equivalent phosphine ligand (DIOP). (**Figure. III. 17**).

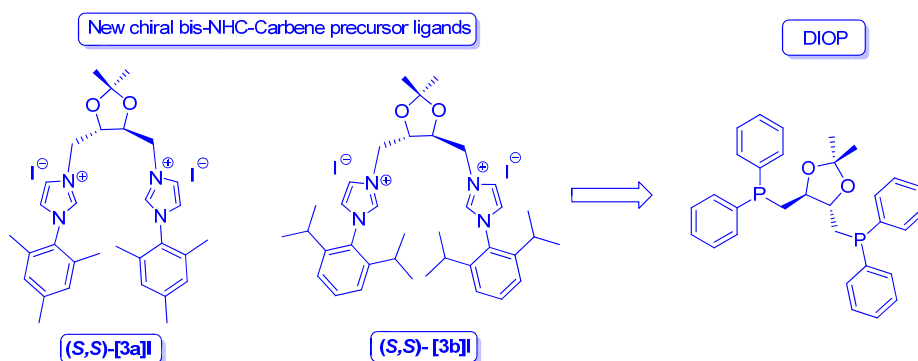


Figure. III. 17. *Bis- N*-heterocyclic carbene precursor salts.

The synthesis strategy involved the preparation of functionalized chiral backbone so that we could directly quaternized the imidazolium moieties obtaining the desired imidazolium salts **(S,S)-[3a]I** and **(S,S)-[3b]I**.

We afforded the dioxolane backbone through manipulation of commercially available enantiopure *L*-tartaric acid^{41,42} improving the methodology described in the literature⁴³ we obtain the (4*R*,5*R*)-*bis*(iodomethyl)-2,2-dimethyl-1,3-dioxolane (**2**) as **Figure. III. 18** shows:

Treatment of tartaric acid with 2,2-dimethoxypropane through acid catalyzed process in methanol gave the chiral dioxolane structure (**IN-1**) in its ester form, which was reduced by NaBH₄ to afford the alcoholic form (**IN-2**) with retention of configuration. Last steps were the tosylation and subsequent S_N2 reaction with NaI to

[41] M. Carmark, C. J. Nelly, *J. Org. Chem.*, **1968**, 33, 2171-2173.

[42] K. Uchida, K. Kato, H. Akita, *Synthesis*, **1999**, 9, 1678-1686.

[43]. L. J. Rubin, H. A. Lardy, H. O. L. Fischer, *J. Am. Chem.Soc.*, **1952**, 74, 425-428.

get the target backbone (**2**) in enantiomerically pure form. We note the formation of the final product after purification by the disappearance of aromatic signals in the ^1H NMR spectra around 7.25 ppm and 7.85 ppm characteristic of the tosyl derivative, yielding a yellow oil.

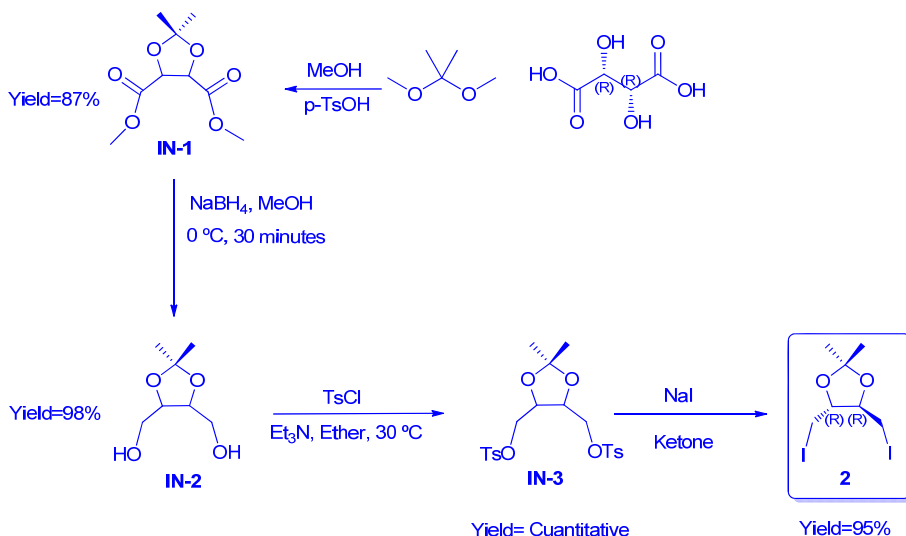


Figure. III. 18. Total synthesis of dioxolane chiral backbone.

We have improved the synthetic method described⁴⁴ for the synthesis of the two imidazoles (**1a**, **1b**). In our pathway, appropriate aniline and ethanodial reacted in the presence of phosphoric acid, ammonium chloride and formaldehyde affording the corresponding yellow solids after purification by flash column chromatography with good yields. Here we have a suitable methodology for the preparation of these compounds in multi-gram scale and from inexpensive and readily available starting materials. (**Figure. III. 19**).

[44] J. Lin, J. Chen, J. Zhao, L. Li, H. Zhang, *Synthesis*, **2003**, 2661-2667.

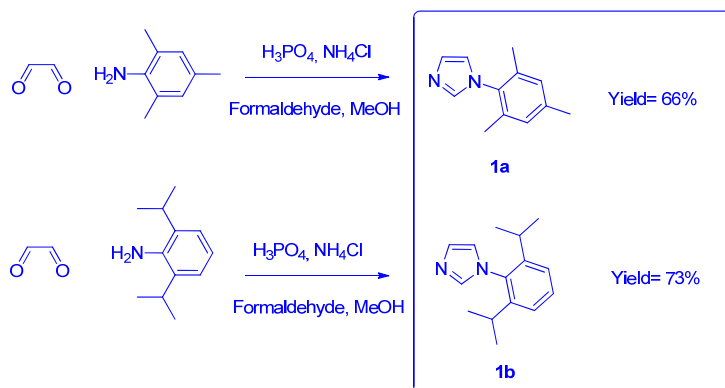


Figure. III. 19. Imidazole synthesis.

In a steel reactor, **2** was heated with 2.2 equivalents of 1-arylimidazoles **1a** or **1b** producing almost quantitative yields of (*S,S*)-[**3a**]**I**, (*S,S*)-[**3b**]**I** as light yellow solids (**Figure. III. 20**). These synthesis routes have been performed by an adaptation of a procedure described previously.⁴⁵

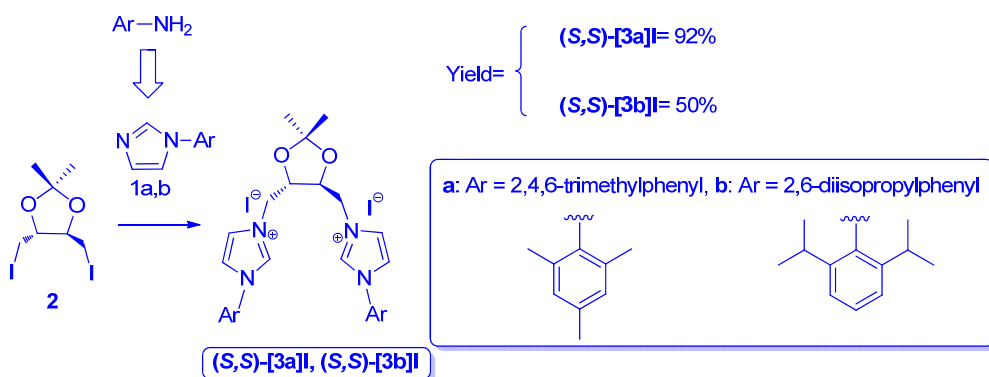


Figure. III. 20. Synthesis of imidazolium ligands salts.

(*S,S*)-[**3a**]**I** and (*S,S*)-[**3b**]**I** have been characterized after isolation. In ^{13}C NMR spectrum the imidazolium carbon (N-CH=N) appears at 137.4 ppm ([**3a**]**I**) and 137.9 ppm ([**3b**]**I**) and in ^1H NMR, the imidazolium proton (N-CH=N) is located downfield at 9.77 ppm ([**3a**]**I**) and 9.66 ppm ([**3b**]**I**).

[45] M.Y. Machado, R. Dorta, *Synthesys*, **2005**, 2473.

We also appreciate how different are the protons of the two CH₂, fact that corroborates the helical structure, at 5.55 ppm and 5.08 ppm for **[3a]I** and 5.5 ppm, 5.25 ppm for **[3b]I**, CH adjacent to the oxygen are represented as a single signal at 4.73 ppm and 4.90 ppm for **[3a]I** and **[3b]I** respectively. It should be noted the appearance of two dioxolane methyl groups as a unique signal which also corroborates the proposed structure, thus, they share the same chemical environment. These signals appear at 1.43 ppm for **[3a]I** and **[3a]I**. (**Figure. III. 21**).

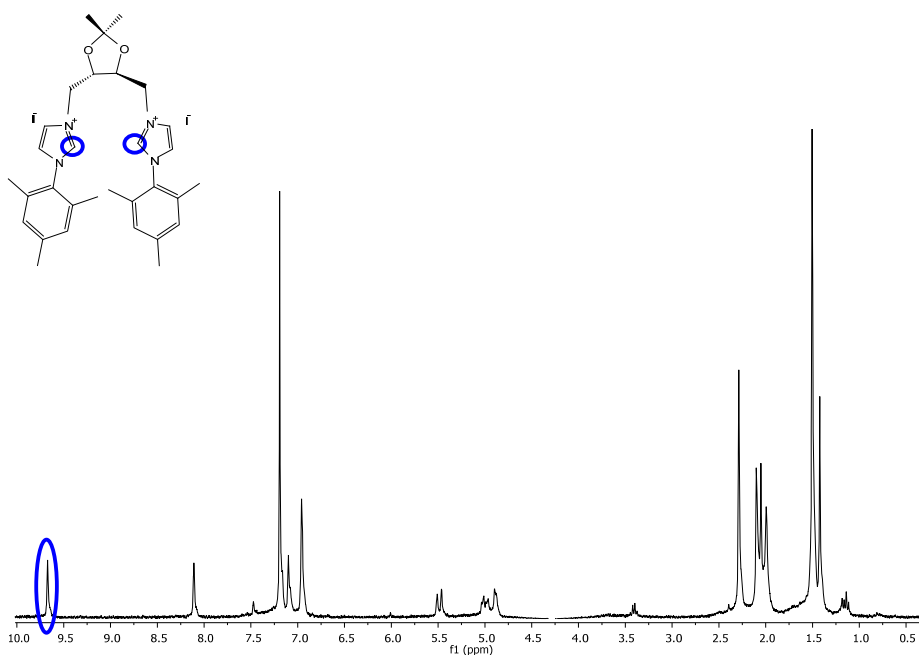


Figure. III. 21. ¹H NMR spectrum for (*S,S*)- **[3a]I**.

ES/MS analyst presents M⁺ ion in the two salts, 500 (M⁺; 100) for **[3a]I** and 584 (M⁺; 100) for **[3b]I** and in IR spectrum shows typical vibrations of C-N, C=C and C=N at 3437 (C-N); 1608 (C=C); 1560-1546 (C=N) for **[3a]I** and 3436 (C-N); 1625 (C=C); 1561-1541 (C=N) for **[3b]I**.

3.2.2 Synthesis of mono-*N*-heterocyclic carbene amine precursor salts.

We have synthesized a new family of chiral *mono*-carbene ligand precursors functionalized with amine pendant groups (**Figure. III. 22**) in order to obtain:

- Ligands to be used as reference systems for homogeneous catalysis.
- Ligands with a pendant alkoxysilyl groups for heterogeneization proposes.

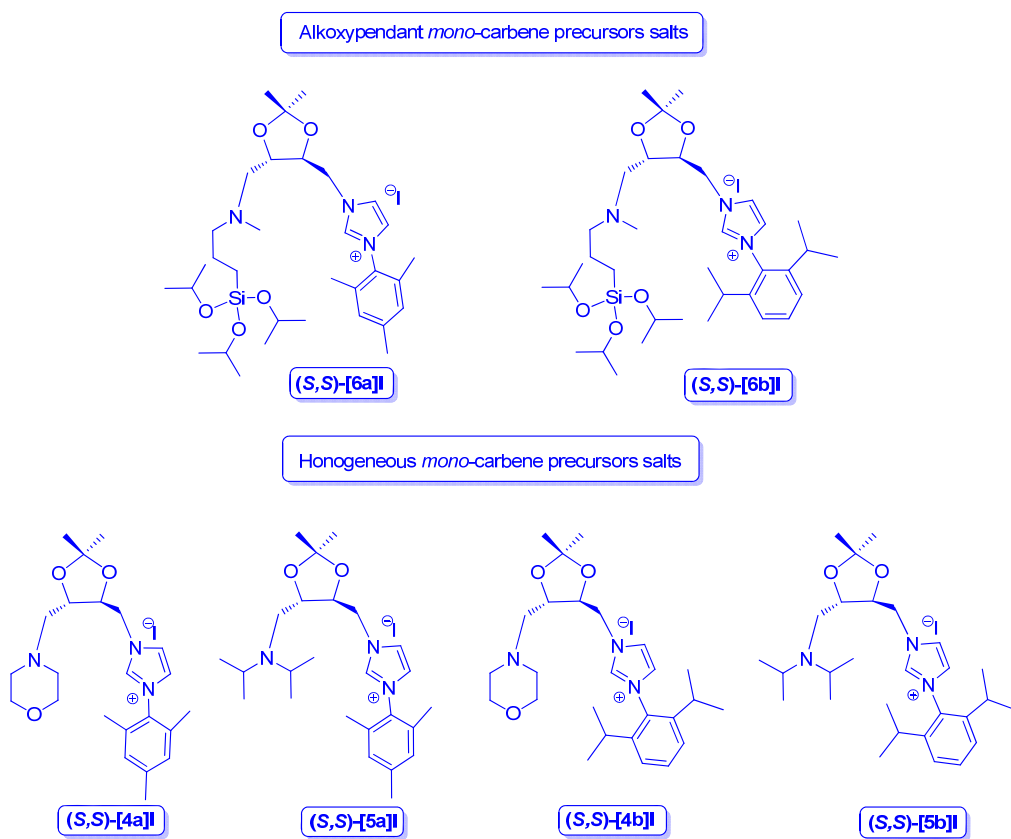


Figure. III. 22. *Mono*-carbene precursor salts.

3.2.2.a Synthesis of mono-*N*-heterocyclic carbene amine precursor salts. Reference systems for homogeneous catalysis.

We have synthesized (NHC)-dioxolane-amine precursors that could be used as ligands for Rh and Pd complexes as soluble reference models and study the influence of the substituents of the ligand (amines) in the catalytic activity.

We use amines such as morpholine or diisopropylamine which lead to the precursors **(*S,S*)-[4a]I**, **(*S,S*)-[4b]I** (morpholine) and **(*S,S*)-[5a]I**, **(*S,S*)-[5b]I** (diisopropyl amine) in excellent yields. (**Figure. III. 23**).

2 was heated with 1.1 equivalents of 1-arylimidazoles **1a** or **1b**. The *mono*-carbenes precursor salts **IN-4a** and **IN-4b** were isolated and purified by flash column chromatography with good yields and they were fully characterized. ¹H NMR presents the typically signal for CH imidazolium salts.

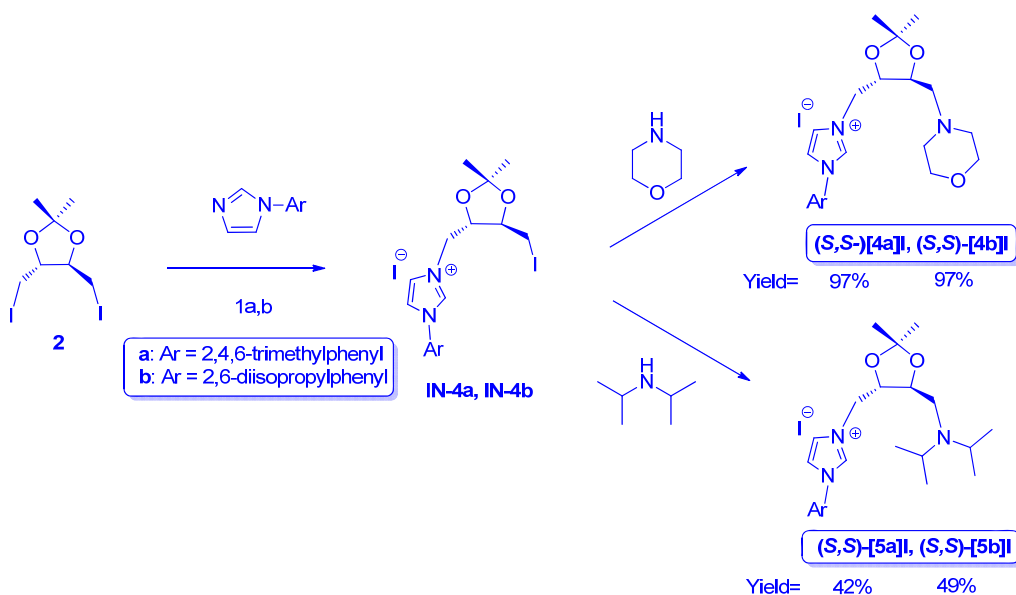


Figure. III. 23. Synthesis of soluble *mono*-NHC-amine ligands.

The two signals for the terminal methyl groups in dioxolane moiety are observed at 1.43 ppm and 1.45 ppm for **IN-4a** and 1.44 ppm and 1.46 ppm for **IN-4b**. This fact corroborates the asymmetry conferred on the molecule. The ES/MS is

according with the molecular ion of the salt with peaks at 441 (M^+ ; 100) for **IN-4a** and 483 (M^+ ; 100) for **IN-4b**.

The second step is a typically S_N2 nucleophilic substitution, but we must take into consideration several factors to obtain the desired product; the choice of amine, the auxiliary base and temperature. (**Figure. III. 24**).

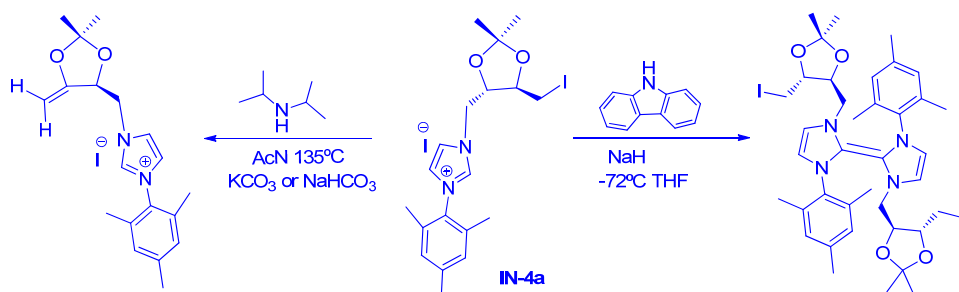


Figure. III. 24. Elimination and dimerization of **IN-4a**.

Treatment of the salts **IN-4a** and **IN-4b** with bases such as NaH leads the formation of free carbene species that reacts immediately with itself, forming a dimeric species. However, bases as K_2CO_3 or $NaHCO_3$ lead the elimination of iodine through $E2$ reaction affording the corresponding olefinic compounds, even at room temperature. Finally morpholine and diisopropylamine were suitable for the substitution reaction and useful for the formation of *mono*-NHC amine ligand precursors. These new ligand precursors have been synthesized by addition of excess corresponding amine to **IN-4a** or **IN-4b** in acetonitrile by microwave heating. (**Figure. III. 23**). These compounds were isolated as dark oils with good yields and totally characterized.

These compounds show similar signals to their starting products **IN-4a** and **IN-4b**. In morpholine derivatives, 1H NMR shows two signals corresponding to the two CH_2 adjacent to nitrogen in morpholine moiety and two CH_2 adjacent to oxygen that appears at 3.75 ppm and 2.71 ppm for **[4a]I** and 3.73 ppm and 2.71 ppm **[4b]I**.

Diisopropylamine compounds, show clearly the methyl groups corresponding of diisopropylamine moieties, as doublets, at 1.20 ppm and 1.11 ppm for **[5a]I** and

NHC's

1.33 ppm and 1.18 ppm for **[5a]I**. The imidazolium proton (N-CH=N) is located downfield for all compounds at 9.89 ppm (**[4a]I**) and 9.77 ppm (**[4b]I**) and 9.81 ppm (**[5a]I**) and 9.73 ppm (**[5b]I**).

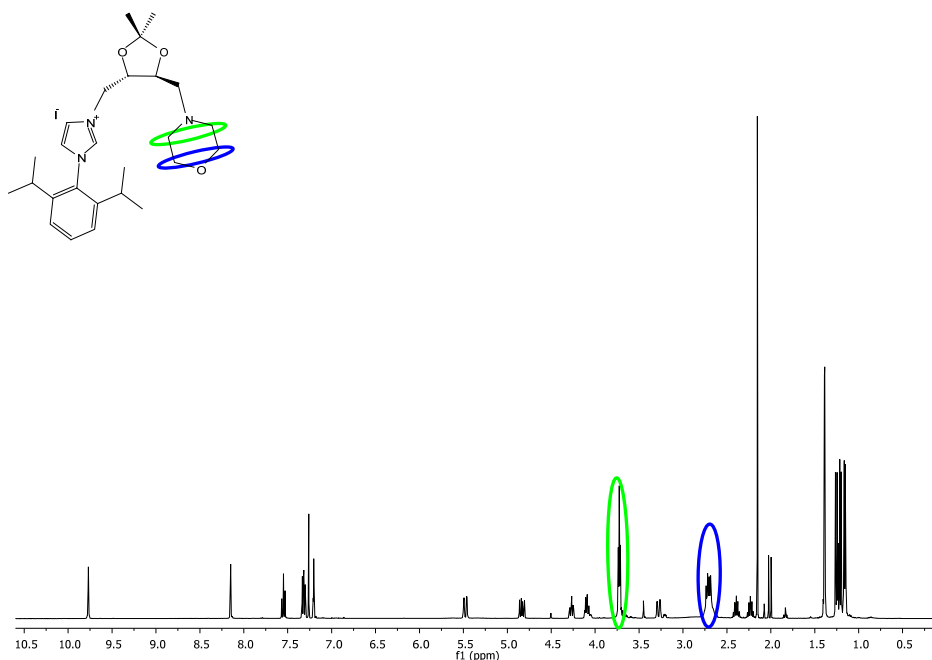


Figure. III. 25. ^1H NMR spectrum for (*S,S*)- **[4b]I**

In ^{13}C NMR spectrum the imidazolium carbon (N-CH=N) appears at 137.6 ppm (**[4a]I**) and (**[4b]I**) and 139.4 ppm (**[5a]I**) and 137.9 (**[5b]I**) and the ES/MS presents the molecular ion of the salt with peaks at 400 (M^+ ; 100) (**[4a]I**), 441 (M^+ ; 100) (**[4b]I**), 414 (M^+ ; 100) (**[5a]I**) and 456 (M^+ ; 100) for **[5b]I**.

3.2.2.b Synthesis of mono-*N*-heterocyclic carbene amine precursor salts with pendant alkoxy silane groups.

(*S,S*)-**[6a]I** and (*S,S*)-**[6b]I** were obtained by a similar method to that described for reference systems (*S,S*)-**[4a]I**, (*S,S*)-**[4b]I** and (*S,S*)-**[5a]I**, (*S,S*)-**[5b]I**.

IN-4a and **IN-4b** were heated in microwave reactor with excess of amine in acetonitrile to afford the functionalized salts (*S,S*)- **[6a]I**, (*S,S*)- **[6b]I** as light yellow

oils. It is important to note that the use of auxiliary bases in the last step give rise to a collection of olefinic products from the elimination reaction as described above. (**Figure. III. 26**).

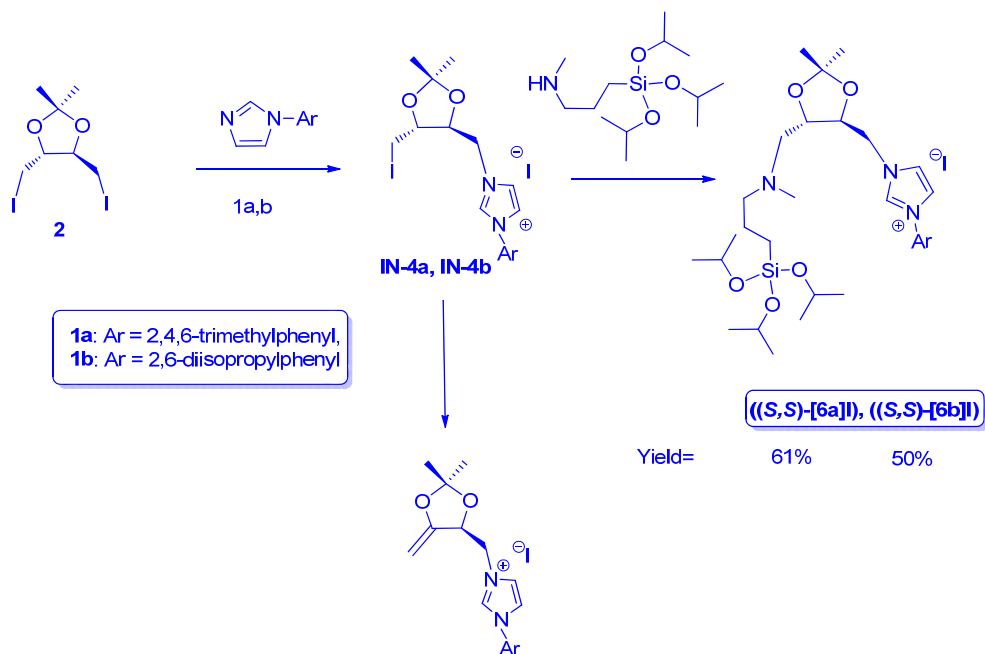


Figure. III. 26. Synthesis of *mono*-NHC amine precursors salts with pendant alkoxy silane groups.

Compounds containing pendant alkoxy silane groups were characterized after purification by flash chromatography. ^{13}C NMR spectrum, shows the imidazolium carbon (N-CH=N) that appears at 138.8 ppm ([**6a**]I) and 138.2 ppm ([**6b**]I). ^1H NMR shows (**Figure. III. 27**) typically signals from pendant alkoxy silane that appears at 0.59-0.54 ppm ($\text{CH}_2\text{-Si}$) as a characteristic multiplet. The two methyl from dioxolane backbone are differenced at 1.40 ppm and 1.37 ppm for [**6a**]I and 1.41 ppm and 1.36 ppm for ([**6b**]I) and the imidazolium proton appears at 9.87 ppm [**6a**]I and 9.88 ppm ([**6b**]I). The IR spectrum shows typical vibrations of Si-O and Si-C bonds at 1038 cm^{-1} (Si-O), 845 cm^{-1} (Si-O) and 762 cm^{-1} (Si-C) and ES/MS analyst presents M^+ ion in the two salts, 590 (M^+ ; 100) for [**6a**]I and 632 (M^+ ; 100) for [**6a**]I. All data confirm the proposed structure.

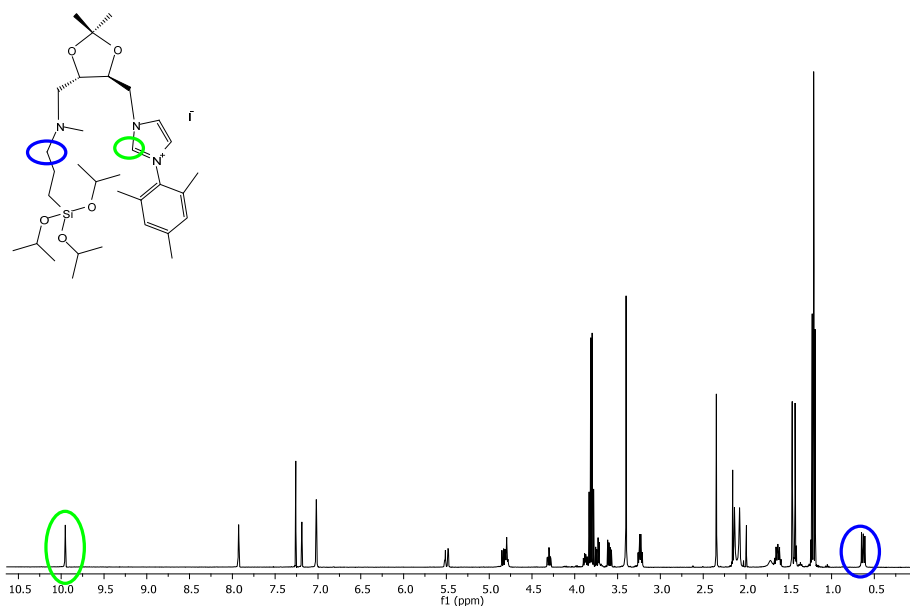


Figure. III. 27. ^1H NMR spectrum for (S,S) -[6a]I.

3.3 Synthesis of complexes.

3.3.1 Synthesis of bis-*N*-heterocyclic carbene complexes.

It is well known that silver (I)-oxide is suitable metal salt for the synthesis of the silver carbene complexes. Treatment of the imidazolium iodide salts ((S,S) -[3a]I, (S,S) -[3b]I) with Ag_2O yielded the silver complexes (S,S) -3a,3bAg. The formation of the carbene complexes 3a,3bAg was established by a peak below at 174 ppm in the ^{13}C NMR spectra which was assigned to the C-imidazol-2-ylidene (carbene) carbon, and by the absence of the downfield peak for the 2*H*-imidazolium proton in the ^1H NMR spectra (below 9.7 ppm).

As Ag-NHC bonds are quite weak⁴⁶ the silver complexes could then be used as carbene transfer reagents to gold, palladium and rhodium according to Lin et al⁴⁷ as

[46]a) C. Boehme, G. Frenking, *Organometallics*, **1998**, 17, 5801; b) D. Nemcsok, K. Wichmann, G. Frenking, *Organometallics*, **2004**, 23, 3640.

discussed previously. The reaction of the silver complexes with $\text{AuCl}(\text{tht})$ (tht = tetrahydrothiophene), $[\text{RhCl}(\text{cod})]_2$, $[\text{PdCl}_2(\text{cod})]$ (cod = 2,5-cyclooctadiene) and $\text{K}[\text{AuCl}_4]$ yielded the respective complexes (*S,S*)-**3aAu(I)**, **3bAu(I)**, **3aRh**, **3aPd**, **3aAu(III)** (Figure. III. 28) with good yield, along with the formation of AgI precipitate.

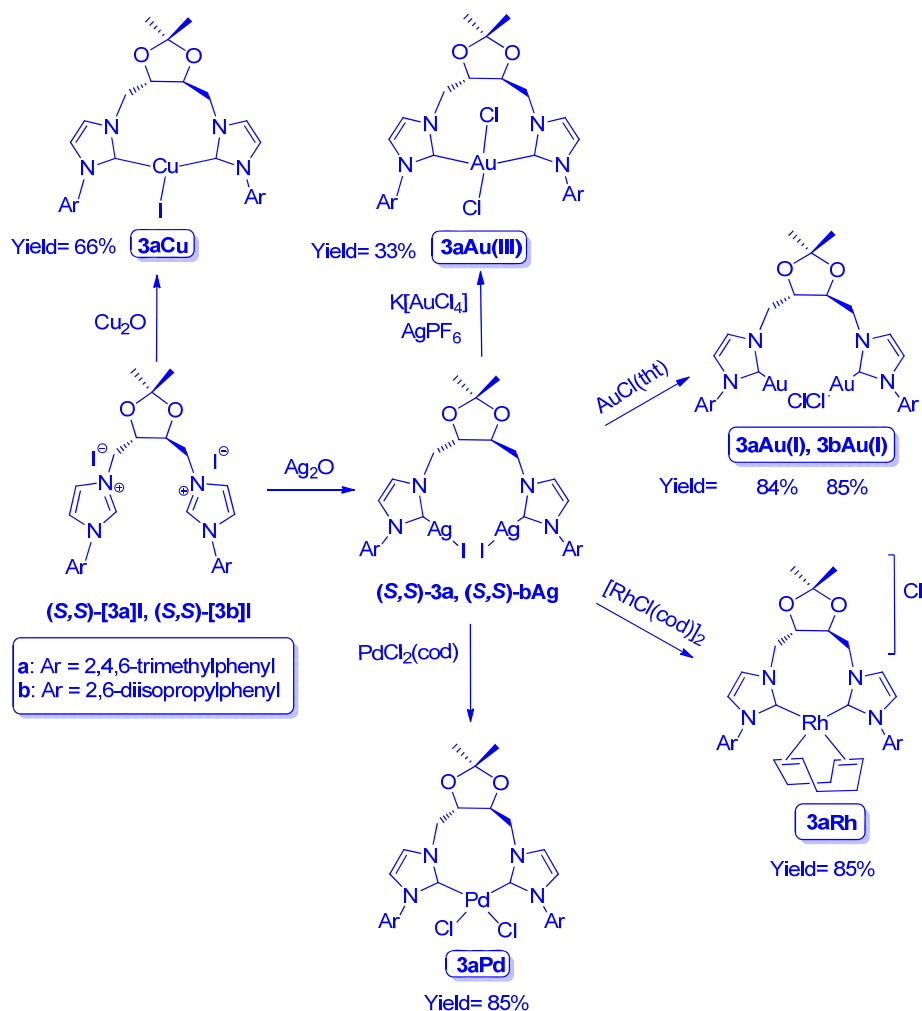


Figure. III. 28. Synthesis of soluble *bis*-NHC-complexes.

[47] a) H. M. J. Wang, I. J. B. Lin, *Organometallics*, **1998**, 17, 972; b) I. J. B. Lin, C. S. Vasam, *Coord. Chem. Rev.*, **2007**, 251, 642; c) J. C. Y. Lin, R. T. W. Huang, C. S. Lee, A. Bhattacharyya, W. S. Hwang, I. J. B. Lin, *Chem. Rev.*, **2009**, 109, 3561.

ESI spectrum for **3aAu(I)** shows a peak at $m/z=927$ which corresponds to the loss of one chloride, $m/z=1011$ for **3bAu(I)**. FT IR spectrum show a medium band at 328 cm^{-1} for **3aAu(I)** and 331 cm^{-1} for **3bAu(I)** assigned to the $\nu(\text{Au-Cl})$ vibration. ^{13}C NMR spectra show all resonances shifted as compared to the uncoordinated ligand with the diagnostic gold-bound (NCN-Au) peak at 177.1 ppm (**3aAu(I)**) or 173.9 ppm (**3bAu(I)**).

^1H NMR spectrum of **3aAu(I)** suggests a high symmetry within the molecule but, if we analyze deeply its configuration through semi-empirical molecular modeling programs, minimizing their energy by MM2, we could see that the two heterocyclic salts moieties are in *anti*-position facing each other. It is also noted as the two heterocycles are not parallel with respect to each other; they are perpendicular as we can see in **Figure. III. 29**. The catalyst has a helicoidally conformation that makes this complex director of chirality.

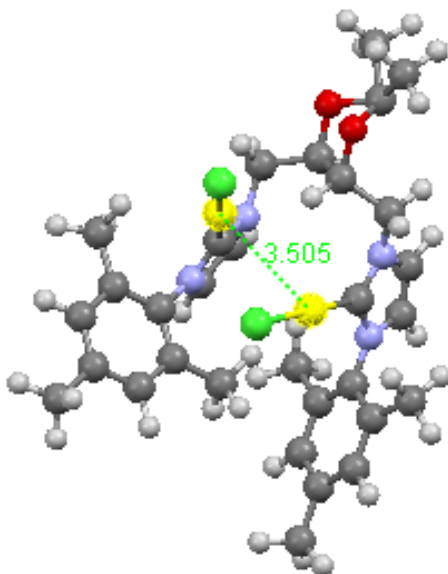


Figure. III. 29. Modelization of (*S,S*)- **3aAu(I)** empiric approximation.

Another fact that deserves mention is that the model suggests aurophilicity in **3aAu(I)** between the two gold atoms, because the calculate distance (3.5 Å) is shorter

than the sum of two van der Waals radii (3.7 Å). Similar effect has been reported for diphosphine ether bridged gold (I) complexes.⁴⁸

[RhCl(cod)(**3a**)] (**3aRh**) shows the ¹H NMR spectrum of the signals due to the cod protons significantly broadened due to fluxionality of the complex. The mesityl rings undergo restricted rotation about the N–C bond as evidenced by the presence of two distinct resonances in the ¹H NMR spectrum for each of the *o*-methyl groups and *m*-protons on the mesityl ring. In ¹³C NMR (NCN-Rh) signal appears at 179.8 ppm. The monomolecular structure is confirmed by the intense MS molecular peak 745 (M⁺) in ESI analysis.

The ¹H NMR spectrum of [PdCl₂(**3a**)] (**3aPd**) shows one set of signal corresponding a symmetric species. In the ¹³C NMR spectrum NCN-Pd signal appears at 175.0 ppm, which is comparable to the chemical shift observed in other *trans*-[PdCl₂(*bis*(NHC))] complexes.⁴⁹ IR spectrum shows a band at 578 cm⁻¹ corresponding to Pd-C vibration and ESI show the molecular peak *m/z*= 677 (M⁺) and the loss of two chlorides *m/z*= 605 (M⁺-2Cl).

The ESI spectrum for **3aAu(III)** shows a peak at *m/z*= 731 which corresponds to the loss of one chloride. ¹³C NMR spectra show all resonances shifted as compared to the uncoordinated ligand with the diagnostic gold-bound (NCN-Au) peak at 173.1 ppm. IR spectrum shows a strong band at 848 cm⁻¹ corresponding to ν(P-F) vibration.

3aCu for comparative proposes in multi-component reaction have been synthesized by reaction with Cu₂O through microwave heating. ¹³C NMR spectra show all resonances shifted as compared to the uncoordinated ligand with the diagnostic Cu-bound (NCN-Au) peak at 182.7 ppm and MALDI show the molecular peak *m/z*= 687 (M⁺).

In general, cationic complexes were generated by halide abstraction via addition of AgPF₆ to a CH₂Cl₂/water solution of (*S,S*)-**3aAu(I)**, **3bAu(I)**, **3aRh**, **3aPd**).

[48] D. V. Partyka, J. B. Updegraff III, M. Zeller, A. D. Hunter, T. G. Gray, *Dalton Trans.*, **2010**, 39, 5388–5397.

[49] a) I. Dinares, C. García de Miguel, M. Font-Bardia, X. Solans, E. Alcalde, *Organometallics*, **2007**, 26, 5125; b) J. Houghton, G. Dyson, R. E. Douthwaite, A. C. Whitwood, B. M. Kariuki, *Dalton Trans.*, **2007**, 28, 3065; c) F. Hannig, G. Kehr, R. Frohlich, G. Erker, *J. Organomet. Chem.*, **2005**, 690, 5959; d) B. P. Morgan, G. A. Galdamez, R. J. Gilliard Jr., R. C. Smith, *Dalton Trans.*, **2009**, 11, 2020.

3.3.2 Synthesis of mono-*N*-heterocyclic amine carbene complexes.

3.3.2.a Synthesis of Rh and Pd mono-*N*-heterocyclic amine complexes. Reference systems for homogeneous catalysis.

The Ag-transmetallation route used to obtain the *bis*-NHC complexes failed to attempt the synthesis of *mono*-NHC amine complexes with morpholine or diisopropylamine substituents. This discrepancy can be explained, in the case of morpholine, by the lower basicity of the amine, but when the amine is very basic as occurs with diisopropylamine, the inhibition of complex formation can be attributed more properly to steric considerations.

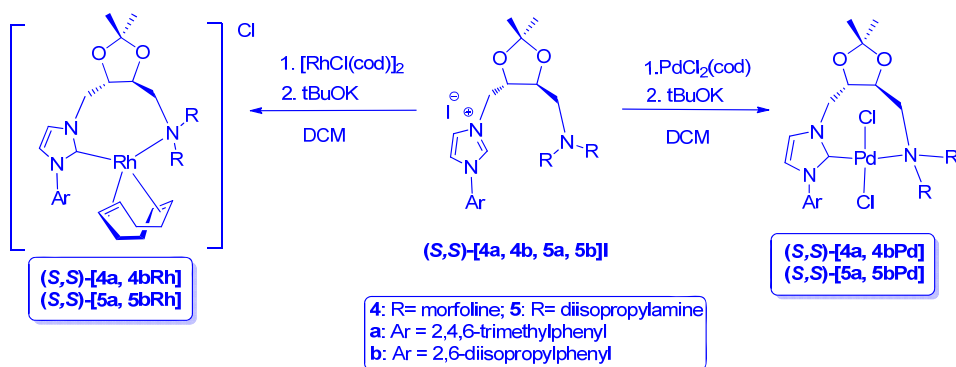


Figure. III. 30. Synthesis of soluble *mono*-NHC-complexes.

Rhodium (I) and palladium (II) NHC-complexes were obtained directly from the corresponding metal precursor ($[\text{RhCl}(\text{cod})]_2$, $\text{PdCl}(\text{cod})_2$) and subsequent deprotonation of the imidazolium salt in the presence of a strong base (KO^tBu). (**Figure. III. 30**). It was not possible to isolate the complexes as pure products and they were used in subsequent reactions as obtained from the reaction mixture. Only **6aRh** has been isolated and fully characterized and data can be seen in the experimental section. NMR spectroscopy shows the signals consistent with a single diastereoisomer including a signal at 168.0 ppm in the ^{13}C NMR spectrum assigned to the rhodium carbene atom and four other rhodium-coupled doublets assigned to the coordinating cod carbon atoms.

The analogous gold(I) complexes were unstable in solution and decompose to gold(0) when we tried to apply as catalysts.

3.3.2.b Synthesis of mono-*N*-heterocyclic carbene amine complexes with pendant alkoxy silane groups.

The abilities of the *N*-methyl-3-(triisopropoxysilyl)propan-1-amine-NHC's-substituted dioxolane ((*S,S*)-[**6a**]**I** and (*S,S*)-[**6b**]**I**) to act as bidentate chelate ligands were demonstrated by the preparation of silver, gold (I), palladium (II) and rhodium (I) complexes. (**Figure. III. 31**)

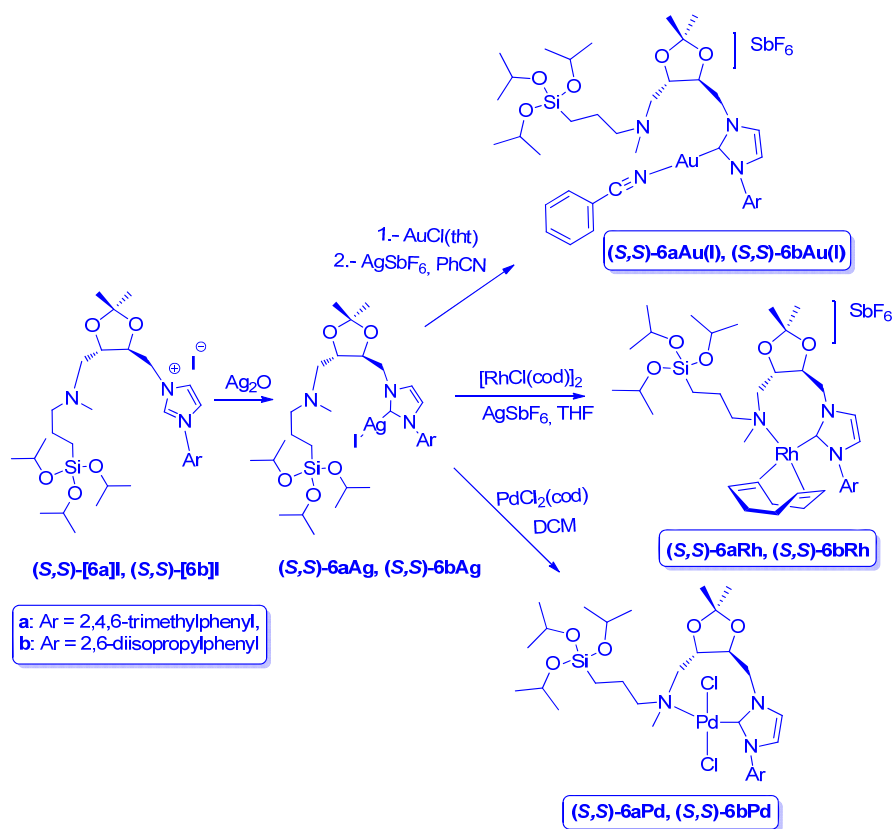


Figure. III. 31. Synthesis *Mono*-NHC amine complexes with pendant alkoxy silane groups.

The treatment of the imidazolium iodide salts (*S,S*)-[**6a**]**I** and (*S,S*)-[**6b**]**I** with Ag_2O yielded the silver complexes **6a**, **6bAg**. The formation of the carbene complexes

6a,6bAg is consistent with peak below 174 ppm in the ^{13}C NMR spectra which was assigned to the *C*-imidazol-2-ylidene (carbene) carbon, and by the absence of the downfield peak for the *H*-imidazolium proton in the ^1H NMR spectra (below 9.8 ppm).

Silver complexes Ag-NHC bonds are quite weak⁴⁶ and could be used as carbene transfer reagents to gold, palladium and rhodium according to Lin et al.⁴⁷

The reaction of the silver complexes with a solution of AgSbF_6 and $\text{AuCl}(\text{tht})$ (tht= tetrahydrothiophene) or $[\text{RhCl}(\text{cod})]_2$ (cationic complexes) or $[\text{PdCl}_2(\text{cod})]$ (cod= 2,5-cyclooctadiene) yielded the respective complexes (*S,S*)-[**6a,6bAu(I)**, **6a,6bRh**, **6a,6bPd**] (Figure. III. 31) in >80% yield along with the formation of AgI precipitate that is removed by filtration over Celite ®. Gold (I) complexes should be obtained in benzonitrile as solvent, leading to stable species that have a benzonitrile molecule as co-ligand. All new complexes were fully characterized after isolation by precipitation with pentane and ethyl ether.

^{13}C NMR spectra for gold (I) species **6aAu(I)** and **6bAu(I)** show all resonances shifted as compared to the respective uncoordinated ligand precursors and the diagnostic gold-bound (NCN-Au) peak at 182.5 ppm (**6a(I)Au**) and 179.2 ppm for (**6b(I)Au**) and signals for the coordinating benzonitrile.

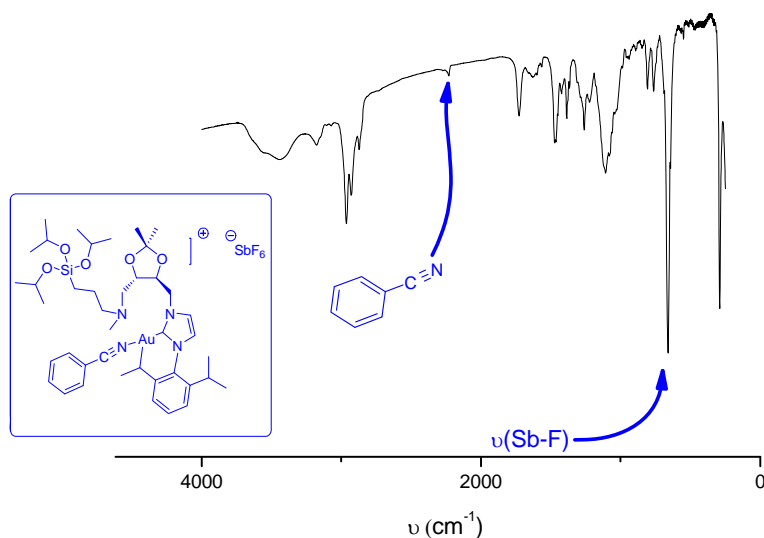


Figure. III. 32. IR spectrum of (*S,S*)-**6bAu(I)**.

The ESI/MS spectrum for **6aAu(I)** shows a peak at $m/z = 786$ which corresponds to the loss of benzonitrile and SbF_6 and $m/z = 949$ for **6bAu(I)** which corresponds to the loss benzonitrile and fluorine. FT IR spectra for the two complexes show a strong band at 655 cm^{-1} assigned to the $\nu(\text{Sb-F})$ vibration a band at 2244 cm^{-1} assigned to the $\nu(\text{CN})$ vibration (benzonitrile).

Palladium (II) complexes show in their ^1H NMR spectrum formation of one signal set consistent with a single diastereoisomer.

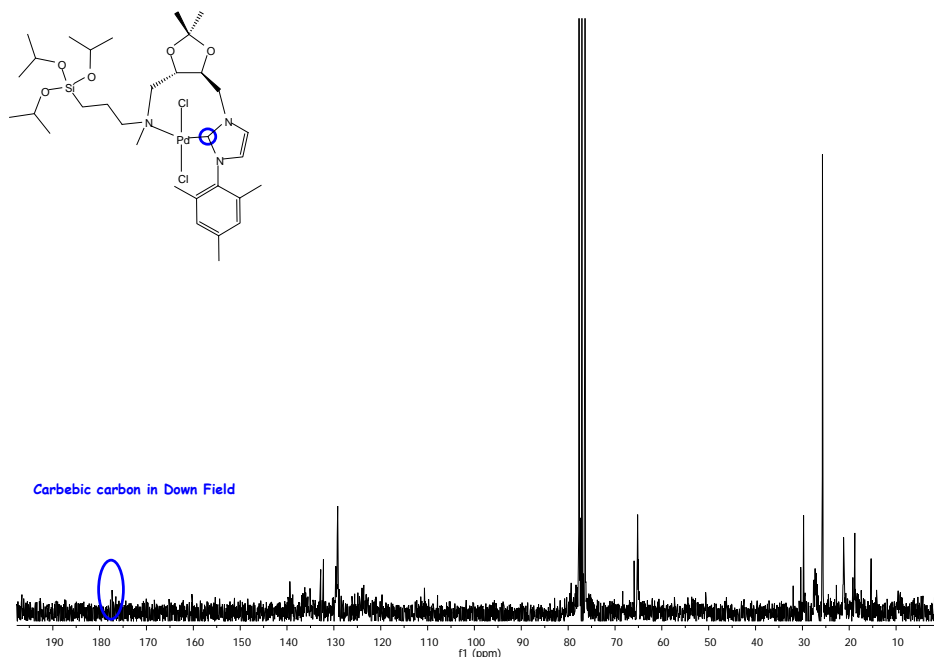


Figure. III. 33. ^{13}C NMR spectrum for (*S,S*)-**6aPd**.

Formation of the carbene complexes **6aPd** and **6bPd** is indicated by a carbene signal at 177.3 ppm and 176.2 ppm respectively, in ^{13}C NMR spectrum, which is a typical value for imidazolinylidene palladium complexes and is shifted more than 20 ppm high field compared to the signal of the silver carbene complex and which is comparable to the chemical shift observed in other $\text{PdCl}_2(\text{NHC})$ complexes.⁴⁹ The mass spectra confirm formation of the mononuclear complex with peaks for **6aPd** at $m/z = 768$ (M^+) and 590 (L) and $m/z = 810$ ($\text{M}^+ + 1$) and 633 ($\text{M}^+ - 3\text{O}^i\text{Pr}$) for **6bPd**.

^1H NMR spectrum for rhodium (I) complexes, **6aRh** and **6bRh** show the resonance due to the cod protons significantly broadened due to fluxionality of the complex, the NCNRh signal at 187.8 ppm (**6aRh**) and 193.2 ppm (**6bRh**). The ESI spectra for **6aRh** shows a peak in $m/z = 674$ according with the hydrolysis of three isopropoxy moieties in the cationic species and $m/z = 878$ for **6bRh** that corresponds with the loss of two fluorine and the hydrolysis of OⁱPr groups of the silyloxy group. All data is according with the proposed structures.

3.4 Heterogeneization of complexes containing pendant alkoxy silane groups to MCM-41.

The most important target in our project is to support the functionalized alkoxy silane complexes on inorganic materials as MCM-41, following a standard method developed in our laboratory. Our method consists of the grafting of a spacer, on the walls of the MCM material. (**Figure. III. 34**).

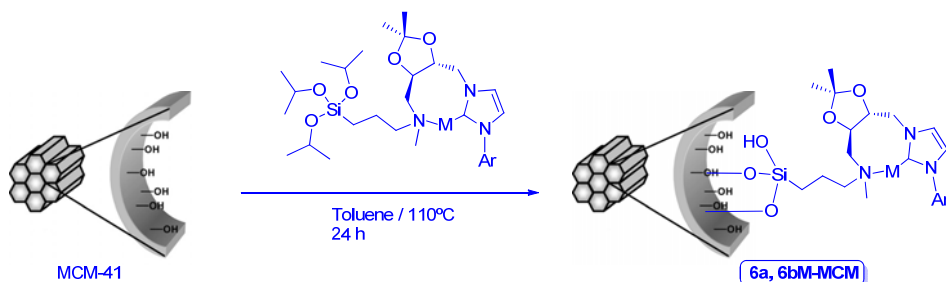


Figure. III. 34. Heterogeneization of *mono*-NHC amine complexes in MCM-41.

MCM-41 is a short-range amorphous material that contains a large number of silanol groups available for grafting; however, it presents a long-range ordering of hexagonal symmetry with regular, monodirectional channels of 3.5 nm diameter (Brunauer–Emmett–Teller (BET) surface area 1030 m²g⁻¹, micropore surface (*t*-plot) 0 m²g⁻¹, external (or mesoporous) surface area 1030 m²g⁻¹).

The complexes (*S,S*)-[**6a,6bAu**, **6a,6bRh**, **6a,6bPd**] were used for the preparation of a new family of materials based on mesoporous MCM-41. The silyloxi-complexes were supported on MCM-41 by addition of the corresponding solution on a

dispersion of MCM-41 in toluene and heating for 24 h to afford the materials **6a**, **6bM-MCM** with metal loadings of 0.4, 0.1 and 1.6 wt% Pd, Rh, Au(I), corresponding to 3.8×10^{-2} , 0.97×10^{-2} and $8.1 \times 10^{-2} \text{ mmol g}^{-1}$, respectively. As can be noted the amount of rhodium complex (the value given corresponds to an average of three experiments) that is immobilized on the support is lower than that achieved with the complexes of palladium and gold, this can only be attributed to increased steric hindrance of the rhodium complex.

In order to obtain gold (III) supported catalysts, oxidation of **6aAu(I)-MCM** was carried out in benzonitrile with phenyliodine (III) dichloride as oxidant reagent, following a recently method reported by Nolan et al.⁵⁰ Thus, after reaction was finished the resulting solid was filtered, washed and dried, affording the white powder solid **6aAu(III)-MCM**.

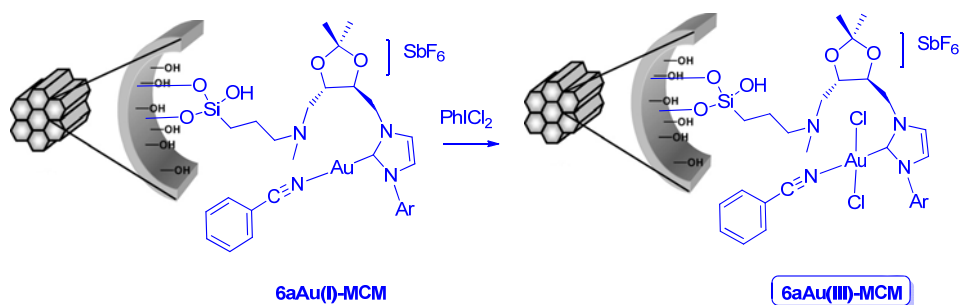


Figure. III. 35. Synthesis of **6aAu(III)-MCM**.

The resulting solids were characterized by FT-IR, Uv-Vis, DFTR and solid state CP MAS ^{13}C NMR and compared with their counterpart before heterogeneization.

[50] S. Gaillard, A. M. Z. Slawin, A. T. Bonura, E. D. Stevens, S. P. Nolan, *Organometallics*, **2010**, 29, 394 – 402.

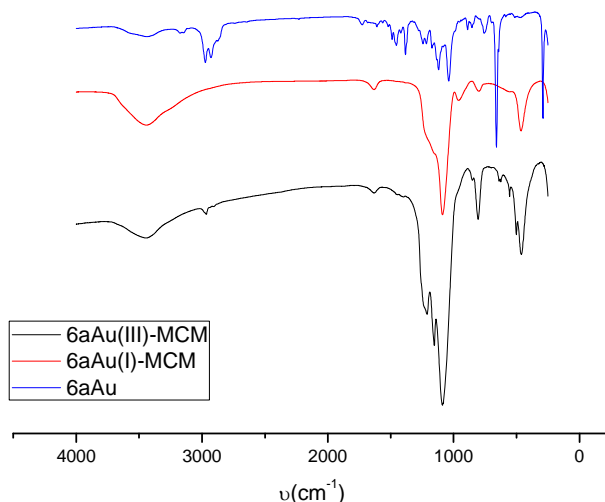


Figure. III. 36. IR spectra of **6a(I)Au** before and after heterogeneization (**6aAu(I)-MCM** and **6aAu(III)-MCM**).

The presence of functional groups characteristic of [complex] propyltriisopropoxysilane in the materials was checked by FT IR spectroscopy. The stretching vibrations modes of the mesoporous framework (Si–O–Si) of the grafted materials are observed at around 1240, 1070, and 810 cm^{-1} . The introduction of the complexes **6aM** and **6bM** in the stepwise pathway leads to the appearance of the ν (C=N) and ν (C=C) stretching modes at 1636 (**6aAu(I)-MCM**) and 1632 cm^{-1} for (**6bAu(I)-MCM**) as a broad signals.

The materials were also characterized by ^{13}C CP MAS solid state NMR. The solid state ^{13}C CP MAS NMR spectra of **6a**, **6bPd-MCM**, **6bRh-MCM** and **6a**, **6bAu-MCM** materials are quite similar, since the spectra are dominated by the resonances of the aliphatic and aromatic groups. These signals appear at ca. 9.5 (Si–CH₂), 18.1 (CH₂–CH₂–CH₂), and 58.5 (NCH₂) ppm for **6aPd-MCM**.

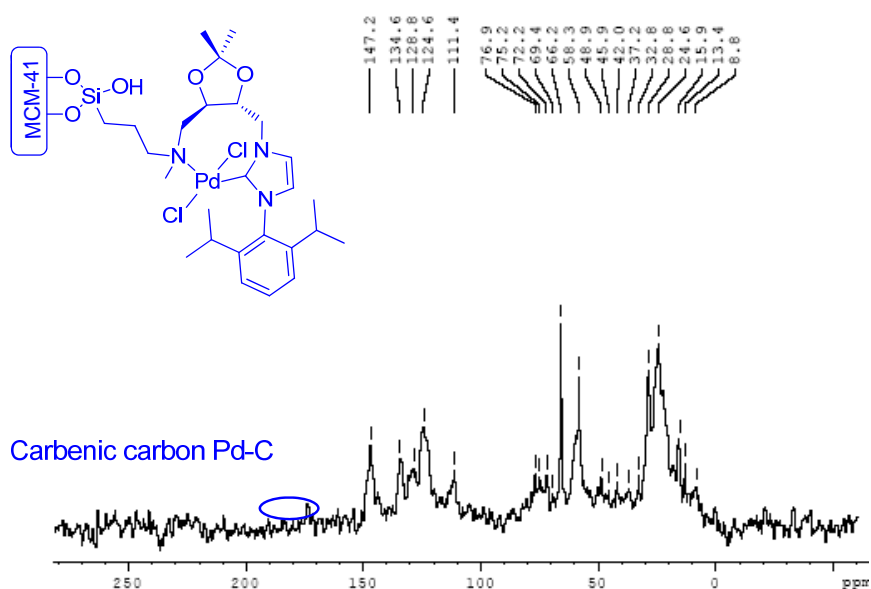


Figure. III. 37. ^{13}C CP MAS solid state NMR of **6bPd-MCM**.

In fact the metal content is small and therefore since the spectra are dominated by the aliphatic and aromatic signals it will mask any resonances from other species in lower concentration. A similar effect has already been described previously. The peaks assigned to the SiO^iPr groups appear at 24.8 (CH_3) and 61.4 (OCH) ppm. A characteristic signal at 175 ppm is observed in the ^{13}C NMR spectrum for the carbene carbon atom in **6bPd-MCM**. (**Figure. III. 37**)

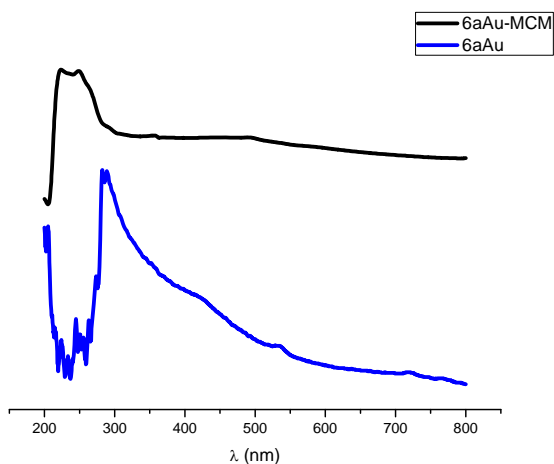


Figure. III. 38. Uv-Vis and DFTR spectrum (S,S) -**6aAu(I)** before and after heterogeneization.

Uv-Vis and DFTR spectra is similar before and after heterogeneization and shows bands at 536, 420, 282 and 273 nm in (S,S) -**6aAu(I)** and 493, 357, 290, 248, 223 nm in **6aAu(I)-MCM**.

3.5 Catalytic activity.

Once all the catalysts were synthesized and characterized both soluble and heterogenized type carbene complexes were tested as catalysts in enantioselective hydrogenation of prochiral substrates in order to study the effect of ligand, metal center, support and substrate on the catalytic activity.

Heterogenized catalysts were recovered and recycled to prove their value as a reusable catalyst.

3.5.1 *Asymmetric hydrogenation of pro-chiral alkenes.*

As we have seen in Chapter I asymmetric hydrogenation is very important in modern organic chemistry and is one of the key steps in many processes for obtaining products in large scale manufacturing and fine chemicals.

Normally in these processes rhodium, iridium and ruthenium have been used as catalysts, these metals have a high economic cost, so this project has tried to obtain competitive results with other metals such as palladium and gold (having smart prices), or rhodium itself but having the advantage to be reused maintaining the activity and enantioselectivity as first cycle.

The rhodium and iridium catalyzed hydrogenation has been extensively studied and some examples of asymmetric induction has been reported.⁵¹ The accepted mechanism can be seen in **Figure. III. 39.**

[51] D. Baskakov, W. A. Herrmann, E. Herdtweck and S. D. Hoffmann, *Organometallics*, **2007**, *26*, 626.

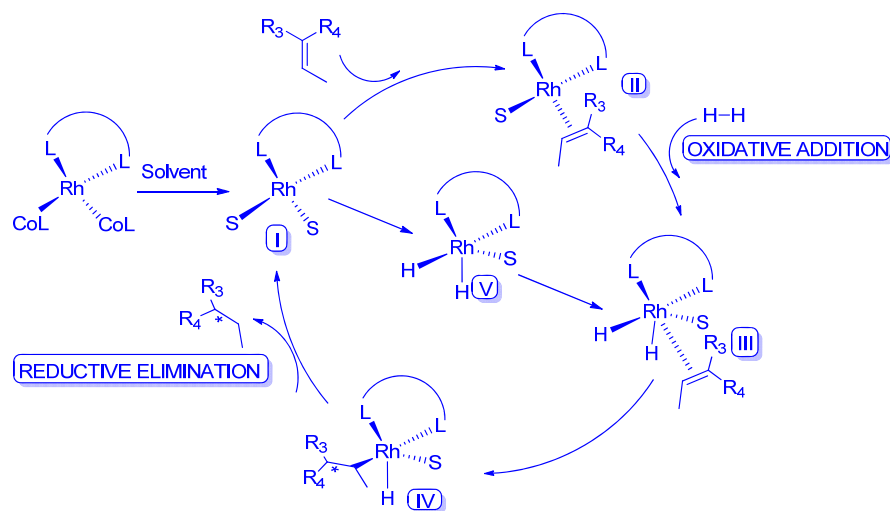


Figure. III. 39. Rhodium and iridium hydrogenation mechanism.

In first step, the active species (I) is formed by substitution of co-ligands for solvent molecules. Then, alkene coordination (II) and oxidative hydrogen addition affords the octahedral species (III) (in this step the rhodium (I) was oxidized to Rh (III)), normally this process is rate-determining step. The next step is the migration of hydride leading the ethyl group and through reductive elimination releases the desired hydrogenated product recovering the active species Rh (I).

Alternatively, the oxidative addition of hydrogen could take place on the initial complex (I) to conduct (V). This route, known as the hydride route, takes place when the oxidative addition of hydrogen is faster than the olefin coordination.

The accumulated evidence concerning the mechanisms of homogeneous catalyzed hydrogenation indicates that three principal modes of hydrogen activation are suitable: oxidative addition (Rh (I) complexes), and homolytic or heterolytic hydrogen cleavage. For Pd (II) and Au (I) complexes, heterolytic cleavage is preferred to give a hydride intermediate which involve charge separation without any oxidation of the metal. Heterolytic cleavage of hydrogen by Pd and Au complexes have been reinforced from our group experiments with more polar and protonic acid media which produces a

significant increase of reaction rate, probably favoring charge separation in the step of formation of intermediate.⁵²

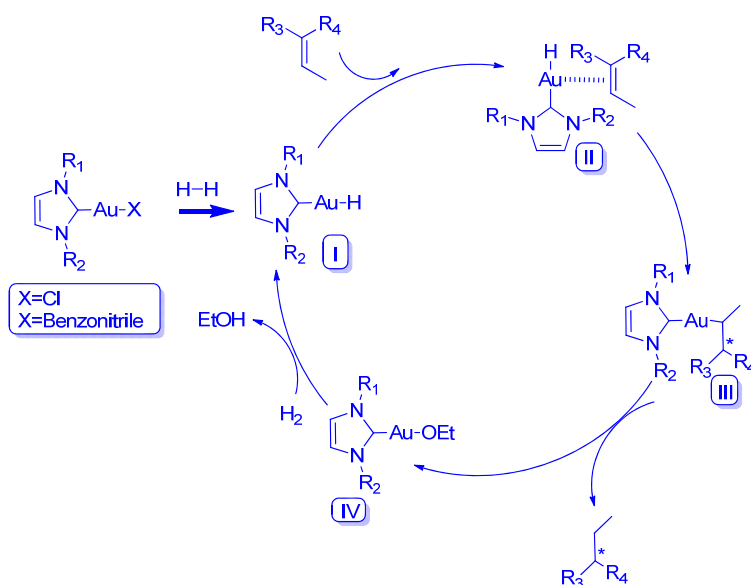


Figure. III. 40. Gold (I) tentative hydrogenation mechanism.

Then, the reaction could start (**Figure. III. 40**) by the addition of H₂ to the catalyst, to give a hydride complex, (I), that involves a hydride ion transfer to the gold, releasing a proton. In the second step, the alkene forms a π -complex (II), with the gold and simultaneous hydride ion transfer from gold to alkene occurs (III). The last step involves the transfer of a proton to the substrate, leading to the separation of the hydrogenated product and the regeneration of the catalyst.

The problem in (NHC)M-catalyzed hydrogenation is the tendency for NHC reductive elimination to the imidazolium salt [NHC-H]⁺. *Bis*-NHC ligands are expected to be resilient to reductive elimination and the efficiency of gold(I)-, palladium- and rhodium-complexes as catalysts for the asymmetric hydrogenation of different alkenes (diethyl itaconate, (*E*)-diethyl 2-benzylidenesuccinate, (*E*)-diethyl 2-

[52] a) A. Comas-Vives, C. González-Arellano, A. Corma, M. Iglesias, F. Sánchez, G. Ujaque, *J. Am. Chem. Soc.*, **2006**, 128, 4756; b) A. Comas-Vives, C. González-Arellano, M. Boronat, A. Corma, M. Iglesias, F. Sánchez, G. Ujaque, *J. Catal.*, **2008**, 254, 226.

methylenesuccinate and (*E*)-diethyl 2-(naphthalen-1-ylmethylene) succinate) was investigated. (Table. III. 1, Table. III. 2, Table. III. 3, Table. III. 4).

3.5.1.a Phosphine versus carbene. Metal and substrate influence.

In order to probe the efficiency of carbene complexes about tertiary phosphines in the same system, we obtained the rhodium (I), palladium (II) and gold (I) complexes with the diphosphine (*R,R*)-DIOP as ligand ((*R,R*)-DIOP= (4*R*,5*R*)-4,5-bis (diphenylphosphino methyl)-2,2-dimethyldioxolane) which have the same backbone as dioxolane NHC's ligands.

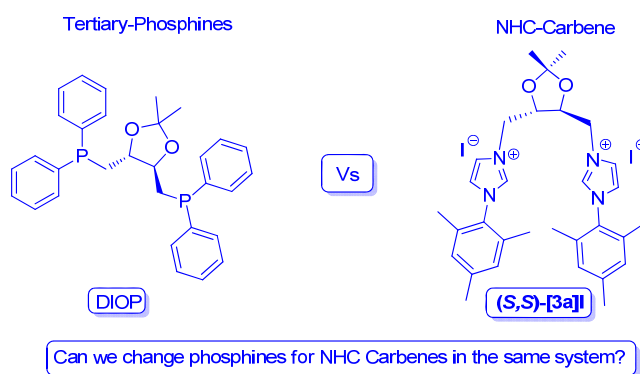


Figure. III. 41. Phosphines versus carbenes.

These complexes of palladium, rhodium and gold were tested as catalyst for the hydrogenation of 2*R*-succinates. Experiments were carried out in an Autoclave Engineers with gentle stirring to ensure that the diffusion is not involved in reaction rates. Hydrogenations were carried out in standard conditions that allow us an effective comparison between catalysts.

The turnover frequency values (**TOF**) were calculated as the reaction rate per active site, namely, the number of substrate molecules that one catalyst molecule can convert into desired product in one second, minute or hour. This value can be expressed by the following equation:

$$TOF = \frac{\text{conversion}(\%) \times (\text{mmol})_{\text{substrate}}}{(\text{mmol})_{\text{catalyst}} \times t}$$

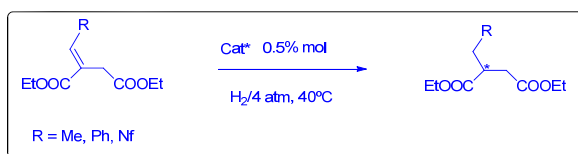


Table. III. 1. Hydrogenation of (*E*)-diethyl 2-*R*-succinates with soluble *bis*-NHC and diphospine catalysts.^{a,b}

Entry	Catalyst	R	TOF ^b	ee % ^c
1	3aRh	methylene	258	10 (<i>S</i>)
2		benzylidene	16	99 (<i>S</i>)
3		naphthylmethylene ^d	10	>95 (<i>S</i>)
4	DiopRh	methylene	579	20 (<i>S</i>)
5		benzylidene	28	99 (<i>S</i>)
6	3aPd	methylene	45	5 (<i>S</i>)
7		benzylidene	17	98 (<i>S</i>)
8		naphthylmethylene ^d	2	>95 (<i>S</i>)
9	DiopPd	methylene	119	11 (<i>S</i>)
10		benzylidene	35	97 (<i>S</i>)
11	3aAu(I)	methylene	2000	15 (<i>S</i>)
12		benzylidene	1250	90 (<i>S</i>)
13		naphthylmethylene ^d	150	95 (<i>S</i>)
14	3bAu(I)	methylene	210	25 (<i>S</i>)
15		benzylidene	50	85 (<i>S</i>)
16		naphthylmethylene ^d	5	90 (<i>S</i>)
17	3a(OPNB)Au(I)	methylene	120	25 (<i>S</i>)
18		benzylidene	15	90 (<i>S</i>)
19		naphthylmethylene ^d	0,5	93 (<i>S</i>)
20	DiopAu(I)	benzylidene	45	98 (<i>S</i>)
21	DuphosAu(I)	benzylidene	906	80 (<i>S</i>) ⁵³

^aEthanol, 4 atm. H₂, 40 °C, Cat.: 0.5 mol%; ^bTOF: h⁻¹ (calculated at maximum rate); ^cHPLC (chiralcel AD-H, λ: 230 nm, Hexane/iPrOH: 98/2, chiralcel OD, λ: 250 nm, Hexane/iPrOH: 95/5); ^d60 °C, 4 atm. H₂.

All NHC's and DIOP complexes showed significant activities (**Table. III. 1**) in the hydrogenation of 2*R*-succinates (diethyl citraconate, (*E*)-diethyl 2-benzylidenesuccinate and (*E*)-diethyl 2-(naphthalen-2-ylmethylene)succinate). Up to 99% ee was obtained with the rhodium *bis*-carbene catalyst for (*E*)-diethyl 2-benzylidenesuccinate. Palladium and gold (I) *bis*-carbene complexes yielded also good

enantioselectivity, being in all cases greater than 97% ee for the same substrate. (**Table. III. 1**, entries 2, 7 and 12).

The reactivity is slightly higher with the diphosphine Rh-complex however the enantioselectivity was similar in the case of succinates with greater steric hindrance. In succinates with low steric hindrance the enantioselectivity undergoes a sharp decline.

The palladium complex $[\text{Pd}(\text{cod})(\text{Diop})]^{2+}$ decomposes in the reaction medium and the cationic gold complex $([\text{Au}(\text{benzonitrile})]_2(R,R)\text{-Diop})$ gives a similar reactivity and enantioselectivity than the corresponding derivative *bis*(NHC)-complex (**3aAu(I)**).

These results for gold (I) *bis*-(NHC)-complex (**3aAu(I)**) are similar to that obtained when freshly prepared $[(\text{AuCl})_2((R,R)\text{-Me-Duphos})]^{53}$ was the catalyst with the difference, that (**3aAu(I)**) complex is stable for at least 3 months and is easier to synthesize and manipulate.

As it can be shown in (**Table. III. 1**, entries 14, 15, 16) the complex **3bAu(I)** which contain a 2,6-diisopropylphenyl on the NHC donor had much slower reaction rates. These results indicate that the bulky substituents severely limit the activity of the catalysts. This effect is most probably due to the inhibition of substrate coordination due to steric interaction with the bulky isopropyl substituent. Dramatic decrease of reactivity was also founded when the chlorine was substituted by OPNB (4-nitrobenzoate), $[\text{Au}(\text{OPNB})]_2((S,S)\text{-3a})$ probably due to increased steric hindrance.

To extend the scope of the complexes as catalysts we have used (*Z*)- α -ethyl benzamidocinnamate as substrate and result that the catalytic activity for **3aRh** is good (TOF= 35 h⁻¹) but the enantiomeric excess is marginal (<10 %). The $[(\text{Diop})\text{Rh}]^+$ gives an ee of 15 % (TOF= 264 h⁻¹) and palladium complex decomposes in the reaction medium under the same conditions.

[53] C. González-Arellano, A. Corma, M. Iglesias, F. Sánchez, *Chem. Commun.*, **2005**, 27, 3451.

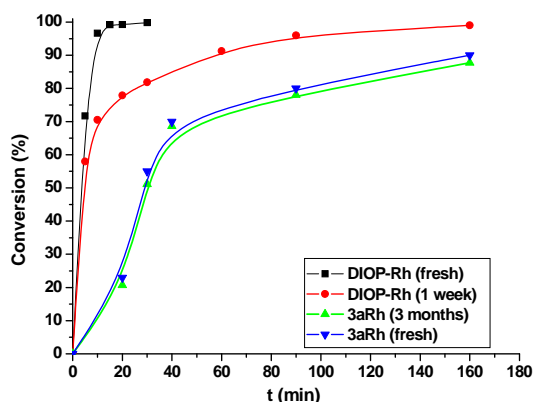


Figure. III. 42. Behavior of phosphine and *bis*-carbene rhodium complexes over time.

Taking account the unstable behavior of phosphine systems, we checked the variation of the catalyst activity over time with *bis*-carbene and *bis*-phosphine (Diop) rhodium (I) systems. It was found that carbene complex **3aRh** maintains its activity for at least three months; however the activity for the **DiopRh** complex decreases over a week. (**Figure. III. 42**).

Now, we can say that these *bis*-NHC systems represent a class of ligands that can be used in place of phosphine ligands in transition- metal catalysis.

3.5.1.b Ligand Influence.

We have seen above, how the activity of *bis*-NHC complexes decreased when we used 2,6-diisopropylphenyl on the NHC donor (**3bAu(I)**) against mesityl-*N* substituted NHC complexes (**3aAu(I)**).

In order to evaluate how affects the modifications in the ligand structure when we replace one of the carbene moieties with amine group, we analyzed the rhodium and palladium *mono*-carbene amine soluble complexes in terms of activity and enantioselectivity and compared with the *bis*-carbene complexes analogues.

Thus, soluble *mono*-NHC amine complexes (*S,S*)-[**4aRh**, **4bRh**, **5aPd**, **5bPd**] were tested in the hydrogenation of diethyl itaconate and (*E*)-diethyl 2-benzylidenesuccinate and gave high activity and enantioselectivity. As can be shown in (**Table. III. 1**) reaction allowed differentiation of the activity between the precatalysts.

These findings are analogous to those found for the related study using *bis*-(NHC)–dioxolane complexes.

Entries 1-6 (**Table. III. 2**) show the effect of modifying the NHC-*N*-substituent, indicating that the rate and enantioselectivity are not very sensitive to changes in this position for *mono*-NHC amine catalysts. As we see in entries 3-6 (**Table. III. 2**), the best results were obtained with complexes derivate from (*S,S*)-[**5a**]I and (*S,S*)-[**5b**]I for both palladium and rhodium complexes, which contain a diisopropylamine moiety against with morpholine derivatives and even with corresponding *bis*-(NHC)–dioxolane complexes (**3aRh** and **3aPd**). (**Figure. III. 43**).

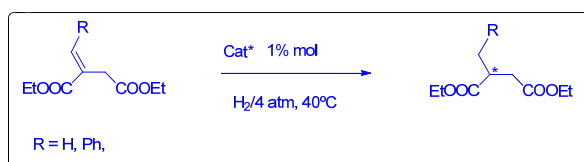


Table. III. 2. Hydrogenation of (*E*)-diethyl 2-*R*-succinates with soluble *mono*-NHC and *bis*-NHC.^{a,b}

Entry	Catalyst	TOF ^b		ee % (<i>S</i>) ^c	
		H	Ph	H	Ph
1	4aRh	207	17	5	99
2	4bRh	164	21	5	99
3	5aRh	492	20	5	99
4	5bRh	226	43	5	99
5	5aPd	293	29	5	99
6	5bPd	338	30	5	99
7	3aRh	258	16	5	99
8	3aPd	45	17	5	98

^aEthanol, 4 atm. H₂, 40 °C, Cat.: 1 mol%; ^bTOF: h⁻¹ (calculated at maximum rate); ^cHPLC (chiralcel AD-H, λ: 230 nm, Hexane/iPrOH: 98/2, chiralcel OD, λ: 250 nm, Hexane/iPrOH: 95/5).

These results involve that it could be better to functionalize the ligand using linear amines rather than cyclical, so, we could support and increase the activity of the system in one step.

Morpholine (**Table. III. 2**, entries 1, 2) and diisopropyl (**Table. III. 2**, entries 3-6) substituents on the dioxolane backbone modify the activity not so the enantioselectivity. All reactions resulted in predominant formation of the *S*-enantiomer as using *bis*-carbene catalysts.

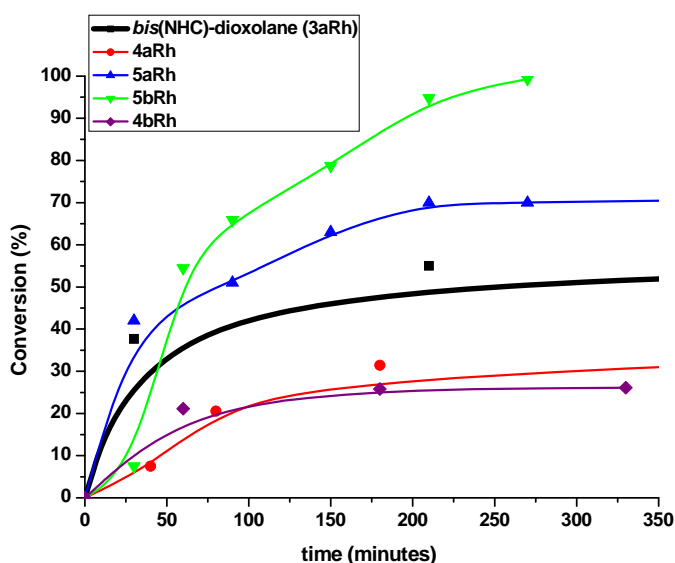


Figure. III. 43. Kinetic profile for catalytic activity of *mono*-carbene Rh reference soluble systems.

3.5.1.c Influence of support.

Heterogenized catalysts were analyzed and the efficiency of gold (I)-, palladium- and rhodium- supported complexes as catalysts for the asymmetric hydrogenation of diethyl itaconate and (*E*)-diethyl 2-benzylidenesuccinate was investigated and compared with that obtained using soluble precatalysts.

The best results were obtained for gold and palladium complexes derived from ligand (*S,S*)-[**6b**]**I** and those derived from ligand (*S,S*)-[**6a**]**I** for rhodium complexes.

All complexes showed significant activities for the hydrogenation of 2-*R*-succinates and high enantioselectivity for (*E*)-diethyl 2-benzylidenesuccinate with 99% ee. (Table. III. 3 and Table. III. 4)

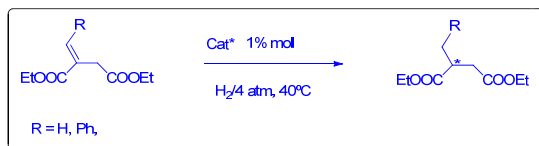


Table. III. 3. Hydrogenation of (*E*)-diethyl 2-*R*-succinates with heterogenized *mono*-NHC.^{a,b}

Entry	Catalyst	R	TOF (h ⁻¹) ^c	ee % (S) ^b
1	6aPd-MCM	H	67	5
2	6aRh-MCM	H	3000	5
3	6aRh-MCM	benzylidene	235	99
4	6bPd-MCM	H	28	5
5	6bPd-MCM	benzylidene	157	99
6	6b(I)Au-MCM	H	1302	5
7	6b(I)Au-MCM	H	17	99
8	6b(I)Au-MCM (four cycles)	benzylidene	40	99

^aEthanol, 4 atm. H₂, 40 °C, Cat.: 1 mol%; ^bTOF: h⁻¹ (calculated at maximum rate); ^cHPLC (chiralcel AD-H, λ: 230 nm, Hexane/iPrOH: 98/2, chiralcel OD, λ: 250 nm, Hexane/iPrOH: 95/5).

As Table. III. 4 shows, in rhodium catalysts, the heterogenized catalysts have higher activity than the corresponding counterparts. These results indicated that the support gives a positive effect in the catalytic properties of these complexes, conferring stability of the active metallic formed in the catalytic process. The fact that the heterogenized catalysts present higher rates is one of the expected features with these materials.

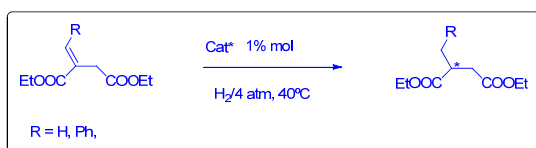


Table. III. 4. Hydrogenation of (*E*)-diethyl 2-*R*-succinates with heterogenized *mono*-NHC amine, soluble and supported.^{a,b}

Metal	Catalyst	R	TOF ^b	ee % ^c
Pd	6bPd-MCM	hydrogen	28	5 (<i>S</i>)
		benzylidene	20	99 (<i>S</i>)
	5aPd	hydrogen	293	5 (<i>S</i>)
		benzylidene	29	99 (<i>S</i>)
	5bPd	hydrogen	338	5 (<i>S</i>)
		benzylidene	30	99 (<i>S</i>)
Rh	6aRh-MCM	hydrogen	3000	5 (<i>S</i>)
		benzylidene	235	99 (<i>S</i>)
	4aRh	hydrogen	207	5 (<i>S</i>)
		benzylidene	17	99 (<i>S</i>)
	5aRh	hydrogen	492	5 (<i>S</i>)
		benzylidene	20	99 (<i>S</i>)
	4bRh	hydrogen	164	5 (<i>S</i>)
		benzylidene	21	99 (<i>S</i>)
	5bRh	hydrogen	226	5 (<i>S</i>)
		benzylidene	43	99 (<i>S</i>)

^aEthanol, 4 atm. H₂, 40 °C, Cat.: 1 mol%; ^bTOF: h⁻¹ (calculated at maximum rate); ^cHPLC (chiralcel AD-H, λ: 230 nm, Hexane/iPrOH: 98/2, chiralcel OD, λ: 250 nm, Hexane/iPrOH: 95/5).

3.5.2 *Recycling experiments in asymmetric hydrogenation of alkenes.*

One of our big goals is the synthesis of recyclable catalytic material and the verification of the permanence of the catalytic properties after several recycling cycles. For this purpose heterogenized catalysts were recovered from the reaction mixture by simple filtration, washed with the solvent itself and dried under vacuum.

Recycle studies using catalysts **6aRh**-, and **6aPd**-, **6bPd-MCM** displayed very similar activities and enantioselectivities as the initial runs and the results are shown in **Table. III. 5** and **Table. III. 6** and even showed marginally better activity.

This increase may result from removal of any residual, species that remain during the filtration steps following the metallation procedure. Catalysts **6bPd-MCM** and **6aRh-MCM** displayed very consistent yield and selectivity over four cycles.

In recycling experiments with **6b(I)Au-MCM** decreased rates were observed, leading to longer reaction times (48 h). These data may suggest a fractional loss of active Au-species with each successive cycle, possibly due to leaching of gold during the washing steps between cycles, catalyst poisoning or loss of crystallinity. Recycle studies using other solvents instead of EtOH displayed similar losses in catalytic activity as using EtOH.

To rule out the loss of crystallinity we study the powder XRD patterns of **6b(I)Au-MCM** (before reaction) and **6b(I)Au-MCM** (after reaction) are given in **Figure. III. 46**. The pattern of the parent, calcined material MCM-41, shows four reflections (only three were showed) in the 2θ range $2-10^\circ$, indexed to a hexagonal cell as (1 0 0), (1 1 0), (2 0 0), and (2 1 0). The d value of the (1 0 0) reflection is 35.2 Å, corresponding to a lattice constant of $a = 40.6 \text{ Å}$ ($=2d_{100}/\sqrt{3}$).

Table. III. 5. Recycling experiments
for **6bPdMCM**.

Run	TOF (h^{-1})	ee % (<i>S</i>)
1	157	99 (<i>S</i>)
2	188	99 (<i>S</i>)
3	177	99 (<i>S</i>)
4	240	99 (<i>S</i>)

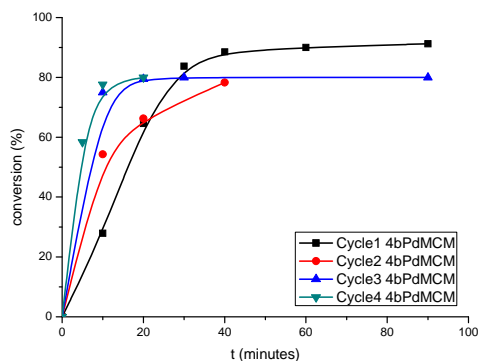


Figure. III. 44. Kinetic profile for catalytic activity **6bPdMCM**.

Table. III. 6. Recycling experiments for
6aRhMCM

Run	TOF (h^{-1})	ee % (<i>S</i>)
1	235	99 (<i>S</i>)
2	1559	99 (<i>S</i>)
3	1745	99 (<i>S</i>)
4	2917	99 (<i>S</i>)

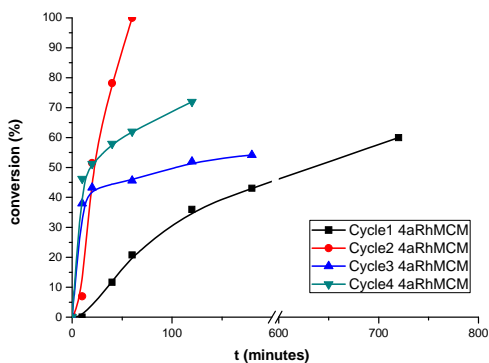


Figure. III. 45. Kinetic profile for catalytic activity **6aRhMCM**.

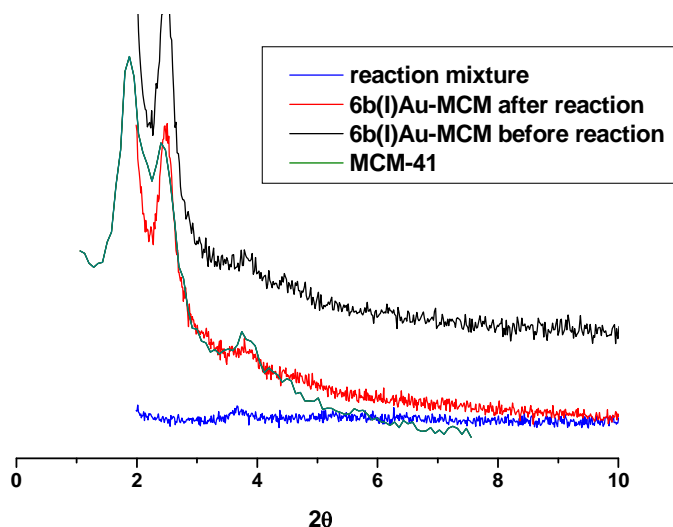


Figure. III. 46. XRD patterns of **6bAu(I)-MCM** (before reaction), **6bAu(I)-MCM** (after reaction), MCM-41 and reaction mixture.

The positions of the peaks of **6b(I)Au-MCM** (before reaction), after functionalizing the walls of the parent host material MCM with [complex]propyltriisopropoxysilane, remain almost unchanged, suggesting the retention of the long range hexagonal symmetry of the host material. The powder patterns also remain unchanged for material **6b(I)Au-MCM** (after reaction). A reduction of the peaks intensities is observed in this case, and becomes more relevant in the metal rich **6b(I)Au-MCM** (before reaction). This is not interpreted as a loss of crystallinity, but rather to a reduction in the X-ray scattering contrast between the silica walls and pore-filling material, a situation well described in the literature,⁵⁴ and also observed for other types of materials.⁵⁵

Catalyst deactivation of **6b(I)Au-MCM** proved to be an initial problem during this work. However, it was observed that this could be minimized by the treatment of recovered material with excess of benzonitrile at 50 °C for 2 hours before the washing steps. Treatment with benzonitrile proved to have a positive effect on catalyst stability

[54] a) B. Marler, U. Oberhagemann, S. Vortmann, H. Gies, *Micropor. Mater.* **1996**, 6, 375–383; b) W. Hammond, E. Prouzet, S. D. Mahanti, T. J. Pinnavaia, *Micropor. Mesopor. Mater.* **1999**, 27, 19–25.

[55] M. Vasconcellos-Dias, C. D. Nunes, P. D. Vaz, P. Ferreira, M. J. Calhorda, *Eur. J. Inorg. Chem.* **2007**, 2917–2925.

over several cycles as seen by overlapping kinetics curves between the first and third cycles after benzonitrile treatment (**Figure. III. 47**).

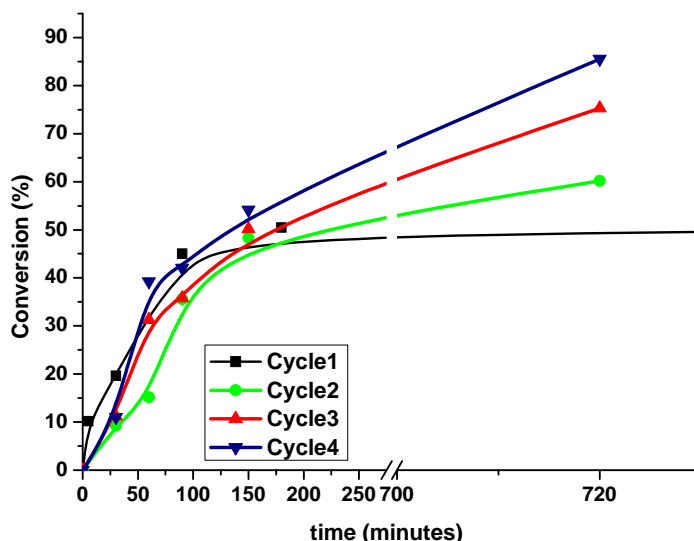
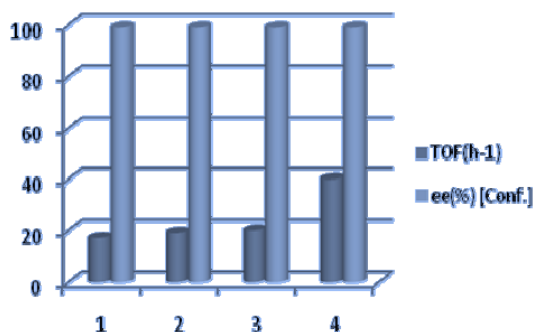


Figure. III. 47. Kinetic profile for recycling of **6bAu(I)MCM** heterogenized complex in the hydrogenation of diethyl (*E*)-diethyl 2-benzylidenesuccinate.

As a result, all recycle experiments were repeated using the benzonitrile washing between cycles (**Table. III. 7**). At slightly longer times (6 h), very high yields ($\geq 97\%$) could be achieved for MCM catalysts over the three cycles tested without any apparent deactivation. Initial runs gave similar results as shown in **Table. III. 7**, and even showed marginally better activity. This increase may result from removal of any residual, non-chiral gold species that remain during the filtration steps following the metallation procedure. Catalyst **6bAu(I)-MCM** displayed very consistent yield and selectivity over four cycles.

Table. III. 7. Recycling experiments for the hydrogenation of (*E*)-diethyl 2-benzylidenesuccinate with supported **6bAu(I)-MCM** catalysts.

Run	TOF (h ⁻¹)	ee % (<i>S</i>)
1	17	99 (<i>S</i>)
2 (washed with ethanol)	0	-
2 (treated with benzonitrile)	19	99 (<i>S</i>)
3 (washed with ethanol)	0	-
3 (treated with benzonitrile)	20	99 (<i>S</i>)
4 (washed with ethanol)	0	-
4 (treated with benzonitrile)	40	99 (<i>S</i>)



The treatment of benzonitrile before the washing steps is through to stabilize the gold center during the washing procedure. The gold complex must dissociate a benzonitrile ligand prior to initiate the catalytic cycle. This vacant coordination site permits the formation of the gold intermediate prior to hydrogen addition across the carbon-carbon double bond of the olefin. After complete consumption of the olefin, a vacant coordination site remains on the gold center. Addition of excess benzonitrile shifts the equilibrium towards binding one benzonitrile co-ligand, thus stabilizing the Au-carbene complex, and inhibiting leaching of gold metal from the ligand. Elemental analysis data indicated that benzonitrile washing did affect the gold content in the recycled catalysts.

Attempts to assess changes to the Au-(NHC) catalysts upon recycling via FT-IR analysis proved that a peak from benzonitrile (2229 cm⁻¹) appears in FT-IR spectra of complexes before heterogeneization (**Figure. III. 32**). No apparent differences between the fresh and recovered catalysts were observed in the IR spectra. In addition, the other frequencies were only minimally visible, due to the low gold loadings on the solid supports compared to analogous studies of soluble complexes.

4 Conclusions.

We developed the synthesis of gold, palladium and rhodium complexes bound to a chiral dioxolane ligand bearing two or one NHC moieties. These *N*-Heterocyclic carbenes (NHC's) represent a class of ligands that can be used in place of phosphine ligands in transition-metal catalysis, which provide more effective metal complexes owing to their stability to air and moisture.

The efficiency of gold, palladium and rhodium, soluble and supported complexes as catalysts for the asymmetric hydrogenation of diethyl itaconate and (*E*)-diethyl 2-benzylidenesuccinate was investigated and compared. All complexes showed significant activities for the hydrogenation of (*E*)-diethyl 2-benzylidenesuccinate with 99% ee.

The heterogenized catalysts could be reused in at least in four cycles without any loss of their performances, even the heterogenized gold (I) catalyst. This fact shows the amazing aptitude of NHC's to stabilize metallic centers in order to improve the catalytic properties.

5 Experimental section.

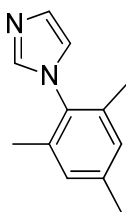
General Remarks: All preparations of metal complexes were carried out under dinitrogen by conventional Schlenk-tube techniques. Solvents were carefully degassed before use. C, H and N analysis were carried out by the analytical department of the Institute of organic chemistry (C.S.I.C.) with a Lecco apparatus. Metal contents were analyzed by atomic absorption using a Perkin Elmer AAnalyst 300 atomic absorption apparatus and plasma ICP Perkin Elmer OPTIMA 2100 DV. IR spectra were recorded on a Bruker IFS 66v/S spectrophotometer (range 4000-200 cm⁻¹) in KBr pellets. ¹H NMR, ¹³C NMR spectra were taken on Varian XR300 and Bruker 200 spectrometers. Chemical shifts being referred to tetramethylsilane (internal standard). Gas chromatography analysis was performed using a Hewlett-Packard 5890 II. The enantiomeric excess was measured by HPLC (Agilent 1200). AuCl(tht),⁵⁶ PdCl₂(cod), [RhCl(cod)]₂,⁵⁷ [Rh(diop)(cod)]PF₆⁵⁸ and diop[AuCl]₂⁵⁹ were obtained as described in literature.

5.1 Synthesis of precursors.

5.1.1 Imidazole synthesis.

For the synthesis of 1-mesityl-1H-imidazole and 1 - (2,6-diisopropilfenil)-1H-imidazol we used an improved process described in the literature.^{44, 60}

5.1.1.a 1-mesityl-1H-imidazole. (1a).



[56] D. Drew, J. R. Doyle, A.G. Shaver, *Inorg. Synth.* **1972**, 13, 47.

[57] G. Giordano and R.H. Crabtree, *Inorg. Synth.* **1990**, 28, 88.

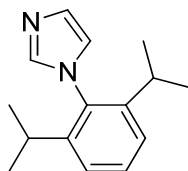
[58] a) K. Tani, T. Yamagata, S. Akutagawa, H. Kumobayashi, T. Takatomi, H. Takaya, A. Miyashita, R. Noyori, S. Otsuka, *J. Am. Chem. Soc.* **1984**, 106, 5208–5217; b) J. A. Osborn, R. R. Schrock, *J. Am. Chem. Soc.* **1973**, 93, 2397–2407.

[59] M. J. Johansson, D. J. Gorin, S. T. Staben, F. Dean Toste, *J. Am. Chem. Soc.*, **2005**, 127, 18002-18003.

[60] A.L. Jonson, *US. Patent*, **1972**, 3637, 731.

To a solution of 2,4,6-trimethylaniline (14.1 mL, 0.1 mol) in 50 mL of methanol were added 0.1 mol of aqueous solution of glyoxal (30%, 6.2 mmol/mL) and the mixture was left stirring at room temperature for 24 h. Note the formation of a yellow precipitate. In this mass reaction was added NH_4Cl (10.7 g, 0.2 mol) followed by aqueous solution of formaldehyde 40% (10 mL, 0.2 mol). The mixture was diluted in methanol (400 mL) and refluxed for 1 h while continuous drip is added 14 mL of aqueous H_3PO_4 85%. The reaction is refluxed for 8 hours and followed by thin layer chromatography (hexane/ethyl acetate (1:1), $R_f = 0.38$). When reaction is complete, the mixture was concentrated to dryness and the residue obtained added on ice water and neutralized with a solution of 40% KOH to pH = 9. The resulting mixture was extracted with diethyl ether (5x150 mL), the organic phases are combined and washed with water and saturated NaCl, dried over Na_2SO_4 and concentrated to dryness and purified by flash chromatography on silica gel to afford a yellow solid. Yield=65%.

5.1.1.b 1-(2,6-diisopropylphenyl)-1H-imidazole. (1b).



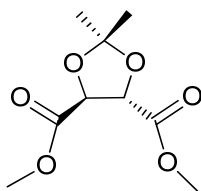
To a solution of 2,6-diisopropylaniline (18.3 mL, 0.1 mol) in 50 mL of methanol were added 0.1 mol of aqueous solution of glyoxal (30%, 6.2 mmol/mL) and the mixture was left stirring at room temperature for 24 h. Note the formation of a yellow precipitate. In this mass reaction was added NH_4Cl (10.7 g, 0.2 mol) followed by aqueous solution of formaldehyde 40% (10 mL, 0.2 mol). The mixture was diluted in 400 mL of methanol and heated at reflux temperature for 1 h while continuous drip is added 14 mL of aqueous H_3PO_4 85%. The reaction is refluxed for 8 hours and followed by thin layer chromatography (hexane/ethyl acetate (1:1), $R_f = 0.41$). After the reaction was complete the mixture was concentrated to dryness and the residue obtained is added on ice water and neutralized with a solution of 40% KOH to pH = 9. The

NHC's

resulting mixture was extracted with diethyl ether (5 x 150 ml), the organic phases are combined and washed with water and saturated NaCl, dried over Na₂SO₄ and concentrated to dryness and purified by flash chromatography on silica gel to afford 16.7 g of yellow solid. Yield = 73%.

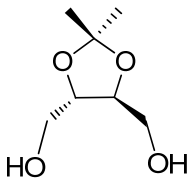
5.1.2 Synthesis of the “ligand backbone”: 4,5-bis(iodomethyl)-2,2-dimethyl-1,3-dioxolane. (2).

5.1.2.a Dimethyl 2,2-dimethyl-1,3-dioxolane-4,5-dicarboxylate. (IN-1).



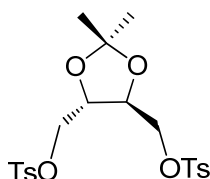
Tartaric acid solution (50 g, 333.3 mmol), 2,2-dimethoxypropane (79 g, 759.9 mmol) and 0.2 g p-toluenesulfonic acid in 20 mL of methanol were heated to reflux for 1.5 hours, giving a red solution, 39.35 g of 2,2-dimethoxypropane and 225 mL of cyclohexane was added to the mixture. The two phases resulting solution was refluxed with constant stirring and distilled using a vigrex column: (53 °C) the acetone-cyclohexane azeotrope and methanol-cyclohexane azeotrope (54.5 °C). After 47 hours the fraction collected at 79 °C was the desired product. Potassium carbonate (0.5 g) was added to neutralize the catalyst. The crude was concentrated to dryness. Yellowish oil was obtained. Yield = 87%.

5.1.2.b (2,2-dimethyl-1,3-dioxolane-4,5-diyl)dimethanol. (IN-2).



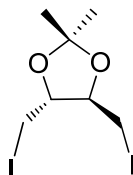
Sodium borohydride (5.9 g, 156.16 mmol) was added dropwise to a solution of dimethyl-2,2-dimethyl-1,3-dioxolane-4,5-dicarboxylate (12.61 g, 57.84 mmol) in methanol at 0 °C. The mixture was stirred at room temperature for 12 hours. Methanol is removed under vacuum, 250 mL of water added and continuously extracted with ethyl acetate. The organic phase was concentrated to dryness and purified by flash column chromatography on silica gel (1:1, hexane / ethyl acetate, $R_f = 0$) and then eluted with ethyl acetate / methanol drops. Yield = 98%.

5.1.2.c 2,2-dimethyl -4,5-ditosylmethyl-1,3-dioxolane. (IN-3).



To (2,2-dimethyl-1,3-dioxolane-4,5-diyl)dimethanol (9.2 g, 56.8 mmol) was added at -10 °C 75 mL of pyridine and stirred for 15 minutes, then added tosylchloride and the mixture stirred vigorously until homogenous mixture and maintained at 0 °C for 12 h. 6 mL of H₂O were added dropwise until precipitate the product. The reaction is quantitative.

5.1.2.d 4,5-bis(iodomethyl)-2,2-dimethyl-1,3-dioxolane. (2).⁴³



To a solution of 2,2-dimethyl -4,5-ditosylmethyl-1,3-dioxolane (4g, 8.51 mmol) in 50 mL of acetone, sodium iodide is added (6 g, 40 mmol) and the mixture refluxed for 48h, when the reaction was over, p-toluensulfonate formed was filtered and washed with acetone. The aqueous layer of the filtrate was concentrated to

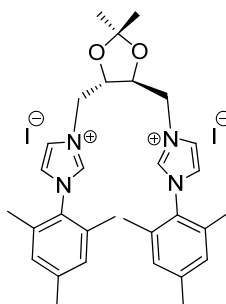
NHC's

dryness; 30 mL of water added and extracted with chloroform, the organic phase washed with saturated sodium thiosulfate and water, dried with anhydrous sodium sulfate and concentrated. Yield = 95%.

5.2 Synthesis of ligands.

5.2.1 Synthesis of soluble bis-*N*-heterocyclic carbene precursor salts.

5.2.1.a 3,3'-((4*S*,5*S*)-2,2-dimethyl-1,3-dioxolane-4,5-diyl) bis(methylene) bis(1-(2,4,6-trimethylphenyl)-1*H*-imidazol-3-ium) iodide. ((*S,S*)-[3a]I).



A mixture of (4*R*,5*R*)-bis(iodomethyl)-2,2-dimethyl-1,3-dioxolane (**2**) (1.14 g, 3 mmol) and 1-(2,4,6-trimethylphenyl)-1*H*-imidazole (**1a**) (1.24 g, 6.6 mmol) was heated in acetonitrile at 140 °C for 48 h. The solvent was removed, the product washed with ethyl ether and filtered to afford the salt (2.07 g, 92%) as a white solid.

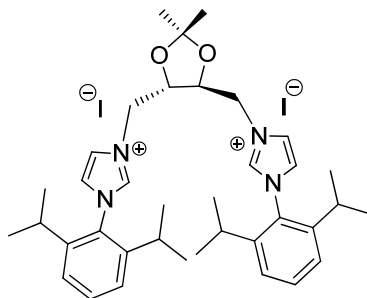
IR (KBr; cm⁻¹): ν = 3437 (C-N); 3049 (C-H); 2984-2928 (C-H); 1608 (C=C); 1560-1546 (C=N); 1445 (C-N); 1202-1163 (C-N).

¹H RMN (CDCl₃) δ (ppm): 9.66 (2H, s, NCH=N); 8.29 (2H, s, CH_{im}); 7.24 (2H, t, CH_{im}); 6.98 (4H, s, H_{arom}); 5.55 (2H, d, CH₂); 5.08 (2H, d, CH₂); 4.73 (2H, d, OCH); 2.31 (6H, s, *p*-CH₃); 2.07 (12H, d, *o*-CH₃); 1.43 (6H, s, CH₃).

¹³C RMN (CDCl₃) δ (ppm): 141.36 (C(*p*-CH₃)); 137.42 (NCH=N); 134.06 (C(*o*-CH₃)); 134.29 (C(*o*-CH₃)); 130.38 (C_{arom}-N); 129.83 (CH_{arom}); 124.91 (CH_{im});

122.89 (CH_{im}); 111.66 (C(CH₃)₂); 75.74 (OCH); 51.10 (CH₂); 27.43 (CH₃); 20.39 (*p*-CH₃); 17.63 (*o*-CH₃).

**5.2.1.b 3,3'-((4*S*,5*S*)-2,2-dimethyl-1,3-dioxolane-4,5-diyl) bis
(methylene)bis(1-(2,6-diisopropylphenyl)-1*H*-imidazol-3-ium)iodide.
(*(S,S)*-[3*b*]I).**



The procedure for (*S,S*)[3*a*]I was followed using (4*R*,5*R*)-bis(iodomethyl)-2,2-dimethyl-1,3-dioxolane (**2**) (0.547 g, 1.433 mmol) and 1-(2,6-diisopropylphenyl)-1*H*-imidazolidine (**1b**) (0.72 g, 3.15 mmol). The product was purified by flash chromatography (acetone/ethyl acetate, 2:1) to give the salt (601 mg, 50%) as a light yellow solid.

IR (KBr, cm⁻¹): ν = 3436 (C-N); 3065 (C-H); 2964-2928 (C-H); 1625 (C=C); 1561-1541 (C=N); 1460 (C-N).

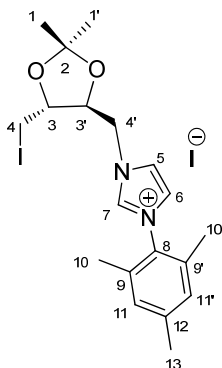
¹H RMN (CDCl₃) δ (ppm): 9.77 (2H, s, NCH=N); 8.45 (2H, s, CH_{im}); 7.54 (2H, t, *p*-H_{arom}); 7.31-7.30 (4H, m, *m*-H_{arom}); 7.20 (2H, t, CH_{im}); 5.6 (2H, dd, CH₂); 5.25 (2H, dd, CH₂); 4.86 (2H, dd, OCH); 2.44-2.42 (2H, m, CH); 2.21-2.19 (2H, m, CH); 1.26, 1.17, 1.16 (24H, d,d,d, CH₃-CH_{arom}); 1.43 (6H, s, CH₃).

¹³C RMN (CDCl₃) δ (ppm): 145.4 (*o*-C_{arom}); 145.7 (*o*-C_{arom}); 137.9 (NCH=N); 132.3 (*p*-C_{arom}); 130.9 (C_{arom}-N); 125.3 (CH_{im}); 125.2 (*m*-C_{arom}); 124.8 (*m*-C_{arom}); 123.9 (CH_{im}); 112.0 (C(CH₃)₂); 76.0 (OCH); 51.3 (CH₂); 28.9, 28.8 (CH); 27.8 (CH₃); 24.7, 24.7, 24.6, 24.2 (CH₃).

5.2.2 Synthesis of mono-*N*-heterocyclic carbene precursor salts.

5.2.2.a Synthesis of intermediates.

1-(((4*S*,5*R*)-5-(iodomethyl)-2,2-dimethyl-1,3-dioxolan-4-yl)methyl)-3-mesityl-1*H*-imidazol-3-ium iodide. (IN-4a).



A mixture of (4*R*,5*R*)-*bis*(iodomethyl)-2,2-dimethyl-1,3-dioxolane (**2**) (3 g, 7.8 mmol) and 1-(2,4,6-trimethylphenyl)-1*H*-imidazole (**1a**) (0.96 g, 5.2 mmol) was heated in acetonitrile at 140 °C for 48 h. The solvent was removed, the desired product was purified by flash column chromatography (ethyl acetate/ketone; 2:1) to afford 1.08 g of white powder solid and recovering 1.71 g of starting material (**2**).

EM (ES) (m/z; %): 442 ($M^+ + 1$; 34); 441 (M^+ ; 100); 313 (34); 187 (34).

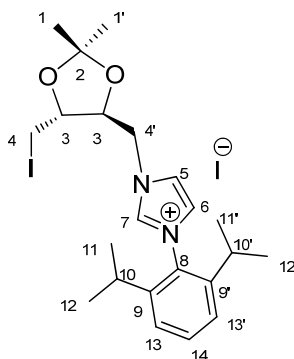
IR (KBr; cm^{-1}): ν = 3115-3056 (C-H); 2984-2931 (H); 1606 ($\nu=\text{C}$); 1559-1547 (C=N); 1482-1447 ($=\text{C}-\text{N}$); 1204-1163 (C-N).

$^1\text{H-NMR}$ (CDCl_3) δ (ppm): 9.89 (s, H_7); 7.98 (s, H_5); 7.21 (s, H_6); 7.03 (s, 2H, H_{11} , $\text{H}_{11'}$); 5.48 (dd, 1H, CH_2 , H_4); 4.83 (dd, 1H, CH_2 , H_4); 4.30 (td, 1H, CH, H_3); 3.88 (m, 1H, CH, H_3); 3.74 (dd, 1H, CH_2 , H_4); 3.59 (dd, 1H, CH_2 , H_4); 2.34 (s, 3H, CH_3 , H_{13}); 2.14 (s, 3H, CH_3 , H_{10} or $\text{H}_{10'}$); 2.07 (s, 3H, CH_3 , H_{10} or $\text{H}_{10'}$); 1.45 (s, 3H, CH_3 , H_1 or H_1'); 1.43 (s, 3H, CH_3 , H_1 or H_1').

$^{13}\text{C-NMR}$ (CDCl_3) δ (ppm): 141.6 (C_{12}); 137.6 (CH, C_7); 134.3 (C_9 or C_9'); 135.0 (C_9 or C_9'); 130.3 (C_8); 129.9 (CH, C_{11} or $\text{C}_{11'}$); 129.8 (CH, C_{11} or $\text{C}_{11'}$); 124.3

(CH, C₅); 122.8 (CH, C₆); 110.8 (C₂); 78.8 (CH, C_{3'}); 77.3 (CH, C₃); 51.7 (CH₂, C_{4'}); 27.5 (CH₃, C₁ or C_{1'}); 27.3 (CH₃, C₁ or C_{1'}); 21.1 (CH₃, C₁₃); 18.0 (CH₃, C₁₀ or C_{10'}); 17.7 (CH₃, C₁₀ or C_{10'}); 6.3 (CH₂, C₄).

3-(2,6-diisopropylphenyl)-1-(((4*S*,5*R*)-5-(iodomethyl)-2,2-dimethyl-1,3-dioxolan-4-yl)methyl)-1*H*-imidazol-3-ium iodide. (IN-4b).



A mixture of (4*R*,5*R*)-bis(iodomethyl)-2,2-dimethyl-1,3-dioxolane (**2**) (3 g, 7.8 mmol) and 1-(2,6-diisopropylphenyl)-1*H*-imidazole (**1b**) (1.2 g, 5.2 mmol) was heated in acetonitrile at 130 °C for 48 h. The solvent was removed, the desired product was purified by flash column chromatography (ethyl acetate/ketone; 1:2) to afford 1.4 g of white powder solid and recovering 0.3 g of starting material (**2**).

EM (ES) (m/z; %): 484 (M⁺+1; 34); 483 (M⁺; 100).

¹H-NMR (CDCl₃) δ (ppm): 9.81 (s, H₇); 8.17 (s, H₅); 7.55 (t, 1H, CH, H₁₄); 7.32 (m, 2H, 2CH, H₁₃, H_{13'}); 7.23 (s, H₆); 5.53 (dd, 1H, CH₂, H_{4'}); 4.99 (dd, 1H, CH₂, H_{4'}); 4.32 (td, 1H, CH, H_{3'}); 3.92 (m, 1H, CH, H₃); 3.79 (dd, 1H, CH₂, H₄); 3.60 (dd, 1H, CH₂, H₄); 2.42 (m, 1H, CH, H₁₀ or H_{10'}); 2.24 (m, 1H, CH, H₁₀ or H_{10'}); 1.46 (s, 3H, CH₃, H₁ or H_{1'}); 1.44 (s, 3H, CH₃, H₁ or H_{1'}); 1.26 (d, 3H, CH₃, H₁₁ or H₁₂ or H_{11'} or H_{11'}); 1.22 (d, 3H, CH₃, H₁₁ or H₁₂ or H_{11'} or H_{11'}); 1.24 (d, 6H, 2CH₃, H₁₁ or H₁₂ or H_{11'} or H_{11'}).

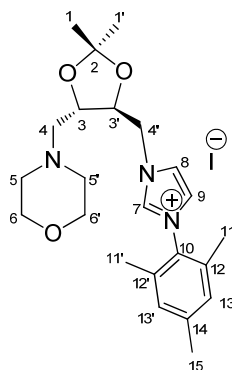
¹³C-NMR (CDCl₃) δ (ppm): 145.4 (C₉ or C_{9'}); 145.26 (C₉ or C_{9'}); 137.7 (CH, C₇); 135.7 (CH, C₁₄); 129.8 (C₈); 127.1 (CH, C₁₃, C_{13'}); 124.4 (CH, C₅); 124.3 (CH, C₆);

NHC's

110.7 (C₂); 81.3 (CH, C₃); 78.2 (CH, C₃); 51.7 (CH₂, C₄); 28.7 (2CH, C₁₀, C_{10'}); 27.6 (CH₃, C₁ or C_{1'}); 27.3 (CH₃, C₁ or C_{1'}); 24.5 (CH₃, C₁₁ or C_{11'} or C₁₂ or C_{12'}); 24.4 (CH₃, C₁₁ or C_{11'} or C₁₂ or C_{12'}); 24.14 (2CH₃, C₁₁ or C_{11'} or C₁₂ or C_{12'}) 6.40 (C₄).

5.2.2.b Synthesis of mono-N-heterocyclic carbene amine precursors salts. Reference systems for homogeneous catalysis.

1-(((4*S*,5*S*)-2,2-dimethyl-5-(morpholinomethyl)-1,3-dioxolan-4-yl)methyl)-3-mesityl-1*H*-imidazol-3-ium iodide. ((*S*,*S*)-[4a]I).



1-(((4*S*,5*R*)-5-(iodomethyl)-2,2-dimethyl-1,3-dioxolan-4-yl)methyl)-3-mesityl-1*H*-imidazol-3-ium iodide (**IN-4a**) (200 mg, 0.3 mmoles) and morpholine (77 μ L, 0.8 mmol) were added to 10 mL of acetonitrile in a steel reactor and was heated in acetonitrile at 130 °C for 48 h. The solvent was removed and the product was isolate and purified by flash column chromatography (keton / ethyl acetate 10:1, R_f= 0.55) to afford 180 mg of yellow oil. Yield= 97%.

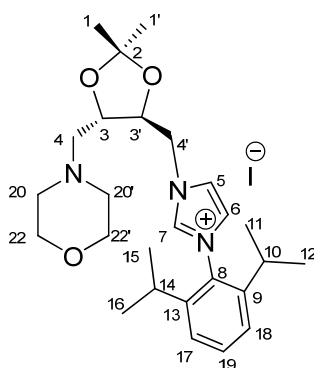
EM (ES) (m/z; %): 401 (M⁺+1; 34); 400 (M⁺; 100).

IR (KBr; cm⁻¹): ν = 3115-3056 (C-H); 2926 (C-H); 1662 (C=C); 1549 (C=N); 1455 (C-N); 1205-1161 (C-N).

¹H RMN (CDCl₃) δ (ppm): 9.89 (t, 1H, H₇); 7.95 (t, 1H, H₈); 7.19 (t, 1H, H₉); 7.02 (s, 2H; H₁₃, H_{13'}, CH); 5.42 (dd, 1H, CH₂, H_{4'}); 4.70 (dd, 1H, CH₂, H_{4'}); 4.31 (td, 1H, CH, H_{3'}); 4.16 (td, 1H, CH, H₃); 3.75 (4H, 2CH₂, H₆, H_{6'}); 3.29 (dd, 1H, CH₂, H₄); 2.72 (m, 5H; 2CH₂, H₅, H_{5'}, 1H, CH₂, H₄); 2.34 (s, 3H, CH_{3Me-p15}); 2.13 (s, 3H, CH₃, H₁₁ or H_{11'}); 2.08 (s, 3H, CH₃, H₁₁ or H_{11'}); 1.39 (s, 6H; 2CH₃, H₁, H_{1'}).

^{13}C RMN (CDCl_3) δ (ppm): 141.6 (C_{14}); 137.6 (CH ; C_7); 134.3 (C_{12} or $\text{C}_{12'}$); 134.1 (C_{12} or $\text{C}_{12'}$); 130.4 (C_{10}); 130.0 (CH ; C_{13} or $\text{C}_{13'}$); 129.9 (CH ; C_{13} or $\text{C}_{13'}$); 124.6 (CH ; C_8); 122.6 (CH ; C_9); 110.7 (C_2); 77.1 (CH ; C_3); 76.9 (CH ; C_3); 66.5 (2CH_2 ; C_6 , C_6'); 59.8 (CH_2 ; C_4); 54.3 (2CH_2 ; C_5 , C_5'); 51.8 (CH_2 ; C_4'); 27.2 (CH_3 ; C_1 or C_1'); 27.3 (CH_3 ; C_1 or C_1'); 21.1 (CH_3 ; C_{15}); 18.1 (CH_3 ; C_{11} or $\text{C}_{11'}$); 17.8 (CH_3 ; C_{11} or $\text{C}_{11'}$).

3-(2,6-diisopropylphenyl)-1-(((4*S*,5*S*)-2,2-dimethyl-5-(morpholinomethyl)-1,3-dioxolan-4-yl)methyl)-1*H*-imidazol-3-ium iodide. ((*S*,*S*)-[4*b*]I).



3-(2,6-diisopropylphenyl)-1-(((4*S*,5*R*)-5-(iodomethyl)-2,2-dimethyl-1,3-dioxolan-4-yl)methyl)-1*H*-imidazol-3-ium iodide (**IN-4b**) (200 mg, 0.3 mmoles) and morpholine (77 μL , 0.8 mmol) were added to 10 mL of acetonitrile in a steel reactor and was heated in acetonitrile at 130 $^{\circ}\text{C}$ for 48 h. The solvent was removed and the product was isolated and purified by flash column chromatography (ketone / ethyl acetate 10:1, R_f = 0.38) to afford 182 mg of yellow oil. Yield= 97%.

EM (ES) (m/z ; %): 443 ($\text{M}^+ + 1$; 34); 441 (M^+ ; 100).

IR (KBr; cm^{-1}): ν = 3871 (C-H); 2966-2870 (C-H); 1622 (C=C); 1563-1547 (C=N); 1455 (C-N); 1245 (C-N).

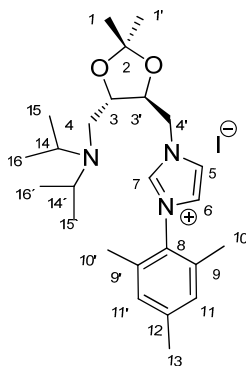
^1H RMN (CDCl_3) δ (ppm): 9.77 (t, 1H, H_7); 8.15 (t, 1H, H_6); 7.55 (t, 1H, CH , H_{19}); 7.32 (m, 2H, 2CH, H_{17} , H_{18}); 7.20 (t, 1H, H_5); 5.48 (dd, 1H, CH_2 , $\text{H}_{4'}$); 4.83 (dd, 1H, CH_2 , $\text{H}_{4'}$); 4.27 (td, 1H, CH , $\text{H}_{3'}$); 4.09 (m, 1H, CH , H_3); 3.73 (t, 4H, 2CH₂, H_{22} ,

NHC's

H_{22'}); 3.28 (dd, 1H, CH₂, H₄); 2.71 (m, 5H, 2CH₂, H₂₀, H_{20'}, 1H, CH₂, H₄); 2.39 (m, 1H, CH, H₁₄ or H₁₀); 2.39 (m, 1H, CH, H₁₄ or H₁₀); 1.39 (d, 6H, 2CH₃, H₁, H_{1'}); 1.25 (d, 3H, CH₃, H₁₅ or H₁₆ or H₁₁ or H₁₂); 1.21 (d, 3H, CH₃, H₁₅ or H₁₆ or H₁₁ or H₁₂); 1.16 (m, 6H, 2CH₃, H₁₅ or H₁₆ or H₁₁ or H₁₂).

¹³C RMN (CDCl₃) δ (ppm): 145.3 (C₉ or C₁₃); 145.2 (C₉ or C₁₃); 137.6 (CH; C₇); 132.1 (CH; C₁₉); 129.8 (C₈); 124.9 (CH; C₁₇ or C₁₈); 124.7 (CH; C₁₇ or C₁₈); 124.5 (CH; C₅); 123.6 (CH; C₆); 110.5 (C₂); 77.4 (CH; C₃); 77.1 (CH; C_{3'}); 66.6 (2CH₂; C₂₂, C_{22'}); 59.7 (CH₂; C₄); 54.4 (2CH₂; C₂₀, C_{20'}); 51.7 (CH₂; C_{4'}); 28.67 (CH; C₁₄ or C₁₀); 28.66 (CH; C₁₄ or C₁₀); 27.2 (CH₃; C₁ or C_{1'}); 27.1 (CH₃; C₁ or C_{1'}); 24.43; 24.41; 24.26; 24.07 (4CH₃; C₁₅, C₁₆, C₁₁, C₁₂).

1-(((4*S*,5*S*)-5-((diisopropylamino)methyl)-2,2-dimethyl-1,3-dioxolan-4-yl)methyl)-3-mesityl-1*H*-imidazol-3-ium iodide. ((*S,S*)-[5*a*]I).



Diisopropylamine (0.7 mL, 4.9 mmol) and 1-(((4*S*,5*R*)-5-(iodomethyl)-2,2-dimethyl-1,3-dioxolan-4-yl)methyl)-3-mesityl-1*H*-imidazol-3-ium iodide (**IN-4a**) (300 mg, 0.49 mmol) were added to 2 mL of acetonitrile in a microwave reactor using the following method:

3 hours, 130 °C, 220 W, 20 bar

30 minutes, 60 °C, 0 W, 0 bar

3 hours, 130 °C, 220 W, 20 bar

When the reaction was finished the solvent was evaporated and 120 mL of chloroform was added and washed with ammonia (3x1 mL). The organic layer dried

over Na_2SO_4 and concentrated. The product was purified by flash column chromatography (acetonitrile / ethyl acetate 1:1, $R_f = 0.35$) to afford 120 mg of dark oil. Yield= 42%.

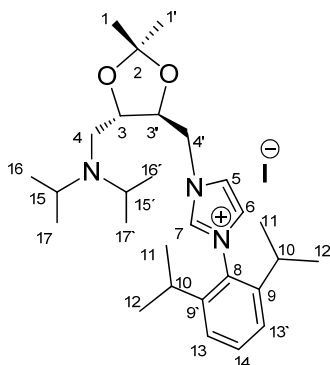
EM (ES) (m/z ; %): 414 (M^+ ; 100); 415 (M^++1 ; 54).

IR (KBr; cm^{-1}): $\nu = 3429$ (C-N); 2967-2932 (C-H); 1609 (C=C); 1547-1502 (C=N); 1459 (=C-N); 1236-1204 (C-N).

^1H NMR (CDCl_3) δ (ppm): 9.81 (s, H_7); 7.75 (s, H_5); 7.19 (s, H_6); 7.00 (s, 2H, 2CH , H_{11} , $\text{H}_{11'}$); 5.23 (dd, 1H, CH , H_4); 4.73 (dd, 1H, CH_2 , H_4); 4.27 (m, 2H, 2CH , H_3 , H_3'); 3.26 (m, 3H, 2CH , H_{14} , $\text{H}_{14'}$, CH_2 , H_4); 2.95 (dd, 1H, CH_2 , H_4); 2.32 (s, 3H, CH_3 , H_{13}); 2.13 (s, 3H, CH_3 , H_{10} or $\text{H}_{10'}$); 2.07 (s, 3H, CH_3 , H_{10} or $\text{H}_{10'}$); 1.43 (s, 3H, CH_3 , H_1 or $\text{H}_{1'}$); 1.38 (s, 3H, CH_3 , H_1 or $\text{H}_{1'}$); 1.21 (d, 6H, 2CH_3 , H_{15} or $\text{H}_{15'}$ or H_{16} or $\text{H}_{16'}$); 1.11 (d, 6H, 2CH_3 , H_{15} or $\text{H}_{15'}$ or H_{16} or $\text{H}_{16'}$).

^{13}C NMR (CDCl_3) δ (ppm): 141.5 (C_{12}); 139.4 (CH , C_7); 134.4 (C_9 or C_9'); 134.2 (C_9 or C_9'); 130.4 (C_8); 129.9 (CH , C_{11} or $\text{C}_{11'}$); 129.8 (CH , C_{11} or $\text{C}_{11'}$); 124.3 (CH , C_5); 123.3 (CH , C_6); 110.3 (C_2); 77.9 (2CH ; C_3 , C_3); 53.1 (CH_2 , C_4); 47.7 (CH_2 , C_4); 49.9 (2C , C_{14} , $\text{C}_{14'}$); 27.2 (CH_3 , C_1 or $\text{C}_{1'}$); 27.1 (CH_3 , C_1 or $\text{C}_{1'}$); 21.5 (2CH_3 , C_{15} or $\text{C}_{15'}$ or C_{16} or $\text{H}_{16'}$); 19.4 (CH_3 , C_{13}); 19.2 (2CH_3 , C_{15} or $\text{C}_{15'}$ or C_{16} or $\text{H}_{16'}$); 18.0 (CH_3 , C_{10} or $\text{C}_{10'}$); 17.6 (CH_3 , C_{10} or $\text{C}_{10'}$).

1-(((4*S*,5*S*)-5-((diisopropylamino)methyl)-2,2-dimethyl-1,3-dioxolan-4-yl)methyl)-3-(2,6-diisopropylphenyl)-1*H*-imidazol-3-iumiodide. ((*S,S*)-[5*b*]I).



Diisopropylamine (0.7 mL, 4.9 mmol) and 3-(2,6-diisopropylphenyl)-1-(((4*S*,5*R*)-5-(iodomethyl)-2,2-dimethyl-1,3-dioxolan-4-yl)methyl)-1*H*-imidazol-3-ium iodide (**IN-4b**) (300 mg, 0.5 mmol) were added to 2 mL of acetonitrile in a microwave reactor using the following method:

3 hours, 130 °C, 220 W, 20 bar

30 minutes, 60 °C, 0 W, 0 bar

3 hours, 130 °C, 220 W, 20 bar

When the reaction was finished the solvent was evaporated and 120 mL of chloroform was added and washed with ammonium (3x1 mL). The organic layer was dried over Na₂SO₄ and concentrated. The product was isolated and purified by flash column chromatography (acetonitrile / ethyl acetate 1:1, R_f = 0.25) to afford 130 mg of dark oil. Yield = 49%.

EM (ES) (m/z; %): 457(M⁺+1; 90); 456 (M⁺; 100).

IR (KBr; cm⁻¹): ν = 3413 (C-N); 3065 (C-H); 2965-2930 (C-H); 1545 (C=N); 1460 (C-N); 1217-1189 (C-N).

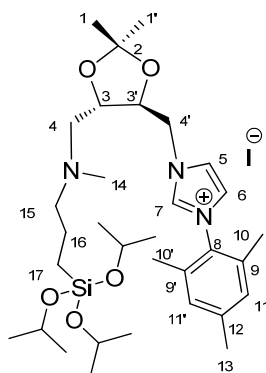
¹H RMN (CDCl₃) δ (ppm): 9.73 (s, 1H, H₇); 7.92 (s, 1H, H₅); 7.53 (t, 1H, CH, H₁₄); 7.30 (m, 2H, 2CH, H₁₃, H_{13'}); 7.20 (s, 1H, H₆); 5.33 (dd, 1H, CH₂, H_{4'}); 4.82 (dd, 1H, CH₂, H_{4'}); 4.36 (m, 2CH, H₃, H_{3'}); 3.37 (m, 3H, 2CH, H₁₅, H_{15'}, 1H, CH₂, H₄); 3.00

(dd, 1H, CH₂, H₄); 2.42 (m, 1H, H₁₀ or H_{10'}); 2.38 (m, 1H, H₁₀ or H_{10'}); 1.45 (s, 3H, CH₃, H₁ or H_{1'}); 1.38 (s, 3H, CH₃, H₁ or H_{1'}); 1.33 (d, 6H, 2CH₃, H₁₆ or H₁₇ or H_{16'} or H_{17'}); 1.27 (d, 3H, CH₃, H₁₁ or H₁₂ or H_{11'} or H_{12'}); 1.22 (d, 3H, CH₃, H₁₁ or H₁₂ or H_{11'} or H_{12'}); 1.18 (d, 6H, 2CH₃, H₁₆ or H₁₇ or H_{16'} or H_{17'}); 1.16 (d, 3H, CH₃, H₁₁ or H₁₂ or H_{11'} or H_{12'}); 1.12 (d, 3H, CH₃, H₁₁ or H₁₂ or H_{11'} or H_{12'}).

¹³C RMN (CDCl₃) δ (ppm): 145.5 (C₉ or C_{9'}); 145.3 (C₉ or C_{9'}); 137.9 (C₇); 132.1 (CH; C₁₄); 124.9 (CH; C₁₃ or C_{13'}); 129.8 (C₈); 124.7 (CH; C₁₃ or C_{13'}); 123.8 (CH; C₅); 123.7 (CH; C₆); 110.5 (C₂); 77.7 (CH; C_{3'}); 77.2 (CH; C₃); 53.3 (CH₂; C_{4'}); 51.7 (2CH; C₁₅, C_{15'}); 47.9 (CH; C₄); 28.7 (CH; C₁₀ or C_{10'}); 28.6 (CH; C₁₀ or C_{10'}); 27.2 (CH₃; C₁ or C_{1'}); 27.1 (CH₃; C₁ or C_{1'}); 21.1 (2CH₃; C₁₆ or C₁₇ or C_{16'} or C_{17'}); 24.4 (2CH₃; C₁₁ or C_{11'} or C₁₂ or C_{12'}); 24.1 (2CH₃; C₁₁ or C_{11'} or C₁₂ or C_{12'}); 19.1 (2CH₃; C₁₆ or C₁₇ or C_{16'} or C_{17'}).

5.2.2.c Synthesis of mono-*N*-heterocyclic carbene amine precursors salts with pendant alkoxy silane groups.

1-(((4*S*,5*S*)-2,2-dimethyl-5-((methyl(3-(triisopropoxysilyl)propyl)amino) methyl)-1,3-dioxolan-4-yl)methyl)-3-mesityl-1*H*-imidazol-3-ium iodide. ((*S,S*)-[6a]I).



N-methyl-3-(triisopropoxysilyl)propan-1-amine (63.5 mg, 0.229 mmol) and 1-(((4*S*,5*R*)-5-(iodomethyl)-2,2-dimethyl-1,3-dioxolan-4-yl)methyl)-3-mesityl-1*H*-imidazol-3-ium iodide, (**IN-4a**), (100 mg, 0.176 mmol) were added to 2 mL of acetonitrile in a microwave reactor at 120 °C, 220 W, during 3 hours. When the

reaction was finished the solvent was evaporated and 120 mL of chloroform added and washed using ammonia (3x1 mL). The organic layer was dried over Na₂SO₄ and evaporated to dryness. The crude was washed with ethyl ether and the precipitate filtered, the solvent was evaporated to afford 63 mg of yellow oil. Yield= 61%.

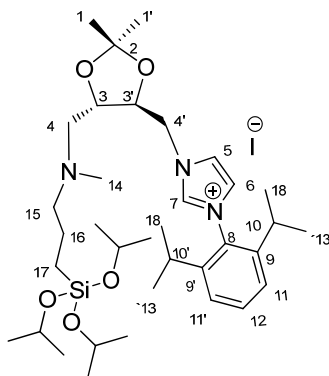
MS (ES⁺) (m/z; %): 590 (M⁺; 100), 591 (M⁺+1; 50).

IR (KBr; cm⁻¹): ν = 2972 (C-H); 2931 (C-H); 1667 (C=N); 1609 (C=N); 1562 (C=N); 1548 (C=N); 1370 (=C-N); 1038 (Si-O); 852(Si-O-C); 752 (Si-C); 734(Si-C).

¹H-NMR (CDCl₃) δ (ppm): 9.87 (s, H₇); 7.82 (t, H₅); 7.17 (t, H₆); 7.00 (s, 2H, H₁₁, H_{11'}); 5.18 (dd, 1H, CH₂, *J*_{3,4'} = 14.8 Hz, *J*_{4',4} = 2.20 Hz, H_{4'}); 4.82 (dd, 1H, CH₂, *J*_{3,4'} = 14.20 Hz, *J*_{3,4'} = 8.06 Hz, H_{4'}); 4.20 (sep, 3H, *J* = 6.10 Hz, 3C-H_{isopr}) 4.15-4.10 (m, 1H, H_{3'}); 3.99-3.94 (m, 1H, H₃); 2.84 (dd, 1H, CH₂, *J*₃₄ = 13.4 Hz, *J*₄₄ = 5.1 Hz, H₄); 2.67 (dd, 1H, CH₂, *J*₃₄ = 13.4 Hz, *J*₄₄ = 6.59 Hz, H₄); 2.42-2.46 (m, 2H, CH₂₍₁₅₎); 2.33 (s, 3H, CH₃, H₁₃); 2.31 (s, 3H, CH₃, H₁₄); 2.13 (s, 3H, CH₃, H₁₀ or H_{10'}); 2.05 (s, 3H, CH₃, H₁₀ or H_{10'}); 1.60-1.50 (m, 2H, CH₂, H₁₆); 1.40 (s, 3H, CH₃, H₁ or H_{1'}); 1.37 (s, 3H, CH₃, H₁ or H_{1'}); 1.26 (d, 18H, *J* = 6.10 Hz, 6CH_{3isopr}); 0.54 (m, 2H, CH₂, H₁₇).

¹³C-NMR (CDCl₃) δ (ppm): 141.4 (C₁₂); 138.8 (CH; C₇); 134.4 (C₉ or C_{9'}); 134.1 (C₉ or C_{9'}); 130.4 (C₈); 129.9 (CH; C₁₁ or C_{11'}); 129.8 (CH; C₁₁ or C_{11'}); 123.9 (CH; C₅); 122.6 (CH; C₆); 110.2 (C₂); 78.8 (CH; C_{3'}); 77.2 (CH; C₃); 64.8 (3xCH_{isopr}); 61.6 (C₁₅); 59.1 (CH₂; C₄); 52.1 (CH₂; C_{4'}); 43.0 (C₁₄); 27.2 (2CH₃; C₁ , C_{1'}); 25.5 (6CH_{3isopr}); 21.0 (CH₃; C₁₃); 20.5 (C₁₆); 18.0 (CH₃; C₁₀ or C_{10'}); 17.6 (CH₃; C₁₀ or C_{10'}); 9.5 (C₁₇).

3-(2,6-diisopropylphenyl)-1-(((4*S*,5*S*)-2,2-dimethyl-5-((methyl(3-(triisopropoxysilyl)propyl)amino)methyl)-1,3-dioxolan-4-yl)methyl)-1*H*-imidazol-3-ium iodide. ((*S,S*-)[6*b*]*I*).



N-methyl-3-(triisopropoxysilyl)propan-1-amine (89 mg, 0.320 mmol) and 3-(2,6-diisopropylphenyl)-1-(((4*S*,5*R*)-5-(iodomethyl)-2,2-dimethyl-1,3-dioxolan-4-yl)methyl)-1*H*-imidazol-3-ium iodide, (**IN-4b**), (150 mg, 0.246 mmol) were added to acetonitrile (2 mL) the mixture was heated in a microwave reactor at 120 °C, 220 W, 3 hours. When the reaction was finished the solvent was evaporated and 120 mL of chloroform added and washed with ammonia (3x1 mL). The organic layer was dried over Na₂SO₄ and concentrated. The crude was washed with ethyl ether the precipitate filtered and the solvent evaporated to afford 100 mg of yellow oil. Yield= 50%.

MS (ES⁺) (m/z; %): 632 (M⁺; 100), 633 (M⁺+1; 50).

IR (KBr; cm⁻¹): ν = 3060 (C_{ar}-H); 2970-2868 (C-H); 1657 (C=C); 1547 (C=N); 1464 (=C-N); 1381 (=C-N); 1038 (Si-O); 845 (Si-O); 762 (Si-C).

¹H NMR (CDCl₃) δ (ppm): 9.88 (s, H₇); 7.97 (t, 1H, *J*_{HH} = 1.77 Hz, H₅); 7.56 (t, 1H, *J*_{HH} = 7.91 Hz, H₁₂); 7.36-7.30 (m, 2H, 2CH, H₁₁, H_{11'}); 7.17 (t, 1H, *J*_{HH} = 1.70 Hz, H₆); 5.22 (dd, 1H, CH₂, *J*_{3,4'} = 13.9 Hz, *J*_{4',4} = 2.29 Hz, H_{4'}); 5.01 (dd, 1H, CH₂, *J*_{3,4'} = 13.9 Hz, *J*_{3,4'} = 8.4 Hz, H_{4'}); 4.21 (sep, 3H, *J* = 6.18 Hz, C-H_{isopr}); 4.18-4.12 (m, 1H, CH, H_{3'}); 4.07-4.00 (m, 1H, CH, H₃); 2.88 (dd, 1H, CH₂, *J*₃₄ = 13.27 Hz, *J*₄₄ = 5.03 Hz, H₄); 2.70 (dd, 1H, CH₂, *J*₃₄ = 13.04 Hz, *J*₄₄ = 6.41 Hz, H₄); 2.51-2.43 (m, 3H, CH₂₍₁₅₎, 1H_{10 or 10'}); 2.32 (s, 3H, CH₃, H₁₄); 2.28-2.23 (m, 1H, CH, H_{10 or 10'}); 1.62-1.54

(m, 2H, CH₂₍₁₆₎); 1.41 (s, 3H, CH₃, H₁ or H_{1'}); 1.36 (s, 3H, CH₃, H₁ or H_{1'}); 1.31-1.23 (m, 12H, 4CH₃; H₁₃, H_{13'}, H₁₈, H_{18'}); 1.26 (d, 18H, $J = 6.18$ Hz, CH_{3isopr}); 0.59-0.54 (m, 2H, CH₂₍₁₇₎).

¹³C NMR (CDCl₃) δ (ppm) = 145.5 (C₉ or C_{9'}); 145.2 (C₉ or C_{9'}); 138.2 (C₇); 132.0 (C₁₂); 129.9 (C₈); 124.8 (CH; C₁₁ or C_{11'}); 124.6 (CH; C₁₁ or C_{11'}); 123.9 (CH; C₅); 123.6 (CH; C₆); 110.3 (C₂); 77.8 (CH; C₃); 76.1 (CH; C₃); 64.8 (3CH_{isopr}); 61.7 (C₁₅); 59.1 (CH₂; C₄); 52.3 (CH₂; C_{4'}); 43.1 (C₁₄); 28.7 (C₁₀ or C_{10'}); 28.5 (C₁₀ or C_{10'}); 27.2 (CH₃; C₁ or C_{1'}); 27.2 (CH₃; C₁ or C_{1'}); 25.6 (6CH_{3isopr}); 24.5 (CH₃; C₁₈ or C_{18'} or C₁₃ or C_{13'}); 24.4 (CH₃; C₁₈ or C_{18'} or C₁₃ or C_{13'}); 24.3 (CH₃; C₁₈ or C_{18'} or C₁₃ or C_{13'}); 24.1 (CH₃; C₁₈ or C_{18'} or C₁₃ or C_{13'}); 20.6 (C₁₆); 9.5 (C₁₇).

5.3 Synthesis of complexes.

5.3.1 Synthesis of bis-*N*-heterocyclic carbene complexes.

General method: to a solution of (*S,S*)-[3a]I (1 mmol, 754 mg) or (*S,S*)-[3b]I (1 mmol, 838 mg) in dichloromethane, Ag₂O (1 mmol, 231 mg) was added and the mixture stirred at room temperature for 24 h under N₂ atmosphere. The mixture was filtered through Celite in order to remove unreacted Ag₂O and other insoluble solids. AuCl(tht) (2 mmol, 632 mg), PdCl₂(cod) (1 mmol, 259 mg) or [RhCl(cod)]₂ (0.5 mmol, 246 mg) was added to the solution of the resulting silver salt in CH₂Cl₂. After 3 h at room temperature, the mixture was filtered through Celite. The solvents were removed in vacuum, and the residue thoroughly washed with diethyl ether and/or pentane. Several attempts to obtain suitable crystals for X-ray diffraction were unsuccessful.

5.3.1.a (*S,S*)-[3a][Au(I)Cl]₂ (3aAu):

Pale yellow. Yield: 84%. M.p.: 138-141 °C. C₃₁H₃₈N₄O₂Au₂Cl₂ (963.5): C: 38.6; H: 4.0; N: 5.8; Au: 40.9; found C: 38.3; H: 4.1; N: 5.5; Au: 40.2 %.

MS (ES⁺) (m/z; %): 927 (M⁺-Cl), 731 (M⁺-AuCl).

IR (KBr, cm⁻¹): $\nu = 3142$ (CH_{arom}); 1605 (C=C); 328 (Au-Cl).

^1H NMR (CDCl_3 , ppm): δ = 7.19 (2H, s, CH_{im}); 7.05-7.00 (4H, m, H_{arom}); 6.94 (2H, s, CH_{im}); 4.81-4.64 (2H, m, CH_2); 4.63-4.58 (2H, m, OCH); 4.53-4.39 (2H, m, CH_2); 2.32 (3H, s, $p\text{-CH}_3$); 2.30 (3H, s, $p\text{-CH}_3$); 2.00 (6H, s, $o\text{-CH}_3$); 1.97 (6H, s, $o\text{-CH}_3$); 1.45 (3H, s, CH_3); 1.35 (3H, s, CH_3).

^{13}C NMR (CDCl_3 , ppm): δ = 177.12 (C-Au); 141.80 (C-N); 141.73 (C-N); 134.75 (C($p\text{-CH}_3$)); 134.70 (C($p\text{-CH}_3$)); 130.77 (CH_{arom}); 130.19 (CH_{arom}); 129.75 (C($o\text{-CH}_3$)); 129.65 (C($o\text{-CH}_3$)); 125.39 (CH_{im}); 124.69 (CH_{im}); 123.32 (CH_{im}); 123.10 (CH_{im}); 112.06 (C(CH_3) $_2$); 76.31 (OCH); 75.67 (OCH); 52.06 (CH_2); 51.20 (CH_2); 27.52 (CH_3); 27.19 (CH_3); 21.24 ($p\text{-CH}_3$); 17.92 ($o\text{-CH}_3$).

5.3.1.b (*S,S*)-[3a]/[Au(OPNB)] $_2$:

A suspension of (*S,S*)-[3a][AuCl] $_2$ (50 mg, 0.052 mmol) and AgOPNB (42 mg, 0.15 mmol, 3 equiv) in chloroform (1.5 mL) was sonicated for 5 min. The resulting off-white dispersion was filtered through a plug of celite (0.5 x 2 cm), washed with chloroform (3 x 2 mL), and concentrated to approximately 1 mL. A white solid formed upon dropwise addition of hexanes. The remaining solvent was removed *in vacuum* to afford (*S,S*)-[3a][Au(I)(OPNB)] $_2$ as an analytically pure white solid. Yield: 61 %. M.p.: 148-150 °C. $\text{C}_{45}\text{H}_{46}\text{N}_6\text{O}_{10}\text{Au}_2$ (1224.8): C: 44.1; H: 3.8; N: 6.9; Au: 32.2; found C: 44.7; H: 4.1; N: 7.4; Au: 31.8 %.

MS (ES^+) (m/z; %): 695 (3aAu).

IR (KBr, cm^{-1}): ν = 3153 (CH_{arom}); 1589 (C=O); 1522, 1333 (NO_2).

^1H RMN (CDCl_3 , ppm): δ = 8.18-8.09 (8H, m, H_{OPNB}); 6.98-6.68 (8H, m, CH_{im} , H_{arom}); 4.76 (2H, m, CH_2); 4.55-4.46 (2H, m, CHO); 4.36-4.28 (2H, m, CH_2); 2.43 (3H, s, $p\text{-CH}_3$); 2.40 (3H, s, $p\text{-CH}_3$); 1.99 (3H, s, $o\text{-CH}_3$); 1.81 (3H, s, $o\text{-CH}_3$); 1.70 (3H, s, $o\text{-CH}_3$); 1.54 (3H, s, $o\text{-CH}_3$); 1.40 (3H, s, OC(CH_3) $_2$); 1.27 (3H, s, OC(CH_3) $_2$).

^{13}C NMR (CDCl_3 , ppm): δ = 185.76 (C-Au); 184.05 (C-Au); 169.00 (CNO $_2$); 149.08 (CNO $_2$); 141.37 (C-N); 139.78 (C-N); 134.80 (C($p\text{-CH}_3$)); 134.50 (C($p\text{-CH}_3$)); 130.53 (C $_{\text{OPNB}}$); 129.79 (CH_{arom}); 129.50, 129.00 (C($o\text{-CH}_3$)); 124.88 (CH_{im}); 124.01 (CH_{im}); 122.86 (C $_{\text{OPNB}}$); 122.01 (CH_{im}); 111.41 (C(CH_3) $_2$); 76.04 (CHO); 75.31 (CHO);

54.49 (CH₂); 50.71 (CH₂); 29.67 (OC(CH₃)₂); 26.88 (OC(CH₃)₂); 21.03 (*p*-CH₃); 17.43 (*o*-CH₃).

5.3.1.c (*S,S*)-[**3b**]/[Au(I)Cl]₂ (**3bAu**).:

Pale yellow. 85%. M.p.: 152-155 °C. C₃₇H₅₀N₄O₂Au₂Cl₂ (1046.6): C: 42.5; H: 4.7; N: 5.4; Au: 37.6; found C: 42.0; H: 4.6; N: 5.5; Au: 37.1 %.

MS (ES⁺) (m/z; %): 1011 (M⁺ - Cl), 815 (M⁺ - AuCl).

IR (KBr, cm⁻¹): ν = 3140 (CH_{arom}); 1610 (C=C); 331 (Au-Cl).

¹H NMR (CDCl₃, ppm): δ = 7.57 (2H, d, CH_{im}); 7.50-7.44 (3H, m, H_{arom}); 7.27-7.21 (3H, m, H_{arom}); 6.96 (2H, s, CH_{im}); 4.82-4.77 (2H, m, CH₂); 4.64-4.61 (2H, m, OCH); 4.53-4.43 (2H, m, CH₂); 2.54-2.48 (2H, m, CH), 2.31-2.23 (m, 2H, CH), 1.66-1.64 (6H, CH₃); 1.36-1.29 (12H, CH₃); 1.17-1.08 (12H, CH₃).

¹³C NMR (CDCl₃, ppm): δ = 173.88 (C-Au); 146.40, 146.00 (C_{arom}-N); 134.33, 131.32 (*p*-CH_{arom}); 127.02 (C(*o*-CH₃)); 125.47 (C(*o*-CH₃)); 124.69 (CH_{im}); 123.32 (CH_{im}); 123.07 (CH_{im}); 112.13 (C(CH₃)₂); 76.65 (OCH); 76.26 (OCH); 52.00 (CH₂); 29.43 (CH); 27.39 (CH₃); 24.77 (CH₃).

5.3.1.d (*S,S*)-[**3a**]/[Au(III)Cl₂]/PF₆ (**3aAu(III)**). :

To a solution of 3,3'-((4*S*,5*S*)-2,2-dimethyl-1,3-dioxolane-4,5-diyl)bis(methylene) bis(1-(2,4,6-trimethylphenyl)-1H-imidazol-3-ium) iodide (0.13 mmol, 100 mg) in dichloromethane, Ag₂O (0.066 mmol, 15 mg) was added and the mixture stirred at room temperature for 24 h under N₂ atmosphere. The mixture was filtered through Celite in order to remove unreacted Ag₂O and other insoluble solids and dried. The crude was solved in acetonitrile and K[AuCl₄] (0.066 mmol, 25 mg) and AgPF₆ (0.099 mmol, 25 mg) were added to the solution of the resulting silver salt. After half hour at room temperature, the mixture was filtered through Celite. The solvents were removed in vacuum, and the residue thoroughly washed with diethyl ether and/or pentane to afford a orange solid. Several attempts to obtain suitable crystals for X-ray diffraction were unsuccessful. Yield: 30%.

IR (KBr, cm⁻¹): ν = 3146 (CH_{arom}); 2994, 2922 (CH); 1735, 1610 (C=N, C=C); 848 (PF₆).

¹H-NMR (CDCl₃, ppm): δ = 9.09-8.86 (m, 2H, CH_{im}); 8.21-7.93 (m, 2H, CH_{im}); 7.03 (s, 4H, H_{arom}); 5.22-5.06 (m, 1H, CH₂); 5.02-4.90 (m, 1H, CH₂); 4.80-4.38 (m, 4H, 2OCH, CH₂); 2.34 (s, 3H, *p*-CH₃); 2.33 (s, 3H, *p*-CH₃); 2.06 (d, 6H, 2*o*-CH₃); 2.03 (d, 6H, 2*o*-CH₃); 1.42 (s, 3H, CH₃); 1.39 (s, 3H, CH₃).

¹³C-NMR (CDCl₃, ppm): δ = 173.1 (2C-Au); 141.5 (C-N); 141.4 (C-N); 134.7 (2C(*p*-CH₃)); 129.9 (4CH_{arom}); 129.5 (2C(*o*-CH₃)); 129.4 (2C(*o*-CH₃)); 124.8 (CH_{im}); 124.7 (CH_{im}); 123.4 (CH_{im}); 123.3 (CH_{im}); 111.6 (C(CH₃)₂); 76.1 (OCH); 76.0 (OCH); 53.3 (CH₂); 51.20 (CH₂); 27.1 (CH₃); 26.9 (CH₃); 21.1 (2C, *p*-CH₃); 17.9 (*o*-CH₃); 17.6 (2*o*-CH₃); 17.4 (*o*-CH₃); 17.3 (*o*-CH₃).

ESI-MS (m/z): 731(L+Au+Cl).

5.3.1.e (*S,S*)-[3a][PdCl₂]. (3aPd):

Red-brown. Yield: 85 %. 188-190 °C. C₃₁H₃₈Cl₂N₄O₂Pd (676.0): C: 54.9; H: 5.9; N: 8.3; Pd: 15.7 % found C: 54.7; H: 5.6; N: 8.1, Pd: 15.1 %.

MS (ES⁺) (m/z; %): 677 (M⁺), 605 (M⁺-2Cl).

IR (KBr, cm⁻¹): ν = 1610 (C=C.); 1241, 1207 (C-O-C); 578 (Pd-C).

¹H NMR (CDCl₃, ppm): δ = 7.10 (2H, s, CH_{im}); 6.95 (4H, s, H_{arom}); 6.83 (2H, s, CH_{imi}); 6.23 (2H, d, *J* = 15 Hz, CH₂); 5.24-4.96 (2H, m, CH₂); 4.90-4.65 (2H, m, OCH); 2.36 (6H, s, *p*-CH₃); 2.10 (6H, s, *o*-CH₃); 2.04 (6H, s, *o*-CH₃); 1.61 (6H, s, (CH₃)₂C-).

¹³C NMR (CDCl₃, ppm): δ = 175.00 (C-Pd); 141.42 (C-N) 137.74 (C(*p*-CH₃)); 130.17 (CH_{arom}); 129.81 (C(*o*-CH₃)); 125.25 (CH_{imi}); 123.19 (CH_{im}); 112.14 (C(CH₃)₂); 77.79 (CHO); 52.82 (CH₂); 27.95 (OC(CH₃)₂); 21.49 (*p*-CH₃); 19.04 (*o*-CH₃).

5.3.1.f (*S,S*)-[3a][RhCl(cod)]. (3aRh):

Green-brown. Yield: 70 %. M.p.: 250 °C (dec.). C₃₉H₅₀ClN₄O₂Rh (745.2): C: 62.9; H: 6.8; N: 7.5; Rh: 13.6 % found C: 62.4; H: 7.3; N: 7.3; Rh: 13.0 %.

MS (ES⁺) (m/z; %): 745 (M⁺).

IR (KBr, cm⁻¹): ν = 1632 (C=C); 1228, 1203 (C-O-C); 525 (Rh-C).

¹H NMR (CDCl₃, ppm): δ = 7.09 (2H, s, CH_{im}); 6.99 (4H, s, H_{arom}); 6.88 (2H, s, CH_{im}); 6.18-6.02 (2H, m, CH₂); 5.20-5.00 (2H, m, CH₂); 4.97-4.54 (4H, m, OCH,

NHC's

CH_{cod}); 3.61-3.29 (2H, m, CH_{cod}); 2.56-2.18 (8H, m, CH_{2(cod)}); 2.40 (3H, s, *p*-CH₃); 2.30 (3H, s, *p*-CH₃); 2.06 (6H, s, *o*-CH₃); 1.97 (6H, s, *o*-CH₃); 1.60 (6H, m, (CH₃)₂C-).

¹³C NMR (CDCl₃, ppm): δ= 179.81 (C-Rh); 141.23 (C-N) 132.20 (C(*p*-CH₃)); 130.17 (CH_{arom}); 129.06 (C(*o*-CH₃)); 126.33 (CH_{im}); 124.20 (CH_{imi}); 111.30 (C(CH₃)₂); 95.30 (CH_{cod}); 78.46 (CHO); 69.33 (CH_{cod}); 53.41 (CH₂); 28.42 (CH_{2(cod)}); 27.72 (OC(CH₃)₂); 21.39 (*p*-CH₃); 18.29 (*o*-CH₃).

5.3.1.g (*S,S*)-[3a][CuI]. (3aCu):.

3,3'-((4*S*,5*S*)-2,2-dimethyl-1,3-dioxolane-4,5-diyl)bis(methylene)bis(1-(2,4,6-trimethylphenyl)-1H-imidazol-3-ium) iodide (50 mg, 0.066mol) and Cu₂O (10.4 mg, 0.077 mmol) were added to 2 mL of toluene in a microwave reactor at 130 °C, 220 W, during 1 hour. When the reaction was finished the solvent was evaporated and the crude was washed with ethyl ether to afford a white powder solid. Yield=66%.

IR (KBr, cm⁻¹): ν = 3137 (CH_{arom}); 2992, 2934 (CH); 1620, 1576 (C=N, C=C).

¹H-NMR (CDCl₃, ppm): δ= 7.67-7.54 (m, 2H, CH_{im}); 7.36 (s, 1H, H_{arom}); 7.16 (s, 1H, H_{arom}); 7.14-7.09 (m, 2H, CH_{im}); 6.89 (s, 1H, H_{arom}); 6.53 (s, 1H, H_{arom}); 5.34 (d, 2H, CH₂); 5.04 (d, 2H, CH₂); 4.47-4.38 (m, 1H, OCH); 4.26-4.15 (m, 1H, OCH); 2.63 (s, 6H, *p*-CH₃); 2.33-2.15 (m, 12H, *o*-CH₃); 1.65 (s, 6H, CH₃).

¹³C-NMR (CDCl₃, ppm): δ= 182.7 (2C-Cu); 152.4 (C-N); 139.2 (C-N); 138.7 (C(*p*-CH₃)); 136.35 (C(*p*-CH₃)); 135.1 (2CH_{arom}); 134.9 (2CH_{arom}); 129.3 (2C(*o*-CH₃)); 129.2 (C(*o*-CH₃)); 129.0 (C(*o*-CH₃)); 122.6 (CH_{im}); 122.2 (CH_{im}); 121.7 (CH_{im}); 120.6 (CH_{im}); 110.1 (C(CH₃)₂); 76.9 (OCH); 76.6 (OCH); 51.8 (CH₂); 51.1 (CH₂); 27.3 (CH₃); 26.8 (CH₃); 21.1 (2 *p*-CH₃); 18.1 (*o*-CH₃); 18.0 (*o*-CH₃); 17.9 (*o*-CH₃); 17.8 (*o*-CH₃).

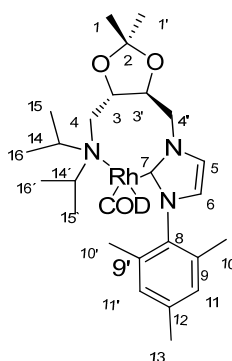
MALDI-MS (m/z): 687(L+Cu+I).

5.3.2 Synthesis of mono-*N*-heterocyclic carbene amine complexes.

5.3.2.a Synthesis of Rh and Pd mono-*N*-heterocyclic amine complexes. Reference soluble systems.

We have synthesized all *mono*-carbene complexes but haven't been possible to isolate and therefore have been generated "in situ" and used in catalytic tests. Only **5aRh** has been fully characterized

((*S,S*)-[**5a**]Rh(cod)). (**5aRh**).:



To a solution of ((*S,S*)-[**5a**]I) (50 mg, 0.0924 mmol) was added [RhCl(cod)]₂ (33 mg, 0.046 mmol) under inert atmosphere. After 3 hours stirring at room temperature, ^tBuOK (10 mg, 0.0924 mmol) was added and mixture heated to 50 °C during 12 hours. The solution was concentrated and the crude washed with pentane to afford 45 mg of yellow solid. Yield= 73%.

EM (ES) : 624 (M⁺).

IR (KBr; cm⁻¹): ν = 3435 (C-N); 2935-2818 (C-H); 1619 (C=C); 1562 (C=N); 1463 (=C-N); 1243 (C-N).

¹H NMR (CDCl₃) δ (ppm): 7.92 (s, H₅); 7.68 (s, H₆); 7.06 (s, 2H, 2CH, H₁₁ or H_{11'}); 6.95 (s, 2H, 2CH, H₁₁ or H_{11'}); 4.95 (dd, 1H, CH₂, H_{4'}); 5.33-5.25 (m, 2H, CH_{cod}); 4.59 (dd, 1H, CH₂, H_{4'}); 4.17 (m, 1H, CH, H₃ or H_{3'}); 4.06 (m, 1H, CH, H₃ or H_{3'}); 3.61-3.29 (m, 2H, CH_{cod}); 3.11 (m, 1H, CH, H₁₄ or H_{14'}); 2.93 (m, 2H, CH₂, H₄, H, CH, H₁₄ or H_{14'}); 2.56-2.18 (m, 8H, CH_{2(cod)}); 2.37 (s, 3H, CH₃, H₁₃); 2.08 (s, 3H, CH₃, H₁₀).

NHC's

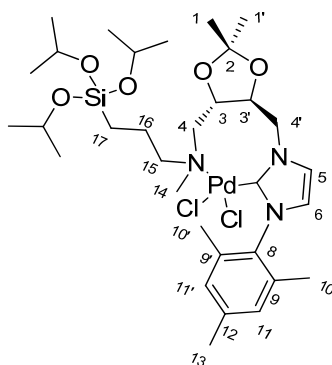
or H_{10'}); 2.04 (s, 3H, CH₃, H₁₀ or H_{10'}); 1.42 (s, 3H, CH₃, H₁ or H_{1'}); 1.38 (s, 3H, CH₃, H₁ or H_{1'}); 1.10 (d, 6H, 2CH₃, H₁₅ or H_{15'} or H₁₆ or H_{16'}); 1.05 (d, 6H, 2CH₃, H₁₅ or H_{15'} or H₁₆ or H_{16'}).

¹³C NMR (CDCl₃) δ (ppm): 168.0 (C-Rh, C₇); 142.4 (C₁₂); 133.3 (C₉, C_{9'}); 130.7 (CH, C₁₁ or C_{11'}); 130.3 (CH, C₁₁ or C_{11'}); 129.9 (C₈); 123.9 (CH, C₅); 123.1 (CH, C₆); 110.8 (C₂); 87.4 (CH_(cod)); 77.4 (CH; C_{3'}, C₃); 69.3 (CH_(cod)); 53.2 (CH₂, C_{4'}); 48.5 (C₁₄ or C_{14'}); 49.2 (C₁₄ or C_{14'}); 47.1 (CH₂, C₄); 27.4 (2CH₃, C₁, C_{1'}); 29.7 (CH_{2(cod)}); 22.2 (2CH₃, C₁₅ or C_{15'} or C₁₆ or C_{16'}); 19.3 (CH₃, C₁₃); 20.0 (2CH₃, C₁₅ or C_{15'} or C₁₆ or C_{16'}); 17.9 (CH₃, C₁₀ or C_{10'}); 17.1 (CH₃, C₁₀ or C_{10'}).

5.3.2.b Synthesis of Mono-N-heterocyclic carbene amine complexes with pendant alkoxy silane group.

Synthesis of mono-N-heterocyclic carbene amine palladium complexes with pendant alkoxy silane groups.

General method: To a solution of ((*S,S*)-[6a]I) (40 mg, 0.056 mmol) or ((*S,S*)-[6b]I) (0.053 mmol, 40 mg) in dichloromethane, Ag₂O (6 mg, 0.028 mmol) was added and the mixture stirred at room temperature for 24 h under N₂ atmosphere. The mixture was filtered through Celite in order to remove unreacted Ag₂O and other insoluble solids. PdCl₂(cod) (21 mg, 0.056 mmol) or (20 mg, 0.053 mmol) respectively was added to the solution of the resulting silver salt in CH₂Cl₂. After 3 h at room temperature, the mixture was filtered through Celite. The solvents were removed in vacuum, and the residue thoroughly washed with diethyl ether and/or pentane.

(*S,S*)-[6a]PdCl₂ (6aPd):

C₃₂H₅₅Cl₂N₃O₅PdSi Calculated for ([Pd]CH₂Cl₂); (C, 46.51; H, 6.74; N, 4.93)
found: C, 46.77; H, 6.68; N, 4.67.

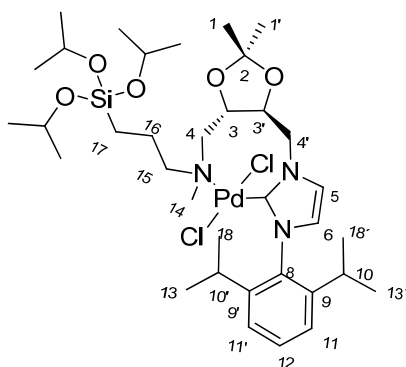
UV-Vis: λ_{max} = 447 nm, 366 nm, 286 nm, 270 nm.

ES (MS): 768 (M⁺); 590 (L)

IR (KBr; cm⁻¹): ν = 3005 (C_{Ar}-H); 2959 (C-H); 2859 (C-H); 1612 (C=C); 1484 (C=N); 1382 (=C-N); 1370 (=C-N); 1038 (Si-O); 887 (Si-O-C); 748 (Si-C); 579 (Pd-C).

¹H NMR (CDCl₃) δ (ppm): 7.68-7.61 (m, 1H, H₅); 7.51-7.47 (m, 1H, H₆); 7.07-6.91 (m, 2H, 2CH, H₁₁, H_{11'}); 4.70 (d, 1H, CH₂, $J_{3,4}$ =14.4 Hz, H_{4'}); 4.42 (d, 1H, CH₂, $J_{3,4}$ =15.95 Hz, H_{4'}); 4.38-4.06 (m, 5H, 3CH_{isopr}, 2CH, H_{3'}, H₃); 2.58-2.53 (m, 1H, CH₂, H₄); 2.47-2.44 (m, 1H, CH₂, H₄); 2.39-2.33 (m, 5H, 1CH₃, H₁₃, CH₂₍₁₅₎); 2.11 (s, 3H, CH₃, H₁₄); 1.60 (s, 6H, 2CH₃, H₁₀, H_{10'}); 1.55-1.54 (m, 2H, CH₂₍₁₆₎); 1.37 (s, 3H, CH₃, H₁ or H_{1'}); 1.32 (s, 3H, CH₃, H₁ or H_{1'}); 1.25-1.16 (m, 18H, 6CH_{3isopr}); 0.84 (m, 2H CH₂₍₁₇₎).

¹³C NMR (CDCl₃) δ (ppm)=177.3 (Pd-C) 139.4 (C₁₂); 136.2 (C₉ or C_{9'}); 135.1 (C₉ or C_{9'}); 132.7 (C₈); 132.2 (2CH; C₁₁, C_{11'}); 129.6 (CH; C₅); 129.1 (CH; C₆); 110.7 (C₂); 79.3 (CH; C_{3'}); 78.3 (CH; C₃); 65.2 (3CH_{isopr}); 65.1 (C₁₅); 65.0 (CH₂; C₄); 64.1 (CH₂; C_{4'}); 50.7 (C₁₄); 29.7 (2CH₃; C₁, C_{1'}); 25.7 (6CH_{3isopr}); 21.1 (CH₃; C₁₃); 19.2 (C₁₆); 18.8 (CH₃; C₁₀ or C_{10'}); 15.3 (CH₃; C₁₀ or C_{10'}); 9.5 (C₁₇).

(S,S)-[6b]PdCl₂. (6bPd):

C₃₅H₆₁Cl₂N₃O₅PdSi Calculated for ([Pd].2CH₂Cl₂); (C, 45.39; H, 6.69; N, 4.29)
found: C, 45.42; H, 6.58; N, 3.69.

UV-Vis: λ_{max} = 476 nm, 353 nm, 285 nm, 271 nm.

ES(MS): 810 (M⁺+1), 633 (M+•-3OⁱPr).

IR (KBr; cm⁻¹): ν = 3133 (C_{ar}-H); 2969, 2918 (C-H); 1458 (=C-N); 1375 (=C-N); 1272 (C-OC); 1035 (Si-O-C); 799 (Si-C); 325 (Pd-Cl).

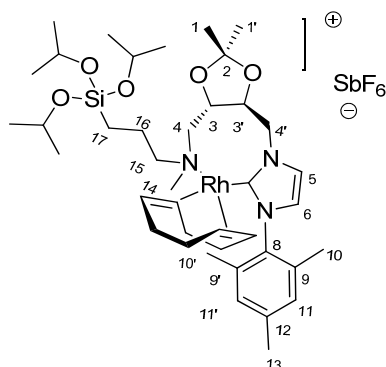
¹H NMR (CDCl₃) δ (ppm): 7.89-7.62 (m, H₅); 7.58-7.44 (m, 4H, 4CH, H₁₂, H₁₁, H_{11'}, H₆); 4.56-4.51 (m, 1H, CH₂, H_{4'}); 4.34-4.09 (m, 4H, 1H, CH₂, H_{4'}, 3CH_{isopr}); 3.49-4.44 (m, 1H, CH, H_{3'}); 3.09-3.00 (m, 1H, CH, H₃); 2.54-2.48 (m, 1H, CH₂, H₄); 2.40-2.34 (m, 1H, CH₂, H₄); 1.61-1.67 (m, 5H, CH₃, H₁₄, CH₂₍₁₅₎); 1.54-1.45 (m, 4H, 2CH, H₁₀, H_{10'}, CH₂₍₁₆₎); 1.43 (s, 3H, CH₃, H₁ or H_{1'}); 1.42 (s, 3H, CH₃, H₁ or H_{1'}); 1.25 (d, 18H, 6CH₃, J =1.9 Hz, CH_{3isopr}); 1.20 (d, 6H, 2CH₃, J = 5.42 Hz, H₁₃ or H_{13'} or H_{18'} or H₁₈); 1.17 (d, 6H, 2CH₃, J = 5.42 Hz, H₁₃ or H_{13'} or H_{18'} or H₁₈); 0.69-0.45 (m, 2H, CH₂₍₁₇₎).

¹³C NMR (CDCl₃) δ (ppm)= 176.2 (C-Pd, C₇); 147.5 (C₉ or C_{9'}); 146.2 (C₉ or C_{9'}); 132.8 (C₁₂); 132.2 (C₈); 126.3 (2CH; C₁₁, C_{11'}); 124.2 (CH; C₅); 124.1 (CH; C₆); 104.1 (C₂); 77.2 (CH; C_{3'}); 76.9 (CH; C₃); 65.8 (3CH_{isopr}); 65.4 (C₁₅); 65.2 (CH₂; C₄); 65.0 (CH₂; C_{4'}); 52.0 (C₁₄); 30.9 (2C, C₁₀, C_{10'}); 30.3 (CH₃; C₁ or C_{1'}); 30.2 (CH₃; C₁ or C_{1'}); 29.7 (2CH₃; C₁₈ or C_{18'} or C₁₃ or C_{13'}); 25.7 (2CH₃; C₁₈ or C_{18'} or C₁₃ or C_{13'}); 25.6 (6CH_{3isopr}); 15.3 (C₁₆); 9.0 (C₁₇).

Synthesis of mono-*N*-heterocyclic carbene amine rhodium complexes with pendant alkoxy silane groups.

General method: To a solution of ((*S,S*)-[6a]I) (40 mg, 0.056 mmol) or ((*S,S*)-[6b]I) (0.053 mmol, 40 mg) in dichloromethane, Ag₂O (6 mg, 0.028 mmol) was added and the mixture stirred at room temperature for 24 h under N₂ atmosphere. The mixture was filtered through Celite in order to remove unreacted Ag₂O and other insoluble solids. A mixture of [RhCl(cod)]₂ (13.8 mg, 0.028 mmol) or (12.8 mg, 0.026 mmol) respectively and AgSbF₆ (19.2 mg, 0.056 mmol) or (18.2 mg, 0.053 mmol) respectively was added to the solution of the resulting silver salt in THF. After 3 h at room temperature, the mixture was filtered through Celite. The solvents were removed in vacuum, and the residue thoroughly washed with diethyl ether and/or pentane.

((*S,S*)-[6a]Rh(COD). (6aRh).):



C₄₀H₆₇F₆N₃O₅RhSbSi Calculated for ([Rh-cod]CH₂Cl₂); (C, 37.18; H, 5.67; N, 4.15); found C, 37.60; H, 5.22; N, 4.59.

UV-Vis: λ_{max} = 287 nm.

MS (ES): 674 (M⁺-3xⁱPr); 464 (L).

IR (KBr; cm⁻¹): ν = 3145 (C_{Ar}-H); 2918 (C-H); 2876 (C-H); 1571 (C=N); 1231 (C-OC); 1107 (Si-O); 861 (Si-O); 703 (Si-C); 655 (Sb-F).

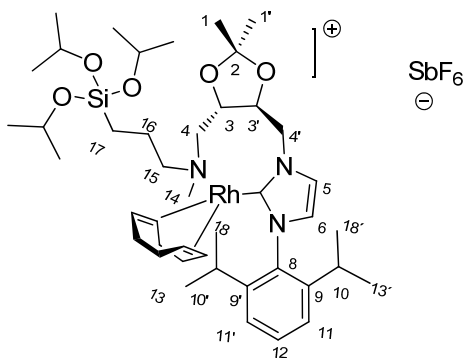
¹H NMR (CDCl₃) δ (ppm): 7.49-7.44 (m, H₅); 7.38-7.33 (m, H₆); 7.08 (s, 1H, CH, H₁₁ or H_{11'}); 6.75 (s, 1H, CH, H₁₁ or H_{11'}); 5.80 (d, 1H, CH₂, J = 12.2 Hz, H₄); 4.78-4.71 (m, 3H, 1H, CH₂, H_{4'}, 2CH_{cod}); 4.54-4.50 (m, 1H, CH, H₃); 4.49-4.36 (m, 2CH_{cod}); 4.33-3.96 (m, 4H, 3CH_{isopr}, 1H, CH, H₃); 3.53-3.42 (m, 1H, CH₂, H₄); 3.26-

NHC's

3.05 (m, 1H, CH₂, H₄); 2.76-2.64 (m, 2H, CH₂₍₁₅₎); 2.38 (s, 3H, CH₃, H₁₃); 2.04-1.96 (m, 11H, 4CH_{2(cod)}, 3H, CH₃, H₁₄); 1.95 (s, 3H, CH₃, H₁₀ or H_{10'}); 1.86 (s, 3H, CH₃, H₁₀ or H_{10'}); 1.45-1.49 (m, 2H, CH₂₍₁₆₎); 1.42 (s, 6H, 2CH₃, H₁, H_{1'}); 1.24-1.15 (m, 18H, 6CH_{3(isopr)}); 0.60-0.51 (m, 2H, CH₂₍₁₇₎).

¹³C NMR (CDCl₃) δ (ppm)= 187.8 (C₇, C-Rh); 139.4 (C₁₂); 138.5 (C₉ or C_{9'}); 136.7 (C₉ or C_{9'}); 134.4 (C₈); 125.5 (2CH; C₁₁, C_{11'}); 123.2 (2CH; C₅, C₆); 111.8 (C₂); 97.3 (2CH_(cod)); 77.2 (CH; C_{3'}); 76.7 (CH; C₃); 69.6 (2CH_(cod)); 65.1 (C₁₅); 64.4 (3CH_{isopr}); 34.1 (CH₂; C₄); 30.78 (C₁₄); 33.7 (CH₂; C_{4'}); 27.1 (4CH_{2(cod)}); 25.5 (2CH₃; C₁, C_{1'}); 25.3 (6CH_{3(isopr)}); 21.1 (CH₃; C₁₃); 19.6 (C₁₆); 17.9 (2CH₃; C₁₀, C_{10'}); 9.2 (C₁₇).

(*S,S*)-[6b]Rh(cod). (6bRh):



C₄₃H₇₃F₆N₃O₅RhSbSi Calculated for ([Rh]CH₂Cl₂); (C, 46.69; H, 6.69; N, 3.40); found C, 46.90; H, 6.83; N, 2.01.

UV-Vis: λ_{max}= 392 nm, 348 nm, 285 nm.

MS (ES): 878 (M⁺-3xⁱPr+SbF₂).

IR (KBr; cm⁻¹): ν = 2959, 2918 (C-H); 1633 (C=C); 1396 (=C-N); 1265 (C-O-C) 1025 (Si-O); 809 (Si-O-C); 655 (Sb-F).

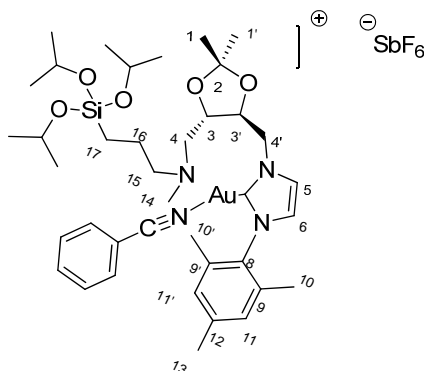
¹H NMR (CDCl₃) δ (ppm): 7.55-7.50 (m, H₅); 7.40-7.34 (m, 1H, H₁₂); 6.97 (s(broad), 2H, 2CH, H₁₁, H_{11'}); 6.93-6.83 (m, H₆); 5.90 (s(broad), 1H, CH₂, H_{4'}); 4.80-4.70 (m, 3H, 1H, CH₂, H_{4'}, 2H, 2CH_(cod)); 4.54-4.50 (m, 1H, CH, H_{3'}); 4.43-4.12 (m, 5H, 3CH_{isopr}, 2CH_(cod)); 3.99-3.89 (m, 1H, CH, H₃); 3.70-3.62 (m, 1H, CH₂, H₄); 3.51-3.41 (m, 1H, CH₂, H₄); 2.26 (s, 3H, CH₃, H₁₄); 1.79-1.64 (m, 10H, CH₂₍₁₅₎, 4CH_{2(cod)}),

1.60-1.52 (m, 4H, 2CH, H₁₀, H_{10'}, CH₂₍₁₆₎); 1.36-1.41 (m, 24H, 2CH₃, H₁, H_{1'}, 6CH₃, CH_{3isopr}); 1.31-1.21 (d, 12H, 4CH₃, H₁₃, H_{13'}, H_{18'}, H₁₈); 0.87-0.81 (m, 2H, CH₂₍₁₇₎).

¹³C NMR (CDCl₃) δ (ppm)=193.2 (C₇, C-Rh); 150.5 (2 C, C₉, C_{9'}); 138.7 (C₁₂); 134.8 (C₈); 129.6 (CH; C₁₁ or C_{11'}); 129.1 (CH; C₁₁ or C_{11'}); 124.5 (2CH, C₅, C₆); 110.1 (C₂); 101.9 (2CH_(cod)); 77.8 (CH; C_{3'}); 77.6 (CH; C₃); 68.2 (2CH_(cod)); 64.8 (3CH_{isopr}); 62.1 (C₁₅); 34.0 (CH₂; C₄); 33.3 (C₁₄); 30.9 (CH₂; C_{4'}); 29.9 (2CH₃; C₁ or C_{1'}); 29.3 (6CH_{3isopr}); 28.7 (2CH₃; C₁₈ or C_{18'} or C₁₃ or C_{13'}); 27.9 (2CH, C₁₀, C_{10'}); 27.1 (4CH_{2(cod)}); 24.5 (CH₃; C₁₈ or C_{18'} or C₁₃ or C_{13'}); 20.2 (C₁₆); 14.3 (CH₃; C₁₈ or C_{18'} or C₁₃ or C_{13'}); 9.02 (C₁₇).

Synthesis of mono-N-heterocyclic carbene amine gold (I) complexes with pendant alkoxy silane groups.

General method: To a solution of ((*S,S*)-[**6a**]**I**) (40 mg, 0.056 mmol) or ((*S,S*)-[**6b**]**I**) (40 mg, 0.053 mmol) in dichloromethane, Ag₂O (6 mg, 0.028 mmol) was added and the mixture stirred at room temperature for 24 h under N₂ atmosphere. The mixture was filtered through Celite in order to remove unreacted Ag₂O and other insoluble solids. A mixture of AuCl(tht) (18 mg, 0.056 mmol) or (17.0 mg, 0.053 mmol) respectively and AgSbF₆ (19.2 mg, 0.056 mmol) or (18.2 mg, 0.053 mmol) respectively was added to a solution of the resulting silver salt in benzonitrile. After 3 h at room temperature, the mixture was filtered through Celite. The solvents were removed in vacuum, and the residue thoroughly washed with diethyl ether and/or pentane.

(*S,S*)-[6a]Au(BzN). (6aAu).:

$C_{39}H_{60}AuF_6N_4O_5SbSi$ Calculated for $(([Au] \ 3BzN)$; (C, 45.77; H, 5.15; N, 5.93); found C, 46.60; H, 5.89; N, 3.77.

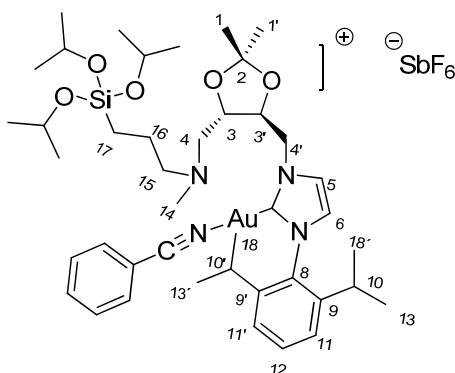
UV-Vis: λ_{max} = 536 nm, 420 nm, 282 nm, 273 nm.

ES (MS): 786(M^+ -BzN); 972(M^+ -1+Na).

IR (KBr; cm^{-1}): ν = 3155 (C_{Ar} -H); 2979 (C-H); 2918 (C-H); 1244, 1216 (C-OC); 1035 (Si-O); 889 (Si-O-C); 853 (Si-C); 756 (Si-C); 655 (Sb-F).

1H -NMR ($CDCl_3$) δ (ppm): 7.66-7.55 (m, 2H, 2*o*-CH, BzN); 7.48-7.38 (m, 3H, *p*-CH, 2*m*-CH, BzN); 6.99-6.88 (m, 2H, H_5 , H_6); 6.89 (s, 1H, CH, H_{11} or $H_{11'}$); 6.86 (s, 1H, CH, H_{11} or $H_{11'}$); 4.74-4.32 (m, 2H, CH_2 , H_4'); 4.26-4.03 (m, 3H, CH_{isopr}); 3.69-3.45 (m, 2H, 2CH, H_3' , H_3); 2.92 (d, 1H, CH_2 , J =9.2 Hz, H_4); 2.71 (d, 1H, CH_2 , J =9.2 Hz, H_4); 2.39-2.34 (m, 2H, $CH_{2(15)}$); 2.27 (s, 3H, CH_3 , H_{13}); 1.98 (s, 3H, CH_3 , H_{14}); 1.96 (s, 3H, CH_3 , H_{10} or $H_{10'}$); 1.95 (s, 3H, CH_3 , H_{10} or $H_{10'}$); 1.49-1.47 (m, 2H, $CH_{2(16)}$); 1.32 (s, 3H, CH_3 , H_1 or $H_{1'}$); 1.30 (s, 3H, CH_3 , H_1 or $H_{1'}$); 1.15-1.10 (m, 18H, CH_{3isopr}); 0.84-0.68 (m, 2H, $CH_{2(17)}$).

^{13}C -NMR ($CDCl_3$) δ (ppm)=182.5 (C-Au; C_7); 139.7 (C_{12}); 134.9 (C_9 or C_9'); 134.8 (C_9 or C_9'); 134.4 (*p*-CH; BzN); 132.8 (2*o*-CH; BzN); 132.6 (C_8); 132.2 (2CH; C_{11} , $C_{11'}$); 129.4 (CH; C_5); 129.3 (CH; C_6); 129.1 (2*m*-CH; BzN); 121.2 (CN; BzN); 112.3 (C-CN; BzN); 111.2 (C_2); 77.80 (CH; C_3'); 77.1 (CH; C_3); 68.1 (C_{15}); 66.6 (2 CH_2 ; C_4 , C_4'); 65.0 (3 CH_{isopr}); 53.4 (C_{14}); 29.7 (2 CH_3 ; C_1 , $C_{1'}$); 25.6 (6 CH_{3isopr}); 21.2 (CH_3 ; C_{13}); 21.1 (C_{16}); 17.1 (CH_3 ; C_{10} or $C_{10'}$); 14.1 (CH_3 ; C_{10} or $C_{10'}$); 10.9 (C_{17}).

(*S,S*)-[6a]Au(BzN). (6bAu):

$C_{42}H_{66}AuF_6N_4O_5SbSi$ Calculated for $([Au]2CH_2Cl_2)$; C, 39.48; H, 4.68; N, 4.19; found C, 38.24; H, 5.35; N, 4.00.

UV-Vis: λ_{max} = 393, 286, 273, 244 nm.

ES (MS): 1044 ($M^+ - 3xiPr + SbF_6^-$); 949 (AuL+Sb).

IR (KBr; cm^{-1}): ν = 3173 ($C_{ar}-H$); 2972, 2931 (C-H); 1721 (C=C); 1468 (=C-N); 1129 (C-O-C); 1043 (Si-O); 807 (Si-O-C); 763 (Si-C); 655 (Sb-F).

1H NMR ($CDCl_3$) δ (ppm): 7.62-7.59 (m, 2H, 2o-CH, BzN); 7.56-7.52 (m, 1H, CH, H_{12}); 7.41-7.41 (m, 3H, *p*-CH, 2 *m*-CH, BzN); 7.38 (br.s., H_5); 7.30 (s.br., H_6); 7.00-6.86 (m, 2H, CH, H_{11} , $H_{11'}$); 4.68-6.64 (m, 1H, CH_2 , $H_{4'}$); 4.48-4.40 (m, 1H, CH_2 , $H_{4'}$); 4.35-4.13 (m, 5H, 3 CH_{isopr} , 2CH, $H_{3'}$, H_3); 3.48-3.41 (m, 1H, CH_2 , H_4); 3.23-3.07 (m, 1H, CH_2 , H_4); 2.96 (br.s., 3H, CH_3 , H_{14}); 2.89-2.83 (m, 1H, CH, H_{10} or $H_{10'}$); 2.82-2.74 (m, 1H, CH, H_{10} or $H_{10'}$); 2.34-2.57 (m., 2H, $CH_{2(15)}$); 1.62-1.58 (m, 2H, $CH_{2(16)}$); 1.39 (br.s., 6H, 2 CH_3 , H_1 , $H_{1'}$); 1.18-1.05 (m, 30H, 10 CH_3 , H_{13} , $H_{13'}$, H_{18} , H_{18} , 6 CH_{3isopr}); 0.65-0.61 (m, 2H, $CH_{2(17)}$).

^{13}C NMR ($CDCl_3$) δ (ppm)= 179.2 (Au-C), 145.9 (C_9 or $C_{9'}$); 145.7 (C_9 or $C_{9'}$); 133.8 (*p*-CH, BzN); 132.8 (2o-CH, BzN); 132.4 (C_{12}); 132.1 (2*m*-CH; BzN); 130.8 (C_8); 129.1 (2CH; C_{11} , $C_{11'}$); 124.3 (CH; C_5); 124.1 (CH; C_6); 122.4 (CN; BzN); 105.6 (C_2); 95.2 (C-CN; BzN); 77.2 (CH; $C_{3'}$); 76.1 (CH; C_3); 65.7 (3 CH_{isopr}); 68.1 (C_{15}); 66.6 (2 CH_2 , C_4 , $C_{4'}$); 53.4 (CH_3 ; C_{14}); 38.7 (2C, C_{10} , $C_{10'}$); 28.9 (CH_3 ; C_1 or $C_{1'}$); 28.7 (CH_3 ; C_1 or $C_{1'}$); 25.4 (6 CH_{3isopr}); 24.4 (CH_3 ; C_{18} or $C_{18'}$ or C_{13} or $C_{13'}$); 24.3

(CH₃; C₁₈ or C_{18'} or C₁₃ or C_{13'}); 24.2 (CH₃; C₁₈ or C_{18'} or C₁₃ or C_{13'}); 24.1 (CH₃; C₁₈ or C_{18'} or C₁₃ or C_{13'}); 22.9 (C₁₆); 10.9 (C₁₇).

5.4 Heterogeneization of complexes containing pendant alkoxy silane groups to MCM-41.

General method: To a suspension of the mesoporous solids, MCM-41, (100 mg) in toluene (25 mL), was added a solution of 10 mg, of complexes in CH₂Cl₂ (5 mL). The slurry was heated at 110 °C for 16 h. The mixture was cooled, and the solid filtered off and washed thoroughly with ethanol, dichloromethane and diethyl ether.

5.4.1 6aPd-MCM.

Found C: 6.35; H: 7.23; N: 5.48; Pd: 0.37 %.

DFTR: λ_{max} (nm)= 576 nm, 521 nm, 362 nm, 336 nm, 286 nm, 258 nm, 225 nm.

IR (KBr): ν = 1629 (C=C) and (C=N); 1223 (Si-O-Si); 1087 (Si-O); 808 (Si-O-C); 812 (Si-C); 566 (Pd-C).

¹³C NMR (300 MHz, Solid Phase, 25 °C, ppm), (Partial): δ = (C-Pd, C₇, No found); 140.1 (C₁₂); 135.4 (2C; C₉, C_{9'}); 132.0-125 (5C; C₈, 2CH; C₁₁, C_{11'}, 2CH; C₅, C₆); 112.2 (C₂); 77.4 (CH; C_{3'}); 72.2 (CH; C₃); 61.4 (CH_{isopr}); 58.4 (C₁₅); 55.3 (CH₂; C₄); 54.0 (CH₂; C_{4'}); 48.4 (CH₃; C₁₄); 30.0 (2CH₃; C₁, C_{1'}); 24.8 (CH_{3isopr}); 18.1-17.0 (3C; CH₃, C₁₃, C₁₆, CH₃, C₁₀ or C_{10'}); 13.3 (CH₃; C₁₀ or C_{10'}); 9.5 (C₁₇).

5.4.2 6bPd-MCM.

Found C: 2.2; H: 4.14; N: 0.80; Pd: 0.4 %.

DFTR: λ_{max} (nm)= 516, 363, 337, 293, 257, 219 nm.

IR (KBr): ν = 1646 (C=C) and (C=N); 1220 (Si-O-Si); 1096 (Si-O); 814 (Si-O-C); 781 (Si-C); 544 (Pd-C).

¹³C NMR (300 MHz, Solid Phase, 25 °C, ppm): δ = 175 (C-Pd, C₇); 147.2 (2C, C₉, C_{9'}); 134.6 (2C, C₁₂, C₈); 128.8 (2CH; C₁₁, C_{11'}); 124.6 (2CH, C₅, C₆); 111.4 (C₂); 76.9 (CH; C_{3'}); 75.2 (CH; C₃); 69.4-66.2 (CH_{isopr}, C₁₅, 2CH₂, CH₂, C_{4'}); 58.3

(CH₃; C₁₄); 32.8 (2C, C₁₀, C₁₀, 2CH₃; C₁, C_{1'}); 28.8 (2CH₃, C₁₈ or C_{18'} or C₁₃ or C_{13'}); 24.6 (CH_{3isopr}, 2CH₃, C₁₈ or C_{18'} or C₁₃ or C_{13'}); 15.9 (C₁₆); 8.8 (C₁₇).

5.4.3 6aRh-MCM.

Found C: 2.87; H: 4.99; N: 0.94; Rh: 0.05 %.

DFTR: λ_{\max} (nm)= 594, 668, 395, 335, 285, 245, 233 nm.

IR (KBr.): ν = 1633 (C=C) and (C=N); 1222 (Si-O-Si); 1089 (Si-O); 802 (Si-O-C); 799 (Si-C); 554 (Rh-C).

¹³C NMR (300 MHz, Solid Phase, 25 °C, ppm): Solid with low load. Signals are not resolved.

5.4.4 6bRh-MCM.

Found C: 4.83; H: 2.42; N: 0.19; Rh: 0.01 %.

DFTR: λ_{\max} (nm)= 512, 363, 337, 288, 257, 219 nm.

IR (KBr.): ν = 1624 (C=C); 1372 (C=N); 1213 (Si-O-Si); 1091 (Si-O); 799 (Si-O-C); 555 (Rh-C).

¹³C NMR (300 MHz, Solid Phase, 25 °C, ppm): δ = 197.0 (C₇, C-Rh); 160.0 (C, C₉, C_{9'}); 136.0 (broad, 2C; CH; C₁₂, C; C₈); 129.9 (2CH; C₁₁, C_{11'}); 124.9 (2CH, C₅, C₆); 110.2 (C₂); 103 (2CH_(cod)); 75.6 (CH; C_{3'}); 73.5 (CH; C₃); 70.0 (2CH_(cod)); 60.8 (3CH_{isopr}); 58.5 (CH₂; C₁₅); 41.8 (CH₂; C₄); 37.9 (CH₃; C₁₄); 32.0 (CH₂; C_{4'}); 30.0-23.0 (broad, 16C; 2CH₃; C₁, C_{1'}; 6CH_{3isopr}; 2CH₃; C₁₈ or C_{18'} or C₁₃ or C_{13'}; 2CH, C₁₀, C_{10'}; 4CH_{2(cod)}); 22.9-8 (broad, 4C; 2CH₃; C₁₈ or C_{18'} or C₁₃ or C_{13'}; CH₂; C₁₆; CH₂; (C₁₇)).

5.4.5 6aAu(I)-MCM.

Found C: 4.59; H: 5.37; N: 0.48; Au: 1.6%.

DFTR: λ_{\max} (nm)= 493, 357, 290, 248, 223 nm.

IR (KBr.): ν = 1632 (C=C) and (C=N); 1209 (C-O-C); 1086 (Si-O); 802 (Si-C).

¹³C NMR (300 MHz, Solid Phase, 25 °C, ppm): δ = 179.0 (C-Au; C₇); 137.0 (C₁₂); 135.0 (broad, 8C; 2C; C₉, C_{9'}, *p*-CH, 2*o*-CH; BzN, C₈, 2CH; C₁₁, C_{11'}); 129.6 (broad, 4C; 2CH; C₅, C₆; 2*m*-CH; BzN); 122.5 (CN; BzN); 111.3 (broad, 2C, C-CN;

BzN; C₂); 78.3 (broad, 2CH; C₃', C₃); 72.0 (CH₂; C₁₅); 59.9 (2CH₂; C₄, C₄'); 58.2 (CH_{isopr}); 58.8 (CH₃; C₁₄); 25.3 (broad, 2CH₃; C₁, C₁' and CH_{3isopr}); 18.7 (broad, 3C; CH₃; C₁₃, CH₂; C₁₆, CH₃; C₁₀ or C₁₀'); 13.4 (CH₃; C₁₀ or C₁₀'); 8.0 (C₁₇).

5.4.6 **6bAu(I)-MCM.**

Found C: 27.21; H: 6.31; N: 1.54; Au: 1.1%.

DFTR: λ_{max} (nm)= 605, 546, 444, 366, 301, 253 nm.

IR (KBr.): ν = 1645 (C=C) and (C=N); 1093 (Si-O); 787 (Si-C).

¹³C NMR (300 MHz, Solid Phase, 25 °C, ppm) (Partial): δ = (C-Au, C₇, No found); 146.2 (2C; C₉, C₉'); (*p*-CH, BzN, No found); (*o*-CH, BzN, No found); (C₁₂, No found); (*2m*-CH; BzN No found); (C₈, No found); 129.0 (2CH; C₁₁, C₁₁'); 123.4 (broad, 3C; 2CH; C₅, C₆, CN; BzN); 106.0 (C₂); 97.0 (C-CN; BzN); 76.7 (CH; C₃'); 74.6 (CH; C₃); (3CH_{isopr}, No found); 68.1 (CH₂; C₁₅, No found); 66.6 (2 CH₂, C₄, C₄', No found); (CH₃; C₁₄, No found); 33.1 (2C, C₁₀, C₁₀'); 29.0 (2CH₃; C₁, C₁'); 24.7 (broad, CH_{3isopr}, 4CH₃; C₁₈, C₁₈', C₁₃, C₁₃'); 21.0 (CH₂; C₁₆); 13.3 (CH₂; C₁₇).

5.4.7 **6aAu(III)-MCM.**

In a round bottom flask 30 mg of **6aAu(I)-MCM41 (1.6%, Au(I))** was dispersed in 5 mL of benzonitrile and added 11mg of phenyliodine (III) dichloride and the mixture stirred at room temperature for 24 h. The solid was filtered and washed with ethyl ether, and dried under vacuum.

Stable white solid. **Found** C: 13.53; H: 2.08; N: 2.03; Cl: 3.83.

IR (KBr.): ν = 2987 (CH); 1635 (C=C, C=N); 1227 (C-O-C); 1088 (Si-O); 848 (PF₆); 801 (Si-C).

5.5 Catalytic Activity.

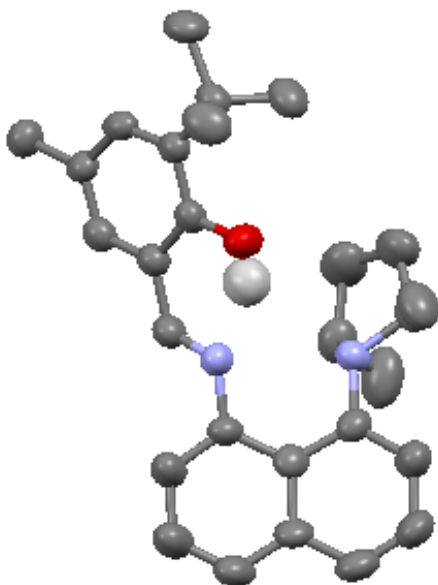
5.5.1 **Hydrogenation of alkenes.**

The catalytic properties, in hydrogenation reactions, of the complexes were examined under conventional conditions for batch reactions in a reactor (Autoclave Engineers) of 100 mL capacity at 40 °C temperature, 4 atm. dihydrogen pressure and the corresponding metal/substrate molar ratio. The evolution of the reaction of

hydrogenated product was monitored by gas-chromatography. The enantiomeric excess was measured by HPLC using chiral column chiralcel OD [diethyl 2-benzylidene succinate, λ : 250 nm, Hexane/iPrOH: 95/5, 0.5 mL/min flow rate, chiralcel AD-H [diethyl itaconate, λ : 230 nm, Hexane/iPrOH: 98/2, 0.4 mL/min flow rate.

5.5.2 *Recycling experiments.*

At the end of the process the reaction mixture was centrifuged, and the catalyst residue washed to completely remove any remaining products and/or reactants. The solid was used again and any change in the catalytic activity was observed. In each of the four runs, up to 95% conversion was reached after 220 min and ee (%) was maintained after 4 cycles.



Synthesis of chiral ligands based on “proton sponges-core”. Soluble and heterogenized rhodium and palladium complexes as enantioselective hydrogenation catalysts.

1 Introduction.

Proton sponges (PS's) are one group of promising catalysts in organic chemistry for their extremely high pK_a , easy molecular modification, possible recyclability, repeated use of recovered materials, simple operation based on the acid–base concept and their lower toxicity.¹

Recently, nitrogen-containing organo-bases, such as, guanidines, amidines, and phosphazenes have been attracting much attention in organic synthesis due the possibility to work with them under mild conditions even in cooperation with organometallic catalysts in catalyzed reactions on selective processes. The use of organic bases has some advantages over ionic bases, such as, milder reaction conditions, better solubility and absence of a coordinating metal ion that derived in more secondary subproducts. From a structural point of view, proton sponges usually presents two very close nitrogen functions that could simultaneously coordinate with a proton, being this effect responsible for their strong basicity, the spatial proximity of both nitrogen functions does these type of molecules also useful as bidentate ligands for obtaining a wide families of organometallic complexes.

In this chapter, we focused on the use tuned proton sponge precursors as building blocks for the synthesis of new ligands with one or two nitrogen and/or one additional oxygen as donor atoms. We synthesized the corresponding rhodium and palladium complexes (soluble and heterogenized on inorganic support) and evaluated theirs catalytic properties.

Despite these kinds of organic compounds show interesting structures as bidentate donors only scarcely reports have studied their properties as ligands in organometallic complexes and further study of their catalytic properties.

[1] P. T. Anastas, J. C. Warner, in *Green Chemistry: Theory and Practice*, **1998**, Oxford University Press, Oxford.

2 State of the art.

2.1 Historical background and general features of proton sponges.

Proton sponges (PS's) are organic diamines with amazing high basicity. This exceptional basicity was reported by Alder² in 1968 for the 1,8-bis(dimethylamino)naphthalene (DMAN) which is considered the first “proton sponge”. This compound has basicity about 10 millions times higher ($pK_a = 12.1$ in water) than other similar organic amines. The basicity of this amine derivate is due to the construction of highly effective conjugation system after protonation under reversible conditions. (**Figure. IV.1**).

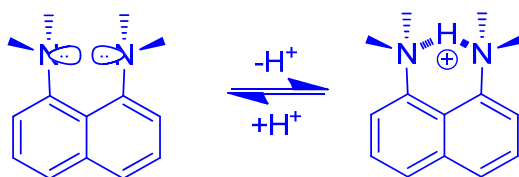


Figure. IV. 1. DMAN.

Another peculiar feature of the DMAN is the slowness of proton addition detachment due to the shielding of inter-nitrogen space by four methyl groups. Thus, the high thermodynamic basicity is associated with its rather low kinetic basicity. This circumstance made it possible to establish a similarity in the behavior of the DMAN and genuine sponges, which slowly absorb water and retain it very strongly so that water is difficult to squeeze out. For this particular reason, DMAN has been named “Proton Sponge®”, which is generally accepted now and is further extended to all other compounds with this type of properties. The concept of “proton sponges” is based on the following principles:

[2] R. W. Alder, P. S. Bowman, W. R. S. Steele, D. R. Winterman, *Chem. Commun.* **1968**,13, 723-724.

- The proper structural organization of the molecule which provides rigid fixation of two nitrogen atoms at a sufficiently close distance from each other.
- The existence in the molecule of a destabilizing repulsion effect of unshared electron pairs of nitrogen atoms.
- The occurrence of a strong intramolecular hydrogen bond (IHB) in the cation, which relieves steric and electronic strains characteristic of a base.
- The presence of a hydrophobic environment at the nitrogen atoms, most often in the form of alkyl groups, which actually accounts for the 'sponge' effect.

In short, we could say that the abnormally high basicity of DMAN is caused by three factors:

- Destabilization of the base due to strong repulsion of unshared electron pairs of nitrogen atoms.
- Formation of a strong IHB in the protonated form.
- Steric strain relief in the molecule upon the transition from a non-planar base to a planar cation.

The influence of the molecular structure on these factors has been studied by means of modifications on the DMAN structure. There are two types of variations in the structure:

- The naphthalene skeleton is maintained with the basic groups at *peri*-position and the changes affect the substituents at the basic group and/or at positions close them, producing changes in their relative orientation and in the hydrophobic proton shielding.
- The skeleton supporting both basic groups is changed, modifying the relative disposition of these groups.

Based on these variations, widely types of proton sponges with different backbones have been reported. (**Figure. IV. 2**). Thus, sponges derived from fluoxerene (**E1**),³ heterofluorene (**E2**),⁴ phenantrene (**E3**), and their analogues (**E4**),⁵ 4,9-dichloroquino[7,8-*h*]quinoline (**E5**),⁶ with and sp^2 -hybridised nitrogen have synthesized and their properties studied.

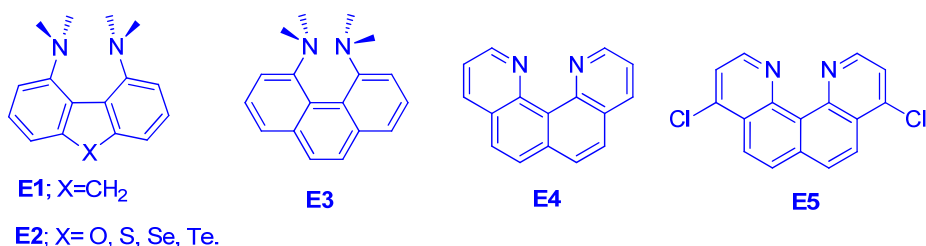


Figure. IV. 2. Proton sponges without-naphthalene backbone.

In this work we have been restricted our study to “naphthalene proton sponges” because are easily functionalized by different routes. Thus, we can find several derivatization products from DMAN (**Figure. IV. 3**), such as, 1,8-bis(dialkylamino) naphthalenes (**E6**), and analogs with amine nitrogen inside into five or six member ring (**E7**),⁷ bridged derivatives (**E8**),⁸ 2,7 functionalized (**E9** and **E10**) even functionalized in others positions for different purposes as heterogenization (**E11**).⁹

The modifications, which only affect basic groups, have a greater influence on the proton transfer rate than on basicity. When the nitrogen substituents are bulkier, the hydrophobic shielding of the proton is more effective, and its intermolecular transfer more difficult.

[3] H. A. Staab, T. Saupe, C. Krieger, *Angew. Chem., Int. Ed. Engl.*, **1983**, 22, 731.

[4] H. A. Staab, M. Hoene, C. Krieger, *Tetrahedron Lett.*, **1988**, 1905.

[5] T. Saupe, C. Krieger, H. A. Staab, *Angew. Chem., Int. Ed. Engl.*, **1986**, 25, 451.

[6] M. A. Zirnstein, H. A. Staab, *Angew. Chem.* **1987**, 99, 460–461; *Angew. Chem. Int. Ed. Engl.* **1987**, 26, 460–461.

[7] V. A. Ozeryanskii, D. A. Shevchuk, A. F. Pozharskii, O. N. Kazheva, A. N. Chekhlov, O. A. Dyachenko, *J. of Mol. Struct.*, **2008**, 892, 63–67.

[8] R. W. Alder, M. R. Bryce, N. C. Goode, N. Miller, J. Owen, *J. Chem. Soc., Perkin Trans.*, **1981**, 1, 2840.

[9] A. Corma, S. Iborra, I. Rodriguez, F. Sanchez, *Journal of Catalysis*, **2002**, 211, 208–215.

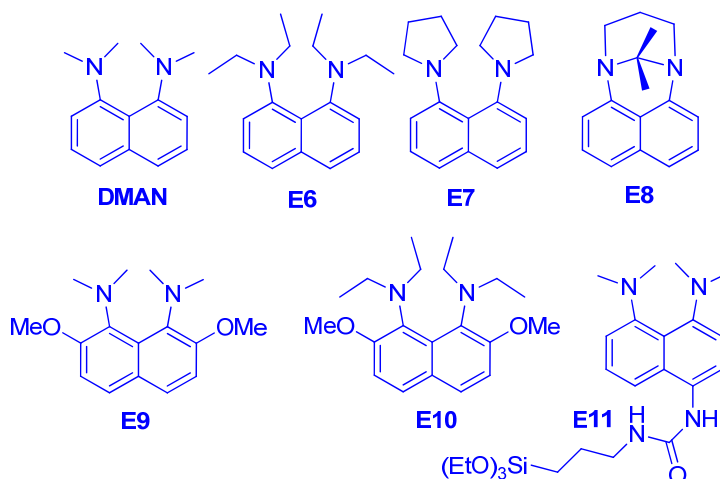


Figure. IV. 3. Proton sponges naphthalene backbone.

Substituents at positions 2 and 7 of the naphthalene ring (**E9** and **E10**), (**Figure. IV. 3**) produce steric interactions with the *N*-substituents, named “buttressing effect”.¹⁰ Their influence on the basicity values is due to the proximity of the lone pairs that destabilize the base and reinforce the intramolecular hydrogen bond (IHB) in the mono-protonated species. Both factors are favorable for an increase in the basicity, while only the second modification slows down the process of proton transfer.

Another modification can be achieved by the union of the nitrogen atoms with an aliphatic chain of variable length, $-(CH_2)_n-$, (**Figure. IV. 3**, **E8**). These changes cause opposite effects in the proton transfer rate and the basicity depending on the chain length; a higher rate and lower basicity and in all cases could be simultaneously shown a different donor capacity to form organometallic complexes.

[10] (a) A. F. Pozharskii, O. V. Ryabtsova, V. A. Ozeryanskii, A. V. Degtyarev, O. N. Kazheva, G. G. Alexandrov, O. A. Dyachenko, *J. Org. Chem.*, **2003**, 68, 10109-10122.

2.2 Synthesis of naphthalene proton sponges.

In general, there are two methods to afford naphthalene proton sponges. The first one is based on the alkylation of 1,8-diaminonaphthalene compounds or its partially alkylated derivatives. This method involves the use of strong bases as sodium or potassium hydrides in anhydrous THF or KOH in DMF, for amine group ionization.¹¹ In these conditions, (**Figure. IV. 4**) the *N*-anions of the original amine and the intermediates, substitution products, promote to a total alkylation. The ionization is favored respect other anilines because the N-H acidity is bigger ($pK_a = 24.5$, DMSO, 25 °C) than ordinary arylamines. This was ascribed to the stabilization of anion (**EInt-1**) through an intramolecular hydrogen bond.¹²

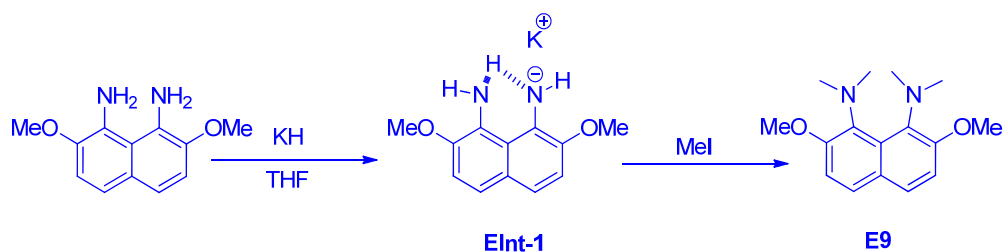


Figure. IV. 4. Synthesis of PS through alkylation.

For the preparation of proton sponges with the amine nitrogen onto five or six member ring (**E7**), (**Figure. IV. 5**), α,ω -dihalogenoalkanes were used as alkylation agents, if the α,ω -dihalogenoalkane has the halogens closely (two or three atoms) the alkylation reaction gives the bridge sponges type (**E7** and **E12**).⁸

The reaction usually needs to heat the mixture with an excess of alkyl halide and when reaction is finished, the proton sponge salt is converted into the base by treatment with an aqueous alkaline solution.

[11] L. A. Kurasov, A. F. Pozharskii, V. V. Kuzmenko *Zh. Org. Khim.* **1981**, 17, 1944.

[12] E. M. Arnett, K. G. Venkatasubramanian, R. T. McIver, E. K. Fukuda, F. G. Bordwell, R. D. Press, *J. Am. Chem. Soc.*, **1982**, 104, 325.

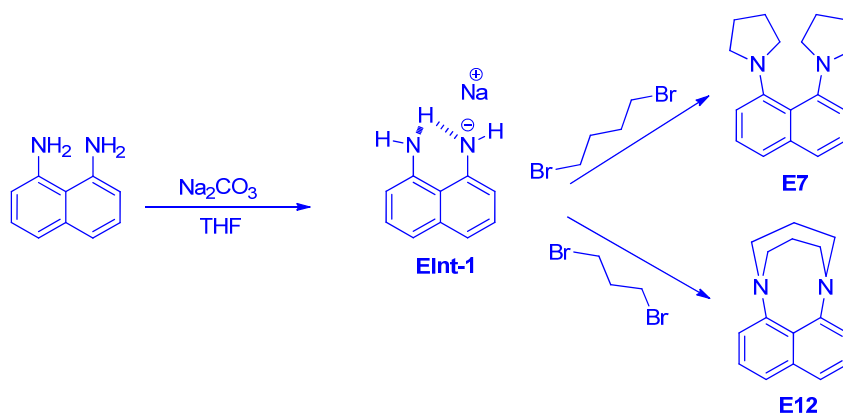


Figure. IV. 5. Synthesis of cyclic amine naphthalene PS's.

The second way to obtain naphthalene proton sponges (**Figure. IV. 6**) uses 1,3-dialkyl-2,3-dihydropyrimidine compound as starting material. The quaternization of pyrimidine derivatives afford the salt intermediate **EInt-2** that is treated with KOH solution to get the tri-alkyl substituted derivative **EInt-3**. In the last step, give the proton sponge by alkylation with desired alkyl halide. This method is usually used to afford proton sponges with different alkyl substituents (**E13**).¹³

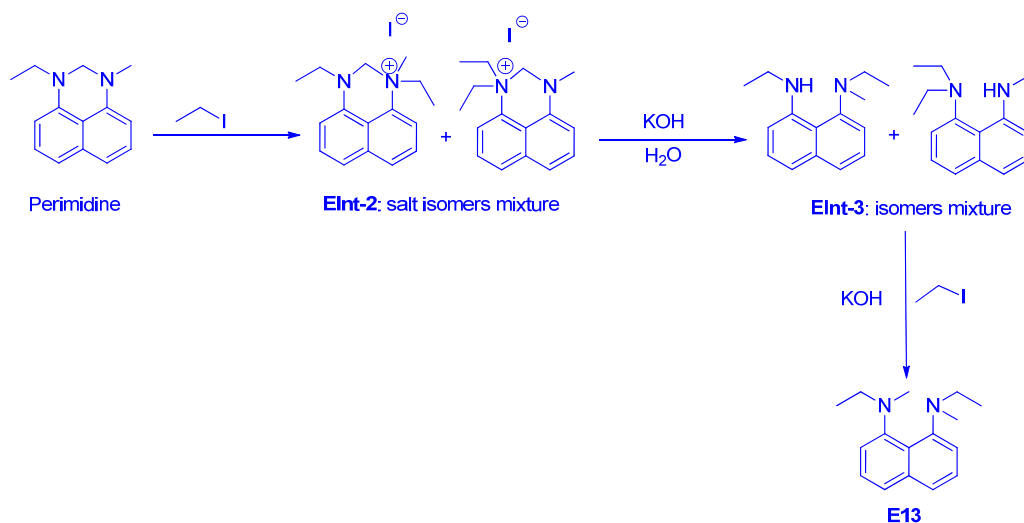


Figure. IV. 6. Synthesis of naphthalene PS from perimidines.

[13] A. F. Pozharskii, L. A. Kurasov, V. V. Kuzmenko, L. L. Popova, *Zh. Org. Khim.*, **1981**, 17, 1005.

Other way to obtain proton sponges with different alkyl substituents was reported in 1999 by Lloyd-Jones,¹⁴ using as starting material (9-BBN)⁺(1,8-diaminonaphthalene)⁺ and subsequent alkylation reactions.

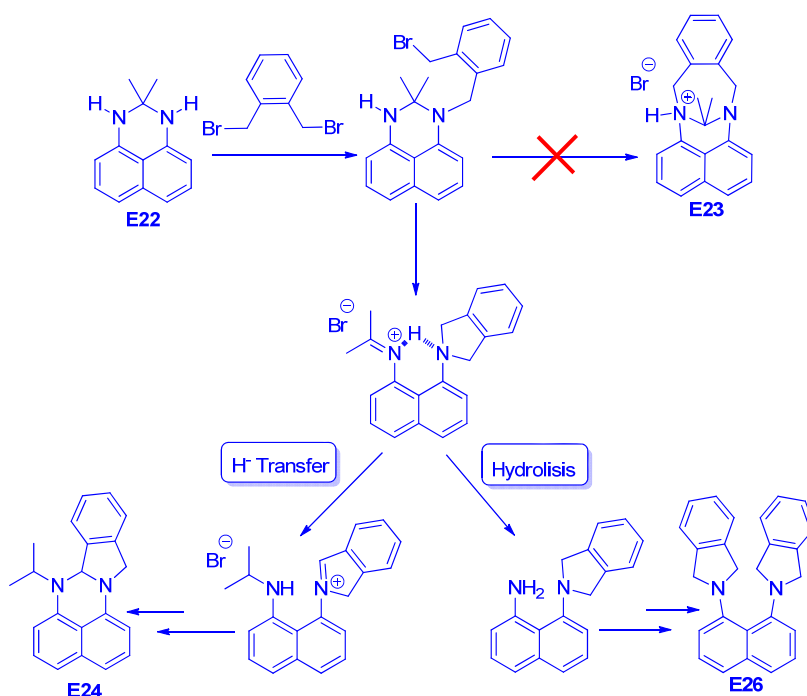


Figure. IV. 7. Perimidine formation through hydride transfer mechanism.

Alder et al¹⁵ in 1981, in attempted to prepare **E23** (**Figure. IV. 7**) from 2,2-dimethyl-1,2-dihydroperimidine by reaction with α,α' -dibromo-*o*-xylene obtained the surprisingly perimidine **E24** and the expected product **E26**. A tentative mechanism was proposed where a hydride transfer makes possible the formation iminium salt which evolves to the cyclized product **E24**. Parallel, rather than the hydride transfer, hydrolysis occurs and becomes to **E26**. Models suggest that **E23** will posses large interactions between the upward methyl groups and either the benzene ring or the upward benicylic protons, depending on which way the benzene ring is flipped. Thus, the transition state is destabilized and preferentially the cyclization occurs on the same nitrogen atom.

[14] J. P. H. Charmant, G. C. Lloyd-Jones, T. M. Peakman, R. L. Woodward, *Eur. J. Org. Chem.*, **1999**, 10, 2501-2510.

[15] R. W. Alder, M. R. Bryce, N. C. Goode, N. Miller; J. Owen, *J. Chem. Soc., Perkin Trans. 1*, **1981**, 2840-2847.

2.3 Chiral proton sponges.

Most of the efforts to modify the first proton sponge aim to increase the basicity and kinetics properties of the original sponge. However, another key point is the quest for chirality. This kind of tunings in a proton sponge make these compounds more useful in regio and enantio selective processes. However, there aren't many papers reporting "chiral proton sponges".

The first chiral generation of proton sponges in its protonated form was reported by Guy. C. Lloyd-Jones et al.¹⁶ These compounds have the stereogenic centre at both nitrogen atoms. (**Figure. IV. 8**).

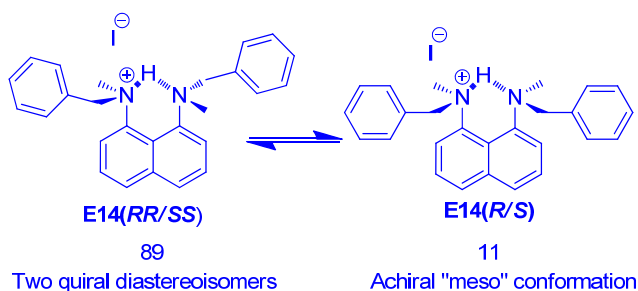


Figure. IV. 8. First chiral generation of proton sponges.

This salt exists as two diastereoisomers: the chiral one **E14 (RR/SS)** and the achiral **E14 (RS)**. The protonation of the two species is locked, thus, they predicted a short and strong hydrogen bond. Unfortunately this bond was weaker than they expected, and they couldn't isolate these species that are a diastereoisomers mixture in rate 89/11.

Other way to lock diastereoisomers mixtures was reported by Pozharskii and Degtyarev,¹⁷ in this case for chelating (2-naphthyl)pyridylmethanols. The resulting mixture of conformers was very interesting in the study of new conformations in PS's, as well as, its influence in the pK_a behavior.

[16] P. Hodgson, G. C. Lloyd-Jones, M. Murray, T. M. Peakman, R. L. Woodward, *Chem. Eur. J.*, **2000**, 6, 4451–4460.

[17] A. V. Degtyarev, A. F. Pozharskii, *Chem. of Heterocyclic Comp.*, **2008**, 44, 1138-1145.

Other approaches to chiral proton sponges were the totally resolution of *bis*-isoquinoline derivatives described by M. C. Elliot et al¹⁸ and the synthesis and catalytic application of Brønsted acid salts of bis(amidine) ligands derived from (+)-*trans*-cyclohexane in asymmetric Aza-Henry reaction reported by N. Johnston et al,¹⁹ in the two cases the amines are quite similar to proton sponge but have not an identifiable increase in Brønsted basicity relative to their component functionality.

In 2008 the first chiral atropisomeric proton sponge was reported by Jean-Paul Mazaleyrat and Karen Wright,²⁰ this work describes the synthesis and basicity properties of several chiral and enantiomerically pure proton sponges based in 1,8-diaminonaphthalene and (*S*)-2,2'-bis(bromomethyl)-1,1'-binaphthyl. (**Figure. IV. 9**).

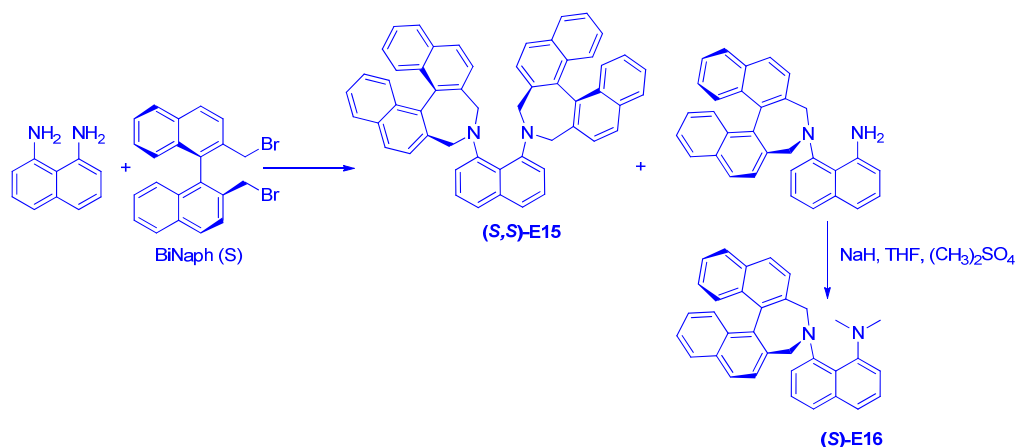


Figure. IV. 9. First chiral atropisomer PS.

Studies in the conformation behavior describes the stability for (*S,S*)-E15 (295-385 K) but in case of (*S*)-E16 “narcissistic” processes was observed. This process involves the interconversion of object and mirror image through a planar transition state (high energy state) with increase of temperature as proposed Alder and co-workers.²¹ In terms of basicity, ¹H NMR of protonated diamines shows a single proton

[18] M. C. Elliott, E. Williams, S. T. Howard, *J. Chem. Soc., Perkin Trans. 2*, **2002**, 201–203.

[19] A. S. Hess, R. A. Yoder, J. N. Johnston, *Synlett*, **2006**, 147–149.

[20] J. P. Mazaleyrat, K. Wright, *Tetrahedron Letters*, **2008**, 49, 4537–4541.

[21] R. W. Alder, J. E. Anderson, *J. Chem. Soc., Perkin Trans. 2*, **1973**, 2086–2088.

at low field in all cases (18.7-20.0 ppm) in agreement with classical proton sponge behavior.

2.4 Proton sponges as ligands for organometallic complexes.

Since several years ago, has been reported approaches of proton sponges complexes by the formation of a diaminoacetal by condensation of 1,8-diaminonaphthalene with the chromium tricarbonyl complex of benzaldehyde²² and the synthesis of a Pd complex with a pincer ligand obtained via a condensation of isophthalic dicarboxaldehyde and 2 equiv of 1,8-diaminonaphthalene.²³

However, there aren't many examples of metallation for naphthalene proton sponges. One of the alternatives is the functionalization with other groups that could bond with the metal, as an example, (**Figure. IV. 10**) J. Scott McIndole²⁴ reported the modification of DMAN to get PS phosphine ligands.

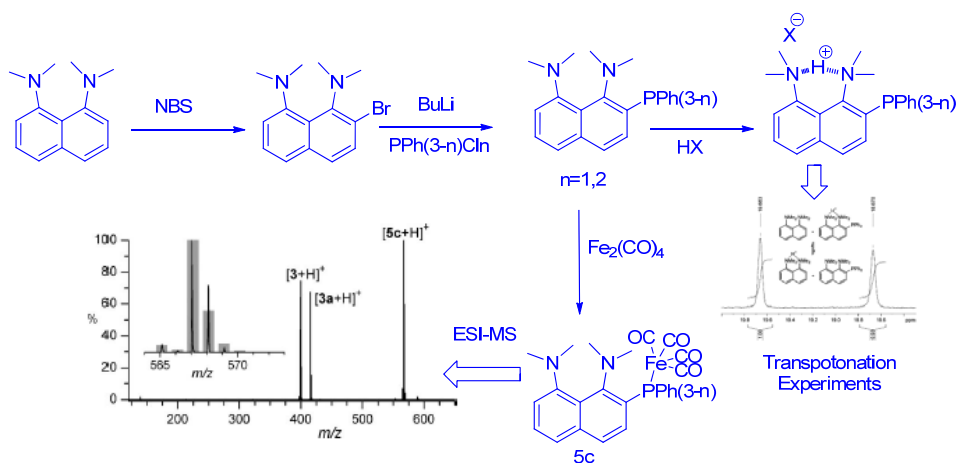


Figure. IV. 10. Useful metallation of phosphine-DMAN.

PS phosphine ligands were used to afford several metal complexes. The capacity of these ligands to associate with metals through the phosphine moiety and the absolute selectivity for protons of the DMAN is interesting and useful in ESI-MAS

[22] S. U. Son, H. Y. Jang, I. S. Lee, Y. K. Chung, *Organometallics*, **1998**, 17, 3236-3239.

[23] I. G. Jung, S. U. Son, K. H. Park, K. C. Chung, J. W. Lee, Y. K. Chung *Organometallics*, **2003**, 22, 4715-4720.

[24] N. J. Farrer, R. McDonald, J. S. McIndoe, *Dalton Trans.*, **2006**, 38, 4570-4579.

spectra in order to detect neutral complexes in low concentration or in presence of abundant competing species, common conditions in catalytic systems.

While DMAN has a high affinity towards H^+ , it is indifferent to other electrophiles, which is in contrast to usual nitrogen bases. Some examples of reactivity of DMAN apart from the previously seen, somewhat surprisingly, its role as a hydride donor in its reaction with *mer*- $RhCl_3(dmsO)_3$ or $[RuCl(dppb)]_2(I-Cl)_3$,²⁵ with fluoroalkyl complexes of iridium,²⁶ or with $B(C_6F_5)_3$ ²⁷ to form the 1,1,3-trimethyl-2,3-dihydroperimidinium cation (TMP^+) in all cases. The mechanism of this interesting behavior was studied by Russell P. Hughes et al²⁶ using the fully perdeuteomethylated analogue of DMAN (DMAN*) and fluoroalkyl iridium complexes to afford hydride-fluoroalkyl iridium deuterium marked complexes. This is proof of their behave as a hydride transfers in these processes. (**Figure. IV. 11**).

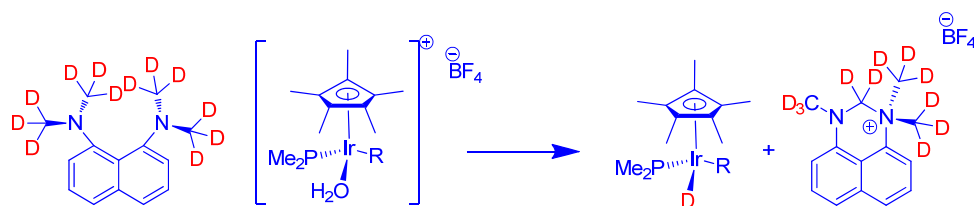


Figure. IV. 11. Hydride transference in Iridium complex.

Thus, until relatively recently, it was believed that DMAN was not suitable as ligand for metal complexes because the methyl groups shield the nitrogen atoms and thereby sufficient thermodynamic stability was not conferred on the complexes that could be formed, but in 2004, Seichi Okeya et al²⁸ reported the first example of a metal complex coordinating (directly) to DMAN, (*via* the amino groups); the reaction with $Pd(hfac)_2$ immediately generates a poorly-characterized charge-transfer product, which

[25] S. N. Gamage, Morris, R. H. Rettig, S. J. Thackeray, D. C. Thorburn, I. S. James, *J. Chem. Soc., Chem. Commun.*, **1987**, 12, 894-895.

[26] R. P. Hughes, I. Kovacic, D. C. Lindner, J. M. Smith, S. Willemsen, D. Zhang, I. A. Guzei, L. R. Arnold, *Organometallics*, **2001**, 20, 3190-3197.

[27] A. Di Saverio, F. Focante, I. Camurati, L. Resconi, T. Beringhelli, G. D'Alfonso, D. Donghi, D. Maggioni, P. Mercandelli, A. Sironi, *Inorg. Chem.*, **2005**, 44, 5030-5041.

[28] T. Yamasaki, N. Ozaki, Y. Saika, K. Ohta, K. Goboh, F. Nakamura, M. Hashimoto, S. Okeya, *Chem. Lett.*, **2004**, 33, 928-929.

after standing for a week forms the cationic complex $[\text{Pd}(\text{hfac})(\text{DMAN})]^+$. The hfac ligand may be substituted for β -diketones and one of these complexes was structurally characterized; coordination causes severe distortion of the proton sponge, the $\text{N} \cdots \text{N}$ distance opening to 2.94 Å from 2.51 Å. The proton sponge ligand is easily displaced, even by water.

Recently, the transition metal complexes of different proton sponges were reported as Pt, Pd, Re and Mn 4,9-dichloroquino[7,8-*h*]quinoline complexes²⁹ and palladium TMGN complex³⁰ (as enantiomeric mixture). The most remarkable structure feature is the non-planar naphthalene aromatic system and the location of the Pd atom in the best plane of naphthalene. The two enantiomers are in the unit cell. (**Figure. IV. 12**). Palladium TMGN complex was tested in catalyzed Heck reaction between phenyl iodide and styrene to give *trans*-stilbene, presenting high activity.

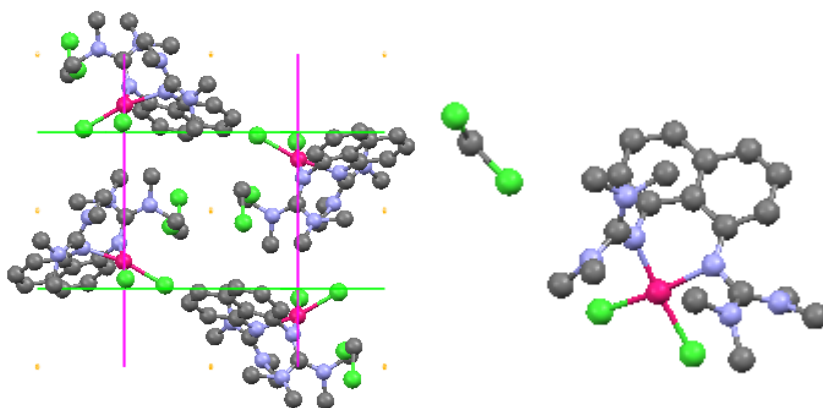


Figure. IV. 12. Palladium TMGN complex.

During this PhD dissertation Brancatelli et al³¹ reported the synthesis of new naphthalene chiral PS's that were coordinated with Ru and used as precatalysts for allylic etherification.

[29] H. U. Wüstefeld, W. C. Kaska, F. Schüth, G. D. Stucky, X. Bu, B. Krebs, *Angew. Chem.* **2001**, *113*, 3280–3282; *Angew. Chem.Int. Ed.* **2001**, *40*, 3182–3184.

[30] U. Wild, O. Hübner, A. Maronna, M. Enders, E. Kaifer, H. Wadepohl, H. J. Himmel *Eur. J. Inorg. Chem.*, **2008**, 4440–4447.

[31] G. Brancatelli, D. Drommi, G. Ferminó, M. Saporita, G. Bottari, F. Faraone, *New J. Chem.*, **2010**, *34*, 2853–2860.

3 Discussion and results.

3.1 Targets.

The aim of this study was to gain insight into the effects of “proton sponge core ligands” properties, such as, the rigidity or flexibility of the chiral chelating ligand and the influence of the donor-atoms, in determining asymmetric induction in the catalytic processes and namely, to establish the relation between regioselectivity induced by the chelated chiral ligands involving each conformational isomer present in solution and the enantiomeric excess of the obtained product. We believe that the potential of this chiral building block to influence asymmetric transformations should be investigated.

Other way, the functionalization of these amazing structurally ligands and supporting on inorganic solid as MCM-41 to convert in efficient, stable and recyclable catalysts is one of our objectives inside the green chemistry philosophy.

3.2 Synthesis of ligands from 8-((2*R*,5*R*)-2,5-dimethylpyrrolidin-1-yl)naphthalen-1-amine.

As part of an ongoing project, this PhD dissertation is focused on the design and synthesis of ligands for asymmetric catalytic reactions. Thus, we developed a modular synthetic strategy for preparing new ligands based on 8-((2*R*,5*R*)-2,5-dimethylpyrrolidin-1-yl)naphthalen-1-amine (type (*R,R*)-**A** or type (*R,R*)-**B** in **Figure. IV. 13**. Nitrogen atoms from pyridine, amine or imine moieties are electronically different and are assumed to provide different binding properties to transition metals.

Although pyridine is a strong electron-donating ligand, the delocalized π -system provides a tool for tuning the electronic nature of this moiety with different substituents. While the different donor abilities of the pyridine, phenol, amine or imine groups can serve as an electronic differentiator for transition metal-catalyzed asymmetric reactions, the *trans*-2,5-disubstituted pyrrolidine moiety can provide a chiral influence for asymmetric discrimination on pro-chiral substrates.

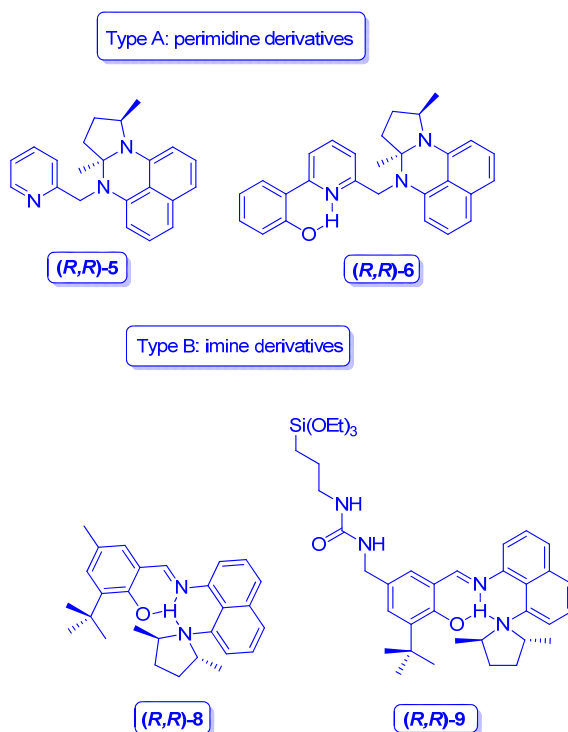


Figure. IV. 13. Chiral perimidine and imine ligands.

Recently, our group have shown that complexes with anionic linear Schiff ligands (**Figure. IV. 14, (a)**) have excellent catalytic activity in several reactions.³² On the other hand, we have also developed a series of novel conformationally restricted ONN-Pincer-type ligands (**Figure. IV. 14, (b)**) resembling coordination environments present in Schiff-base ligands.³³

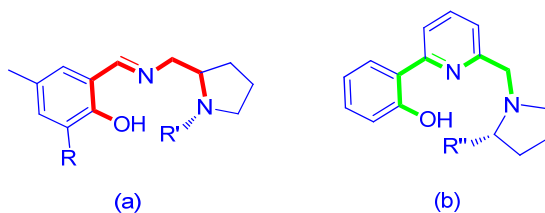


Figure. IV. 14. Schiff-base ligands previously described.

[32] a) C. González-Arellano, A. Corma, M. Iglesias, F. Sánchez, *Adv. Synth. Catal.*, **2004**, 346, 1316-1328; b) C. González-Arellano, E. Gutiérrez-Puebla, M. Iglesias, F. Sánchez, *Eur. J. Inorg. Chem.* **2004**, 9, 1955-1962.

[33] a) N. Debono, M. Iglesias, F. Sánchez, *Adv. Synth. Catal.*, **2007**, 349, 2470-2476; b) C. del Pozo, N. Debono, A. Corma, M. Iglesias, F. Sánchez, *ChemSusChem*, **2009**, 2, 650-657.

To study the scope and efficiency of these systems, we modified the ligands by variation of the substituent on the pyridine ring or on the imine group to create different electronic properties. Thus, we have synthesized, characterized and studied the reactivity of the metal complexes of the chiral perimidine **(R,R)-5**, **(R,R)-6**, and imino derivatives **(R,R)-8**, and **(R,R)-9** obtained via condensation of an aldehyde and the proton sponge precursor 8-((*R,R*)-2,5-dimethylpyrrolidin-1-yl)naphthalen-1-amine that exhibit unusual structures and interesting reactivity. (**Figure. IV. 15** and **Figure. IV. 17**).

We have derivatized the original proton sponge (DMAN) using 8-((2*R*,5*R*)-2,5-dimethylpyrrolidin-1-yl) naphthalen-1-amine (**(R,R)-4**), (previously obtained by the treatment of 1,8-dimethylaminonaphthalene with (2*S*,5*S*)-hexane-2,5-diyl dimethanesulfonate (**IN-6**)), as a building block to obtain the new chiral ligands.

IN-6 has been synthesized by enantioselective catalyzed reduction of hexane-2,5-dione by yeast (*Saccharomyces cerevisiae*) affording the enantiomeric pure dialcohol **IN-5**. Treatment of **IN-5** with 2-chloro-1,3,5-trimethylbenzene provided the protected alcohol **IN-6** which by cyclization reaction with 1,8-dimethylaminonaphthalene affords **(R,R)-4**. (**Figure. IV. 15**).

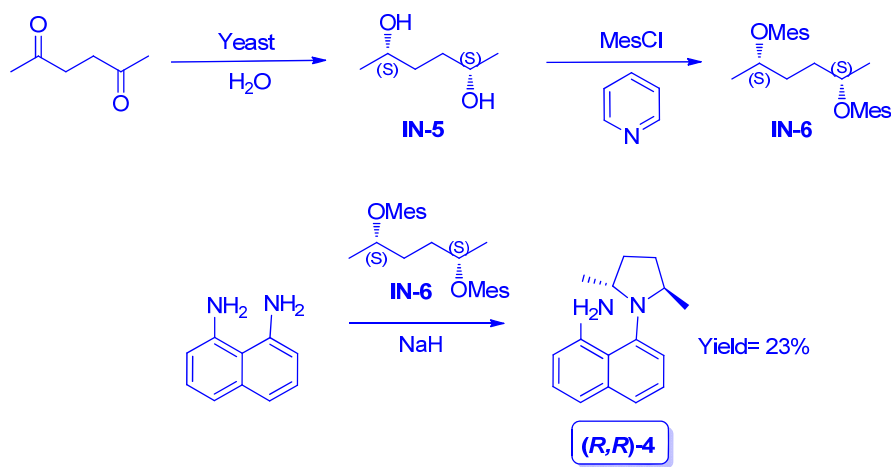


Figure. IV. 15. Synthesis of starting material **(R,R)-4**.

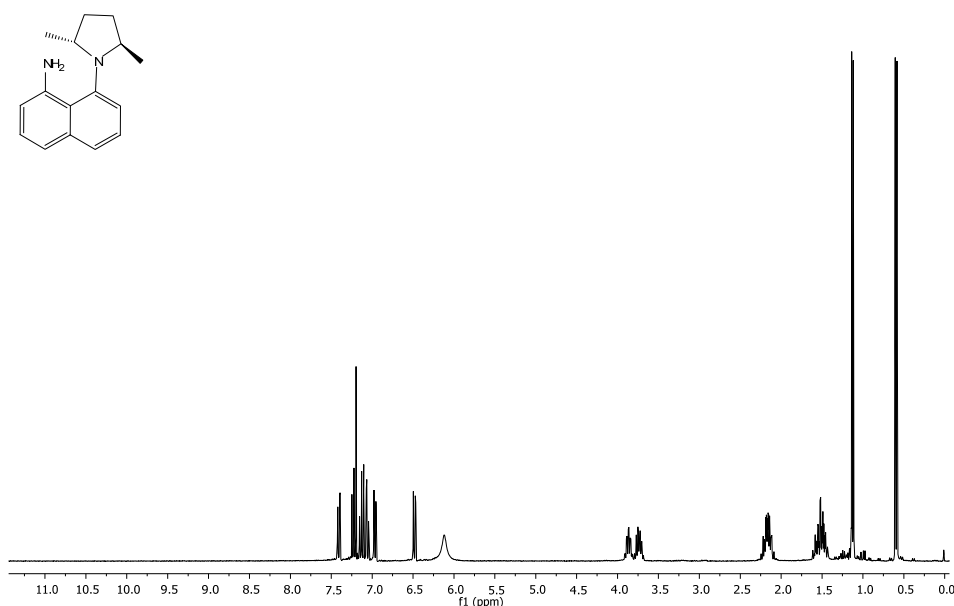


Figure. IV. 16. ^1H -NMR spectrum of **(*R,R*)-4**.

(*R,R*)-4 have been characterized after isolation. Only one diastereoisomer was detected (**Figure. IV. 16**) and its ^1H NMR shows two signals corresponding to the two methyl groups in pyrrolidine moiety as doublets at 0.64 ppm and 1.17 ppm respectively. CH_2 appears as multiplets at 1.57 ppm and 2.22 ppm and CH at 3.77 ppm and 3.90 ppm. MS/IE presents the molecular ion 240 (M^+ ; 100). All data is according with the proposed structure.

(*R,R*)-4 has been derivatized by reaction with different aldehydes in order to obtain pincer-type ligands containing such functionality. Treatment of pyridine-2-carbaldehyde, 6-(2-hydroxyphenyl)pyridine-2-carbaldehyde, 3-*tert*-butyl-2-hydroxy-5-methylbenzaldehyde, *N*-(3-*tert*-butyl-5-formyl-4-hydroxybenzyl)-*N'*-[3-(triethoxysilyl)propyl]urea with 8-((2*R*,5*R*)-2,5-dimethylpyrrolidin-1-yl)naphthalen-1-amine in ethanol at room temperature in the presence of molecular sieves (4 Å) gave compounds of type **A** or **B** (**Figure. IV. 17**), in moderate to good yields (40-70 %). All new compounds have been characterized by ^1H NMR, ^{13}C NMR, FTIR spectroscopy and EI

mass spectrometry. In some cases X-Ray single diffraction crystal structure were studied.

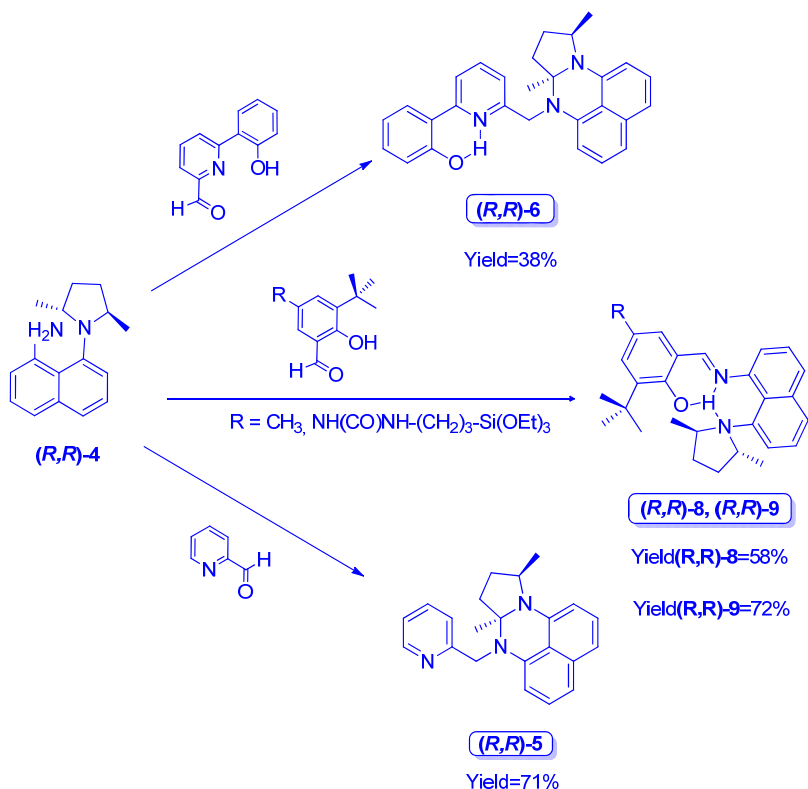


Figure. IV. 17. Synthesis of new chiral ligands with proton sponge core.

Initially, we expected an imino compound as product in all cases. However, the ¹H NMR spectra of **A** type compounds obtained from pyridine-2-carbaldehyde and 6-(2-hydroxyphenyl)pyridine-2-carbaldehyde did not match with the ¹H NMR spectra of the expected imino compounds, as we could see the signals of diastereotopic CH₂-N groups as ABXY system at 4.82 ppm, 4.57 ppm (**(R,R)-5**), and 4.70 ppm, 4.45 ppm (**(R,R)-6**). Thus, we suspected that the products type **A** were not imino compounds. They are chiral perimidines. (**Figure. IV. 18**)

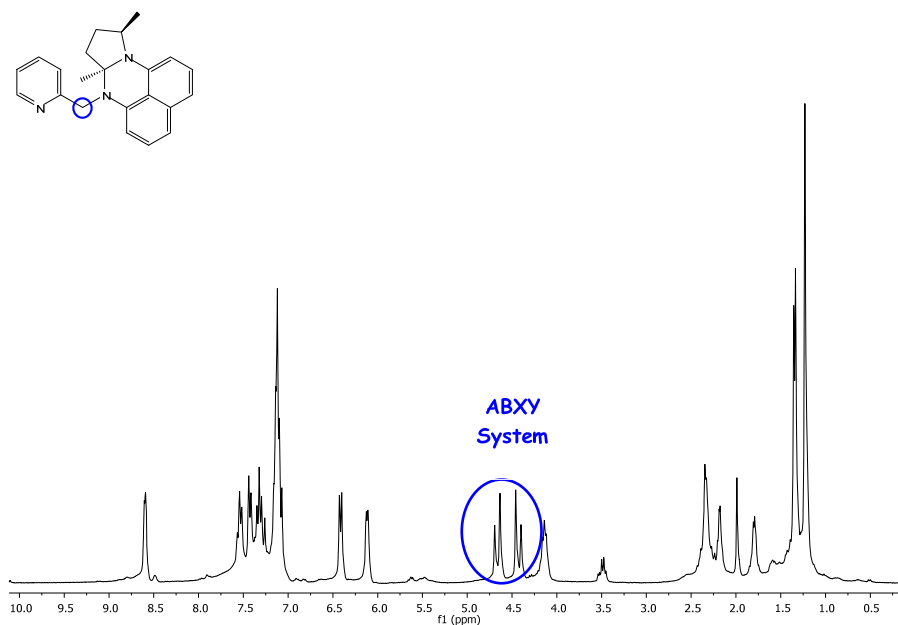


Figure. IV. 18. ^1H -NMR spectrum of **(*R,R*)-5**.

Single crystal X-ray diffraction studies have been performed on **(*R,R*)-6**. **Figure. IV. 19** shows the molecular structure with the atomic numbering. Crystal data and structure refinement details of **(*R,R*)-6** are given in Table S1 (Experimental Section).

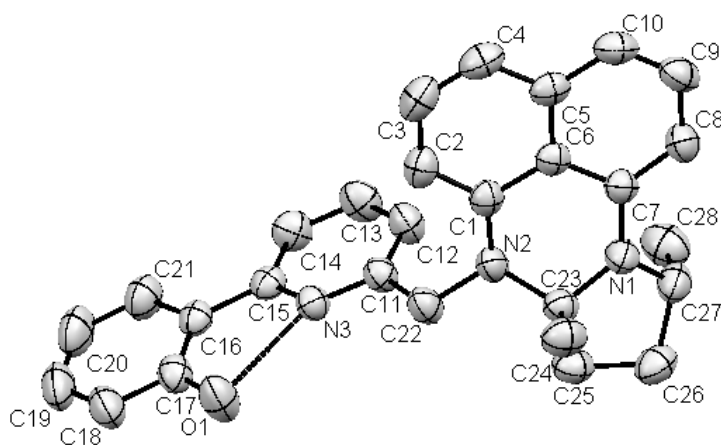


Figure. IV. 19. Molecular structure of **(*R,R*)-6**.

The structure consists of a central pyridine ring that is substituted at its 2-position by a phenol group and at its 6-position by an amine-containing CH₂(7a*R*,10*R*)-7a,10-dimethyl-7a,8,9,10-tetrahydro-7H-pyrrolo[1,2-*a*]perimidine unit.

The amine group is inclined essentially orthogonal to the plane of the adjacent pyridyl unit. The phenol moieties are almost co-planar with respect to the pyridine unit [tors.: C(17)–C(16)–C(15)–N(3) -4.7 (3)] and are disposed mutually *cis* as a result of a hydrogen bonding interaction between the phenol hydrogen atom and the neighboring pyridine nitrogen [N(3)–H(1) 1.852 (2) Å; O(1)–N(3) 2.576 (2) Å]. The ipso carbons, C(1) and C(7), deviate slightly from the naphthalene plane 0.032(6) and 0.081(6) Å, respectively. The torsion angle between C(7)–N(2) and C(1)–N(4) is 7.0 (2)°, as the protonated form of DMAN. The N(1)–N(2) distance (2.378 (3) Å) is shorter than an idealized value, 2.51 Å. This distortion of N::N could come from the stress caused by the cyclization.

When we use (*R,R*)-**5** and (*R,R*)-**6** as chiral chelate ligands, the nitrogen atom N(1) is not in the direction of metal atom and the metal is far away. Thus, (*R,R*)-**5** and (*R,R*)-**6** act as chiral N,N or N,N,O ligands, not as N,N,N- or N,N,N,O ligand. The mass spectrum of (*R,R*)-**6** reveal protonated molecular ion peak.

Treatment of 3-*tert*-butyl-2-hydroxy-5-methylbenzaldehyde or *N*-(3-*tert*-butyl-5-formyl-4-hydroxyphenylcarbamoyl)-4-(triethoxysilyl)butanamide and 8-[(2*R*,5*R*)-2,5-dimethylpyrrolidin-1-yl]naphthalen-1-amine in ethanol gave 2-*tert*-butyl-6-[(*E*)-({8-[(2*R*,5*R*)-2,5-dimethylpyrrolidin-1-yl]-1-naphthylimino)methyl]-4-methylphenol ((*R,R*)-**8**) and *N*-(3-*tert*-butyl-5-((*E*)-(8-((2*R*,5*R*)-2,5-dimethylpyrrolidin-1-yl)naphthalen-1-ylimino)methyl)-4-hydroxybenzylcarbamoyl)-4-(triethoxysilyl)butanamide ((*R,R*)-**9**), ligands type **B**, as yellow oils in good yields.

Mass spectrum of (*R,R*)-**8** reveals protonated molecular ion peak while in IR spectrum show the characteristic frequencies for imino functionalities at 1618 cm⁻¹. In their ¹H NMR spectrum, the imine compounds gave a singlet at 8.26 ppm ((*R,R*)-**8**), 8.32 ppm ((*R,R*)-**9**) consistent with the presence of CH=N protons, phenol hydrogen atom appears at low field, as a broad singlet at 13.86 ppm ((*R,R*)-**8**), 14.11 ppm ((*R,R*)-**9**). (Figure. IV. 20). These values suggest that the proton of the phenol is forming a

hydrogen bond with the nitrogen atoms which stabilizes the imino compounds and prevents the cyclization.

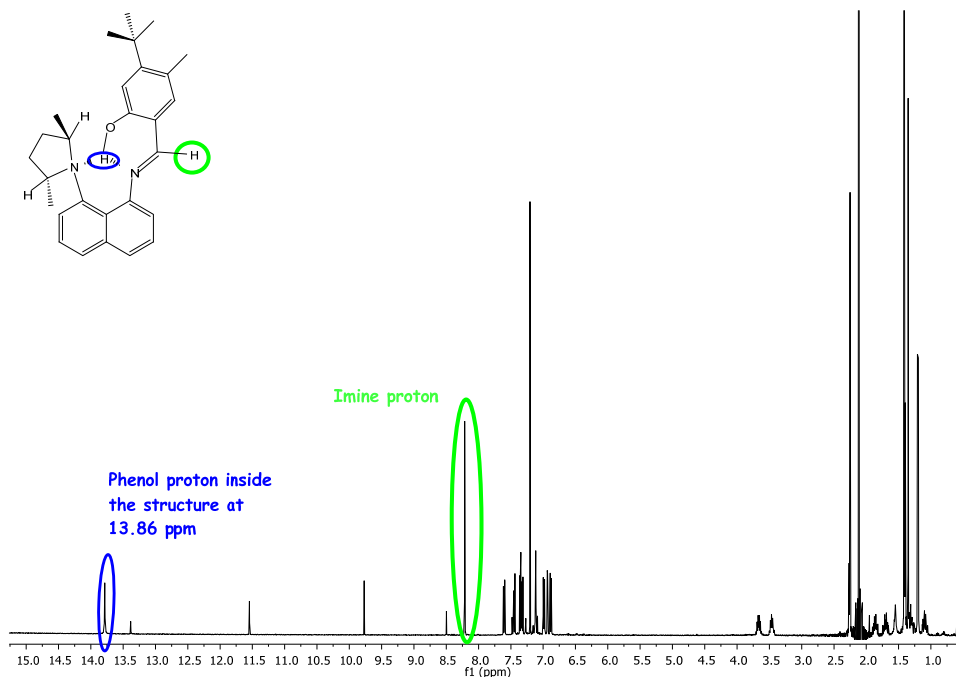


Figure. IV. 20. ^1H -NMR spectrum of **(R,R)-8**.

To support the spectroscopic data, crystals of **(R,R)-8** have been grown and studied by single crystal X-ray diffraction. A perspective view is depicted in **Figure. IV. 21**; crystal data and structure refinement details of **(R,R)-8** are given in Table S2. (Experimental Section).

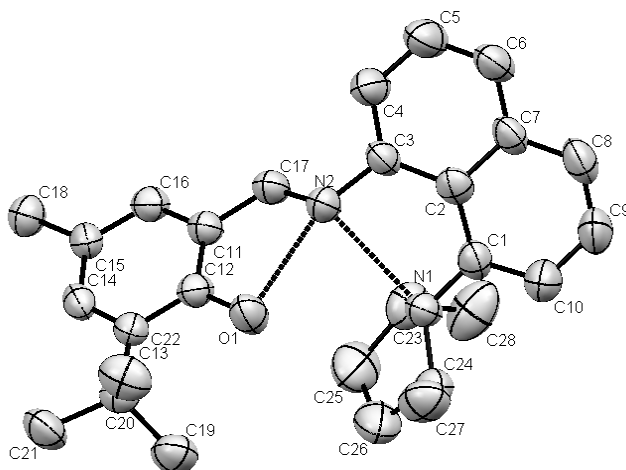


Figure. IV. 21. Molecular structure of **(*R,R*)-8**.

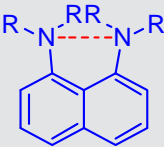
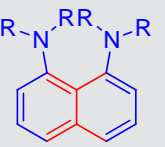
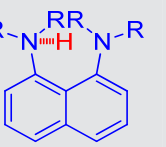
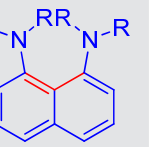
The diamine group is inclined essentially orthogonal to the plane of the phenol unit (46.80°). There is a hydrogen bonding interaction between the phenol hydrogen atom, the neighboring imine nitrogen [N(2)-H(1) 1.850 (3) Å; O(1)-N(2) 2.591 (3) Å] and the amine group [N(1)-N(2) 2.756 Å; N(1)-H(1) 2.940 (3) Å]. The ipso carbons, C(1) and C(3), deviate slightly from the naphthalene plane 0.110 and 0.021 Å, respectively. The torsion angle between C(1)-N(1) and C(3)-N(2) is $-13.4 (2)^\circ$. In this case the N(1)-N(2) distance (2.756 (4) Å) is larger than an idealized value, 2.51 Å. The stereochemistry of **(*R,R*)-8** is the same as that of 8-((2*R*,5*R*)-2,5-dimethylpyrrolidin-1-yl)naphthalen-1-amine, as expected, **(*R,R*)-8** and **(*R,R*)-9** act as tridentate ligands when coordinated to metals.

In both families, the absolute configuration of asymmetric carbons is maintained throughout the process; starting from *R* configuration, we obtain *R* configuration.

As we have seen, one of the features of the conventional proton sponges is the distortion from the planarity with respect to other typically aromatic anilines; in **Table IV.1** we compare DMAN with our derivatives. The perimidine derivate **(*R,R*)-6** does not behave such as proton sponge, the naphthalene ring with pyrrolidine moiety is

totally planar and the distance between nitrogens is typically from (1,8)-diaminonaphthalene.

Table IV. 1. Comparison of angles and distances.

	N::N distance	Torsion angle	N..H distance	CCC angle
				
DMAN	2.810 Å	8.9°, 10.5°	-	125.8 °
DMANH	2.720 Å	1.7°	1.16 Å	125.7 °
(R,R)-8	2.756 Å	4.0 °	1.85 Å	125.7 °
(R,R)-6	2.378 Å	0 °, 2.8 °	-	120.2 °

In the other hand, **(R,R)-8** preserves PS behavior even having the phenolic proton inside its structure, the distance between nitrogens is closely with DMAN, the CCC angle is identical but the torsion of the ring is less than DMAN, this leads us to think that **(R,R)-8** is less basic than DMAN, but it could have conditions to be used as base catalyst.

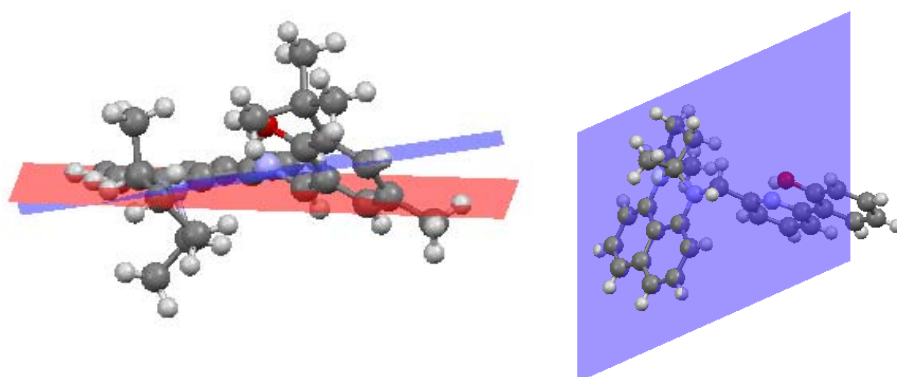


Figure. IV. 22. Twisted naphthalene in **(R,R)-8** (left) and planarity of naphthalene in **(R,R)-6** (right).

3.2.1 Scope of the cyclization reaction to afford chiral perimidines.

Perimidines³⁴ are tricyclic heterocycles consisting of a dihydropyrimidine ring *ortho*- and peri-fused to a naphthalene fragment and as mentioned above, may be used as starting material for the synthesis of proton sponges.¹³ These structures have been shown to be interesting candidates for biological activity studies and find widespread application in industry, agriculture and medicine.³⁵ A generally applied synthetic route towards perimidines comprises the reaction of 1,8-diaminonaphthalene with a carbonyl compound such as carboxylic acids, anhydrides, acid halides, ketones or aldehyde reagents.³⁶ In the latter case 2,3-dihydro-1*H*-perimidines are produced which can be easily converted to perimidines by dehydrogenation. The preparation of (2,3-dihydro-1*H*)-perimidines has been subject of many investigations using Lewis acid promoted reactions³⁷ or other methods.³⁸ On the other hand, recent literature has witnessed the communication of various multi-perimidinal systems that find use as ligand scaffolds for catalytically active complexes,³⁹ and as fragments of *N*-salicylideneaniline structures.⁴⁰

[34] a) K. Undheim, C. Benneche, in: *Comprehensive Heterocyclic Chemistry II* (Eds.: A. R. Katritzky, C. W. Rees, E. F. Scriven), Pergamon, Oxford, **1996**; (b) A. F. Pozharskii, V. V. Dalnikovskaya, *Russ. Chem. Rev.* **1981**, *50*, 816–835.

[35] a) J. M. Herbert, P. D. Woodgate, W. A. Denny, *J. Med. Chem.*, **1987**, *30*, 2081–2086; (b) X. Bu, L. W. Deady, G. J. Finlay, B. C. Baguley, W. A. Denny, *J. Med. Chem.*, **2001**, *44*, 2004–2014; c) D. R. Luthin, A. K. Rabinovich, D. R. Bhumralkar, K. L. Youngblood, R. A. Bychowski, D. S. Dhanoa, J. M. May, *Bioorg. Med. Chem. Lett.*, **1999**, *9*, 765–770.

[36] For some examples see: a) V. Paragamian, M. B. Baker, B. M. Puma, J. Jr. Reale, *J. of Heterocycl. Chem.* **1968**, *5*, 591–597; b) A. Shaabani, A. Maleki, *Chem. Pharm. Bull.*, **2008**, *56*, 79–81; c) J. B. Hendrickson, M. S. Hussoin, *J. Org. Chem.*, **1987**, *52*, 4137–4139; d) J. J. Vanden Eynde, F. Delfosse, A. Mayence, Y. V. Haverbeke, *Tetrahedron*, **1995**, *51*, 5813–5818; e) V. A. Ozeryanskii, E. A. Filatova, V. I. Sorokin, A. F. Pozharskii, *Russ. Chem. Bull.* **2001**, *50*, 846–853.

[37] a) A. Maquestiau, L. Berte, A. Mayence, L. Vanden Eynd, *Synth. Commun.*, **1991**, *21*, 2171–2180; b) A. Mobinikhaledi, P. J. Steel, *Synthesis and Reactivity in Inorganic, Metal-Organic, and Nano-Metal Chemistry*, **2009**, *39*, 133–135; c) S. L. Zhang, J. M. Zhang, *Chin. J. Chem.*, **2008**, *26*, 185–189; d) J. Zhang, S. Zhang, *Synth. Commun.*, **2007**, *37*, 2615–2614.

[38] a) L. W. Deady, T. Rodemann, *J. Heterocycl. Chem.*, **1998**, *35*, 1417–1419; b) N. Morita, J. I. Dickstein, S. I. Miller, *J. Chem. Soc. Perkin Trans., 1* **1979**, *1*, 2103–2106; c) I. Yavari, F. Jahanimoghaddam, F. Adib, H. R. Bijanzadeh, *Tetrahedron*, **2002**, *58*, 6901–6906; d) I. A. S. Smellie, A. Fromm, R. M. Paton, *Tetrahedron Lett.*, **2009**, *50*, 4104–4106; e) A. Mobinikhaledi, N. Foroughifar, N. Basaki, *Turk. J. Chem.*, **2009**, *33*, 555–560; f) M. Tajbakhsh, M. M. Heravi, B. Mohajerani, A. Ahmadi, *J. Mol. Catal. A*, **2006**, *247*, 213–215.

[39] I. G. Jung, S. U. Son, K. H. Park, K. C. Chung, J. W. Lee, Y. K. Chung, *Organometallics*, **2003**, *22*, 4715–4720.

[40] M. Sauer, C. Yeung, J. H. Chong, B. O. Patrick, M. J. MacLachlan, *J. Org. Chem.* **2006**, *71*, 775–788.

Reaction of pyridine-2-carbaldehyde or 6-(2-hydroxyphenyl)pyridine-2-carbaldehyde, with 8-((2*R*,5*R*)-2,5-dimethylpyrrolidin-1-yl)naphthalen-1-amine leads to the formation of perimidine derivatives (**(*R,R*)-5** and **(*R,R*)-6**).

In order to get more information about the cyclization reaction, we here report a versatile approach towards a small library of functionalized chiral perimidines. The results (**Figure. IV. 23**) show that the transformation is not influenced by the nature of the aromatic aldehyde, (activated or deactivated ring, **(*R,R*)-7a, 7c**), but does affect the position of the phenol group, that must be alpha with aldehyde group to prevent the cyclization (**(*R,R*)-10**).

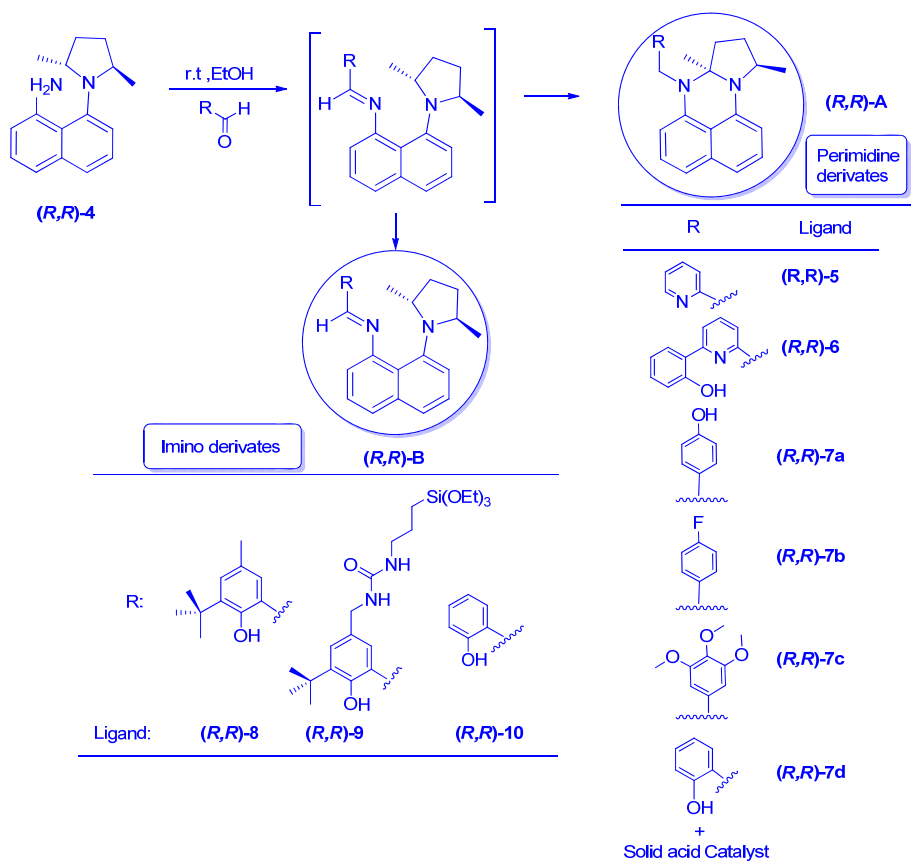


Figure. IV. 23. Synthesis of various substituted (7*aR*,10*R*)-7,7*a*,10-trimethyl-7*a*,8,9,10-tetrahydro-7H-pyrrolo[1,2-*a*]perimidines.

On the other hand, the cyclization occurs when the phenolic group is in (*m*, *p*) position, or in alpha position and the reaction takes place in acid medium (**(*R,R*)-7d**). In these cases the imino structure is not stabilized with the phenolic hydrogen bond and the cyclized product appears. It is important to note that once formed the imino compound ((**(*R,R*)-8**, (**(*R,R*)-9** or (**(*R,R*)-10**) this results to be stable and the cyclization does not occur over increase of the temperature. All compounds showed ^1H NMR and ^{13}C NMR consistent with proposed structures.

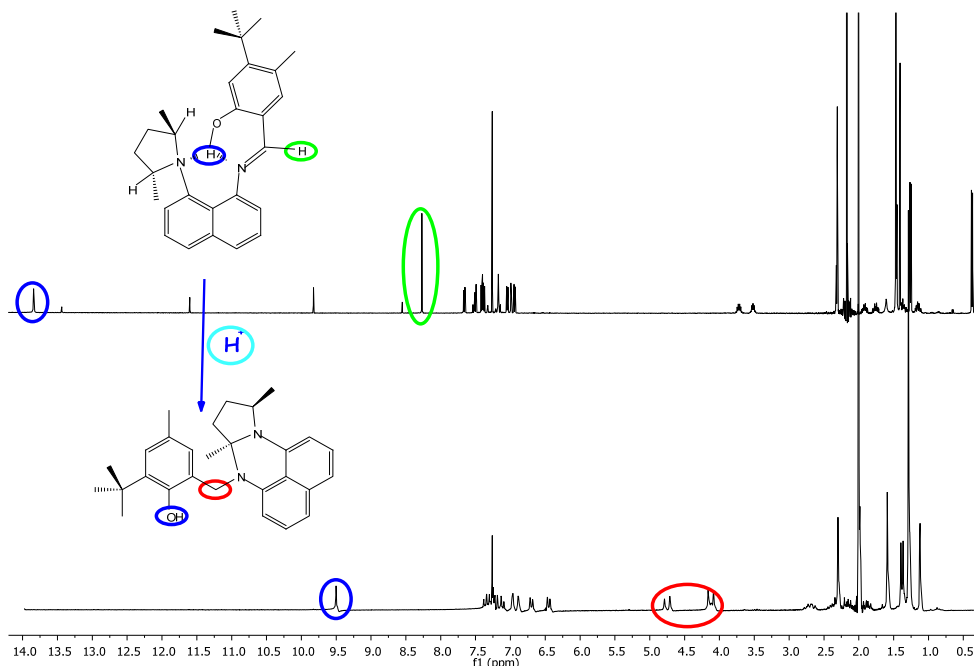


Figure. IV. 24. ^1H -NMR spectrum of (**(*R,R*)-8**) before (up) and after (down) acid treatment.

(**(*R,R*)-8**) becomes in its cyclized derivative in presence of acetic acid or NH_4Cl . In this case the proton of the phenol group is outside the structure and is represented as a singlet at 9.51 ppm and characteristically CH_2 protons of ABXY CH_2 system at 4.68 ppm and 4.20 ppm is present in ^1H NMR spectrum. (**Figure. IV. 24**).

There are few examples of this type of transformation.^{27,15,41} The proposed mechanism involves a hydride transfer that enables the transformation that starts with the formation of an iminium salt before the final cyclization as shown in **Figure. IV. 25**.

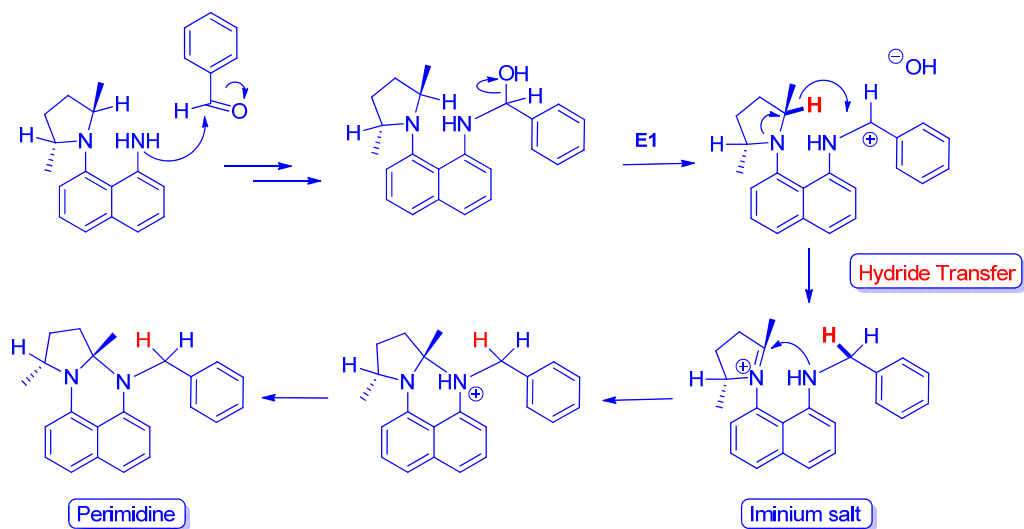


Figure. IV. 25. Proposed mechanism for perimidine synthesis

[41] a) A. Peters, U. Wild, O. Hübner, E. Kaifer, H. J. Himmel *Chem. Eur. J.*, **2008**, *14*, 7813-7821; b) A. F. Pozharskii, *Russ. Chem. Rev.*, **1998**, *67*, 3-27; c) M. M. Belmonte, E. C. Escudero-Adán, J. Benet-Buchholz, R. M. Haak, A. W. Kleij, *Eur. J. Org. Chem.*, **2010**, 4823-4831.

3.3 Synthesis of rhodium and palladium complexes.

Several rhodium and palladium complexes with **(R,R)-5**, **(R,R)-6**, **(R,R)-8**, and **(R,R)-9** as ligands were prepared by standard methods (**Figure. IV. 27**, **Figure. IV. 28** and **Figure. IV. 29**).

3.3.1 Synthesis of perimidine derivative complexes.

3.3.1.a Synthesis of palladium complexes.

Reactions of **(R,R)-5** and **(R,R)-6** with $[\text{Pd}(\text{cod})\text{Cl}_2]$ or $\text{Pd}(\text{AcO})_2$ were carried out at room temperature in CH_2Cl_2 or EtOH solution in a 1:1 complex: ligand ratio. The products, **5Pd**, **6Pd** ($[\text{Pd}((\text{R,R})\text{-5})\text{Cl}_2]$, $[\text{Pd}((\text{R,R})\text{-6})\text{AcO}]$), were obtained in almost quantitative yields as stable brown solids by careful precipitation from pentane; and characterized by elemental analysis, ESI-MS and ^1H ^{13}C NMR spectroscopy. Thus, the ESI-MS spectra of **5Pd** and **6Pd** show peaks from the fragments due to elimination of the ion chloride $[\text{M}^+ - \text{Cl}]$ (471.3 for **5Pd**) or acetate $[\text{M}^+ - \text{OAc}]$ (585.5 for **6Pd**). All assignments were confirmed by good agreement between the observed and calculated isotopic distributions.

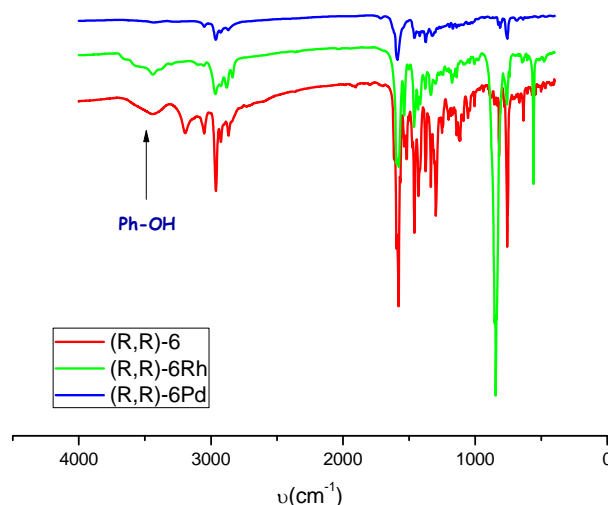


Figure. IV. 26. IR of **(R,R)-6** and its rhodium and palladium metal complexes.

The absence of the $\nu(\text{OH})$ band (present in the spectrum of the free ligand **(R,R)-6** at $\sim 3430\text{ cm}^{-1}$) is in accordance with loss of the $-\text{OH}$ proton (**Figure. IV. 26**) for **6Pd**.

The IR spectrum of **6Pd** also shows strong bands at 1290 and $\sim 1600\text{ cm}^{-1}$ assigned to the symmetric and asymmetric $\nu(\text{COO})$ vibrations, respectively, in agreement with those expected for monocoordinate acetate ligands.⁴² New bands at 555 cm^{-1} are ascribed to $\nu(\text{Pd}-\text{O})$ (**6Pd**).

Diamagnetic palladium complexes have been characterized by ^1H and ^{13}C NMR. All assignments are based on several correlations in the 2D spectra. They are fully consistent with the structures depicted in **Figure. IV. 27** and **Figure. IV. 28**. In all cases, the spectra show the simultaneous occurrence of two set of signals which are attributable on the one hand to the substituted pyridine entity and on the other hand to the amine sponge derivative part of the ligand. In the ^1H NMR spectra all the resonances were high field shifted as compared to the uncoordinated ligand and they were in agreement with metallation of the ligand with coordination of the metal atom *via* the pyridine nitrogen atom.

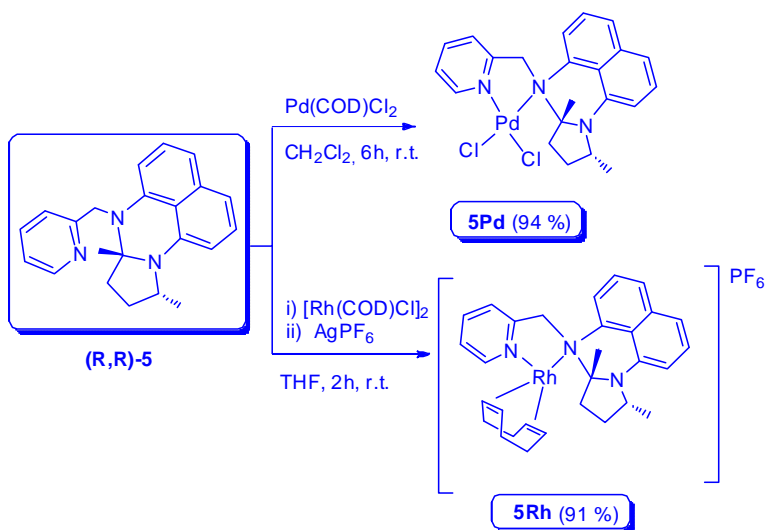


Figure. IV. 27. Synthesis of **(R,R)-5** perimidine-complexes.

[42] K. Nakamoto, *IR and Raman Spectra of Inorganic and Coordination Compounds*, 5th, ed., WILEY & SONS: New York, **1997**.

Deprotonation of the –OH group in **6Pd** was confirmed by the absence of OH resonance in the ^1H spectrum. The ^1H NMR spectrum shows the signal of the *MeCOO* protons as a singlet at 1.88 ppm (**6Pd**). The ^{13}C NMR spectrum of **6Pd** showed the signals assigned to the ligand OAc group.

3.3.1.b Synthesis of rhodium complexes.

The cationic complexes, $[\text{Rh}(\text{cod})(\text{L}^*)]\text{PF}_6$, (**5Rh**, **6Rh**) ($\text{L}^* = (\text{R,R})\text{-5}$, $(\text{R,R})\text{-6}$), were synthesized by the reaction of $[\text{RhCl}(\text{cod})]_2$ with a stoichiometric amount of solid AgPF_6 and, subsequently after 1 h the corresponding L^* chiral ligand, in THF solution. Filtration through Celite and evaporation of the solvent yielded a solid product, which was recrystallized by carefully addition of diethyl ether. The experimental data allowed us to establish that both $(\text{R,R})\text{-5}$ and $(\text{R,R})\text{-6}$ ligand act, in the formation of complexes, as chelating ligand. In the ^1H NMR spectrum the cyclooctadiene resonances are observed as four broad lines between 1.8 ppm and 4.8 ppm due to fluxionality in the conformation of the cyclooctadiene chelate. Complexes exhibit four signals in their ^{13}C spectrum attributable to the carbon atoms of the cod ligand.

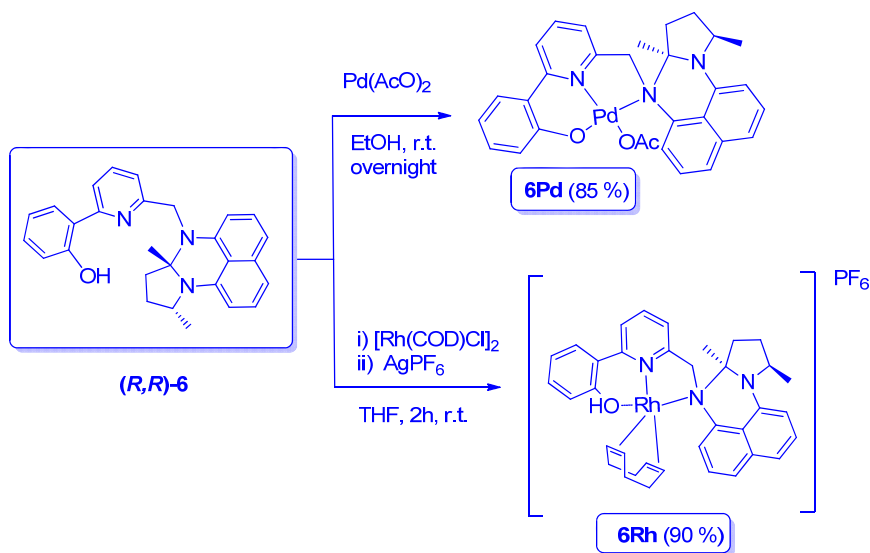


Figure. IV. 28. Synthesis of $(\text{R,R})\text{-6}$ perimidine-complexes.

Elemental analysis and the ESI-MS spectra (540.3 for **5Rh** and 632.3 for **6Rh** corresponding to $[M^+ - PF_6])$ are consistent with the proposed formulation shown in **Figure. IV. 27** and **Figure. IV. 28**, but a single crystal structure has not yet to be obtained. The $-OH$ group deprotonation was not observed for rhodium complex with ligand **(R,R)-6**, the infrared spectrum presents a signal corresponding to $\nu(OH)$ at 3443 cm^{-1} . (**Figure. IV. 26**).

3.3.2 *Synthesis of imino complexes.*

3.3.2.a *Synthesis of palladium complexes.*

The reactions between the imino compounds **(R,R)-8** or **(R,R)-9** with $Pd(OAc)_2$ were carried out at room temperature in EtOH solution, respectively, in a 1:1 complex:ligand ratio.

The products, $[Pd(L^*)(OAc)]$, **8Pd**, **9Pd** ($L^* = \text{(R,R)-8, (R,R)-9}$) were obtained in almost quantitative yields as stable solids. These complexes were characterized by electro-spray mass spectrometry. Thus, the ESI-MS spectrum of **8Pd** shows the peak from the fragment due to elimination of the acetate at m/z 519.3 $[M^+ - OAc]$. All assignments were confirmed by good agreement between the observed and calculated isotopic distributions. In **8Pd**, the absence of the $\nu(OH)$ band (present in the IR spectrum of the free ligand **(R,R)-8** at $\sim 3430\text{ cm}^{-1}$) is in accordance with loss of the $-OH$ proton. The IR spectrum also showed a band at 1585 cm^{-1} assigned to coordinated $C=N$, about 30 cm^{-1} less than the free ligand, as expected for coordination of the imine. The IR spectrum also shows strong bands at 1320 and 1650 cm^{-1} assigned to the symmetric and asymmetric $\nu(COO)$ vibrations, respectively, in agreement with those expected for monocoordinate acetate ligands.⁴² A New band at 541 cm^{-1} is ascribed to $\nu(Pd-O)$ for **8Pd**.

Diamagnetic palladium complexes have been characterized by 1H and ^{13}C NMR spectroscopy. All assignments are based on several correlations in the 2D spectra. They are consistent with the structures depicted in **Figure. IV. 29**. In all cases, the spectra show the simultaneous occurrence of two set of signals which are

attributable on the one hand to the substituted pyridine entity and on the other hand to the amine sponge derivative part of the ligand.

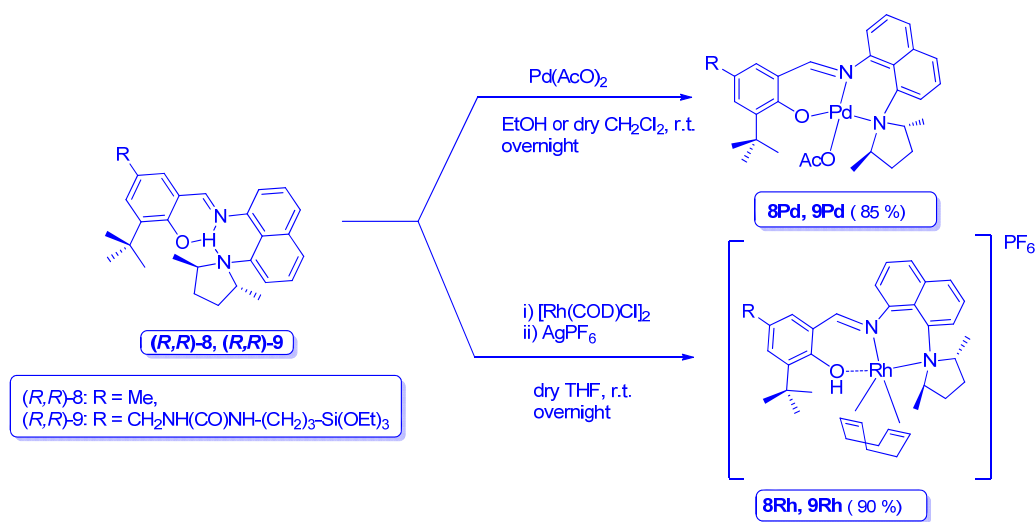


Figure. IV. 29. Synthesis of Rh and Pd imino-complexes.

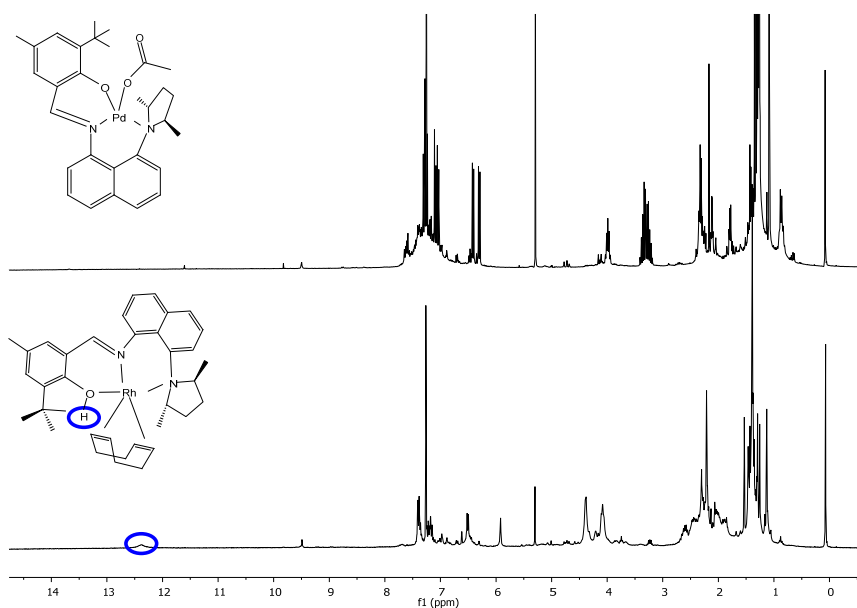


Figure. IV. 30. ^1H -NMR spectrum of (*(R,R)*-8Pd (deprotonated) and (*(R,R)*-8Rh (protonated)).

In the ^1H NMR spectra all the resonances were high field shifted as compared to the uncoordinated ligand and they were in agreement with metallation of the ligand with coordination of the metal atom *via* the pyridine nitrogen atom. In the ^1H NMR of both **8Pd** and **9Pd**, the absence of the OH resonance corroborates the deprotonation of the –OH group. (**Figure. IV. 30**).

The ^1H NMR spectrum of **8Pd** showed a singlet at 7.99 ppm due to imine proton shifted upfield 0.27 ppm compared with the free ligand. Also, the acetate group was observed as a singlet at 1.34 ppm. The ^{13}C NMR spectrum of **8Pd** showed the imine carbon at 153.7 ppm (160.4 ppm for **9Pd**) and two signals for acetate at 29.7 ppm and 197.1 ppm.

3.3.2.b *Synthesis of rhodium complexes.*

Cationic complexes, $[\text{Rh}(\text{cod})(\text{L}^*)]\text{PF}_6$, (**8Rh**, **9Rh**) ($\text{L}^* = (\text{R},\text{R})\text{-8}$ and $(\text{R},\text{R})\text{-9}$), were synthesized by the reaction of $[\text{RhCl}(\text{cod})]_2$ with a stoichiometric amount of solid AgPF_6 and, subsequently after 30 min. the corresponding L^* -chiral ligand, in THF solution. Filtration through Celite and evaporation of the solvent yielded a solid product, which was recrystallized using Et_2O . The ^1H NMR spectrum of the isolated product **8Rh** showed four broad lines between 1.8 and 4.8 ppm, due to fluxionality in the conformation of the cod chelate, a singlet at 5.96 ppm due to the imine (5.93 ppm **9Rh**), and a broad singlet at 12.41 ppm (9.82 ppm for **9Rh**) assigned to the unprotonated OH group. Complexes exhibit four signals in the ^{13}C spectrum attributable to the carbon atoms of the cod ligand. ESI-MS spectrum show the mass for the molecular peak at 625.5 for **8Rh** $[\text{M}^+ - \text{PF}_6]$, but a single crystal structure has yet to be obtained. IR spectrum show the corresponding to $\nu(\text{OH})$ at 3408 cm^{-1} . The $\nu(\text{C}=\text{N})$ stretching was observed at 1619 cm^{-1} .

3.4 Heterogeneization of complexes containing pendant alkoxy silane groups to MCM-41.

The pure siliceous MCM-41 (MCM) parent material was derivatized following the strategy depicted in **Figure. IV. 31**. Supported complexes, were obtained by refluxing a mixture of the precursor **9Pd** or **9Rh** and the support, in toluene, with metal loadings of approximately 0.20-0.30 mmol-metal.g⁻¹ support. These materials were characterized by elemental analysis of C, H, N, M, FT IR, DRUV and CP-MAS solid state, ¹³C NMR spectroscopy. Heterogeneization reactions yielded materials with the expected ratios of metal to nitrogen loadings. In general these results showed us that little other than the expected reactions are occurring on the functionalized silica surface.

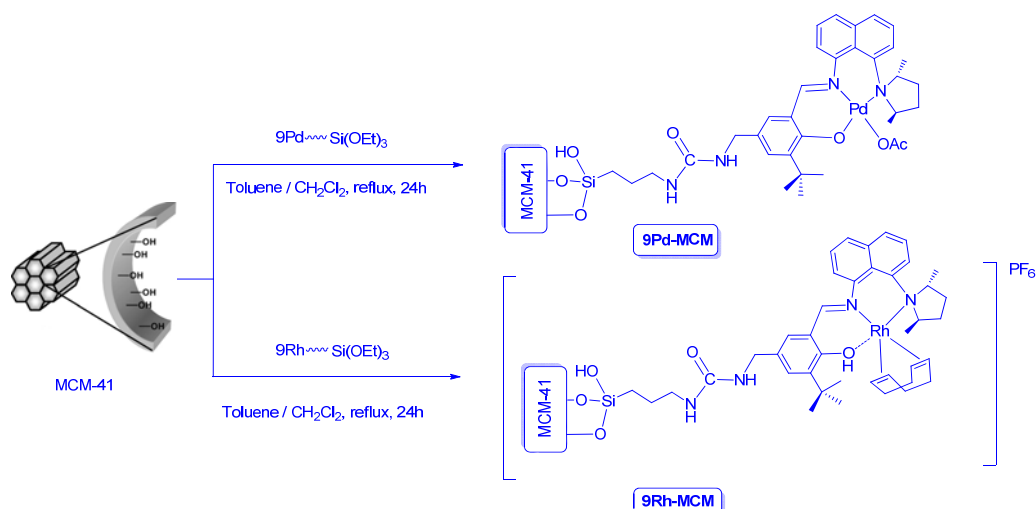


Figure. IV. 31. Heterogeneization of imino complexes.

The presence of functional groups characteristic of **9Pd** or **9Rh** in the materials was checked by FTIR spectroscopy. The stretching vibrations modes of the mesoporous framework (Si–O–Si) of the grafted material **9Pd-MCM** or **9Rh-MCM** are observed at around 1240, 1070, and 810cm⁻¹, as in the parent MCM, while new bands appear at ca. 2950 and 2850cm⁻¹, assigned to the $\nu(\text{C-H})$ stretching of the aliphatic linear chain in MCM-Pr and pyrrolidine ring.

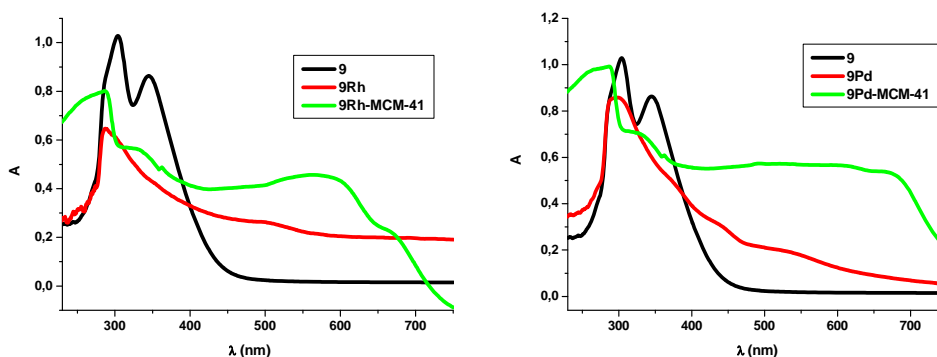


Figure. IV. 32. UV (before and after heterogeneization DFTR (after heterogeneization) of ligand and metal complexes.

The presence of ligands leads to the appearance of the $\nu(\text{C}=\text{N}$, $\text{C}=\text{O}$, $\text{C}=\text{C}$) stretching modes at $1640\text{--}1570\text{ cm}^{-1}$. New band in at $\text{ca. } 550\text{ cm}^{-1}$ is ascribed to $\nu(\text{Pd-O})$.

The complexes immobilized on supports have been characterized by diffuse reflectance spectroscopy. (**Figure. IV. 32**). The complexes show several strong bands in the UV region agreeing with the assignment of the bands as intraligand transitions in the aromatic ring, and charge-transfer transition. The diffuse reflectance spectra of complexes are almost identical before and after heterogeneization process, indicating that the complexes maintain their geometry and their electronic surrounding even after heterogeneization without significant distortion.

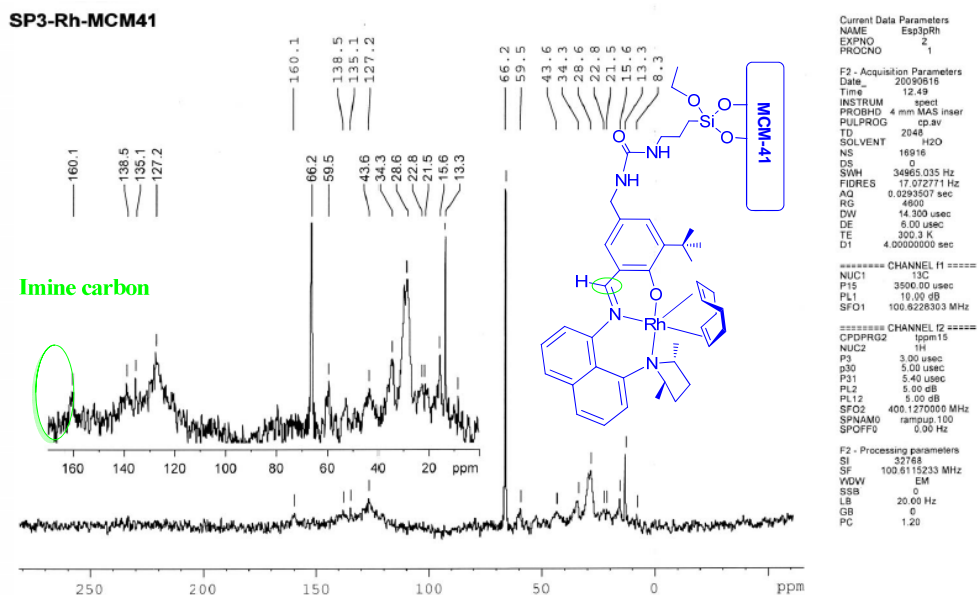


Figure. IV. 33. ^{13}C CP MAS solid state NMR of **9Rh-MCM**.

The materials were also characterized by cross-polarization magic-angle spinning ^{13}C CP MAS solid state NMR. The solid state ^{13}C CP MAS NMR spectra of **9Pd-MCM**, **9Rh-MCM** materials are quite similar, since the spectra are dominated by the resonances of the aliphatic and aromatic groups. These signals appear at 8.6 and 8.3 ppm ($\text{Si}-\text{CH}_2$), 28.6 ppm ($\text{CH}_2-\text{CH}_2-\text{CH}_2$), 44.0-43.6 ppm ($\text{N}-\text{CH}_2$); aromatic region at 130.3-156.4 ppm, 160.5 ppm, 160.1 ppm ($\text{N}=\text{CH}$) and 198 ppm (OAc). The majority of peaks corresponding to the ^{13}C NMR spectrum of soluble complexes were present in the ^{13}C spectra of their heterogenized counterparts. (**Figure. IV. 33**).

3.5 Catalytic activity.

3.5.1 Asymmetric hydrogenation of pro-chiral alkenes.

In order to evaluate the catalytic performances of these new Rh(I) and Pd(II) complexes, we have tested them in asymmetric hydrogenation reactions of 2*R*-succinates using experimental conditions that could permit us a comparative study of different catalysts and substrates. Results are summarized in **Table IV. 2**.

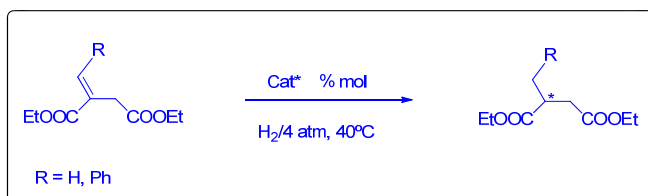


Table IV. 2. Catalytic hydrogenation of (*E*)-diethyl 2-*R*-succinates with palladium and rhodium-complexes.^a

Entry	Catalyst ^s	H		Ph	
		ee (%) ^c	TOF ^b	ee (%) ^c	TOF ^b
1	5Pd	≤ 5	588	50	118
2	5Rh	≤ 5	600	97	36
3	6Pd	≤ 5	582	10	109
4	6Rh	≤ 5	590	60	92
5	8Pd	≤ 5	600	85	158
6	8Rh	≤ 5	602	95	108
7	9Pd-MCM	≤ 5	1176	80	210
8	9Rh-MCM	≤ 5	1164	90	300
9	3Pd (ref.32a)	6	3368	12	640
10	3Pd-MCM (ref. 32a)	≤ 10	4980	≤ 10	900
11	6bPd (ref. 33a)	≤ 5	2800	15	565
12	13Pd-MCM (ref. 33b)	10	234	30	78

^aEthanol, 4 atm. H₂, 40 °C, Cat.: 0.1 mol% for diethyl itaconate, 1 mol% for (*E*)-diethyl 2-benzylidenesuccinate; ^bTOF: h⁻¹ (calculated at maximum rate); ^cHPLC (chiralcel AD-H, λ: 230 nm, Hexane/iPrOH: 98/2, chiralcel OD, λ: 250 nm, Hexane/iPrOH: 95/5), (*S*) isomer.

The hydrogenation of (*E*)-diethyl 2-benzylidenesuccinate or diethyl itaconate with Rh- and Pd-complexes were carried out under standard conditions (EtOH as the solvent, 4 atm hydrogen pressure, 40 °C). Obviously for preparative application a tuning of experimental conditions has to be done for each case. We choose two substrates with extremely different steric hindrance as a model to make a comparative study of the catalysts properties. In all cases, with all catalysts, complete conversion of substrate was observed.

3.5.1.a Ligand influence.

Table IV. 2 also shows the effect of ligand substituents have on activity and enantioselectivity in the hydrogenation process. If we compare the imino ligands with the perimidine ligands for same metal in the hydrogenation of (*E*)-diethyl 2-benzylidenesuccinate, we evaluate the effect of changing the structure of the ligand within the family of catalysts.

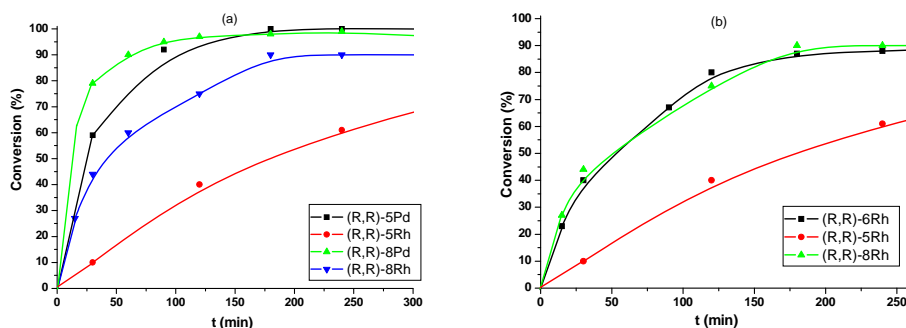


Figure. IV. 34. (a) Kinetic profile for all soluble catalysts. (b) Kinetic profile for Rh soluble catalysts.

In terms of activity, we studied the kinetic profiles for both families in Rh complexes (**Figure. IV. 34 (b)**). We conclude that the complexes derived from (*R,R*)-**5** are less active than the others. The imine catalyst (derived from (*R,R*)-**8**) presents slightly better activity than derivatives from (*R,R*)-**6**.

For the study of the enantiomeric excess induced by the catalyst we could analyze the asymmetric induction for palladium complexes. (**Figure. IV. 35**).

Perimidine complexes show less asymmetric induction than imine catalysts. This fact could be explained by the distance of the metal center from the chiral moiety of the ligand in each case. Thus, in imino catalysts, the metal is closely to the pyrrolidine because it is inside the structure, in the other hand, in perimidine complexes the metal center is outside the structure and it is so far from the chiral pyrrolidine moiety. Then, we could sort these ligands by asymmetric induction depending on the type of ligand.

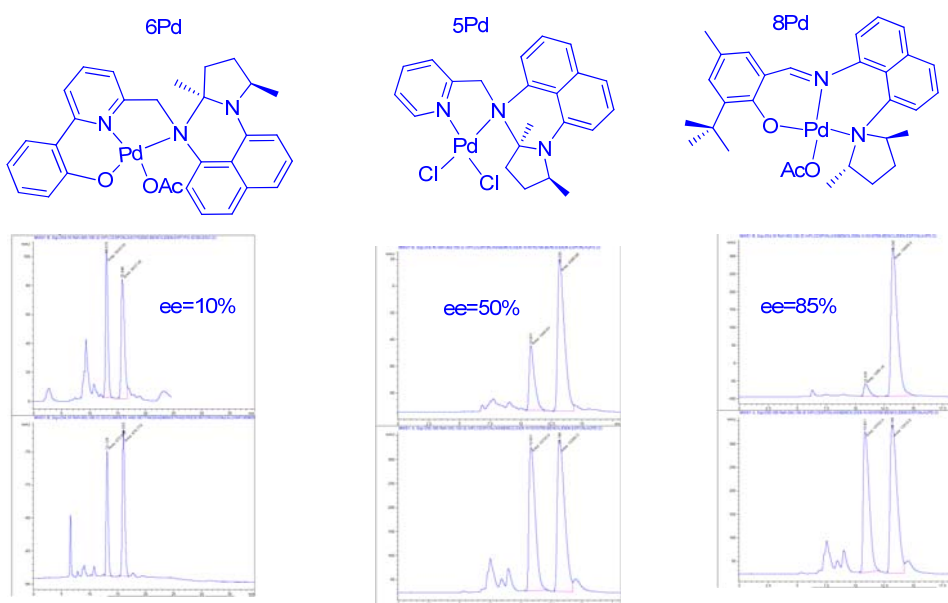


Figure. IV. 35. Ligand influence in asymmetric induction.

3.5.1.b Proton sponge core ligands versus proline Schiff base ligands.

Other way, if we compare, focusing on palladium catalysts, (**Figure. IV. 36**) the catalytic activity of complex **6Pd**, in this work, with that of previously reported for (S)-N-(*tert*-butyl)-1-((6-(2-hydroxyphenyl)pyridine-2-yl)methyl)pyrrolidine-2-carboxamide as ligand (complex **6bPd** in reference [33]a) and **13Pd-MCM-41** in

reference [33]b), which have the prolinamide as chiral group, (the three catalysts are ONN-Pincer-type) in the hydrogenation of (*E*)-diethyl 2-benzylidenesuccinate it appears that although the latter has a better catalytic activity (TOF: 565 h⁻¹, **Table IV. 2.** entry 11 vs 109 h⁻¹, **Table IV. 2.** entry 3), the enantiomeric excess is comparable in both cases (15% vs 10%).^{33a} Similarly in this case the enantioselectivity increases considerably when the catalyst is heterogenized (**Table IV. 2.** entry 12).^{33b}

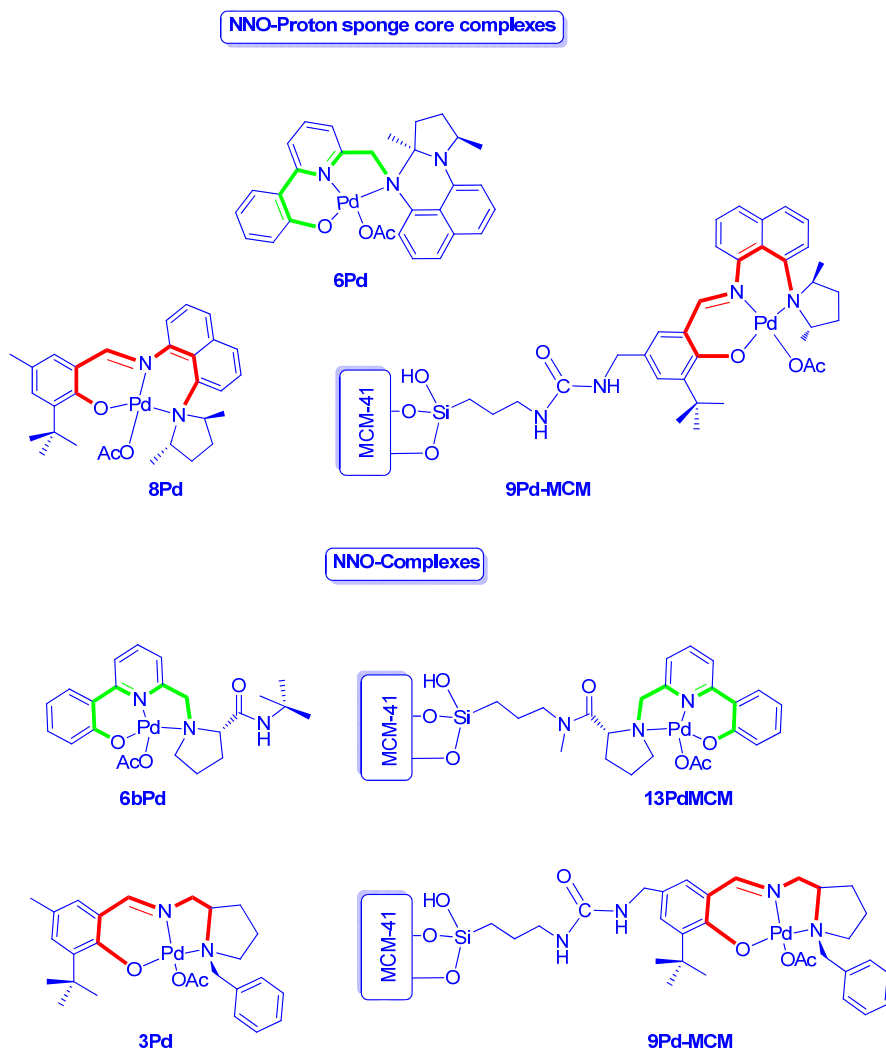


Figure. IV. 36. Catalytic behavior NNO versus proton sponge-core NNO for palladium complexes.

If we now compare the results obtained with the complexes derived from **(R,R)-8** with those previously reported for catalysts with a phenol-imino-amino ligand, 2-(((1-benzylpyrrolidin-2-yl)methylene)amino)-6-(*tert*-butyl)-4-methylphenol as ligand, (complex **3Pd**, **3Pd-MCM-41** in reference [32]a) we found that the most active catalysts are those with the Schiff base system derived with a proline derivative group (**Table IV. 2**, entries 9, 10). However, the highest enantioselectivity is obtained with the catalyst from proton sponge systems. (**Table IV. 2** entries 5,7)

3.5.1.c Influence of support

Because the soluble catalyst show lower activity than the heterogenized, we confirmed that the presence of site-isolated metal complexes grafted onto MCM-41 was responsible for enhanced conversion and that the reaction is truly heterogeneous. (**Figure. IV. 37**).

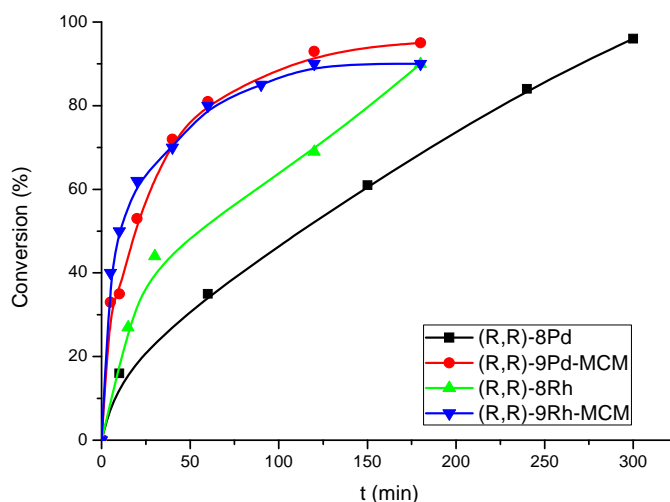


Figure. IV. 37. Kinetic profile soluble versus heterogenized catalysts.

3.5.2 Recycling experiments in asymmetric hydrogenation of alkenes.

From an environmental point of view, it is desirable to minimize the amount of waste for each organic transformation. Reusability is an important feature to be monitored for application of heterogenized single-site catalysts. Before reuse, the

catalyst was separated from the reaction mixture by filtration and washed with ethanol. After the first run, the reaction reached >99% after 3 h and this remained steady up to the 4th run, proving that the catalyst is highly stable and simple to recycle.

Table IV. 3. Recycling experiments of 9Rh-MCM in the catalytic hydrogenation of (*E*)-diethyl 2-benzylidenesuccinate.

Run	TOF (h ⁻¹)	ee % (<i>S</i>)
1	300	90 (<i>S</i>)
2	285	88 (<i>S</i>)
3	290	85 (<i>S</i>)
4	310	90 (<i>S</i>)

The catalytic materials were easily separated from the substrate/ product solution by simple filtration subsequent washing, and then added fresh substrate, and solvent without further addition of catalyst. The recycling process could be repeated four times with no significant loss in selectivity, and minimal losses in activity (**Table IV. 3, Figure. IV. 38**). Furthermore, the filtrate, which was colorless, was placed in a catalyst free autoclave and fresh substrate was added. Dihydrogen pressure was applied, however no further conversion was observed. This demonstrates that no metal leaching from the silica surface is occurring. The metal content (loading) of the recycled catalytic material was the same as the starting catalytic material suggesting little, if any, metal leaching. Hot filtration experiments and ICP measurements were independently carried out to rule out the possibility of leaching.

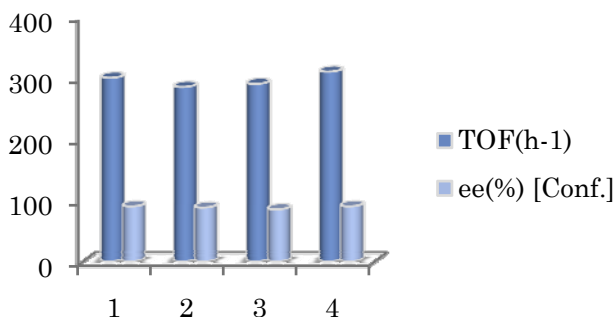


Figure. IV. 38. Recycling of **9Rh-MCM**.

In order to check the stability of metal complexes supported on the solid matrix, we have characterized the solid before and after reaction. As can be deduced from IR, ^{13}C NMR and UV-vis spectra the nature of supported species is very similar and the most important signals for ligands appear in the same position after reaction.

4 Conclusions.

In this chapter we report the synthesis of the first pincer type complexes derived from a chiral proton sponge precursor, as well as, a surprising cyclization transformation that takes place in soft conditions to afford perimidine derivatives from several aldehydes and 8-((2*R*,5*R*)-2,5-dimethylpyrrolidin-1-yl)naphthalen-1-amine with good yields. The complexes derived from both types of ligands present high activity and enantioselectivity in hydrogenation of prochiral olefins. The supported complexes in MCM-41 show better activity than the soluble counterpart, and they could be recycled for subsequent cycles without loss of any material's features.

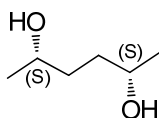
5 Experimental section.

General Remarks: All manipulations were carried out by using standard Schlenk vacuum-line techniques under an atmosphere of oxygen-free argon. All solvents for synthetic use were dried and distilled, under an argon atmosphere, by standard procedures.⁴³ Elemental analyses were performed with a Lecco microanalyzer, by the analytical department of the Instituto de Química Orgánica (C.S.I.C.). Metal contents were analyzed by atomic absorption spectroscopy using a Perkin Elmer AAnalyst 300 atomic absorption apparatus and plasma ICP Perkin Elmer OPTIMA 2100 DV. Infrared spectra were recorded on a Bruker IFS 66v/S spectrophotometer (range 4000–200 cm⁻¹) in KBr pellets. ¹H and ¹³C{¹H} NMR spectra and bidimensional experiments (HMQC, HMBC and COSY) were recorded with a Bruker AMX-300 and 500 instruments. DEPT-135 spectra were used to assign CH, CH₂ and CH₃ resonances. Chemical shifts are referenced to tetramethylsilane (internal standard). ¹³C MAS or CP/MAS NMR spectra of powdered samples, in some cases also with a Toss sequence, in order to eliminate the spinning side bands, were recorded at 100.63 MHz, 6 μs 90° pulse width, 2 ms contact time and 5-10 recycle delay, using a Bruker MSL 400 spectrometer equipped with an FT unit. The spinning frequency at the magic angle (54°44') was 4 KHz. Optical rotation values were measured at the sodium-D line (589 nm) with a Perkin Elmer 241 MC polarimeter. The reaction was monitored by gas chromatography on an HP5890 II GC-MS chromatograph, cross-linked methyl silicone column (SPB): 25 m x 0.2 mm x 0.33 mm; helium as carrier gas, 10 psi; injector temperature: 230 °C; detector temperature: 250 °C; The enantiomeric excess was measured by HPLC (Agilent 1200) using chiral column chiralcel OD (diethyl 2-benzylidene succinate, (λ: 254 nm, Hexane/ⁱPrOH: 95/5, 0.5 mL/min), chiralcel AD-H (diethyl itaconate, λ: 230 nm, Hexane/ⁱPrOH: 98/2, 0.4 mL/min.).

[43] D. D.Perrin, S. L. F.Armarego, D. R. Perrin in *Purification of Laboratory Chemicals*, PERGAMON PRESS, New York, **1980**.

5.1 Synthesis of precursors.

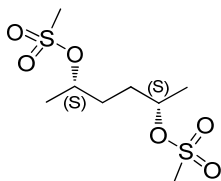
5.1.1 (2*S*,5*S*)-hexane-2,5-diol. (IN-5).



To a 5 L beaker was added yeast (200 g) and sugar (350 g) in 1.7 L of water with mechanical stirring at 30 °C. Over an hour and a half the hexane-2,5-dione (10 mL) was added. The reaction was followed by TLC. When the reaction was complete, the reaction mixture was filtered over celite.

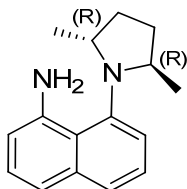
Volume of filtrate was reduced to 1 L and extracted continuously with ethyl acetate. The organic phase was evaporated to dryness and distilled under reduced pressure, collecting the fraction between 70 °C–90 °C at 1 mmHg. Yield= 85%.

5.1.2 (2*S*,5*S*)-hexane-2,5-diyl dimethanesulfonate. (IN-6).



In a two-necked flask was added a solution of (2*S*,5*S*)-hexane-2,5-diol (9.2 g, 0.0779 mol) and triethylamine (27 mL) in toluene (10 mL). The mixture was cooled to -5 °C and mesyl chloride is added dissolved in 10 mL of toluene. Always working in inert atmosphere the reaction allowed evolving without the temperature rise of 15 °C for 1 hour. Water (25 mL) was added and the organic layer was separated, the aqueous phase was extracted with toluene (1x20 mL). They gather organic phases were dried with anhydrous magnesium sulfate and concentrated to obtain 30% of the initial volume of reaction. Yield was quantitative.

5.1.3 8-((2*R*,5*R*)-2,5-dimethylpyrrolidin-1-yl)naphthalen-1-amine. ((*R*,*R*)-4).



In a three-necked flask, under inert atmosphere was placed sodium hydride (60% dispersed in oil) (15.09 g, 0.6287 mol), using a transfer NaH was washed 4 times with pentane. Diglyme solution of naphthalene-1,8-diamine (8.53 g, 0.05391 mol) was added and stirred at room temperature for 30 minutes. (2*S*,5*S*)-hexane-2,5-diyl dimethanesulfonate (**IN-6**) in toluene was added (19.22 g, 0.07005 mol) dropwise. The reaction mixture was left stirring at room temperature for 12 hours, the mixture heated to 120° C for 24 hours more. The reaction was followed by TLC (dichloromethane /ethyl acetate 20:1, *R_f* = 0.8). When the reaction finished, methanol (10 mL) and a saturated solution of sodium chloride were added. The organic phase separated and the aqueous phase extracted with petroleum ether (4x100 mL). The combination of the organic extracts concentrated to dryness and distilled under reduced pressure to remove the diglyme. The residue was purified by flash silica gel column chromatography (ethyl acetate /heptane 1:15), affording 2.8g of a dark red oil. Yield 23%.

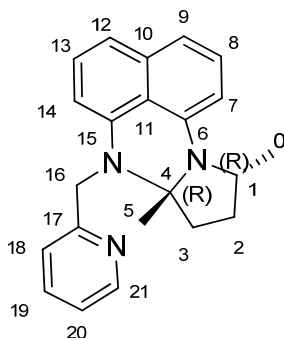
MS (EI, *m/z*, %): 240.0 (M^+), 225.0 ($M^+ - CH_3$).

¹H NMR (CDCl₃) δ (ppm): 7.45 (d, 1H, H_{Nph}, *J*_{HH} = 8.0 Hz); 7.26 (t, 1H, H_{Nph}, *J*_{HH} = 7.0 Hz); 7.17 (t, 1H, H_{Nph}, *J*_{HH} = 8.0 Hz); 7.10 (d, 1H, H_{Nph}, *J*_{HH} = 8.0 Hz); 7.01 (d, 1H, H_{Nph}, *J*_{HH} = 7.0); 6.52 (d, 1H, H_{Nph}, *J*_{HH} = 8.0 Hz); 6.15 (broad, 2H, NH₂); 3.90 (m, 1H, CH); 3.77 (m, 1H, CH); 2.22 (m, 2H, CH₂), 1.57 (m, 2H, CH₂); 1.17 (d, 3H, CH₃, *J*_{HH} = 7.0 Hz); 0.64 (d, 3H, CH₃, *J*_{HH} = 7.0 Hz).

¹³C NMR (CDCl₃) δ (ppm): 146.1; 143.5; 137.2; 126.4; 124.8; 124.6; 120.7; 119.1; 117.0; 109.2; 59.6; 52.2; 32.1; 30.8; 20.1; 16.6.

5.2 Synthesis of ligands.

5.2.1 (7*aR*,10*R*)-7*a*,10-dimethyl-7-(pyridin-2-ylmethyl)-7*a*,8,9,10-tetrahydro-7*H*-pyrrolo[1,2-*a*]perimidine.((*R*,*R*)-5).



To a solution of 8-[(2*R*,5*R*)-2,5-dimethylpyrrolidin-1-yl]naphthalen-1-amine (300 mg, 1.25 mmol) in absolute ethanol (20 mL) and in the presence of molecular sieves (2g, 4 Å) was added a ethanolic solution (10 mL) of 3 pyridine-2-carbaldehyde (133 mg, 1.25 mmol). The reaction mixture was stirred overnight at room temperature and filtered. The residue was dried under reduced pressure and purified by flash chromatography, $R_f = 0.25$ (5:1 heptane/ethyl acetate) to obtain a pale pink solid (290 mg, yield: 71%). M.p.: 58-60 °C. $C_{22}H_{23}N_3$ (329.4).

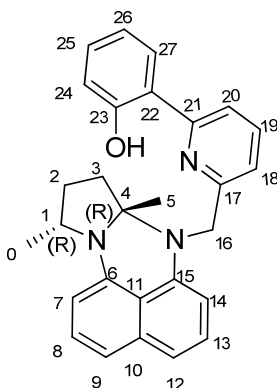
MS (EI, m/z , %): 329.0 (M^+), 314.0 ($M^+ - CH_3$), 252.0 ($M^+ - Py$).

IR (KBr; cm^{-1}): $\nu = 3048$ (w) (CH_{arom}); 2970 (m) (CH_{alip}), 2922 (m); (C=C), (C=N) 1582 (s), 1435 (s), 1418 (s); 1374 (m), 1337 (s); 810 (s), 756 (s); 639 (m), 607 (w), 517 (m).

1H NMR ($CDCl_3$) δ (ppm): 8.75 (ddd, 1H, H_{21} , $J_{HH} = 0.9, 1.6, 4.8$ Hz); 7.70 (dt, 1H, H_{19} , $J_{HH} = 1.7, 7.5$ Hz); 7.58 (d, 1H, H_{18} , $J_{HH} = 7.3$ Hz); 7.45 (t, 1H, H_{13} , $J_{HH} = 7.7$ Hz); 7.33–7.22 (m, 4H, H_8, H_9, H_{12}, H_{20}); 6.56 (d, 1H, H_{14} , $J_{HH} = 7.3$ Hz); 6.25 (dd, 1H, H_7 , $J_{HH} = 3.0, 5.2$ Hz); 4.82 (d, 1H, H_{16} , $-CH_2-$, ABXY, $J_{HH} = 17.6$ Hz); 4.57 (d, 1H, H_{16} , $-CH_2-$, ABXY, $J_{HH} = 17.6$ Hz); 4.29 (m, 1H, H_1 , $-CH_{pyrr}$); 2.55–2.47 (m, 2H, 2 $-CH_{2pyrr}$); 2.34 (m, 1H, $-CH_{2pyrr}$); 1.95 (m, 1H, $-CH_{2pyrr}$); 1.49 (d, 3H, H_0 , $-CH_3$, $J_{HH} = 6.6$ Hz); 1.37 (s, 3H, H_5 , $-CH_3$).

^{13}C NMR (CDCl_3) δ (ppm): 159.6 (C_{17}); 149.1 (C_{21}); 141.9 (C_{15}); 138.9 (C_6); 137.0 (C_{19}); 134.8 (C_{10}); 127.0 (C_{13}); 126.8 (C_9); 121.8 (C_{20}); 120.8 (C_{18}); 117.1 (C_8); 115.3 (C_{12}); 114.9 (C_{11}); 104.5 (C_7); 103.9 (C_{14}); 78.5 (C_4); 53.8 (C_{16} , $-\text{CH}_2-$); 52.6 (C_1); 36.8 (C_3); 29.5 (C_2); 20.0 (C_0 , $-\text{CH}_3$); 18.5 (C_5 , $-\text{CH}_3$).

5.2.2 2-(6-[(*7aR*,*10R*)-*7a*,*10*-dimethyl-*7a*,*8*,*9*,*10*-tetrahydro-*7H*-pyrrolo[1,2-*a*]perimidin-7-yl)methyl} pyridin-2-yl)phenol. ((*R*,*R*)-6).



To a solution of 8-[(*2R*,*5R*)-2,5-dimethylpyrrolidin-1-yl]naphthalen-1-amine (50 mg, 0.208 mmol) in absolute ethanol (2 mL) and in the presence of molecular sieves (2 g, 4 Å) was added a ethanolic solution (4 mL) of 6-(2-hydroxyphenyl)pyridine-2-carbaldehyde (41.4 mg, 0.208 mmol). The reaction mixture was stirred overnight at room temperature and filtered. The residue was dried under reduced pressure and purified by flash chromatography (15:1 heptane/ethyl acetate) to afford a pale pink solid (33 mg, yield: 38%). M.p.: 90-93 °C. Anal. Calc. for $\text{C}_{28}\text{H}_{27}\text{N}_3\text{O}$ (421.5): C: 79.8; H: 6.5; N: 10.0. Found: C: 79.6; H: 6.8; N: 10.2 %.

MS (EI, m/z , %): 421.0 (M^+), 406.0 ($\text{M}^+ - \text{CH}_3$).

IR (KBr; cm^{-1}): ν = 3435 (m) (OH); 3194 (w), 3051 (w) (CH_{arom}); 2963 (m), 2925 (m), 2867 (m) (CH_{alip}); 1596 (s), 1578 (vs), 1458 (s), 1430 (s) ($\text{C}=\text{C}$), ($\text{C}=\text{N}$); 1374 (m), 1335 (m), 1299 (s); 818 (s), 756 (s), 633 (w).

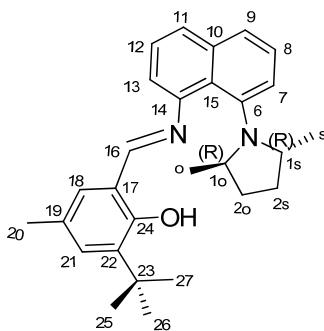
^1H NMR (CDCl_3) δ (ppm): 13.60 (s br, 1H, OH); 7.84 (dd, 1H, H_{27} , $J_{\text{HH}} = 1.5$, 8.0 Hz); 7.79 (s br, 1H, H_{20}); 7.71 (t, 1H, H_{19} , $J_{\text{HH}} = 7.7$ Hz); 7.39–7.31 (m, 3H, H_9 ,

H₁₃, H₂₅); 7.15 (s br, 1H, H₁₈); 7.13 (d, 1H, H₈, $J_{\text{HH}} = 4.4$ Hz); 7.08 (d, 1H, $J_{\text{HH}} = 3.7$ Hz) and 7.04 (d, 1H, $J_{\text{HH}} = 4.4$ Hz) (H₁₂ and H₂₄); 6.95 (dt, 1H, H₂₆, $J_{\text{HH}} = 1.5, 7.3$ Hz); 6.44 (d, 1H, H₁₄, $J_{\text{HH}} = 7.3$ Hz); 6.11 (t, 1H, H₇, $J_{\text{HH}} = 4.4$ Hz); 4.70 (d, 1H, H₁₆, -CH₂-, ABXY, $J_{\text{HH}} = 17.6$ Hz); 4.45 (d, 1H, H₁₆, -CH₂-, ABXY, $J_{\text{HH}} = 17.6$ Hz); 4.16 (m, 1H, H₁, -CH_{pyrr}); 2.42–2.32 (m, 2H, -CH_{2pyrr}); 2.25–2.18 (m, 1H, -CH_{2pyrr}); 1.84–1.81 (m, 1H, -CH_{2pyrr}); 1.37 (d, 3H, H₀, -CH₃, $J_{\text{HH}} = 5.9$ Hz); 1.25 (s, 3H, H₅, -CH₃).

¹³C NMR (CDCl₃) δ (ppm): 159.9 (C₂₂); 157.5 (C₂₃); 156.7 (C₁₇); 141.7 (C₁₅); 138.8 (C₆), 138.7 (C₁₉); 134.9 (C₁₀); 131.5 (C₉); 127.1 (C₁₃); 126.4 (C₂₇); 126.3 (C₁₈); 124.7 (C₂₁); 119.2 (C₂₄); 118.9 (C₂₅); 118.6 (C₂₆); 117.5 (C₈); 117.4 (C₂₀); 115.4 (C₁₂); 114.9 (C₁₁); 104.5 (C₇); 104.1 (C₁₄); 78.5 (C₄); 53.2 (C₁₆, -CH₂-); 52.7 (C₁); 36.9 (C₃); 29.5 (C₂); 20.0 (C₀, -CH₃); 18.6 (C₅, -CH₃).

X-ray crystal data for ((R,R)-6): Formula: C₂₈ H₂₇ N₃ O₁; Unit cell parameters: a 10.414(3) b 13.565(3) c 15.401(4); Space group P212121; CCDC 805292.

5.2.3 2-tert-butyl-6-((E)-(8-((2R,5R)-2,5-dimethylpyrrolidin-1-yl)naphthalen-1-ylimino)methyl)-4-methylphenol.((R,R)-8):



To a solution of 3-tert-butyl-2-hydroxy-5-methylbenzaldehyde (176 mg, 0.915 mmol) in absolute ethanol (20 mL) was added 8-[(2R,5R)-2,5-dimethylpyrrolidin-1-yl]naphthalen-1-amine (200 mg, 0.915 mmol). After stirring at room temperature for 24 h, the reaction mixture was filtered and washed with ethanol. The residue was dried under reduced pressure and purified by flash chromatography (10:1 heptane/ethyl

Proton Sponges

acetate) to obtain a microcrystalline orange solid (199 mg, 58%). M.p.: 73–75 °C. Anal. Calc. for C₂₈H₃₄N₂O (414.6): C, 81.1; H, 8.3; N, 6.8. Found: C: 81.0; H: 8.5; N: 6.5 %.

MS (EI, *m/z*, %): 414.0 (M⁺), 399.0 (M⁺–CH₃), 223.0 (M⁺–CH₃–^tBu–Ar–OH–imine).

IR (KBr; cm^{–1}): ν = 3445 (m) (OH); 3049 (w) (CH_{arom}); 2961 (m), 2920 (m), 2870 (m) (CH_{alip}); 1618 (s), 1564 (vs), 1439 (s) (C=C), (C=N); 1370 (m), 1330 (s).

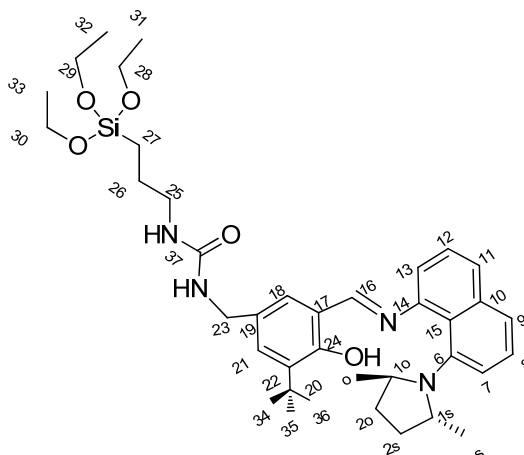
UV-Vis: λ_{max} = 302 nm, 343 nm.

¹H NMR (CDCl₃) δ (ppm): 13.86 (s br, 1H, OH); 8.26 (s, 1H, H₁₆, N=CH); 7.67 (dd, 1H, H₉, J_{HH} = 1.3, 8.4 Hz); 7.50 (d, 1H, H₁₁, J_{HH} = 8.0 Hz); 7.43–7.37 (m, 2H, H₈, H₁₂); 7.18 (d, 1H, J_{HH} = 1.8 Hz) and 6.99 (d, 1H, J_{HH} = 1.8 Hz) (H₁₈ and H₂₁); 7.05 (d, 1H, H₁₃, J_{HH} = 7.5 Hz); 6.94 (dd, 1H, H₇, J_{HH} = 1.3, 7.1 Hz); 3.75–3.66 (m, 1H) and 3.51–3.46 (m, 1H) (H_{1s} and H_{1o}, –CH_{pyrr}); 2.30 (s, 3H, H₂₀, –CH₃); 1.96–1.86 (m, 1H) and 1.80–1.70 (m, 1H) (H_{2s} and H_{2o}, –CH_{2pyrr}); 1.46 (s, 9H, H_{25,26,27}); 1.39–1.33 (m, 1H) and 1.18–1.09 (m, 1H) (H_{2s} and H_{2o}, –CH_{2pyrr}); 1.25 (d, 3H, –CH₃, J_{HH} = 6.2 Hz) and 0.36 (d, 3H, –CH₃, J_{HH} = 6.2 Hz) (H_o and H_s).

¹³C NMR (CDCl₃) δ (ppm): 161.0 (C₁₆, N=CH); 158.2 (C₂₄); 147.2 (C₁₄); 143.7 (C₆); 137.2 (C₂₂); 136.9 (C₁₀); 131.0 (C₁₉); 130.8 (C₁₈); 130.1 (C₂₁); 128.1 (C₁₅); 126.5 (C₉); 125.7 (C₁₂); 125.4 (C₈); 122.4 (C₁₁); 119.1 (C₁₇); 118.5 (C₁₃); 118.0 (C₇); 58.8 (C_{1s}); 51.4 (C_{1o}); 34.7 (C₂₃); 31.6 (C_{2o}); 29.4 (3C, C_{25,26,27}); 29.2 (C_{2s}); 20.7 (C_{2o}, CH₃–Ph); 18.3 (C_o, CH_{3pyrr}); 17.5 (C_s, CH_{3pyrr}).

X-ray crystal data for ((R,R)-8): Formula: C₂₈ H₃₄ N₂ O₁; Unit cell parameters: a 9.8047(8) b 8.8134(8) c 14.0070(12) beta 91.3630(10); Space group P2₁; CCDC 805293.

5.2.4 *N*-(3-*tert*-butyl-5-((*E*)-(8-((2*R*,5*R*)-2,5-dimethyl pyrrolidin-1-yl)naphthalen-1-ylimino)methyl)-4-hydroxybenzylcarbamoyl)-4-(triethoxysilyl)butanamide. (*R,R*)-9.



Using a similar procedure to that described for (*R,R*)-8, from *N*-(3-*tert*-butyl-5-formyl-4-hydroxyphenylcarbamoyl)-4-(triethoxysilyl)butanamide (0.378 g, 0.832 mmol) and 8-[(2*R*,5*R*)-2,5-dimethylpyrrolidin-1-yl]naphthalen-1-amine (200 mg, 0.832 mmol) in absolute ethanol (3 mL). After purification by flash chromatography (4:1 heptane/ethyl acetate) orange oil was obtained (405 mg, 72%).

¹H NMR (CDCl₃) δ (ppm): 14.11 (s br, 1H, OH); 8.32 (s, 1H, H₁₆, N=CH); 7.65 (dd, 1H, H₉, *J*_{HH} = 1.1, 7.9 Hz); 7.50 (d, 1H, H₁₁, *J*_{HH} = 7.9 Hz); 7.44-7.37 (m, 2H, H₈, H₁₂); 7.27 (d, 1H, H₁₈, *J*_{HH} = 2.7 Hz); 7.16 (d, 1H, H₂₁, *J*_{HH} = 2.7 Hz); 7.05 (d, 1H, H₁₃, *J*_{HH} = 7.7 Hz); 6.93 (dd, 1H, H₇, *J*_{HH} = 1.0, 7.2 Hz); 4.34 (s, 2H, H₂₃, -CH₂-); 3.80 (q, 6H, H_{28,29,30}, *J*_{HH} = 7.0 Hz); 3.75-3.69 (m, 1H, H₁₀, -CH_{pyrr}); 3.54-3.48 (m, 1H, H_{1s}, -CH_{pyrr}); 3.23-3.16 (m, 2H, H₂₅, -CH₂-); 1.98-1.87 (m, 1H, H₂₀, -CH_{2pyrr}); 1.75-1.70 (m, 1H, H_{2s}, -CH_{2pyrr}); 1.69-1.61 (m, 2H, H₂₆, -CH₂-); 1.46 (s, 9H, H_{34,35,36}); 1.42-1.30 (m, 1H, H_{2o}, -CH_{2pyrr}); 1.26 (d, 3H, H_o, -CH₃, *J*_{HH} = 5.6 Hz); 1.20 (t, 9H, H_{31,32,33}, *J*_{HH} = 7.0 Hz); 1.13-1.10 (m, 1H, H_{2s}, -CH_{2pyrr}); 0.65 (m, 2H, H₂₇, -CH₂-Si); 0.39 (d, 3H, H_s, -CH₃, *J*_{HH} = 5.6 Hz).

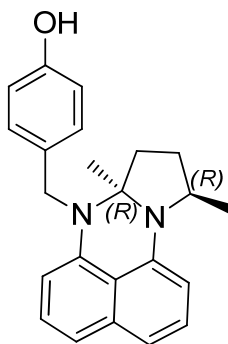
¹³C NMR (CDCl₃) δ (ppm): 160.5 (C₁₆, N=CH); 159.9 (C₃₇, C=O); 158.0 (C₂₄); 146.9 (C₁₄); 143.7 (C₆); 138.0 (C₂₂); 136.9 (C₁₀); 130.5 (C₁₉); 129.4 (C₁₈); 129.2

(C₂₁); 128.1 (C₁₅); 126.9 (C₉); 125.8 (2C, C₁₂, C₈); 122.5 (C₁₁); 119.2 (C₁₇); 118.7 (C₁₃); 118.0 (C₇); 58.9 (C_{1s}); 58.5 (3C, C_{28,29,30}); 51.5 (C₁₀); 44.6 (C₂₃, -HN-CH₂-Ph); 43.0 (C₂₅, -CH₂-); 34.9 (C₂₀); 31.6 (C₂₀); 29.4 (3C, C_{34,35,36}); 29.2 (C_{2s}); 23.6 (C₂₆, -CH₂-); 18.4 (C_o, CH₃); 18.3 (3C, C_{31,32,33}); 17.5 (C_s, CH₃); 7.6 (C₂₇, -CH₂-Si).

5.3 Cyclization scope.

General: To a solution of 8-[(2*R*,5*R*)-2,5-dimethylpyrrolidin-1-yl]naphthalen-1-amine (40 mg, 0.166 mmol) in absolute ethanol (3 mL) and in presence of molecular sieves (2g, 4 Å) was added a ethanolic solution of corresponding aldehyde (0.166 mmol). The reaction mixture was stirred overnight at room temperature and filtered. The residue was dried under reduced pressure and purified by flash chromatography, (heptane/ethyl acetate).

5.3.1 4-(((7*aR*,10*R*)-7*a*,10-dimethyl-7*a*,8,9,10-tetrahydro-7*H*-pyrrolo[1,2-*a*]perimidin-7-yl)methyl)phenol.(*R*,*R*)-7*a*.



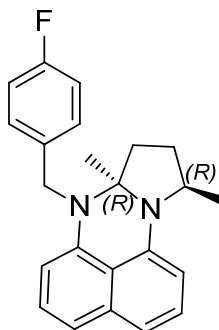
Dark solid. η = 85 %. Anal. Calc. for C₂₃H₂₄N₂O (344.2): C, 80.20; H, 7.02; N, 8.13; Found: C: 80.43; H: 7.0; N: 8.30 %.

MS (EI, *m/z*, %): 344.0 (M⁺), 329.0 (M⁺-CH₃).

¹H NMR (CDCl₃) δ (ppm): 7.25-7.17 (m, 3H, CH_{Nh}); 7.08-6.97 (m, 3H, 2CH_{Ph}, 1CH_{Nph}); 6.68 (d, 2H, CH_{Ph}, *J*_{HH} = 8.6 Hz); 6.31 (d, 1H, H_{Nph}, *J*_{HH} = 7.4 Hz); 6.07 (d, 1H, H_{Nph}, *J*_{HH} = 7.4 Hz); 4.58 (s br, 1H, OH); 4.45 (d, 1H, -CH₂-, ABXY, *J*_{HH} = 16.5 Hz); 4.12 (d, 1H, -CH₂-, ABXY, *J*_{HH} = 16.5 Hz); 4.01 (m, 1H, H₁, -CH_{pyrr}); 2.29-2.22 (m, 2H, -CH_{2pyrr}); 2.09-2.04 (m, 1H, -CH_{2pyrr}); 1.74-1.68 (m, 1H, -CH_{2pyrr}); 1.26 (d, 3H, -CH₃, *J*_{HH} = 6.1 Hz); 1.15 (s, 3H, -CH₃).

^{13}C NMR (CDCl_3) δ (ppm): 156.8 ($\text{C}_{\text{Ar}}\text{-OH}$); 141.3 (C_{Ar}); 138.3 (C_{Ar}); 134.6 (C_{Ar}); 128.4 (C_{Ar}); 127.1 (2C_{Ar}); 126.5 (C_{Ar}); 121.8 (C_{Ar}); 120.2 (C_{Ar}); 120.1 (C_{Ar}); 116.9 (C_{Ar}); 115.8 (C_{Ar}); 115.6 (C_{Ar}); 109.1 (C_{Ar}); 104.3 (C_{Ar}); 79.4 ($\text{-CN-CH}_3\text{pyrr}$); 52.5 ($\text{-CH-CH}_3\text{pyrr}$); 52.4 ($\text{-CH}_2\text{-}$); 36.8 ($\text{-CH}_2\text{pyrr}$); 29.5 ($\text{-CH}_2\text{pyrr}$); 19.9 (-CH_3); 16.6 (-CH_3).

5.3.2 (7a*R*,10*R*)-7-(4-fluorobenzyl)-7a,10-dimethyl-7a,8,9,10-tetrahydro-7*H*-pyrrolo[1,2-*a*]perimidine.(*R,R*)-7b.



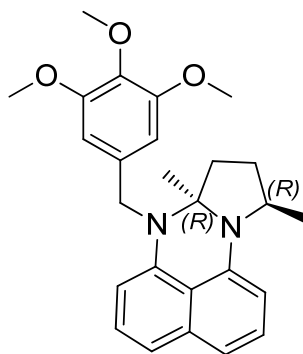
Dark solid. η = 50 %. Anal. Calc. for $\text{C}_{23}\text{H}_{23}\text{FN}_2$ (346,2): C, 79.74; H, 6.69; N, 8.09.

MS (EI, m/z , %): 346.0 (M^+), 331.0 ($\text{M}^+ - \text{CH}_3$).

^1H NMR (CDCl_3) δ (ppm): 7.32-7.19 (m, 3H, CH_{Nph}); 7.09-6.87 (m, 5H, 4 CH_{Ph} , 1 CH_{Nph}); 6.32 (d, 1H, H_{Nph} , $J_{\text{HH}} = 7.4$ Hz); 6.02 (d, 1H, H_{Nph} , $J_{\text{HH}} = 7.4$ Hz); 4.47 (d, 1H, $\text{-CH}_2\text{-}$, ABXY, $J_{\text{HH}} = 17$ Hz); 4.16 (d, 1H, $\text{-CH}_2\text{-}$, ABXY, $J_{\text{HH}} = 16.7$ Hz); 4.01 (dd, 1H, H_1 , -CH_{pyrr} , $J_{\text{HH}} = 12.8, 6.5$ Hz); 2.33–2.21 (m, 2H, $\text{-CH}_2\text{pyrr}$); 2.13-2.03 (m, 1H, $\text{-CH}_2\text{pyrr}$); 1.78-1.71 (m, 1H, $\text{-CH}_2\text{pyrr}$); 1.27 (d, 3H, -CH_3 , $J_{\text{HH}} = 6.2$ Hz); 1.13 (s, 3H, -CH_3).

^{13}C NMR (CDCl_3) δ (ppm): 165.4 ($\text{C}_{\text{Ar}}\text{-F}$); 147.1 (C_{Ar}); 141.8 (C_{Ar}); 134.9 (C_{Ar}); 127.5 (C_{Ar}); 127.3 (C_{Ar}); 126.9 (C_{Ar}); 126.7 (C_{Ar}); 126.6 (C_{Ar}); 116.9 (C_{Ar}); 115.6 (C_{Ar}); 115.3 (C_{Ar}); 115.2 (C_{Ar}); 104.5 (C_{Ar}); 104.4 (C_{Ar}); 103.8 (C_{Ar}); 84.0 ($\text{-CN-CH}_3\text{pyrr}$); 52.6 ($\text{-CH-CH}_3\text{pyrr}$); 50.9 ($\text{-CH}_2\text{-}$); 36.8 ($\text{-CH}_2\text{pyrr}$); 29.5 ($\text{-CH}_2\text{pyrr}$); 20.0 (-CH_3); 18.5 (-CH_3).

5.3.3 (7a*R*,10*R*)-7a,10-dimethyl-7-(3,4,5-trimethoxybenzyl)-
7a,8,9,10-tetrahydro-7*H*-pyrrolo[1,2-*a*]perimidine.(*R,R*)-
7c.



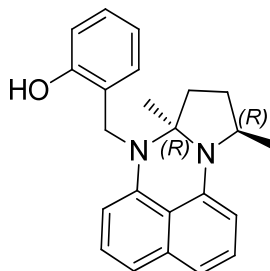
Dark solid. η = 86 %. Anal. Calc. for $C_{26}H_{30}N_2O_3$ (418,2): C, 74.61; H, 7.22; N, 6.69.

MS (EI, m/z , %): 418.0 (M^+), 403.0 ($M^+ - CH_3$).

1H NMR ($CDCl_3$) δ (ppm): 7.46-7.38 (m, 2H, H_{Nbh}); 7.31-7.38 (m, 2H, H_{Nph}); 6.77 (s, 2H, H_{Ph}); 6.53 (d, 1H, H_{Nph} , $J_{HH} = 7.3$ Hz); 6.53 (d, 1H, H_{Nph} , $J_{HH} = 6.4$ Hz); 4.65 (d, 1H, $-CH_2-$, ABXY, $J_{HH} = 16.8$ Hz); 4.31 (d, 1H, $-CH_2-$, ABXY, $J_{HH} = 17.7$ Hz); 4.30-4.26 (m, 1H, H_1 , $-CH_{pyrr}$); 3.94 (s, 3H, OMe); 3.90 (s, 6H, 2OMe); 2.52-2.42 (m, 2H, $-CH_{2pyrr}$); 2.34-2.24 (m, 1H, $-CH_{2pyrr}$); 1.96-1.92 (m, 1H, $-CH_{2pyrr}$); 1.45 (d, 3H, $-CH_3$, $J_{HH} = 6.1$ Hz); 1.31 (s, 3H, $-CH_3$).

^{13}C NMR ($CDCl_3$) δ (ppm): 153.5 ($2C_{Ar}$); 142.2 (C_{Ar}); 138.9 (C_{Ar}); 135.2 ($2C_{Ar}$); 134.8 (C_{Ar}); 126.8 (C_{Ar}); 126.7 (C_{Ar}); 116.8 (C_{Ar}); 115.3 (C_{Ar}); 115.0 (C_{Ar}); 106.6 (C_{Ar}); 104.4 (C_{Ar}); 103.8 (C_{Ar}); 102.5 (C_{Ar}); 78.41 ($-CN-CH_{3pyrr}$); 60.8 (OMe); 56.9 ($-CH-CH_{3pyrr}$); 55.9 (OMe); 52.7 (OMe); 51.9 ($-CH_2-$); 36.8 ($-CH_{2pyrr}$); 29.5 ($-CH_{2pyrr}$); 20.0 ($-CH_3$); 18.6 ($-CH_3$).

5.3.4 2-(((7a*R*,10*R*)-7a,10-dimethyl-7a,8,9,10-tetrahydro-7*H*-pyrrolo[1,2-*a*]perimidin-7-yl)methyl)phenol.(*R,R*)-7*d*.



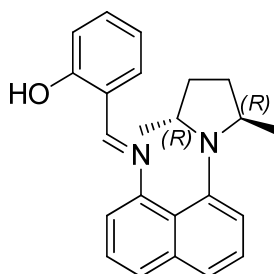
Dark solid. η = 96 %. Anal. Calc. for $C_{23}H_{24}N_2O$ (344.2): C, 80.20; H, 7.02; N, 8.13; Found: C: 79.98; H: 6.96; N: 8.30 %.

MS (EI, m/z , %): 344.0 (M^+), 329.0 ($M^+ - CH_3$).

1H NMR ($CDCl_3$) δ (ppm): 9.40 (s, 1H, OH); 7.30-7.0 (m, 6H, 5H_{Nph}, 1H_{Ph}); 6.83 (t, 1H, H_{Ph}, J_{HH} = 7.5 Hz); 6.65 (d, 1H, H_{Nph}, J_{HH} = 8.1 Hz); 6.52 (d, 1H, H_{Ph}, J_{HH} = 7.5 Hz); 6.37 (d, 1H, H_{Ph}, J_{HH} = 7.5 Hz); 4.75 (d, 1H, -CH₂-, ABXY, J_{HH} = 16.0 Hz); 4.14 (d, 1H, -CH₂-, ABXY, J_{HH} = 16.0 Hz); 4.05 (m, 1H, H₁, -CH_{pyrr}); 2.72-2.62 (m, 1H, -CH_{2pyrr}); 2.43-2.30 (m, 1H, -CH_{2pyrr}); 2.25-2.20 (m, 1H, -CH_{2pyrr}); 1.92-1.80 (m, 1H, -CH_{2pyrr}); 1.37 (d, 3H, -CH₃, J_{HH} = 6.2 Hz); 1.14 (s, 3H, -CH₃).

^{13}C NMR ($CDCl_3$) δ (ppm): 156.8 (C_{Ar}-OH); 141.3 (2C_{Ar}); 138.3 (C_{Ar}); 134.6 (C_{Ar}); 128.4 (C_{Ar}); 127.1 (2C_{Ar}); 126.5 (C_{Ar}); 121.7 (C_{Ar}); 120.3 (C_{Ar}); 120.1 (C_{Ar}); 116.8 (C_{Ar}); 115.6 (C_{Ar}); 108.2 (C_{Ar}); 105.2 (C_{Ar}); 104.3 (C_{Ar}); 79.4 (-CN-CH_{3pyrr}); 56.6 (-CH-CH_{3pyrr}); 52.6 (-CH₂-); 36.8 (-CH_{2pyrr}); 29.5 (-CH_{2pyrr}); 19.9 (-CH₃); 16.6 (-CH₃).

5.3.5 2-((*E*)-((8-((2*R*,5*R*)-2,5-dimethylpyrrolidin-1-yl)naphthalen-1-yl)imino)methyl)phenol.(*R,R*)-10.



Yellow oil. η = 85 %. Anal. Calc. for $C_{23}H_{24}N_2O$ (344.2): C, 80.20; H, 7.02; N, 8.13

MS (EI, m/z , %): 344.0 (M^+), 329.0 ($M^+ - CH_3$).

1H NMR ($CDCl_3$) δ (ppm): 13.5 (s br, 1H, OH); 8.25 (s, 1H, H_{16} , $N=CH$); 7.69 (dd, 1H, H_{Nph} , $J_{HH} = 1.1, 8.1$ Hz); 7.53 (dd, 1H, H_{Nph} , $J_{HH} = 1.2, 8.0$ Hz); 7.46–7.40 (m, 2H, H_{Nph}); 7.37–7.30 (m, 2H, H_{Ph}); 7.07–7.05 (m, 2H, H_{Ph} , H_{Nph}); 7.02 (dd, 1H, H_{Ph} , $J_{HH} = 1.3, 7.2$ Hz); 6.92 (td, 1H, H_{Nph} , $J_{HH} = 1.1, 7.5$ Hz); 3.81–3.64 (m, 1H) and 3.60–3.45 (m, 1H) ($2-CH_{pyrr}$); 2.02–1.87 (m, 1H) and 1.77–1.68 (m, 1H) ($-CH_{2pyrr}$); 1.36–1.25 (m, 1H) and 1.25–1.10 (m, 1H) ($-CH_{2pyrr}$); 1.26 (d, 3H, $-CH_3$, $J_{HH} = 5.9$ Hz) and 0.36 (d, 3H, $-CH_3$, $J_{HH} = 6.5$ Hz).

^{13}C NMR ($CDCl_3$) δ (ppm): 161.2 (C_{16} , $N=CH$); 156.3 ($C_{Ar}-OH$); 143.5 (C_{Ar}); 132.5 (C_{Ar}); 131.7 (C_{Ar}); 128.4 (C_{Ar}); 126.9 (C_{Ar}); 125.7 (C_{Ar}); 122.5 (C_{Ar}); 120.7 (C_{Ar}); 120.1 (C_{Ar}); 118.7 (C_{Ar}); 118.5 (C_{Ar}); 117.1 (C_{Ar}); 115.6 (C_{Ar}); 108.2 (C_{Ar}); 104.4 (C_{Ar}); 58.2 (CH_{pyrr}); 51.4 (CH_{pyrr}); 31.2 ($-CH_{2pyrr}$); 30.0 (CH_{2pyrr}); 18.4 (CH_{3pyrr}); 17.5 (CH_{3pyrr}).

5.4 Synthesis of complexes

(*R,R*)-5Pd: Pd(cod)Cl₂ (43 mg, 0.152 mmol) in CH_2Cl_2 (10 mL) was added to a solution of (*R,R*)-5 (50 mg, 0.152 mmol) in the same solvent and the mixture was stirred at room temperature for 6 h. After the solvent had been removed under vacuum to 0.5 mL, the product was precipitated by careful addition of pentane and collected by filtration, to afford a stable light brown solid (73 mg, 94%). Anal. Calc. for $C_{22}H_{23}Cl_2N_3Pd$ (506.8): C, 52.1; H, 4.6; N, 8.3. Found: C, 52.5; H, 4.8; N, 7.7 %.

MS (ES^+ , m/z): 471.3 ($M^+ - Cl$), 435.3 ($M^+ - 2Cl$), 329.3 ($M^+ - 2Cl - Pd$).

IR (KBr; cm^{-1}): $\nu = 3049$ (w) (CH_{arom}); 2965 (m), 2925 (m) 2875 (m) (CH_{alip}); 1609 (s) 1587 (vs), 1420 (s) ($C=C$), ($C=N$); 1373 (m), 1338 (m), 811 (s), 758 (s), 638 (w), 603 (w), 514 (w).

1H NMR ($CDCl_3$) δ (ppm): 9.04 (m, 1H_{py}); 7.63 (m, 1H_{py}); 7.56 (m, 1H_{py}); 7.28 (m, 1H_{py}); 7.13 (d, 2H_{Nph}, $J_{HH} = 8.0$ Hz); 7.05 (d, 2H_{Nph}, $J_{HH} = 7.3$ Hz); 6.38 (dd, 2H_{Nph}, $J_{HH} = 1.0, 6.4$ Hz); 5.97 (d, 1H, $-CH_2-$, ABXY, $J_{HH} = 18.1$ Hz); 5.61 (d, 1H, -

CH₂-, ABXY, $J_{\text{HH}} = 18.1$ Hz); 4.03 (m, 1H, -CH_{pyrr}); 2.89–2.56 (m, 2H, -CH_{2pyrr}); 2.37–2.17 (m, 2H, -CH_{2pyrr}); 1.25 (d, 3H, -CH₃, $J_{\text{HH}} = 10.2$ Hz); 0.89 (s, 3H, -CH₃).

¹³C NMR (CDCl₃) δ (ppm): 161.7 (C_{Py}); 152.1 (C_{Py}); 141.2 (C_{Nph}); 139.0 (C_{Py}); 134.8 (C_{Nph}); 127.1 (C_{Py}); 124.0 (2C_{Nph}); 123.7 (C_{Py}); 118.0 (2C_{Nph}); 116.7 (2C_{Nph}); 105.1 (2C_{Nph}); 79.2 (-CN-CH_{3pyrr}); 55.6 (-CH₂-); 52.7 (-CH-CH_{3pyrr}); 36.6 (-CH_{2pyrr}); 31.0 (-CH_{2pyrr}); 20.0 (-CH₃); 18.1 (-CH₃).

(*R,R*)-5Rh: AgPF₆ (38.5 mg, 0.152 mmol) in THF (10 mL) was added to a solution of [Rh(cod)Cl]₂ (37 mg, 0.076 mmol) in THF (10 mL) and the mixture was stirred vigorously at room temperature for 30 min. The resulting AgCl was filtered off and the yellow solution was treated with **(*R,R*)-5** (50 mg, 0.152 mmol) in the same solvent. The mixture was stirred at room temperature for 2 h. After the solvent had been removed under vacuum to 0.5 mL, the product was precipitated by careful addition of Et₂O and collected by filtration, to afford a stable dark green solid (95 mg, 91%). Anal calcd. for C₃₀H₃₅F₆N₃PRh (685.5): C, 52.5; H, 5.1; N, 6.1. Found: C, 52.3; H, 5.0; N, 5.8 %.

MS (ES⁺, m/z): 540.3 (M⁺-PF₆), 432.3 (M⁺-PF₆-cod), 330.3 (M⁺-cod-Rh).

IR (KBr; cm⁻¹): $\nu = 2962$ (m), 2924 (m), 2886 (m), 2839 (m) (CH_{alip}); 1614 (s), 1587 (s), 1413 (m) (C=C), (C=N); 1378 (m), 1335 (m); 842 (vs) (PF)); 762 (m); 558 (s).

¹H NMR (CDCl₃) δ (ppm): 8.00 (m, 1H_{Py}); 7.85 (m, 1H_{Py}); 7.73 (m, 1H_{Py}); 7.50 (m, 1H_{Py}); 7.40 (dd, 2H_{Nph}, $J_{\text{HH}} = 1.0, 7.9$ Hz); 7.24 (d, 2H_{Nph}, $J_{\text{HH}} = 7.9$ Hz); 6.53 (d, 2H_{Nph}, $J_{\text{HH}} = 7.4$ Hz); 5.82 (d, 1H, -CH₂-, ABXY, $J_{\text{HH}} = 16.2$ Hz); 4.41 (d, 1H, -CH₂-, ABXY, $J_{\text{HH}} = 16.0$ Hz); 4.05 (m, 2H, -CH=C_{cod}); 3.87 (m, 1H, -CH_{pyrr}); 3.58 (m, 2H, -CH=C_{cod}); 2.58 (m, 2H, -CH_{2cod}); 2.33 (m, 2H, -CH_{2cod}); 2.21 (m, 2H, -CH_{2cod}); 1.87 (m, 2H, -CH_{2cod}); 1.68 (d, 3H, -CH₃, $J_{\text{HH}} = 6.0$ Hz); 1.58 (m, 2H, -CH_{2pyrr}); 1.32 (m, 2H, -CH_{2pyrr}); 1.15 (s, 3H, -CH₃).

¹³C NMR (CDCl₃) δ (ppm): 160.7 (C_{Py}); 146.2 (C_{Py}); 141.0 (C_{Py}); 138.5 (C_{Nph}); 134.5 (C_{Nph}); 128.0 (2C_{Nph}); 126.4 (C_{Py}); 123.7 (C_{Py}); 117.5 (2C_{Nph}); 115.8 (2C_{Nph}); 105.7 (2C_{Nph}); 87.0 (2C, -CH=CH_{cod}); 83.0 (2C, -CH=CH_{cod}); 77.2 (-CN-CH_{3pyrr}); 57.9

Proton Sponges

(-CH₂-); 51.6 (-CH-CH₃_{pyrr}); 39.6 (-CH₂_{pyrr}); 30.3 (2C, 2 -CH₂_{cod}); 29.9 (2C, 2 -CH₂_{cod}); 29.4 (-CH₂_{pyrr}); 20.3 (-CH₃); 15.6 (-CH₃).

(R,R)-6Pd: Pd(AcO)₂ (26.7 mg, 0.119 mmol) in CH₂Cl₂ (10 mL) was added to a solution of **(R,R)-6** (50.1 mg, 0.152 mmol) in the same solvent and the mixture was stirred at room temperature overnight. After the solvent had been removed under vacuum to 0.5 mL, the product was precipitated by careful addition of pentane and collected by filtration, to afford a stable brown solid (65 mg, 85%). Anal. Calcd. for C₃₀H₂₉N₃O₃Pd (586.0): C, 61.5; H, 5.0; N, 7.2. Found C, 61.8; H, 4.9; N, 7.9%.

MS (ES⁺, *m/z*): 585.5 (M⁺), 526.5 (M-CH₃CO₂), 421.5 (M⁺-CH₃CO₂-Pd).

IR (KBr; cm⁻¹): ν = 3055 (w) (CH_{arom}); ν_{CHalip} 2964 (m), 2924 (w), 2891 (vw); 1624 (s) (C=O); 1596 (vs), 1573 (s), 1467 (s) (C=C), (C=N); 1406 (s), 1378 (m), 1360 (m); 1317 (s), (C-O); 821 (m), 755 (m), 686 (w) (OCO); 555 (vw) (Pd-O).

¹H NMR (CDCl₃) δ (ppm): 9.35 (dd, 1H_{Py}, *J*_{HH} = 1.1, 7.5 Hz); 7.80 (m, 1H_{Nph}); 7.79 (m, 1H_{Nph}); 7.73 (d, 1H_{Py}, *J*_{HH} = 7.8 Hz); 7.61 (dd, 1H_{Py}, *J*_{HH} = 1.0, 7.9 Hz); 7.55 (d, 1H_{Ph}, *J*_{HH} = 8.1 Hz); 7.40 (dd, 1H_{Nph}, *J*_{HH} = 1.0, 7.9 Hz); 7.30 (d, 1H_{Nph}, *J*_{HH} = 7.9 Hz); 7.20 (m, 1H_{Ph}); 7.19 (m, 1H_{Ph}); 6.85 (m, 1H_{Nph}); 6.68 (m, 1H_{Ph}); 6.57 (d, 1H_{Nph}, *J*_{HH} = 7.5 Hz); 4.57 (d, 1H, -CH₂-, ABXY, *J*_{HH} = 17.2 Hz); 4.22 (d, 1H, -CH₂-, ABXY, *J*_{HH} = 17.1 Hz); 4.05 (m, 1H, -CH_{pyrr}); 2.68 (dd, 1H, -CH₂_{pyrr}, *J*_{HH} = 6.8, 12.1 Hz); 2.37 (m, 1H, -CH₂_{pyrr}); 1.91 (m, 1H, -CH₂_{pyrr}); 1.88 (s, 3H, CH₃CO₂-); 1.65 (s, 3H, -CH₃); 1.62 (m, 1H, -CH₂_{pyrr}); 1.35 (d, 3H, -CH₃, *J*_{HH} = 6.2 Hz).

¹³C NMR (CDCl₃) δ (ppm): 197.0 (CH₃CO₂-); 164.4 (C-O, C_{Ph}); 161.0 (C_{Nph}); 153.2 (C_{Nph}); 142.4 (C_{Py}); 138.8 (C_{Nph}); 136.5 (C_{Nph}); 134.3 (C_{Py}); 132.1 (C_{Ph}); 128.5 (C_{Ph}); 127.6 (C_{Py}); 127.1 (C_{Nph}); 126.9 (C_{Py}); 123.6 (C_{Py}); 122.6 (C_{Ph}); 121.8 (C_{Ph}); 120.1 (C_{Nph}); 117.0 (C_{Nph}); 116.2 (C_{Nph}); 116.0 (C_{Ph}); 113.7 (C_{Nph}); 105.4 (C_{Nph}); 86.2 (-CN-CH₃_{pyrr}); 66.5 (-CH₂-); 51.7 (-CH-CH₃_{pyrr}); 34.9 (-CH₂_{pyrr}); 28.7 (-CH₂_{pyrr}); 24.3 (CH₃CO₂-); 22.2 (-CH₃); 20.0 (-CH₃).

(R,R)-6Rh: AgPF₆ (48 mg, 0.190 mmol) in THF (10 mL) was added to a solution of [Rh(cod)Cl]₂ (46.4 mg, 0.095 mmol) in THF (10 mL) and the mixture was stirred vigorously at room temperature for 30 min. The resulting AgCl was filtered off and the yellow solution was treated with **(R,R)-6** (80 mg, 0.190 mmol) in the same

solvent. The mixture was stirred at room temperature for 2 h. After the solvent had been removed under vacuum to 0.5 mL, the product was precipitated by careful addition of Et₂O and collected by filtration, to afford a stable (in solid state) dark yellow solid (133 mg, 90%). C₃₆H₃₉F₆N₃OPRh (777.6).

MS (ES⁺, *m/z*): 632.3 (M⁺), 523.3 (M⁺–H⁺–cod).

IR (KBr; cm^{–1}): ν = 3443 (m) (OH); 3101 (vw), 3058 (vw) (CH_{arom}); 2964 (m), 2926 (m), 2880 (m), 2837 (m) (CH_{alip}); 1596 (s), 1578 (s), 1537 (s), 1461 (s) (C=C), (C=N); 1378 (m), 1335 (m), 1299 (m); 843 (vs) (PF); 760 (m), 557 (s).

¹³C NMR (CDCl₃) δ (ppm): 158.3 (C_{Ph}); 154.5 (C_{Ph}); 152.0 (C_{Py}); 140.2 (C_{Nph}); 138.5 (2C, C_{Nph}, C_{Py}); 135.4 (C_{Nph}); 133.5 (C_{Nph}); 127.6 (2C, C_{Nph}, C_{Ph}); 126.3 (2C_{Py}); 119.1 (5C, 3C_{Ph}, C_{Nph}, C_{Py}); 115.3 (2C_{Nph}); 104.6 (2C_{Nph}); 80.9 (5C, 2 -CH=CH-cod, -CN-CH_{3pyrr}); 53.4 (-CH₂-); 53.3 (-CH-CH_{3pyrr}); 39.0 (-CH_{2pyrr}); 30.6 (5C, 4 -CH_{2cod}, -CH_{2pyrr}); 19.7 (-CH₃); 19.5 (-CH₃).

(***R,R***)-**8Pd**:Pd(AcO)₂ (21.6 mg, 0.096 mmol) in EtOH (10 mL) was added to a solution of (***R,R***)-**8** (40 mg, 0.096 mmol) in the same solvent and the mixture was stirred at room temperature overnight. After the solvent had been removed under vacuum to 0.5 mL, the product was precipitated by careful addition of pentane and collected by filtration, to afford a stable light brown solid (48 mg, 85%). C₃₀H₃₆N₂O₃Pd (579.0).

MS (ES⁺, *m/z*): 519.3 (M⁺–OAc), 415.5 (L).

IR (KBr; cm^{–1}): ν = 3053 (w) (CH_{arom}); 2960 (vs), 2921 (vs), 2867 (s) (CH_{alip}); 1650 (s) (C=O); 1585 (vs), 1572 (vs), 1529 (s) (C=C), (C=N); 1457 (s), 1426 (s), 1373 (s), 1320 (s) (C–O); 819 (m), 765 (m); 710 (w) (OCO); 541 (vw) (Pd–O).

¹H NMR (CDCl₃) δ (ppm): 7.99 (s, 1H, N=CH); 7.30 (d, 1H_{Nph}, *J*_{HH} = 6.4 Hz); 7.28 (m, 1H_{Nph}); 7.27 (d, 1H_{Nph}, *J*_{HH} = 6.4 Hz); 7.26 (d, 1H_{Nph}, *J*_{HH} = 5.9 Hz); 7.10 (d, 1H_{Ph}, *J*_{HH} = 2.2 Hz); 7.05 (d, 1H_{Ph}, *J*_{HH} = 2.2 Hz); 6.41 (d, 1H_{Nph}, *J*_{HH} = 7.5 Hz); 6.31 (d, 1H_{Nph}, *J*_{HH} = 7.5 Hz); 4.00 (dc, 1H, -CH_{pyrr}, *J*_{HH} = 1.3, 6.4 Hz); 2.37–2.30 (m, 1H, -CH_{2pyrr}); 2.15–2.11 (m, 1H, -CH_{2pyrr}); 2.10–2.00 (m, 1H, -CH_{2pyrr}); 1.82–1.76 (m, 1H, -CH_{2pyrr}); 1.40 (s, 3H, -CH_{3Ph}); 1.34 (d, 3H, -CH_{3pyrr}, *J*_{HH} = 7.0 Hz); 1.34 (s, 3H,

Proton Sponges

CH₃CO₂-); 1.32 (d, 3H, -CH₃_{pyrr}, $J_{\text{HH}} = 6.0$ Hz); 1.29-1.27 (m, 1H, -CH_{pyrr}); 1.09 (s, 9H, 3 -CH₃_{*t*-Bu}).

¹³C NMR (CDCl₃) δ (ppm): 197.1 (CH₃CO₂-); 153.7 (N=CH); 142.0 (C_{Nph}); 141.1 (C_{Ph}); 139.2 (C_{Nph}); 136.9 (C_{Ph}); 136.4 (C_{Ph}); 135.1 (C_{Ph}); 134.3 (C_{Nph}); 130.2 (C_{Nph}); 130.3 (C_{Nph}); 127.8 (C_{Nph}); 126.9 (C_{Nph}); 116.1 (C_{Ph}); 115.2 (C_{Ph}); 114.9 (C_{Nph}); 103.3 (C_{Nph}); 102.7 (C_{Nph}); 52.2 (-CH-CH₃_{pyrr}); 36.4 (-CH₂_{pyrr}); 29.7 (CH₃CO₂-); 29.7 (-CH-CH₃_{pyrr}); 29.6 (-CH₃_{Ph}); 29.4 (-CH₂_{pyrr}); 22.7 (C_{*t*-Bu}); 20.1 (-CH₃_{pyrr}); 18.1 (3C, 3 -CH₃_{*t*-Bu}); 14.9 (-CH₃_{pyrr}).

(*R,R*)-8Rh: AgPF₆ (24.4 mg, 0.096 mmol) in THF (10 mL) was added to a solution of [Rh(cod)Cl]₂ (23.5 mg, 0.048 mmol) in THF (10 mL) and the mixture was stirred vigorously at room temperature for 30 min. The resulting AgCl precipitated was filtered off and the yellow solution was treated with (*R,R*)-8 (40 mg, 0.096 mmol) in the same solvent. The mixture was stirred at room temperature for 2 h. After the solvent had been removed under vacuum to 0.5 mL, the product was precipitated by careful addition of Et₂O and collected by filtration, to afford a stable dark beige solid (67 mg, 90%). C₃₆H₄₆F₆N₂OPRh (770.6).

MS (ES⁺, m/z): 625.5 (M⁺ - PF₆), 415.5 (L).

IR (KBr; cm⁻¹): ν = 3408 (m) (OH); 3054 (vw) (CH_{arom}); 2962 (m), 2921 (m), 2882 (m), 2838 (m) (CH_{alip}); 1619 (m), 1591 (s), 1467 (m), 1432 (m) (C=C), (C=N); 1375 (m), 1300 (s), 1231 (m); 843 (vs) (PF); 755 (w), 731 (w); 558 (m), 500 (m).

¹H NMR (CDCl₃) δ (ppm): 12.41 (s br, OH); 7.44-7.34 (m, 3H_{Nph}); 7.26-7.16 (m, 3H_{Nph}); 6.53 (m, 1H_{Ph}); 6.51 (m, 1H_{Ph}); 5.96 (s, 1H, N=CH); 4.79-4.69 (m, 1H, -CH₂_{pyrr}); 4.41-4.39 (m, 2H, -CH=C_{cod}); 4.24-4.19 (m, 1H, -CH₂_{pyrr}); 4.11-4.07 (m, 2H, -CH=C_{cod}); 3.29-3.20 (m, 1H, -CH_{pyrr}); 2.66-2.55 (m, 2H, -CH₂_{cod}); 2.52-2.38 (m, 2H, -CH₂_{cod}); 2.31-2.28 (m, 1H, -CH₂_{pyrr}); 2.22 (s, 3H, -CH₃_{Ph}); 2.08-1.96 (m, 2H, -CH₂_{cod}); 1.95-1.84 (m, 2H, -CH₂_{cod}); 1.46 (d, 3H, -CH₃_{pyrr}, $J_{\text{HH}} = 8.8$ Hz); 1.40 (s, 9H, -CH₃_{*t*-Bu}); 1.28 (d, 3H, -CH₃_{pyrr}, $J_{\text{HH}} = 11.5$ Hz); 0.91-0.86 (m, 1H, -CH₂_{pyrr}).

¹³C NMR (CDCl₃) δ (ppm): 171.2 (N=CH); 158.3 (C_{Ph}); 148.4 (C_{Nph}); 143.6 (C_{Nph}); 138.0 (C_{Ph}); 134.6 (C_{Nph}); 131.7 (C_{Ph}); 130.9 (C_{Ph}); 127.8 (C_{Ph}); 127.6 (C_{Nph}); 126.3 (C_{Nph}); 126.3 (2C_{Nph}); 122.7 (C_{Nph}); 120.1 (C_{Ph}); 116.1 (C_{Nph}); 115.3 (C_{Nph}); 83.0

(2C, -CH=CH_{cod}); 80.8 (2C, -CH=CH_{cod}); 52.5 (-CH-CH_{3pyrr}); 52.3 (-CH-CH_{3pyrr}); 35.1 (C_{t-Bu}); 32.7 (-CH_{2pyrr}); 30.3 (2C, 2 -CH_{2cod}); 29.8 (3C, 3 -CH_{3t-Bu}); 29.7 (2C, 2 -CH_{2cod}); 29.5 (-CH_{2pyrr}); 20.0 (-CH_{3Ph}); 18.5 (-CH_{3pyrr}); 8.8 (-CH_{3pyrr}).

(R,R)-9Pd: Pd(AcO)₂ (10.11 mg, 0.045 mmol) in dry CH₂Cl₂ (10 mL) was added to a solution of **(R,R)-9** (30.5 mg, 0.045 mmol) in the same solvent and the mixture was stirred at room temperature overnight. After the solution was purified through celite and subsequent the solvent was removed under vacuum to 0.5 mL, the product was precipitated by careful addition of pentane and collected by filtration, to afford a stable dark red solid (33 mg, 87%). C₄₀H₅₈N₄O₇PdSi (840.5).

UV-Vis: λ_{max} (nm) = 531, 434, 376, 296.

¹H NMR (CDCl₃) δ (ppm): 8.32 (s, 1H, N=CH); 7.68 (d, 1H_{Nph}, J_{HH} = 8.0 Hz); 7.50 (t, 1H_{Nph}, J_{HH} = 7.3 Hz); 7.44-7.40 (m, 2H_{Nph}); 7.36 (d, 1H_{Ph}, J_{HH} = 2.2 Hz); 7.17 (d, 1H_{Ph}, J_{HH} = 2.2 Hz); 7.06 (d, 1H_{Nph}, J_{HH} = 6.6 Hz); 6.94 (d, 1H_{Nph}, J_{HH} = 7.3 Hz); 4.34 (d, 2H, -CH₂-Ph, J_{HH} = 4.4 Hz); 3.78 (c, 6H, -O-CH₂-CH₃, J_{HH} = 7.3 Hz); 3.53-3.42 (m, 1H, -CH_{pyrr}); 3.24-3.15 (m, 3H, 1H, -CH_{pyrr}, 2H, -CH₂₋); 1.97-1.85 (m, 2H, -CH_{2pyrr}); 1.71-1.58 (m, 1H, -CH_{2pyrr}); 1.67-1.60 (m, 2H, -CH₂₋); 1.47 (s, 9H, -CH_{3t-Bu}); 1.30-1.28 (m, 4H) (1H, -CH_{2pyrr}) (3H, CH₃CO₂₋); 1.25-1.23 (m, 6H, -CH_{3pyrr}); 1.21 (t, 9H, -O-CH₂-CH₃, J_{HH} = 7.3 Hz); 0.68-0.60 (m, 2H, -CH₂-Si).

¹³C NMR (CDCl₃) δ (ppm): 197.2 (CH₃CO₂₋); 160.4 (N=CH); 159.8 (C=O); 158.2 (C_{Ph}); 146.9 (C_{Nph}); 138.5 (C_{Nph}); 137.9 (C_{Ph}); 133.7 (C_{Nph}); 130.1 (C_{Ph}); 129.4 (C_{Ph}); 129.1 (C_{Ph}); 128.1 (C_{Nph}); 126.8 (C_{Nph}); 125.4 (2C_{Nph}); 122.4 (C_{Nph}); 119.1 (C_{Ph}); 118.6 (C_{Nph}); 117.9 (C_{Nph}); 58.9 (-CH-CH_{3pyrr}); 58.4 (3C, 3 -O-CH₂-CH₃); 51.3 (-CH-CH_{3pyrr}); 44.5 (-CH₂₋); 42.9 (-CH₂₋); 34.8 (C_{t-Bu}); 31.5 (-CH_{2pyrr}); 29.7 (CH₃CO₂₋); 29.3 (3C, 3 -CH_{3t-Bu}); 29.1 (-CH_{2pyrr}); 25.6 (-CH_{3pyrr}); 23.5 (-CH₂₋); 18.2 (3C, 3 -O-CH₂-CH₃); 17.4 (-CH_{3pyrr}); 7.5 (-CH₂-Si).

(R,R)-9Rh: AgPF₆ (8.21 mg, 0.0325 mmol) in dry THF (10 mL) was added to a solution of [Rh(cod)Cl]₂ (7.93 mg, 0.0162 mmol) in the same solvent and the mixture was stirred vigorously at room temperature for 30 min. The resulting AgCl precipitated was filtered off and the yellow solution was treated with **(R,R)-9** (22 mg, 0.0325 mmol) in dry THF. The mixture was stirred at room temperature overnight. After the

solution was purified through celite and subsequent the solvent was removed under vacuum to 0.5 mL, the product was precipitated by careful addition of Et₂O:pentane (1:1) and collected by filtration, to afford a stable dark green solid (27.5 mg, 82%). C₄₈H₇₃F₆N₄O₅PRhSi (1061.4).

UV-Vis: λ_{max} (nm)= 512, 356, 287.

¹H NMR (CDCl₃) δ (ppm): 9.82 (s br, OH); 7.37-7.18 (m, 3H_{Nph}); 7.12-6.98 (m, 3H, 2H_{Ph}, 1H_{Nph}); 6.65 (d, 1H_{Nph}, J_{HH} = 6.6 Hz); 6.43 (d, 1H_{Nph}, J_{HH} = 6.6 Hz); 5.93 (s, 1H, N=CH); 4.73-4.65 (m, 1H, -CH_{2pyrr}); 4.44-4.37 (m, 2H, -CH=C_{cod}); 4.31-4.05 (m, 5H) (1H, -CH_{2pyrr}, 2H, -CH=C_{cod}, 2H, -CH_{2Ph}); 3.76 (m, 6H, -O-CH₂-CH₃); 3.25 (m, 3H) (1H, -CH_{pyrr}, 2H, -CH₂₋); 2.66-2.54 (m, 2H, -CH_{2cod}); 2.45-2.31 (m, 2H, -CH_{2cod}); 2.28-2.24 (m, 1H, -CH_{2pyrr}); 2.24-2.04 (m, 4H, -CH_{2cod}); 1.89-1.83 (m, 2H, -CH₂₋); 1.51-1.49 (m, 3H, -CH_{3pyrr}); 1.37 (m, 9H, 3 -CH_{3_t-Bu}); 1.25-1.22 (m, 12H, CH_{3pyrr}, -O-CH₂-CH₃); 1.12-1.00 (m, 1H, -CH_{2pyrr}); 0.89-0.74 (m, 2H, -CH₂-Si).

¹³C NMR (CDCl₃) δ (ppm): 166.4 (N=CH); 155.8 (br, 2C, C_{Ph}, C₃₇, C=O); 148.9 (C_{Nph}); 141.6 (C_{Nph}); 138.5 (C_{Ph}); 136.6 (C_{Nph}); 134.7 (C_{Ph}); 128.9 (C_{Ph}); 127.0 (C_{Ph}); 126.7 (C_{Nph}); 125.5 (C_{Nph}); 124.9 (C_{Nph}); 124.4 (C_{Nph}); 122.0 (C_{Nph}); 120.3 (C_{Ph}); 115.9 (C_{Nph}); 115.4 (C_{Nph}); 80.4 (2C, -CH=CH_{cod}); 79.6 (2C, -CH=CH_{cod}); 65.8 (3C, -O-CH₂-CH₃); 53.4 (-CH-CH_{3pyrr}); 52.4 (-CH-CH_{3pyrr}); 43.0 (-CH₂₋); 42.5 (-CH₂₋); 34.7 (C_{t-Bu}); 30.3 (2C, -CH_{2cod}); 30.0 (-CH_{2pyrr}); 29.7 (2C, -CH_{2cod}); 29.4 (3C, -CH_{3_t-Bu}); 29.1 (-CH_{2pyrr}); 22.7 (-CH₂-Si); 19.9 (3C, 3 -O-CH₂-CH₃); 16.2 (-CH_{3pyrr}); 7.9 (2C, -CH_{3pyrr}, -CH₂-Si).

5.5 Heterogeneization on MCM-41.

A solution of metal complex (***R,R***)-**9Pd** or (***R,R***)-**9Rh** (0.022 mmol), bearing a triethoxysilyl group, in CH₂Cl₂ (5 mL) was added to a well-stirred toluene suspension (25 mL) of the mesoporous solid (MCM-41, 150 mg). The slurry was heated at 110 °C for 16 h. After the mixture was cooled, the solid was filtered off, washed thoroughly with ethanol and diethyl ether and dried under vacuum, to afford the respective heterogenized complexes in almost quantitative yields.

(*R,R*)-9Pd-MCM: stable dark brown-reddish solid. Elemental analysis indicated 1.4 mass % Pd. Found C: 5.4; H: 1.4; N: 0.73%.

DFTR: λ_{\max} (nm)= 675, 619, 488, 363, 329, 287, 263, 231.

IR (KBr; cm^{-1}): ν = 1641 (s), 1575 (s) (C=O), (C=N); 1085 (Si-O), 544 (vw) (Pd-O).

^{13}C NMR (300 MHz, Solid, 25 °C, ppm): δ = 198.0 (CH_3CO_2^-); 160.5 (N=CH); 158.0 (C=O); 140.4–121.0 (^{15}C , 5C_{Ph} and 10C_{Nph}); 120.7 (C_{Ph}); 59.5 (-O- CH_2 - CH_3); 59.0 (- CH_{pyrr}); 51.3 (- CH_{pyrr}); 44.0 (- CH_2 -); 43.00 (- CH_2 -); 34.6 ($\text{C}_{t\text{-Bu}}$); 28.0 (6C, 3 - $\text{CH}_{3t\text{-Bu}}$, 2 - $\text{CH}_{2\text{pyrr}}$, CH_3CO_2^-); 23.6 (- CH_2 -); 16.0 (4C, 3 -O- CH_2 - CH_3 , - $\text{CH}_{3\text{pyrr}}$); 13.3 (- $\text{CH}_{3\text{pyrr}}$); 8.6 (- CH_2 -Si).

(*R,R*)-9Rh-MCM: stable dark green solid. Elemental analysis indicated 1.4 mass % Rh. Found C: 5.1; H: 1.4; N: 0.6%.

DFTR: λ_{\max} (nm)= 666, 561, 362, 331, 287, 255, 226.

IR (KBr; cm^{-1}): ν = 1638 (s) (C=O), 1580 (C=N), (C=C); 1085 (Si-O), 803 (vs) (PF).

^{13}C NMR (300 MHz, Solid, 25 °C, ppm): δ = 160.1 (N=CH); 152.0 (C=O); 140.4–115.0 ($^{16}\text{C}_{\text{arom}}$, 6C_{Ph} and 10C_{Nph}); 80.0 (4C, 2- $\text{CH}=\text{CH}_{\text{cod}}$); 59.5 (-O- CH_2 - CH_3); 53.00 (2C, 2- CH_{pyrr}); 43.6 (2C, 2 - CH_2 -); 34.3 ($\text{C}_{t\text{-Bu}}$); 28.6 (9C, 4- $\text{CH}_{2\text{cod}}$, 3- $\text{CH}_{3t\text{-Bu}}$, 2- $\text{CH}_{2\text{pyrr}}$); 21.5 (-O- CH_2 - CH_3 , - CH_2 -); 15.6 (- $\text{CH}_{3\text{pyrr}}$); 8.3 (2C, - $\text{CH}_{3\text{pyrr}}$, - CH_2 -Si).

5.6 Catalytic Activity.

5.6.1 Hydrogenation of alkenes.

The catalytic properties, in the hydrogenation of (*E*)-diethyl 2-benzylidenesuccinate, diethyl itaconate and diethyl citraconate of the complexes were examined under conventional conditions for batch reactions in a reactor (Autoclave Engineers) of 100 mL capacity at 40 °C temperature, 4 atm dihydrogen pressure and 1/1000 mol for diethyl itaconate, 1/100 mol for (*E*)-diethyl 2-benzylidenesuccinate metal/substrate molar ratio. The evolution of the hydrogenated reaction product was monitored by gas chromatography. Specifically: To a suspension of the catalyst, **9Rh-MCM** (15 mg) in Ethanol (40 mL), was added a solution of 23 mg (1 mmol) of (*E*)-

diethyl 2-benzylidene succinate (0.082 mmol). (15 mg of **9Rh-MCM** ($8.2 \cdot 10^{-4}$ mmol of Rh)), 23 mg of (*E*)-diethyl 2-benzylidene succinate (0.082 mmol), 40ml of Ethanol) and the mixture stirred at 40 °C, 1000 rpm. The evolution of the reaction was monitored by gas chromatography.

5.6.2 Recycling Experiments.

At the end of the process the reaction mixture was centrifuged, and the catalyst residue washed to completely remove any remaining products and/or reactants. The solid was used again and any change in the catalytic activity was observed. In each of the four runs, up to 95% conversion was reached after 220 min and ee (%) was maintained after 4 cycles.

5.7 Single-Crystal X-ray diffraction.

Data for (*R,R*)-**6** and (*R,R*)-**8** were collected on a Bruker Smart CCD diffractometer equipped with a normal focus, 2.4 kW sealed tube X-ray source (MoK α radiation, $\lambda = 0.71073$ Å) operating at 40 kV and 8 mA. Data were collected at room temperature over a hemisphere of the reciprocal space in a combination of several sets of exposures. Each exposure of 20s covered 0.5 or 0.3° in ω . Unit cell dimensions were determined by a least-squares fit of 60 reflections with $I > 20\sigma(I)$. The structures were solved by direct methods. The final cycles of refinement were carried out by full-matrix least-squares analyses with anisotropic thermal parameters for all non-hydrogen atoms. The final cycles of refinement were carried out by full-matrix least-squares analyses using SMART software for data collection and data reduction and SHELXTL44, and anisotropically refined (Hydrogen atoms were geometrically situated) by full-matrix least-squares methods on F2 (SHELXL- 97)

[44] Siemens SHELXTL, version 5.0, Siemens Analytical X-ray Instruments, Inc., Madison, WI, 1995.

Table S1. Crystallographic and refinement data for (R,R)-6.

Identification code	(R,R)-6
Empirical formula	C ₂₈ H ₂₇ N ₃ O
Formula weight	421.53
Temperature	296(2) K
Wavelength	0.71073 Å
Crystal system, space group	Orthorhombic, <i>P</i> 2 ₁ 2 ₁ 2 ₁
Unit cell dimensions	<i>a</i> = 10.414 (3) Å <i>b</i> = 13.565 (3) Å <i>c</i> = 15.401(4) Å
Volume	2175.6 (10) Å ³
Z, Calculated density	4, 1.287 Mg/m ³
Absorption coefficient	0.079 mm ⁻¹
F(000)	896.0
Crystal size	0.4 x 0.3 x 0.2
Theta range for data collection	2.36° to 25.40° -12° ≤ h ≤ 12
Limiting indices	-16 ≤ k ≤ 16 -18 ≤ l ≤ 18
Reflections collected / unique	15489 / 2280
Completeness to theta = 25.00°	57 %
Absorption correction	Semi-empirical from equivalents
Refinement method	Full-matrix least-squares on F ²
Data / restraints / parameters	2280 / 0 / 293
Goodness-of-fit on F ²	1.148
Final R indices [I > 2σ(I)]	R1 = 0.0376, wR2 = 0.0812
R indices (all data)	R1 = 0.0475, wR2 = 0.0846
Largest diff. peak and hole	0.111 and -0.100 e·Å ⁻³

Table S2. Crystallographic and refinement data for (R,R-8).

Identification code	(R,R-8)
Empirical formula	C ₂₈ H ₃₄ N ₂ O
Formula weight	414.57
Temperature	296(2) K
Wavelength	0.71073 Å
Crystal system, space group	Monoclinic, <i>P</i> 2 ₁
Unit cell dimensions	<i>a</i> = 9.8047 (8) Å; <i>α</i> = 90 ° <i>b</i> = 8.8134 (8) Å; <i>β</i> = 91.363 (1) <i>c</i> = 14.0070 (12) Å; <i>γ</i> = 90 °
Volume	1210.04 (18) Å ³
Z, Calculated density	2, 1.138 Mg/m ³
Absorption coefficient	0.069 mm ⁻¹
F(000)	448.0
Crystal size	0.45 x 0.3 x 0.2
Theta range for data collection	2.31° to 25.39° -11 ≤ <i>h</i> ≤ 11 -10 ≤ <i>k</i> ≤ 10 -16 ≤ <i>l</i> ≤ 16
Limiting indices	
Reflections collected / unique	8037 / 4000
Completeness to theta = 25.00°	90 %
Absorption correction	Semi-empirical from equivalents
Max. and min. transmission	0.986 and 0.974
Refinement method	Full-matrix least-squares on F ²
Data / restraints / parameters	4000 / 0 / 287
Goodness-of-fit on F ²	1.074
Final R indices [I > 2σ(I)]	R1 = 0.0636, wR2 = 0.1125
R indices (all data)	R1 = 0.1082, wR2 = 0.1281
Largest diff. peak and hole	0.119 and -0.194 e·Å ⁻³

Artículo I. $R1 = [\Sigma(|F_o| - |F_c|)] / \Sigma|F_o|$; $wR2 = \Sigma(w|F_o|^2 - |F_c|^2) / \Sigma[w(|F_o|^2)^{1/2}]$ $w = 1/[\sigma^2|F_o|^2 + (0.0410p)^2]$ where $p = (|F_o|^2 + 2|F_c|^2)/3$



Gold complexes catalyzed synthesis of propargylamines via multi-component reaction.

1 Introduction.

Multi-component reactions (MCR's), by virtue of their convergence, easy of execution and generally high yields of products, have attracted considerable attention and emerged as a powerful tool in the synthesis of biologically important compounds for reducing operative steps and enhancing synthesis efficiency.

Propargylamines are important skeletons or synthetically versatile building blocks for the preparation of many nitrogen-containing biologically active compounds.¹ The conventional methods for their synthesis involve the amination of propargylic halides, phosphates or triflates.² Another possible way is the reaction of lithium acetylides or Grignard reagents with imines or their derivatives.³ However, these methods require the use of stoichiometric amounts of organometallic reagents and strictly controlled reaction conditions. Furthermore, protection of sensitive functional groups, such as aldehyde, is also necessary. Thus, the development of a new efficient method has been an interesting synthetic challenge.

Three component reactions represent the smartest way to obtain building blocks of natural products in one step. The study of reaction conditions and design of catalyst that resulted efficient, selective and recyclable in this transformation is very important in order to get improved methodology for the future implementation at industrial scale.

[1] a) A. Jenmalm, W. Berts, Y. L. Li, K. Luthman, I. Csöreg, U. Hacksell, *J. Org. Chem.*, **1994**, 59, 1139; b) M. A. Huffman, N. Yasuda, A. E. DeCamp, E. J. J. Grabowski, *J. Org. Chem.*, **1995**, 60, 1590; c) M. Miura, M. Enna, K. Okuro, M. Nomura, *J. Org. Chem.*, **1995**, 60, 4999; d) G. Dyker, *Angew. Chem., Int. Ed.*, **1999**, 38, 1698.

[2] a) I. E. Kopka, Z. A. Fataftah, M. W. Rathke, *J. Org. Chem.*, **1980**, 45, 4616–4622; b) Y. Imada, M. Yuassa, S. I. Nakamura, S. I. Murahashi, *J. Org. Chem.*, **1994**, 59, 2282–2284; c) S. Czerneck, J. M. Valery, *J. Carbohydr. Chem.*, **1990**, 9, 767–773.

[3] a) D. Enders, U. Reinhold, *Tetrahedron: Asymmetry*, **1997**, 8, 1895–1946; b) R. Bloch, *Chem. Rev.*, **1998**, 98, 1407–1438; c) C. W. Ryan, C. Ainsworth, *J. Org. Chem.*, **1961**, 26, 1547–1550; d) F. Tubéry, D. S. Grierson, H. P. Husson, *Tetrahedron Lett.*, **1987**, 28, 6457–6460; e) M. E. Jung, A. Huang, *Org. Lett.*, **2000**, 2, 2659–2661; f) T. Murai, Y. Mutoh, Y. Ohta, M. Murakami, *J. Am. Chem. Soc.*, **2004**, 126, 5968–5969.

2 State of the art.

2.1 Multi-component reactions. Historical background.

In a MCR process several starting materials assemble to form complex products. Thus, MCR's are convergent reactions in contrast with the classical divergent multi-step synthesis. Ideal MCR consists in the addition all the reactants, reagents and catalysts together in an unlikely order, under the same conditions.

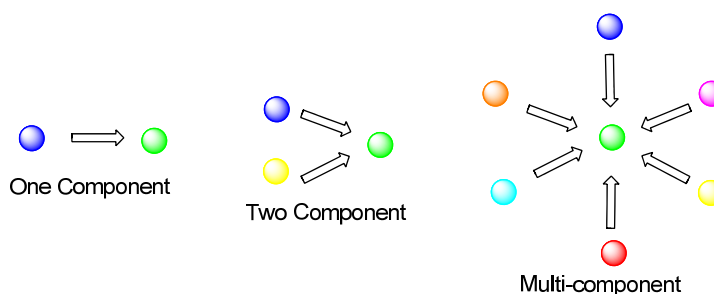


Figure. V. 1. Representation of divergent one and two component processes and converged multi-component reactions.

Although multi-component reactions look very recent, its origin started in 1980 with the discovery of the three component reaction for the synthesis of α -cyanoamines through amine, carbonyl compound and hydrogen cyanide condensation reported by Strecker.⁴ Since then, there have been many reactions that have been called MCR's.⁵

Such as examples sorted by date; the Hantzsch dihydropyridine synthesis (1882), Radziszewski imidazole synthesis (1882), Hantzsch pyrrole synthesis (1890), Biginelli reaction (1891), Mannich reaction (1912), Robinson tropinone synthesis (1917), Passerini reaction (1921), Bucherer-Bergs hydantoin synthesis (1934), Asinger reaction (1958), and Ugi reaction (1959) have been reported along the twentieth century. (**Figure. V. 2**).

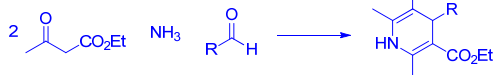
[4] A. Strecker, *Justus Liebigs Ann. Chem.*, **1850**, 75, 27–45.

[5] For some recent reviews, see: a) J. Zhu, H. Bienaymé, *Multicomponent Reactions*, **2005**, Wiley-VCH, Weinheim; b) A. Dömling, I. Ugi, *Angew. Chem. Int. Ed.*, **2000**, 39, 3168–3210; c) A. Dömling, *Chem. Rev.*, **2006**, 106, 17–89; (d) D. J. Ramón, M. Yus, *Angew. Chem., Int. Ed.*, **2005**, 44, 1602–1634; (e) C. Simon, T. Constantieux J. Rodriguez, *Eur. J. Org. Chem.*, **2004**, 4957–4980; (f) D. Tejedor, F. Garcia-Tellado, *Chem. Soc. Rev.*, **2007**, 36, 484–491; (g) V. Nair, C. Rajesh, A. U. Vinod, S. Bindu, A. R. Sreekanth, J. S. Mathen, L. Balagopal, *Acc. Chem. Res.*, **2003**, 36, 899–907.

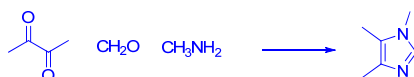
Strecker (1850)



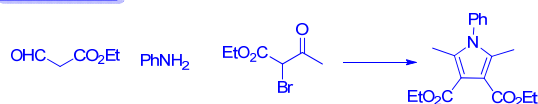
Hantzsch (1882)



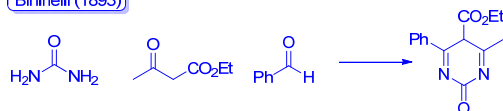
Radziszewski (1882)



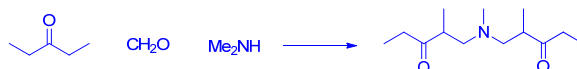
Hantzsch (1890)



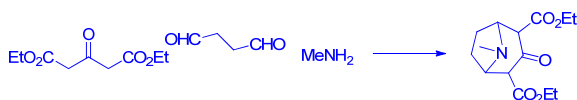
Binelli (1893)



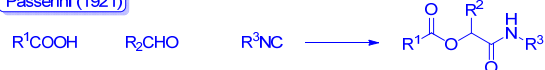
Mannich (1912)



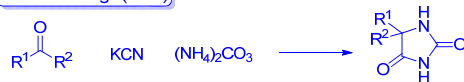
Robinson (1917)



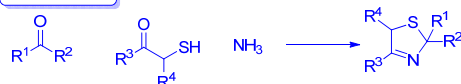
Passerini (1921)



Bucherer-Bergs (1934)



Asinger (1958)



Ugi (1959)

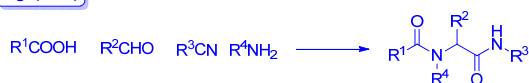


Figure. V. 2. Historical background of MCR's.

The Ugi reaction is the MCR widely study and used than any other MCR and has also developed the concept of combining several multi-component reactions.

Thus, new MCR's can be discover by mixing two or more MCR's in one pot. In 1993 D. Ugi et al⁶ reported a seven-component coupling that we can see it as the combination of an Asinger and Ugi reaction. This fact made that hundred of MCR's have reported over the years and since 1995 has attached attention from not only the academic but also the industrial sector.

2.2 Gold-catalyzed multi-component reactions.

Metal-mediated intermolecular multi-component reaction are well suited for the design of “ideal” multi-component reactions and open a widely scope in these transformations because the behavior of metal centers in order to create new C-C and C-X bonds inside a sequence of steps.

Between the transition metals, palladium⁷ is the most used but nickel and ruthenium have become very popular and recently three component reactions have been reported using several metals centers. The metal center helps to run the reaction under mild conditions and, often, with high levels of chemo-, regio-, and stereoselectivities.

In our case, we focused on the propargylamines synthesis through metal catalyzed A³ transformation owing to the importance of these organic compounds and the high synthetic efficiency of the three-component coupling reaction (alkyne–amine–aldehyde) through C–H activation.

Many efforts have been made to improve the three-component reaction by use transition-metal based catalysts, even in chiral versions, such as copper,⁸ iridium,⁹ silver,¹⁰ zinc¹¹ and iron.¹²

[6] A. Dömling I. Ugi. *Angew. Chem.* **1993**, *105*, 634; *Angew. Chem. Int. Ed. Engl.* **1993**, *32*, 563.

[7] G. Balme, E. Bossharth, N. Monteiro, *Eur. J. Org. Chem.*, **2003**, 4101–4111.

[8] a) L. Shi, Y. Q. Tu, M. Wang, F. M. Zhang and C. A. Fan, *Org. Lett.*, **2004**, *6*, 1001; b) H. Z. S. Huma, R. Halder, S. S. Kalra, J. Das, J. Iqbal, *Tetrahedron Lett.*, **2002**, *43*, 6485; c) G. W. Kabalka, L. Wang and R. M. Pagni, *Synlett*, **2001**, 676; S. B. Park, H. Alper, *Chem. Commun.*, **2005**, 1315.

[9] a) C. Fischer, E. M. Carreira, *Org. Lett.*, **2001**, *3*, 4319–4321; b) S. Sakaguchi, T. Mizuta, M. Furuwan, T. Kubo, Y. Ishii, *Chem. Commun.*, **2004**, 1638.

As discussed in Chapter III gold complexes have emerged as promising catalyst for C-C bond formation reactions through alkyne activation. Thus, gold catalyst also can run MCR's with high efficiency and selectivity.

There are many examples of homogeneous MCR gold catalysis processes:

In 2003 Chao-Jun Li et al.¹³ reported the efficient A³ coupling of aldehyde alkyne and amines via C-H activation catalyzed by gold (I) and gold (III) salts in aqueous media without any other additive to obtain propargylamines. (**Figure. V. 3**).

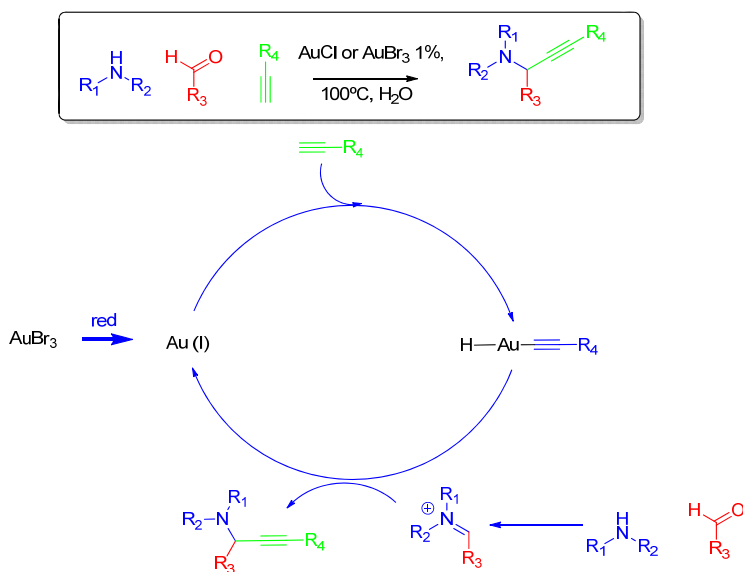


Figure. V. 3. Gold A³ reaction in water. Tentative mechanism.

This transformation was carried out with AuCl and AuBr₃ but did not occur when the catalyst was gold (0). The catalysts were applied to several aldehydes and dialkylamines and studied the influence of the different substrates. Thus, primary

-
- [10] a) W. Yan, R. Wang, Z. Xu, J. Xu, L. Lin, Z. Shen, Y. Zhou, *J. Mol. Catal. A: Chem.*, **2006**, 255, 81; b) B. M. Choudary, C. Sridhar, M. L. Kantam, B. Sreedhar, *Tetrahedron Lett.*, **2004**, 45, 7319; c) M. L. Kantam, B. V. Prakash, C. R. V. Reddy, B. Sreedhar, *Synlett*, **2005**, 2329; d) K. M. Reddy, N. S. Babu, I. Suryanarayana, P. S. S Prasad, N. Lingaiah, *Tetrahedron Lett.*, **2006**, 47, 7563; e) R. Maggi, A. Bello, C. Oro, G. Sartori, L. Soldi, *Tetrahedron*, **2008**, 64, 1435.
 [11] E. Ramu, R. Varala, N. Sreelatha, S. R. Adapa, *Tetrahedron Lett.*, **2007**, 48, 7184.
 [12] K. Cao, F. Zhang, Y. Tu, X. Zhuo, C. Fan, *Chem. Eur. J.*, **2009**, 15, 6332-6334.
 [13] C. Wei, C. J. Li, *J. Am. Chem. Soc.*, **2003**, 125, 9584.

amines resulted inert or with low activity in this transformation presumably for complexation with the catalyst.

Tentative mechanism was proposed involving the activation of C-H bond from the alkyne by Au(I) species (for AuBr₃, Au(I) species could be formed “*in situ*” for reduction of Au(III) by the alkyne) and the gold acetylenic complex formed reacts with the immonium ion generated in the reaction mixture.

Chi-Ming Che et al¹⁴ published gold (III) Salen complexes that catalyzed A³ formation of chiral propargylamines from chiral amines; the reaction took place in water at 40°C. In this work, there are reported a widely scope of the reactions using optically pure proline compounds and several aldehydes and alkynes with excellent yields and diastereoselectivities.

In this case should be noted that the diastereoselectivity is given by the nature of the optically pure amine, and chiral catalyst doesn't induce chirality. Thus, the chiral amine transfer chirality to the nearly sp³ carbon formed.

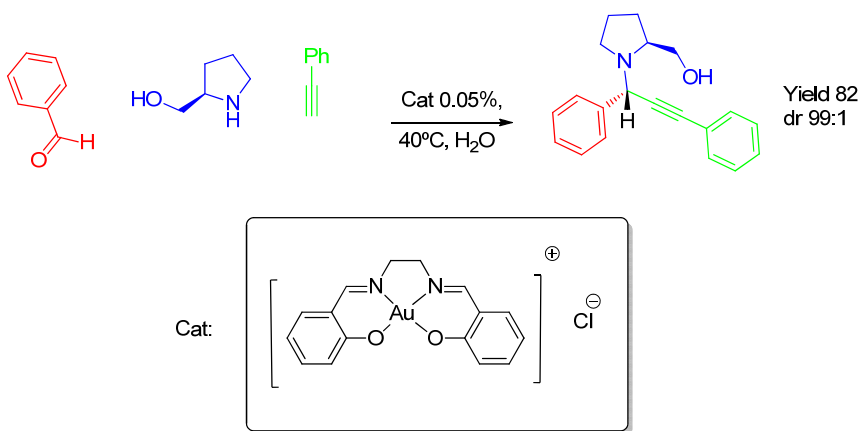


Figure. V. 4. Diastereoselective MCR catalyzed by gold (III) Salem complex.

This reaction was tested for the synthesis of artemisinin derivatives that are active against a human hepatocellular carcinoma as example of use in pharmaceutical

[14] V. K. Y. Lo, Y. Liu, M. K. Wong, C. M. Che, *Org. Lett.*, **2006**, 8, 1529.

industry of these kind of transformation. (**Figure. V. 5**). In this case, the new stereogenic center was not controlled resulting low diastereoselectivity.

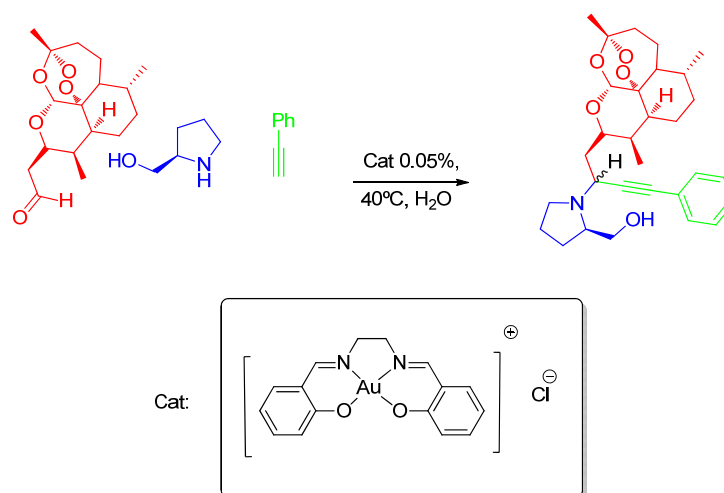


Figure. V. 5. Synthesis of propargylamine- based artemisinin derivatives.

Other useful example of how the starting materials not only conserve chirality but also is transferred to the final product was reported by Chao-Jun Li et al¹⁵. In this work the optically pure protected glyceraldehyde (*R*)-(+)-2,2-dimethyl-1,3-dioxolane-4-carboxaldehyde, was used with piperidine and phenylacetylene to obtain the corresponding propargylamine in high diastereoselectivity and good yield using AuI as catalyst. (**Figure. V. 6**).

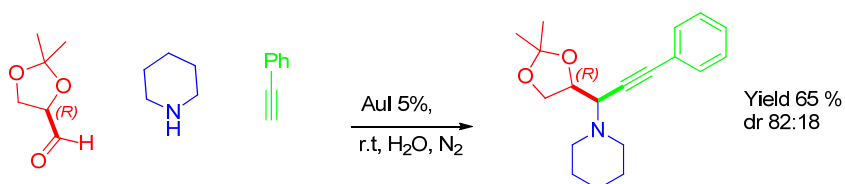


Figure. V. 6. Diastereoselective gold catalyzed MCR.

[15] B. Huang, X. Yao and C. J. Li, *Adv. Synth. Catal.*, **2006**, 348, 1528.

Besides the selectivity another challenge in this type of transformation is to take one more step namely MCR+1. Yauanhong Liu et al¹⁶ reported a gold (III) catalyzed multi-component coupling/cycloisomerization reaction in one pot using heteroaryl aldehydes, secondary amines and alkynes under solvent free conditions or in water. This methodology provides a fast access to substituted aminoindolizines with high atom economy and high catalytic efficiency due to the large number of bonds formed. Gold catalyst is involve in the two cascade reactions and works under mild conditions. (**Figure. V. 7**).

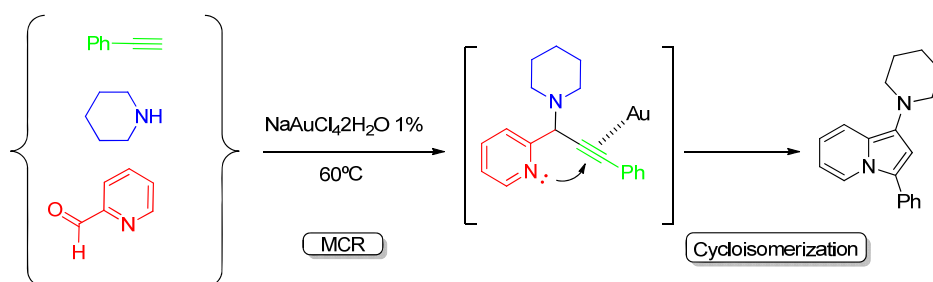


Figure. V. 7. Gold (III) catalyzed multi-component coupling/cycloisomerization reaction.

Last examples work in homogeneous conditions, but besides the potential of homogeneous catalysis has limitations for a sustainable catalytic process; the fast reduction of cationic gold species into inactive metallic atoms is unavoidable when the gold catalysts activate alkenes or alkynes. This fact make impossible to recycle these systems, in this way heterogeneous gold was stabilized by Avelino Corma et al¹⁷ through supporting gold catalysts in which partially charged and electron-deficient gold atoms are stabilized and supported on nanocrystalline ZrO₂ and CeO₂. (**Figure. V. 8**).

[16] B. Yan, Y. Liu, *Org. Lett.*, **2007**, 9, 4323-4326.

[17] X. Zhang, A. Corma, *Angew. Chem., Int. Ed.*, **2008**, 47, 4358.

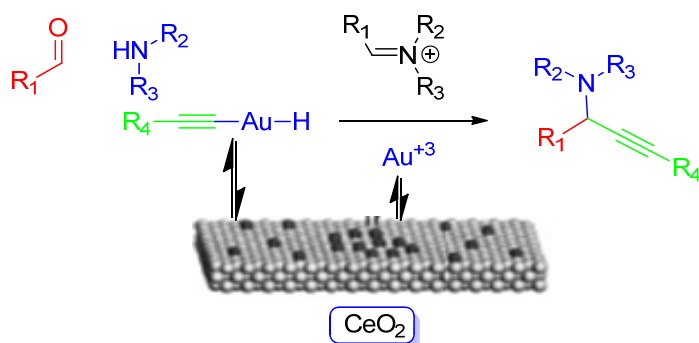


Figure. V. 8. Tentative mechanisms for heterogeneous gold catalyzed MCR.

Au/CeO₂ resulted more active than soluble AuCl₃ that decomposes after 2 hours and can work with several solvents as methanol, THF and water. A widely scope has been studied even the one pot synthesis of functionalized indoles by cyclization reaction after MCR process. But recycling experiments didn't reported in the communication.

Lo and co-workers¹⁸ developed a soluble gold-based complex, which was successfully used in aqueous media for the preparation of propargylamines with good yield and able to be reused for three cycles with minimal loss of activity. In this case the catalyst can be recycled in the reaction mixture adding more starting material when the reaction finished.

[18] V. K. Y. Lo, K. K. Y. Kung, M K. Wong, C. M. Che, *J. Organomet. Chem.*, **2009**, 694, 583–591.

3 Discussion and results.

3.1 Targets.

As we have seen the use of gold soluble catalysts for MCR's are widely used but have some disadvantages, such as, they are expensive, usually not recyclable, and their separation from the reaction mixture is tedious. Other metal-based heterogeneous catalysts were also used successfully in the A³-reaction, e.g. AgI-tungstophosphoric acid,^{10d} CuI anchored on a silica gel support¹⁹ or on USY-zeolite,²⁰ Cu (II) salt on a hydroxyapatite support,²¹ or *N*-heterocyclic carbene–Cu (I) on a silica support.²² The main disadvantages of these methods are the high cost of the catalyst, the tedious preparation, the sensitivity of copper (I) compounds, or problems with the reusability/recyclability.

Thus, our aim in this chapter is to test our previously described gold compounds, as catalysts in multi-component reaction for the synthesis of propargylamines, in order to study new applications for these catalysts and compare soluble and heterogeneous behavior confronting Au (I) versus Au (III) compounds. At the same time, it will study the scope of these reaction and recycling experiments.

3.2 Multi-component reaction. Optimal conditions.

Since MCR's catalysis with gold salts/complexes indicates that Au (III) and Au (I) could be active species,¹³ we examined here the applicability of heterogenized (NHC)-gold catalysts in the three-component reaction and show that are highly active, selective, and recyclable catalysts.

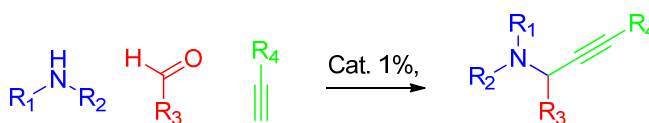


Figure. V. 9. Metal-catalyzed three-component synthesis of propargylamines.

[19] B. Sreedhar, P. S. Reddy, C. S. V. Krishna, P. V. Babu, *Tetrahedron Lett.*, **2007**, 48, 7882–7886.

[20] M. K. Patil, M. Keller, B. M. Reddy, P. Pale, J. Sommer, *Eur. J. Org. Chem.*, **2008**, 4440–4445.

[21] B. M. Choudary, C. Sridhar, M. L. Kantam and B. Sreedhar, *Tetrahedron Lett.*, **2004**, 45, 7319–7321.

[22] M. Wang, P. Li, L. Wang, *Eur. J. Org. Chem.*, **2008**, 2255–2261.

Looking for optimal catalyst, different transition metal complexes with *N*-heterocyclic carbene based on dioxolane backbone synthesized in Chapter III and (NHC)NN-Au(III) ligands recently reported in our group,²³ soluble and heterogenized on MCM-41 have been tested. (**Figure. V. 10**).

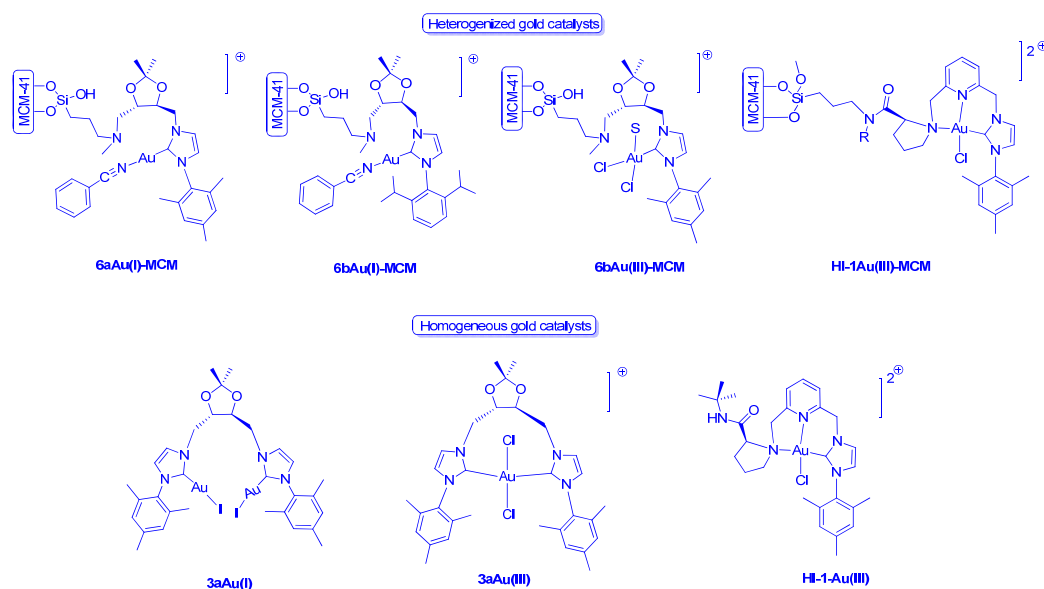


Figure. V. 10. Supported and soluble gold (I) and gold (III) catalysts.

The catalytic behavior of heterogenized gold complexes was compared with their respective counterparts for the synthesis of propargylamines.

To screen the supported catalysts and reaction conditions, we selected a commonly used amine, piperidine, a reactive aldehyde, benzaldehyde, and phenylacetylene as common substrates. The results are shown in **Table. V. 1**.

[23] C. del Pozo, A. Corma, M. Iglesias, F. Sánchez, *Organometallics*, **2010**, 29, 4491-4498.

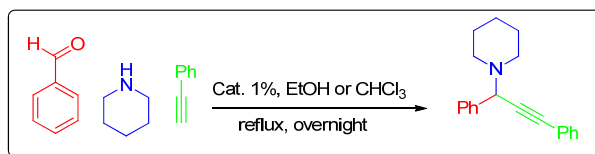


Table. V. 1. Screening of catalysts and reaction conditions for the catalytic three-component reaction.^a

Entry	Catalysts	solvent	T (°C)	Yield (%) ^b
1	6aAu(I)-MCM	EtOH	r.t	Traces
2		EtOH	reflux	41
3		CHCl ₃	reflux	85
4	6bAu(I)-MCM	EtOH	r.t	Traces
5		EtOH	reflux	Traces
6	3aAu(I)	EtOH	reflux	Traces
7		CHCl ₃	reflux	99
8	6aAu(III)-MCM	EtOH	reflux	Traces
9		CHCl ₃	reflux	80
10	3aAu(III)	EtOH	50°C	Traces
11		EtOH	reflux	22
12		CHCl ₃	reflux	99
13	HI-1Au(III)-MCM	EtOH	50°C	64
14		CHCl ₃	reflux	65
15	HI-1-aAu(III)	EtOH	50°C	33
16		CHCl ₃	reflux	94
17	3aCu(I)	CHCl ₃	40°C	5 (Homocoupling)
18	K[AuCl ₄]	CHCl ₃	reflux	63
19	No catalyst	CHCl ₃	reflux	0

^aUnless otherwise noted, all reactions were performed with aldehyde (0.19 mmol), piperidine (0.22 mmol), phenyl acetylene (0.28 mmol), catalyst (1 mol%), in EtOH or CHCl₃ (2 mL) at corresponding temperature for 24 h. ^bYields of isolated product based on aldehyde.

Preliminary experiments in various solvents revealed that the reaction was dependent on temperature and solvent polarity. Indeed reaction yields were higher in ethanol at reflux temperature than at room temperature (**Table. V. 1**, entries 1 and 2, 10 and 11), and higher in chloroform than in ethanol (**Table. V. 1**, entries 3, 7, 9, 12, 14,

16-19). This fact suggests that the solvent can be involved in the reaction mechanism stabilizing the intermediate state.

On the other hand **Table. V. 1** also shows that gold (I) and gold (III) was more effective than copper (I) for this system, which behaves mainly as a catalyst for phenylacetylene homocoupling (**Table. V. 1**, entry 17). The copper-catalyzed-reaction was also performed at -20 °C to avoid the homocoupling of the alkyne.

Thus, the optimal catalytic conditions chosen are: 1 mol% of catalyst, in chloroform at reflux (70 °C) and aldehyde, amine and alkyne in a 1:1.2:1.5 molar ratio. Under these solvent and temperature conditions, the catalyst nature proved to be critical (soluble or supported). As expected for MCR's in which three molecules have to meet within the support pores, the shapes of the MCM-41 have a marked influence on the reaction efficiency. The reaction efficiency seemed directly correlated with the channel pore size (compare entries **Table. V. 1**, 3 and 7, 9 and 12 or 14 and 16). In this MCR, the three starting reagents have to meet and react within the large pores of the support, which could accommodate three molecules together and their intermediates gave slightly worse results than soluble systems but competitive onto the possibility of recycling material.

No conversion was found in the absence of catalyst under identical conditions (**Table. V. 1**, entry 19) and the KAuCl₄ catalyzed reaction yields 63% of product (**Table. V. 1**, entry 18). These results clearly emphasize the role of the support itself and gold. Thus, working with chloroform as solvent and at 70 °C the nature of the catalyst has an important impact on conversion and selectivity.

3.2.1 Scope of the reaction.

We explored the scope of the reaction for the MCR with these soluble and heterogenized gold catalysts and studied the role of each reagent in this three-component process (**Table. V. 2** and **Table. V. 3**).

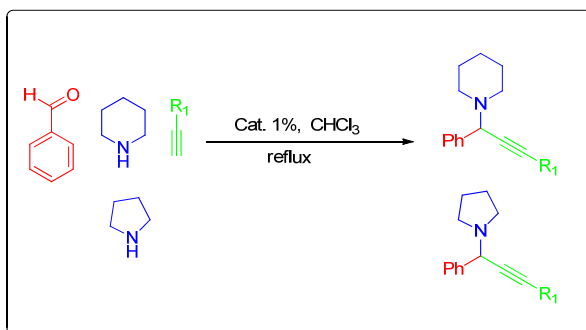
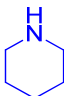
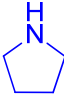
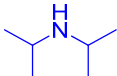
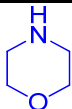


Table. V. 2. Effect of alkyne and amine on the catalytic three-component reaction.^a

Entry	Catalysts	amine	R ¹	Yield (%) ^b
1	6aAu(I)-MCM		Ph	85
2			MePh	82/48h
3			C ₈ H ₁₇	97/48h
4	6aAu(I)-MCM		Ph	40
5	3aAu(I)		Ph	20
6	3aAu(III)		Ph	48
7	HI-1Au(III)-MCM		Ph	49
8	HI-1Au(III)		Ph	93
9	3aCu(I)		Ph	21
10	6aAu(I)-MCM		Ph	Traces
11	6aAu(I)-MCM		Ph	Traces

^aConditions: benzaldehyde (0.19 mmol), amine (0.22 mmol), alkyne (0.28 mmol), catalyst (1 mol%), in CHCl₃ (2 mL) at 70 °C for 24 h. ^bYields of isolated product based on aldehyde.

The effect of the amine was examined with submitting amines of increasing bulkiness or of decreasing nucleophilicity to the reaction with benzaldehyde and phenylacetylene (**Table. V. 2**, entries 1 and 4-11). The reaction with secondary amines proceeded efficiently to afford the corresponding propargylamines.

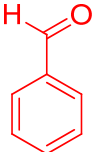
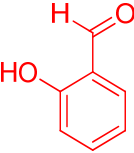
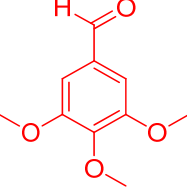
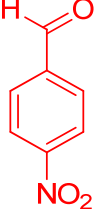

The reactions with piperidine give total complete benzaldehyde conversion with an isolated yield higher than 85%. Experiments with pyrrolidine as amine show that yields drop drastically with different catalysts. Only soluble **HI-1Au(III)** (93% isolated yield) and its heterogenized counterpart **HI-1Au(III)-MCM** (49% isolated yield) maintaining the activity showed with piperidine (**Table. V. 2**, entries 7 and 8 comparing with **Table. V. 1**, entries 14 and 16). When pyrrolidine is the amine, we could also observe beneficial support effect, which showed beneficial behavior for the same system working with gold (I) dioxolane NHC system (**Table. V. 2**, entries 4 and 5).

Pyrrolidine is more basic and less nucleophilic base than piperidine, this fact makes this system less favorable for the formation of the immonium ion intermediate, generated “in situ” through amine attack to the carbonyl aldehyde carbon. This step acts as a bottleneck onto the mechanism and slows the overall reaction. The more bulky diisopropylamine also gave the expected propargylamine, but as expected, the yield of isolated product is marginal. With morpholine only traces of the corresponding propargylamine was observed due to the presence in the former an electron-withdrawing oxygen atom in β -position to the nitrogen atom in a cyclohexyl structure that makes morpholine less nucleophilic than piperidine. In conclusion, it appears that this gold system works reasonably well for the reaction when the bases are nucleophilic enough to form the immonium ion in the first reaction step, according with the proposed mechanisms in **Figure. V. 3** (homogeneous catalysis) and **Figure. V. 8** (heterogeneous catalysis).

The effect of the alkyne on the MCR with heterogenized **Au(I)-MCM** catalyst was also investigated. Phenylacetylene was highly reactive; usually giving good to high yields of adducts (**Table. V. 2**, entries 1–3). Tollyl-acetylene was less effective than phenylacetylene, giving the expected adduct in high yields after 48 h (**Table. V. 2**,

entry 2). Aliphatic reacted as well as aromatic alkynes, as exemplified with 1-decyne, which gave the expected adduct in a high yield but longer reaction times, similar to that obtained with tolyl-acetylene (**Table. V. 2**, entry 3).

Table. V. 3. Catalytic three-component reaction between, piperidine, phenyl acetylene and different aldehydes.^a

Entry	Catalysts	aldehyde	Yield (%) ^b
1	HI-1Au(III)		94
2	HI-1Au(III)-MCM		65
3	HI-1Au(III)		50
4	HI-1Au(III)-MCM		40
5	3aAu(I)		37
6	HI-1Au(III)		64
7	HI-1Au(III)-MCM		30
8	6aAu(I)-MCM		3
9	HI-1Au(III)		5
10	HI-1Au(III)-MCM		0
11	HI-1Au(III)-MCM		74
12	6aAu(I)-MCM		80

^a Conditions: aldehyde (0.19 mmol), piperidine (0.22 mmol), phenyl acetylene (0.28 mmol), catalyst (1 mol%), in CHCl₃ (2 mL) at 70 °C for 24 h. ^b Yields of isolated product based on aldehyde.

The effect of the aldehyde was then examined in **Table. V. 3**. Piperidine and phenylacetylene were used as amine and alkyne respectively. With these reagents, benzaldehyde gave high isolated yield of the expected adduct with several catalyst, whereas the more electron-rich 3,4,5-trimethoxybenzaldehyde or 2-hydroxybenzaldehyde (**Table. V. 3**, entries 4–7) led to a slightly lower yield of products. However, *p*-nitrobenzaldehyde did not give any adduct, and only a mixture of resinous compounds was observed (**Table. V. 3**, entries 9–10). The same behavior was observed with the less nucleophilic morpholine. With no conjugated aldehydes such as heptanal, the MCR proceeded smoothly with piperidine and phenylacetylene leading to the expected adduct in good yield (**Table. V. 3**, entries 11, 12). It has to be remarked here that while unwanted trimerization of aliphatic aldehydes is a major limitation of the A^3 coupling reactions catalyzed by soluble catalysts, no trimer could be detected with the heterogenized gold catalyst.

3.2.2 *Multi-component reaction and acid catalysis.*

In order to study the possibility of a four-component reaction we have studied the A^3 reaction with ethynyltrimethylsilane as acetylenic starting material (**Table. V. 4**). This system offers the opportunity that once the three-component reaction is finished, deprotection of acetylene may occur taking place additional step, thus open new possibilities of reaction through Sonogashira reaction, alcohol or water addition etc...

Table. V. 4 shows also the important effect of the support (MCM-41) in the selectivity of the process. Thus soluble catalyst **HI-1Au(III)** with high selectivity gives almost exclusively the protected product A (**Table. V. 4**, entries 1 and 3), on the contrast, $K[AuCl_4]$ (**Table. V. 4**, entry 5) does not confer this selectivity in the process. By other hand, MCM-41 supported complex **HI-1Au(III)-MCM** afforded almost exclusively the desilylated product B, due to the slightly acidity of the support itself that acts here as an acid catalyst. So we have a clear example of how the support modifies the catalytic properties of the heterogenized catalyst. Then, we can see the heterogenized catalyst acts as a bifunctional solid catalyst with active metal and acid centers in the same material.

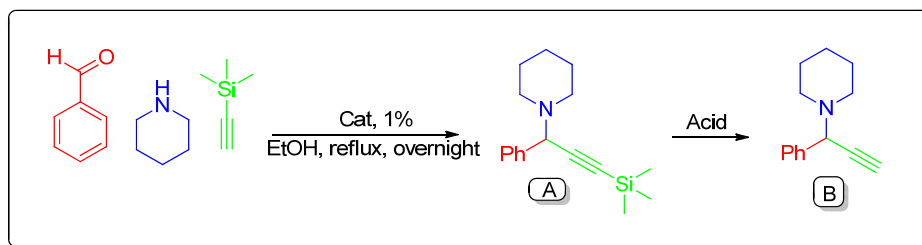


Table. V. 4. Catalytic A³ reaction with ethynyltrimethylsilane substrate.^a

Entry	Catalysts	Temperature	Product	Yield (%) ^b
1	HI-1Au(III)	50°C	A	60%
2	HI-1Au(III)-MCM	50°C	A/B 50:50	50%
3	HI-1Au(III)	80°C	A/B 95:5	63%
4	HI-1Au(III)-MCM	80°C	A/B 2:98	40%
5	K[AuCl ₄]	80°C	A/B 76:24	42%

^aUnless otherwise noted, all reactions were performed with aldehyde (0.19 mmol), piperidine (0.22 mmol), ethynyltrimethylsilane (0.28 mmol), catalyst (1 mol%), in EtOH (2 mL) at corresponding temperature for 24 h. ^b Yield of the mixture.

3.2.3 Tentative MRC mechanism for supported gold systems.

MCR's proceed through the initial formation of an iminium intermediate from the starting amine and aldehyde. This iminium compound reacts with the alkyne, usually in the presence of a metal as catalyst. However, the iminium formation, which proceeds through an aminal, and this equilibrium could be influenced by the support. The acidity of the MCM-41 could indeed favor iminium formation, and interactions of the oxygen or nitrogen atoms with the zeolite frame could also facilitate the reaction. The fact that some heterogenized systems are more active than soluble ones tends to support an active role of the MCM-41 in the formation of this intermediate.

Under our conditions, the gold atoms probably act as the catalyst. Upon coordination, the alkyne is probably deprotonated, either by the starting amine or the intermediate aminal. The gold acetylide thus formed could then add concomitantly to the iminium compound produced within the support.

3.2.4 Recycling.

As we have shown in other chapters, heterogenized catalysts offer easy of handling and purification through simple filtration. They also allow catalyst recovery and recycling, another interesting eco-friendly aspect of these catalysts. In order to examine this possibility, we performed the condensation reaction between piperidine, benzaldehyde, and phenylacetylene several times with the same supported catalyst, the latter being filtered and reused after each run with reactivation. As shown in **Table V. 5**, the heterogenized catalysts could be recycled up to at least three times. We made also an experiment in recycling, in which we used the **6aAu(III)-MCM41** catalyst until we observe less activity and have found that it remains up to 12 cycles without loss of activity.

Once the catalyst was recovered from the reaction mixture, was treated with benzonitrile at 70 °C for 5 h after each cycle (there is no reaction if the catalyst is used without washing with benzonitrile). This fact suggests the formation of a stable acetylene-gold species in the course of the reaction, for recycling these materials is necessary to give up the acetylene moiety and replace it with benzonitrile. All heterogenized catalysts were recycled for the model reaction (phenylacetylene, benzaldehyde and piperidine) (**Table V. 5**). As can be seen heterogenized complexes with dioxolane backbone ligands (Au(I) and Au(III)) were reused at least three cycles but Au(III)-pincer derivative were used only one time and deactivate.

Table V. 5. Recycling experiments.

Entry	Catalysts	Cycle 1	Cycle 2	Cycle 3
1	6aAu(I)-MCM41	99	78	73
2	6aAu(III)-MCM41	99	83	85
3	HI-1Au(III)-MCM41	65	-	-

After 3 runs leaching or gold reduction was not observed for all heterogenized catalyst even in gold (I) catalysts types. In order to confirm the absence of gold soluble

species in the reaction mixture, the reaction mixture was filtered after reaction and the powder XRD patterns of **6aAu(I)-MCM-41** (before reaction) and **6aAu(I)-MCM-41** (after reaction) and the dried filtered crude have been analyzed in **Figure V. 11**.

As in the case of hydrogenation reaction, the positions of the peaks of **6aAu(I)-MCM-41** (before reaction), remain almost unchanged, suggesting the retention of the long range hexagonal symmetry of the host material. The powder patterns also remain unchanged for material **6aAu(I)-MCM-41** (after reaction). A reduction of the peaks intensities is observed in this case; this is not interpreted as a loss of crystallinity, but rather to a reduction in the X-ray scattering contrast between the silica walls and pore-filling material, a situation well described in the literature,²⁴ and also observed for other types of materials.²⁵ In case of reaction mixture any peaks were observed, this fact suggest that any metal species is in solution in the course of the reaction.

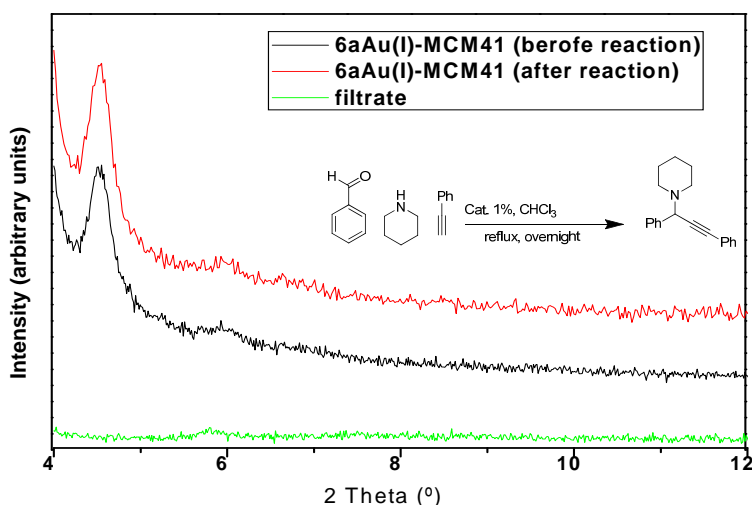


Figure V. 11. XRPD patterns of **6aAu(I)-MCM-41** (before reaction), recovered **6aAu(I)-MCM-41** (after reaction) and liquid solution.

[24] Reference 54 Chapter III.

[25] Reference 55 Chapter III.

4 Conclusions.

In conclusion, heterogenized and soluble catalysts based on gold have been successfully developed for the one-pot A^3 coupling reaction. The catalytic activity of MCM-41 heterogenized gold-complexes is high and the catalysts result air stable for months and can readily be recovered and reused. The process is simple and general and produces propargylamines in good to excellent yields.

5 Experimental section

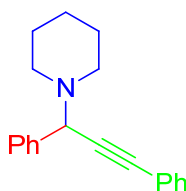
General Remarks: Solvents were carefully degassed before use. ^1H -NMR, ^{13}C -NMR spectra were taken on Varian XR300 and Bruker 200 spectrometers. Chemical shifts being referred to tetramethylsilane (internal standard). Gas chromatography analysis was performed using a Hewlett-Packard 5890 II.

5.1 General procedure for the three-component coupling reaction:

All commercially available reagents were purchased from Aldrich and used as received. The desired amount of supported gold catalyst was added to a mixture of benzaldehyde (20 mg, 1.88 mmol), piperidine (19.3 mg, 2.26 mmol) and phenylacetylene (28.9 mg, 2.82 mmol) in 2.0 mL of CHCl_3 with dodecane as an internal standard. The A^3 coupling reaction was performed in a closed Schlenk flask with stirring (1000 rpm) at 70 °C under inert atmosphere. After a given reaction time, the product mixtures were cooled to room temperature and centrifuged. The reaction mixture was analyzed by GC to determine the aldehyde conversion. The pure product was obtained by flash chromatography and identified by GC/MS and/or ^1H NMR spectroscopy.

5.2 MCR pure products.²⁶

1-(1,3-diphenylprop-2-ynyl)piperidine

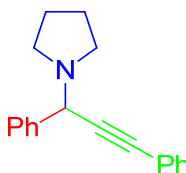


¹H-NMR (CDCl₃, ppm): δ = 7.65-7.62 (m, 2H); 7.52-7.49 (m, 2H); 7.36-7.29 (m, 6H); 4.79 (s, 1H); 2.56-2.48 (M, 4H); 1.72-1.51 (m, 4H); 1.46-1.43 (m, 2H).

¹³C-NMR (CDCl₃, ppm): δ = 138.4; 131.8; 128.6 (three signals overlap); 128.3 (three signals overlap); 128.1 (three signals overlap); 127.5; 123.3; 87.8; 86.0; 62.3, (two signals overlap); 50.6; 26.1; 24.4.

MS (m/z, %): 274 (M⁺; 20); 232 (8); 198 (63); 191 (100); 164 (8).

1-(1,3-diphenylprop-2-ynyl)pyrrolidine

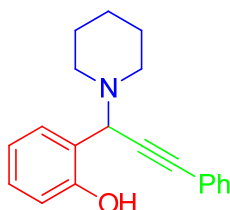


¹H-NMR (CDCl₃, ppm): δ = 7.68-7.64 (m, 2H); 7.57-7.51 (m, 2H), 7.44-7.37 (m, 2H), 7.37-7.30 (m, 4H), 4.93 (s, 1H), 2.80-2.68 (m, 4H), 1.90-1.78 (m, 4H).

¹³C-NMR (CDCl₃, ppm): δ = 138.5; 131.8; 128.3 (four signals overlap); 128.1 (four signals overlap); 126.9; 123.8; 86.7; 86.2; 59.1; 50.3 (two signals overlap); 23.4 (two signals overlap).

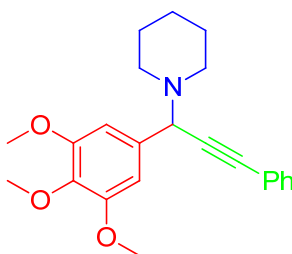
MS (m/z, %): 261(M⁺, 25); 232(7), 191(100).

[26] R. Enugala, V. Ravi, S. Nuvula, A. Srinivas, *Tetrahedron Letters*, **2007**, 48, 7184 – 7190.

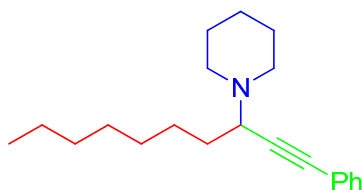
2-(3-phenyl-1-(piperidin-1-yl)prop-2-yn-1-yl)phenol

$^1\text{H-NMR}$ (CDCl_3 , ppm): δ = 9.70 (s, 1 H, OH); 6.80-7.60 (m, 9H); 5.10 (s, 1H); 2.70 (m, 4H); 1.30-1.75 (m, 6H).

MS (m/z, %): 290 (M^+ , 10).

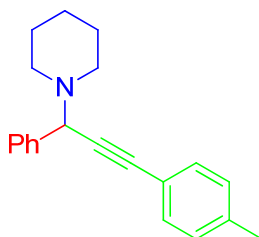
1-(3-phenyl-1-(3,4,5-trimethoxyphenyl)prop-2-yn-1-yl)piperidine

MS (m/z, %): 365 (M^+ , 10); 281 (100).

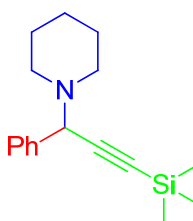
1-(1-Phenyldec-1-yn-3-yl)piperidine

$^1\text{H-NMR}$ (CDCl_3 , ppm): δ = 7.46-7.44 (m, 2H), 7.33-7.30 (m, 3H), 3.52-3.48 (m, 1H), 2.71-2.51 (m, 4H), 1.75-1.43 (m, 8H), 1.36-1.25 (m, 10H), 0.89 (t, 3H).

MS (m/z, %): 297 (M^+), 198 (100).

1-(1-phenyl-3-(p-tolyl)prop-2-yn-1-yl)piperidine

MS (m/z, %): 289 (M⁺, 24).

1-(1-phenyl-3-(trimethylsilyl)prop-2-yn-1-yl)piperidine

¹H-NMR (CDCl₃, ppm): δ = 7.57-7.53 (m, 2H); 7.33-7.29 (m, 3H); 4.57 (s, 1H); 2.44-2.41 (m, 4H); 1.54-1.46 (m, 4H); 1.45-1.41 (m, 2H); 0.22 (s, 9H).

¹³C-NMR (CDCl₃, ppm): δ = 138.5; 128.5 (two signals overlap); 128.0 (two signals overlap); 127.3; 102.1; 92.1; 62.5; 50.4 (two signals overlap); 26.1 (two signals overlap); 24.4; 0.12 (three signals overlap).

MS (m/z, %): 271(M⁺, 10); 194 (100).



General conclusions

1 Conclusions.

In this thesis dissertation, the synthesis of new complexes from two different families has been developed. We have used these new complexes as soluble catalysts in homogeneous catalytic processes. For heterogeneization on inorganic support a new methodology has been established to support the soluble catalysts through functionalization the corresponding ligand with trialkoxysilane groups and posterior immobilization through covalent bond with superficial silanol of MCM-41. With each family, we have studied the catalytic behavior in asymmetric hydrogenation of soluble and heterogenized catalysts paying attention in the role of support on reactivity and selectivity. Gold catalysts have been tested in multi-component reaction for the synthesis of propalgyamines as example of stability and applicability of the supported catalysts. As a consequence of our experiments could be deduced the following conclusions, presented in four different groups:

a) Preparation of soluble ligands and complexes.

We developed a convergent, general and reproducible synthetic route, due to its modularity and efficiency, allows for the synthesis of two families of ligands: based on dioxolane backbone bearing *N*-heterocyclic carbene moieties and based on proton sponges as building block.

- Soluble *N*-heterocyclic carbene precursor salts have been obtained by synthesis of optically pure dioxolane backbone from tartaric acid and subsequently reaction with corresponding imidazole or/and amine affording *bis-N*-heterocyclic carbene precursor salts and *mono-N*-heterocyclic carbene amine precursor salts respectively.
- Soluble proton sponge ligands have been obtained by condensation of 8-((2*R*,5*R*)-2,5-dimethylpyrrolidin-1-yl) naphthalen-1-amine with several aldehydes affording the corresponding perimidines or imine ligands.
- Soluble Au (I), Au (III), Cu (II), Rh (I), Pd (II) *bis-N*-heterocyclic carbene complexes have been obtained by the transmetalation with AuCl(tht) (tht= tetrahydrothiophene), [RhCl(cod)]₂, [PdCl₂(cod)] (cod= 2,5-cyclooctadiene)

and $\text{K}[\text{AuCl}_4]$ from the corresponding silver complex. Copper complex was obtained from direct reaction with Cu_2O .

- Soluble Rh (I) and Pd (II) *mono-N*-heterocyclic carbene amine complexes have been obtained from the corresponding metal precursor ($[\text{RhCl}(\text{cod})]_2$, $\text{PdCl}(\text{cod})_2$) and subsequent deprotonation of the imidazolium salt in the presence of a strong base (KO^tBu).
- Soluble Rh (I) and Pd (II) proton sponge complexes have been obtained by reaction with $[\text{Pd}(\text{cod})\text{Cl}_2]$ or $\text{Pd}(\text{AcO})_2$ and $[\text{RhCl}(\text{cod})]_2$ respectively.

b) Preparation of ligands and complexes containing pendant trialkoxysilane groups.

- Proton sponge core ligands and *N*-heterocyclic carbene precursor salts bearing trialkoxysilane groups were obtained by similar routes as soluble ligands.
- Au (I), Rh (I) and Pd (II) *mono-N*-heterocyclic carbene amine complexes bearing trialkoxysilane groups were accessible by silver carbene transmetallation.
- Rh (I) and Pd (II) proton sponge complexes containing pendant trialkoxysilane groups were obtained by similar route as soluble ones.

c) Heterogeneization of metal complexes on MCM-41.

- Complexes containing pendant trialkoxysilane groups were immobilized on MCM-41 via covalent bonds between the solid containing silanol groups through controlled hydrolysis of RO-Si bonds from the ligand and reaction with silanol groups (Si-OH) from the support.

d) Study of catalytic behavior.

1. Asymmetric Hydrogenation reaction.

- Complexes from *N*-heterocyclic carbene and proton sponge families were efficient and enantioselective as catalyst in the asymmetric hydrogenation of pro-chiral succinates.

- Activity and enantioselectivity of soluble Au (I), Rh (I) and Pd (II) *bis-N*-heterocyclic carbene complexes resulted competitive and more stable confronting with the Diop phosphine analogous complexes.
- Soluble Rh (I) and Pd (II) *mono-N*-heterocyclic carbene amine complexes with diisopropylamine moiety resulted more active than morpholine ones and even than *bis-N*-heterocyclic carbene complexes.
- Activity and enantioselectivity of supported *mono-N*-heterocyclic carbene amine complexes resulted competitive with their soluble counterparts, being the best results for the complexes derived from 2,6-diisopropylphenyl imidazolium (for gold (I) and palladium (II)) and derived from mesityl imidazolium (for rhodium (I)). Heterogenized *N*-heterocyclic carbene amine Rh (I) complex presents higher activity than Rh (I) homogeneous references.
- Soluble imine Rh (I) and Pd (II) complexes based on proton sponges present higher activity and enantioselectivity than the perimidine complexes.
- Heterogenized Rh (I) and Pd (II) proton sponge complexes present higher activity and enantioselectivity than their soluble counterparts in the asymmetric hydrogenation of pro-chiral succinates.
- Heterogenized catalyst from both families are recyclable at least for four cycles without any loss of their performance repeating high enantioselectivity and activity in each cycle.

2. Synthesis of propalylamines via multi-component reaction

- Heterogenized and soluble gold (I) and gold (III) *N*-heterocyclic carbene complexes are active in multi-component reaction for the synthesis of propalylamines
- The process is simple and general and produces propalylamines in good to excellent yields and heterogenized catalysts are stable and can be reused for at least three cycles with almost no loss of activity.

All previous points are very close with green chemistry, such as the developed of new chemical processes that can be replace the unacceptable ones. For this aim is necessary the application of new catalysts more efficient and selective while recyclable so that industrial processes become less polluting for the reduction of toxic and hazardous solvents and reagents in the large scale chemical industry.

2 Conclusiones

En el presente trabajo de tesis doctoral, se ha desarrollado la síntesis de nuevos complejos metálicos provenientes de dos familias diferentes. Estos nuevos complejos pueden ser utilizados como catalizadores solubles en procesos catalíticos homogéneos. Para la heterogenización de estos complejos se ha estudiado una nueva metodología en la cual los catalizadores solubles son inmovilizados mediante la funcionalización de sus ligandos con grupos trialcóhoxisilano y posterior reacción con grupos silanol del soporte (MCM-41), así, quedan inmovilizados por medio de enlace covalente. Con cada familia, se ha estudiado el comportamiento catalítico en hidrogenación asimétrica prestando atención en las diferencias entre la catálisis en fase homogénea y heterogénea. Por otro lado, los catalizadores de oro sintetizados han sido probados en la síntesis de propargilaminas por medio de reacción multi-componente, como ejemplo de la estabilidad, la aplicabilidad y reciclabilidad de estos nuevos catalizadores. Teniendo presente estas ideas, se llevaron a cabo los siguientes pasos:

a) Preparación de ligandos y complejos solubles

Hemos desarrollado una ruta sintética que debido a su modularidad y eficiencia es convergente, general y reproducible y que además permite la síntesis de dos familias de ligandos quirales como son: la familia de los carbenos *N*-heterocíclicos con esqueleto dioxolano y la familia de ligandos basados en esponjas de protones.

- Las sales precursoras de los carbenos *N*-heterocíclicos solubles han sido obtenidos por la síntesis del esqueleto dioxolano ópticamente puro a partir del ácido tartárico y posterior reacción con los imidazoles correspondientes y /o aminas proporcionándonos las sales precursoras de carbenos *bis-N*-heterocíclicos y *mono-N*-heterocíclicos amina, respectivamente.
- Los ligandos solubles derivados de esponja de protones se han obtenido por condensación de 8-((2*R*,5*R*)-2,5-dimetilpirrolidin-1-il) naftalen-1-amina con varios aldehídos dando lugar a los correspondientes ligandos de tipo perimidina o imina.

- Los complejos solubles *bis-N*-heterocíclicos carbeno de Au (I), Au (III), Rh (I), Pd (II) se han obtenido a partir del correspondiente complejo de plata por transmetalación con AuCl(tht) (tht = tetrahidrotiofeno), [RhCl (cod)]₂, [PdCl₂(cod)] (cod= 2,5-ciclooctadieno) y K[AuCl₄] respectivamente. El complejo de cobre se obtuvo por reacción directa con Cu₂O.
 - Los complejos solubles *mono-N*-heterocíclicos carbeno amina de Rh (I) y Pd (II) se han obtenido a partir del precursor metálico correspondiente ([RhCl(cod)]₂ y PdCl(cod)₂) y posterior deprotonación de la sal de imidazolio con la presencia de una base fuerte (KO^tBu).
 - Los complejos derivados de la esponja de protones de Rh (I) y Pd (II) se obtuvieron por la reacción directa de los ligandos con los correspondientes productos de partida [[Pd(cod)Cl₂]] ó Pd(AcO)₂ y [RhCl(cod)]₂.
- b) Preparación de los ligandos y complejos funcionalizados con grupos trialcoxisilano.
- Los ligandos derivados de esponja de protones y las sales precursoras de carbeno *N*-heterocíclicos funcionalizados con grupos trialcoxisilano se obtuvieron a partir de rutas sintéticas similares a las utilizadas para los correspondientes solubles.
 - Los complejos carbeno *N*-heterocíclicos amina funcionalizados con grupos trialcoxisilano de Au (I), Rh (I) y Pd (II) fueron sintetizados por transmetalación a partir de los correspondientes complejos de plata.
 - Los complejos derivados de esponja de protones de Rh (I) y Pd (II) funcionalizados con grupos trialcoxisilano se obtuvieron a partir de rutas de síntesis similares a las utilizadas para los correspondientes solubles.
- c) Heterogenización de los complejos metálicos en MCM-41.
- Los complejos funcionalizados con grupos trialcoxisilano fueron inmovilizados en MCM-41 por medio de enlace covalente entre el sólido que contiene grupos silanoles en la superficie y los grupos RO-Si del complejo por medio de una hidrólisis controlada.

d) Estudio del comportamiento catalítico.1. Hidrogenación asimétrica.

- Los complejos correspondientes a las dos familias sintetizadas resultaron eficientes y enantioselectivos como catalizadores en la hidrogenación asimétrica de succinatos pro-quirales.
- La actividad y enantioselectividad para los complejos carbeno *bis-N*-heterocíclico de Au (I), Rh (I) y Pd (II) resultaron competitivas frente a los complejos fosfina análogos Diop, además de ser más estables.
- Los complejos carbeno *mono-N*-heterocíclico amina solubles de Rh (I) y Pd (II) que contienen diisopropilamina como sustituyente resultaron más activos que los análogos con morfolina como sustituyente e incluso que los correspondientes complejos carbeno *bis-N*-heterocíclico.
- La actividad y enantioselectividad de los complejos soportados *mono-N*-heterocíclico carbeno amina resultaron competitivas frente a sus homólogos solubles, siendo los mejores resultados para los complejos de derivados de 2,6-diisopropilfenil imidazolio (para oro (I) y paladio (II)) y los derivados de mesitil imidazolio (para rodio (I)). Los complejos heterogeneizados *N*-heterocíclicos carbeno amina de Rh (I) presentan una mayor actividad que sus referencias homogéneas.
- Los complejos imina basado en esponja de protones de Rh (I) y Pd (II) presentan mayor actividad y enantioselectividad que los complejos perimidínicos.
- Los complejos imina derivados de esponja de protones heterogeneizados de Rh (I) and Pd (II) presentan mayor actividad y enantioselectividad que sus homólogos solubles.
- Los catalizadores heterogeneizados de las dos familias pueden ser reciclados al menos durante cuatro ciclos sin perder ninguna de sus características obteniéndose altas actividades y enantioselectividades.

2. Síntesis de propalgilaminas vía reacción multi-componente.

- Los complejos carbeno *N*-heterocíclico tanto solubles como heterogeneizados de oro (I) y oro (III) resultaron activos en reacciones multi-componente para la síntesis de propalgilaminas
- La reacción multi-componente es simple y general, y produce propalgilaminas con buenos rendimientos. Los catalizadores heterogeneizados resultaron estables en las condiciones de reacción y pueden ser reutilizados en al menos tres ciclos con mínimas pérdidas de actividad.

Todos los puntos anteriores se encuentran muy relacionados con la química sostenible, como es el desarrollo de procesos químicos nuevos, remplazando los procesos instaurados que no respetan en medioambiente. Para que este objetivo se lleve a cabo es necesario la aplicación de nuevos catalizadores más eficientes y selectivos, que al mismo tiempo sean reciclables para que los procesos industriales sean menos contaminantes reduciendo la utilización de disolventes y reactivos tóxicos y/o peligrosos en la industria química a gran escala.

Chapter V II



Articles

1 Articles.

- **Development of homogeneous and heterogenized rhodium (I) and palladium (II) complexes with ligands based on a chiral proton sponge building block and their application as catalysts.** G. Villaverde,^{a,b} A. Arnanz,^a M. Iglesias,^{a*} N. Snejko,^a M. A. Monge,^a and F. Sánchez^{b*}. *Dalton Transactions*. **2011**. Published on web. DOI: 10.1039/c1dt10597c.
- **Chiral NHC-Complexes with Dioxolane Backbone Heterogenized on MCM-41. Catalytic activity.** G. Villaverde,^[a,b] A. Corma,^[c] M. Iglesias,^{*[a]} and F. Sánchez^{*[b]}. *ChemCatChem*, **2011**, 3, 1320-1328.
- **New chiral ligands bearing two *N*-Heterocyclic carbene moieties at a dioxolane backbone. Gold, palladium and rhodium complexes as enantioselective catalysts.** A. Arnanz,^a C. González-Arellano,^a A. del Valle,^b G. Villaverde,^b A. Corma,^c M. Iglesias,^{*a} and F. Sánchez^{b*} *Chem. Commun.*, **2010**, 46, 3001 – 3003.

New chiral ligands bearing two *N*-heterocyclic carbene moieties at a dioxolane backbone. Gold, palladium and rhodium complexes as enantioselective catalysts†

Avelina Arnanz,^a Camino González-Arellano,^a Alberto Juan,^b Gonzalo Villaverde,^b
Avelino Corma,^c Marta Iglesias^{*a} and Félix Sánchez^{*b}

Received (in Cambridge, UK) 28th October 2009, Accepted 13th February 2010

First published as an Advance Article on the web 8th March 2010

DOI: 10.1039/b922534j

Biscarbene ligands with two imidazolin-2-ylidene moieties at a chiral dioxolane backbone were used as ligands for gold, rhodium and palladium complexes. All new complexes showed varying degrees of enantioselectivity toward hydrogenation of prochiral alkenes with ees up to 95%.

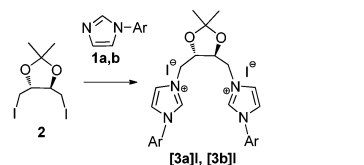
The creation of an asymmetric environment around a metallic centre in order to accommodate the partners of an organic transformation, allows enantioselectivity induction in catalytic processes.¹ A classical approach to achieve this goal is the use of enantiomerically pure ligands containing donor atoms (mainly nitrogen and phosphorus) with a defined symmetry.² The backbone is one of the key aspects to take into account in the design of chiral ligands. Keeping this idea in mind, we have worked with a family of ligands containing a chiral dioxolane backbone. Transition metal complexes supported by ligands bearing *N*-heterocyclic carbene (NHC) groups are emerging as effective catalysts for enantioselective and non-stereospecific organic transformations.³ The attraction of this ligand design⁴ and catalysis is straightforward: NHC supported complexes have the potential to promote any reaction catalyzed by traditional tertiary phosphine- and phosphite-based catalysts.⁵ While the promise of similar reactivity is inviting, the hope of increased efficiency, lower toxicity, air stability, and electronic and structural diversity⁶ makes NHCs a logical and smart choice for exploration. The popular and highly successful motif of chelating diphosphorus-based ligands, particularly chiral versions, prompted our investigation into chiral di-NHC ligands. These ligands often display significant advantages over the analogous phosphine-containing compounds.⁷ Few ligands have been synthesized thus far, and the available structural diversity for NHCs is low in comparison to established phosphorus systems.

In catalytic systems, NHCs have been shown to prevent the formation of elemental metal, a problem often associated with weak ligand–metal interactions.⁸ The literature abounds with examples of chiral monodentate carbene complexes designed for asymmetric synthesis,⁹ but, until recently, C₂-symmetric bidentate carbene complexes were scarce.¹⁰ In a recent paper a comprehensive list was presented describing the synthesis of all chiral di-NHC ligands and complexes reported to date, including pertinent catalytic and structural features.¹¹

Thus far, there have been few reports regarding the use of chiral NHC-metal complexes in asymmetric catalysis.¹² To date, the best enantioselectivities for any reaction featuring a catalyst with a bidentate chiral di-NHC ancillary ligand were reported by Shi *et al.*^{10b} (binaphthyl-*bis*-NHC–Rh). The complex is an excellent precatalyst for the enantioselective hydrosilylation of methyl ketones. Marshal *et al.*^{10a} capitalized on naturally derived tartaric acid to form ligands containing *trans*-2,2-dimethyl-1,3-dioxolane and were able to form Pd(II) complexes featuring *cis*-chelate orientation. Machado and Dorta have synthesized the analogous chiral diimidazole version but do not report metalation attempts or catalysis.¹³

Mindful of this, we began the synthesis of stable C₂-symmetric diimidazolidinylidene ligands bridged by a *trans*-2,2-dimethyl-1,3-dioxolane backbone to use as phosphine substitutes in catalytic asymmetric transformations. We prepared different chelated gold, rhodium and palladium complexes to see how the carbene substituent affects the catalytic activity. These complexes were screened for catalytic activity in the hydrogenation of prochiral alkenes.

The manipulation of L-tartaric acid using modified described methods¹⁴ gave access to (4*R*,5*R*)-*bis*-(iodomethyl)-2,2-dimethyl-1,3-dioxolane (**2**), which, when heated with 1-arylimidazoles **1a,b**,¹⁵ produced quantitative yields of the salts [**3a**]⁺, [**3b**]⁺ as light yellow solids (Scheme 1). These syntheses have been performed by an adaptation of a



a: Ar = 2,4,6-trimethylphenyl, b: Ar = 2,6-diisopropylphenyl

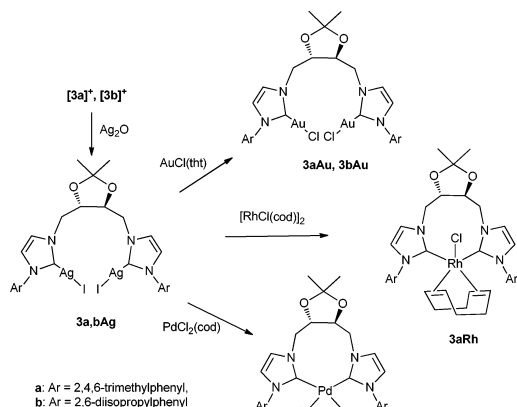
Scheme 1 Synthesis of chiral *bis*-NHC ligand precursor.

^a Instituto de Ciencia de Materiales de Madrid, CSIC, C/Sor Juana Inés de la Cruz 3, Cantoblanco, 28049 Madrid, Spain. E-mail: marta.iglesias@icmm.csic.es; Fax: (+) 34 (91) 3720623; Tel: (+) 34 (91) 3349000

^b Instituto de Química Orgánica General, CSIC, C/ Juan de la Cierva, 3, 28006 Madrid, Spain. E-mail: felix-igo@icmm.csic.es; Fax: (+) 34 (91) 5644853; Tel: (+) 34 (91) 5622900

^c Instituto de Tecnología Química, CSIC-UPV, Avda de los Naranjos, s/n, 46022 Valencia, Spain. E-mail: acorma@itq.upv.es; Fax: (+) 34 (96) 3877809; Tel: (+) 34 (96) 3877800

† Electronic supplementary information (ESI) available: Experimental procedures, and compound characterization details. See DOI: 10.1039/b922534j



Scheme 2 Synthesis of bis-NHC-complexes

procedure described previously.^{10f,13} The imidazolium carbon (N-CH=N) appears at 137.42 ppm (**3aI**) and 137.90 (**3bI**).

It is well known that silver(i) oxide is a suitable metal salt for the synthesis of the corresponding carbene complexes. The treatment of the imidazolium iodide salts (**3aI**, **3bI**) with Ag₂O yielded the silver complexes (**4S,5S**)-**3a,3bAg**. The formation of the carbene complexes **3a,3bAg** was established by a weak peak below δ 174 ppm in each ¹³C-¹H NMR spectrum which was assigned to the C-imidazol-2-ylidene (carbene) carbon, and by the absence of the downfield peak for the 2H-imidazolium proton in each ¹H NMR spectrum (below δ 9.7 ppm). (Scheme 2).

As Ag–NHC bonds are quite weak¹⁶ the silver complexes could then be used as carbene transfer reagents to gold, palladium and rhodium according to Lin *et al.*¹⁷ The reaction of the silver complexes with AuCl(tht) (tht = tetrahydrothiophene), [RhCl(cod)]₂ and [PdCl₂(cod)] (cod = 2,5-cyclooctadiene) yielded the respective complexes (**4S,5S**)-**3aAu**, **3bAu**, **3aRh**, **3aPd**, (Scheme 2) in > 80% yield along with the formation of AgI precipitate.

The ESI spectrum for (**3aAu**) shows a peak at m/z = 927 which corresponds to the loss of one chloride (m/z = 1011 for (**3bAu**)). FT IR spectra show a strong band at 328–331 cm^{−1} assigned to the ν (Au–Cl) vibration. ¹³C NMR spectra show all resonances shifted as compared to the uncoordinated ligand with the diagnostic gold-bound (NCN–Au) peak at 177.1 ppm (**3aAu**) or 173.9 ppm (**3bAu**).

The ¹H NMR spectrum of [RhCl(cod)(**3a**)] (**3aRh**) shows the resonance due to the cod protons significantly broadened due to fluxionality of the complex. The mesityl rings undergo restricted rotation about the N–C bond as evidenced by the presence of two distinct resonances in the ¹H NMR spectrum for each of the *o*-methyl groups and each of the *m*-protons on the mesityl ring. The (NCN–Rh) signal appears at δ = 179.8 ppm in the ¹³C NMR spectrum. The monomolecular structure is confirmed by the intense MS molecular peak 745 (M⁺).

The ¹H-NMR spectrum of [PdCl₂(**3a**)] (**3aPd**) shows one signal set of a symmetric species. In the ¹³C NMR spectrum

Table 1 Hydrogenation of (*E*)-diethyl 2-*R*-succinates with bis-NHC and diphosphine catalysts^{a,c}

Entry	Catalyst	R	TOF ^b	ee (%)
1	3aRh	Methylene	258	10 (S)
2	3aRh	Benzylidene	16	99 (S)
3	3aRh	Naphthylmethylene ^d	10	> 95 (S)
4	DIOP-Rh	Methylene	579	20 (S)
5	DIOP-Rh	Benzylidene	28	99 (S)
6	3aPd	Methylene	45	5 (S)
7	3aPd	Benzylidene	17	98 (S)
8	3aPd	Naphthylmethylene ^d	2	> 95 (S)
9	DIOP-Pd	Methylene	119	11 (S)
10	DIOP-Pd	Benzylidene	35	97 (S)
11	3aAu	Methylene	2000	15 (S)
12	3aAu	Benzylidene	1250	90 (S)
13	3aAu	Naphthylmethylene ^d	150	95 (S)
14	3bAu	Methylene	210	25 (S)
15	3bAu	Benzylidene	50	85 (S)
16	3bAu	Naphthylmethylene ^d	5	90 (S)
17	3a(OPNB)Au	Methylene	120	25 (S)
18	3a(OPNB)Au	Benzylidene	15	90 (S)
19	3a(OPNB)Au	Naphthylmethylene ^d	0.5	93 (S)
20	DIOP-Au	Benzylidene	45	98 (S)
21	Duphos-Au	Benzylidene	906	80 (S) ²¹

^a Ethanol, 4 atm. H₂, 40 °C, cat.: 0.5 mol%. ^b TOF: h^{−1} (calculated at maximum rate). ^c HPLC (Chiralcel AD-H, λ : 230 nm, hexane/iPrOH: 98/2, Chiralcel OD, λ : 250 nm, hexane/iPrOH: 95/5). ^d 60 °C, 4 atm. H₂.

formation of the carbene complex is indicated by a carbene signal at 175.0 ppm, which is comparable to the chemical shift observed in other *trans*-[PdCl₂(bis(NHC))] complexes.¹⁸ Cationic complexes were generated by halide abstraction *via* addition of AgPF₆ in a CH₂Cl₂–water solvent system.

The problem in (NHC)-catalyzed hydrogenation is the tendency for NHC reductive elimination to the imidazolium salt [NHC–H]⁺. Not surprisingly, there is to date only a single example of enantioselective alkene hydrogenation using chiral monodentate NHC complexes.¹⁹ Bis-NHC ligands are expected to be resilient to reductive elimination but only one report of hydrogenation of alkenes has been described.^{12f} The efficiency of gold-, palladium- and rhodium-complexes as catalysts for the asymmetric hydrogenation of different alkenes (diethyl itaconate, (*E*)-diethyl 2-benzylidenesuccinate, and (*E*)-diethyl 2-naphthylmethylenesuccinate) was investigated (Table 1). All complexes showed significant activities. In the hydrogenation of (*E*)-diethyl 2-benzylidenesuccinate up to 99% ee was obtained with the rhodium catalyst. Palladium and gold complexes also yielded good enantioselectivity (Table 1).

For comparison purposes, we obtained the rhodium and palladium complexes with the diphosphine (*R,R*)-DIOP as ligand ((*R,R*)-DIOP = (4*R*,5*R*)-4,5-*bis*-(diphenylphosphino-methyl)-2,2-dimethyldioxolane) which has the same skeleton as the *biscarbene* ligand studied in this paper). The reactivity is slightly higher with the diphosphine Rh-complex ([Rh(cod)(DIOP)]⁺), however the enantioselectivity was similar in the case of succinates with greater steric hindrance. The palladium complex [Pd(cod)(DIOP)]²⁺ and cationic gold complex ([Au(benzonitrile)]₂(*R,R*)-DIOP)²⁺²⁰ activities and enantioselectivities were similar to those obtained with the

corresponding derivative *bis*(NHC)-complex (**3aAu**). These results are similar to that obtained when freshly prepared [(AuCl)₂((*R,R*)-Me-Duphos)]²¹ was the catalyst with the difference that the **3aAu** complex is stable for at least 3 months and is easier to synthesize and manipulate.

To extend the scope of the complexes as catalysts we have used (*Z*)- α -ethyl benzamidocinnamate as a substrate with the result that the catalytic activity for **3aRh** is good (TOF = 35 h⁻¹) but the enantiomeric excess is marginal (<10%). The [Rh(cod)(DIOP)]⁺ gives an ee of 15% (TOF = 264 h⁻¹) and the palladium complex decomposes in the reaction medium under the same conditions.

An important fact is to check is how the catalyst activity varies over time; it was found that the carbene complex maintains its activity for at least three months, however the activity for the [Rh(cod)(DIOP)]⁺ complex decreases over a week (Fig. S2†).

As can be seen from Table 1, the complex **3bAu**, which contains a 2,6-diisopropylphenyl on the NHC donor, had much slower reaction rates. These results indicate that the bulky substituents severely limit the activity of the catalysts. This effect is most probably due to the inhibition of substrate coordination due to steric interaction with the bulky isopropyl substituent. Dramatic decrease of reactivity was also founded when the chlorine was substituted by OPNB (4-nitrobenzoate), [Au(OPNB)]₂((*S,S*)-**3a**), probably due to increased steric hindrance.

In summary, we report the synthesis of gold, palladium and rhodium complexes bound to a chiral dioxolane ligand bearing two NHC moieties. To the best of our knowledge, this is the first example of the use of chiral *bis*(NHC)-metal catalysts in asymmetric hydrogenation with high enantioselectivity. These *N*-heterocyclic carbenes represent a class of ligands that can be used in place of phosphine ligands in transition-metal catalysis, which provide more effective metal complexes owing to their stability to air and moisture.

The authors thank the Dirección General de Investigación Científica y Técnica of Spain (Project MAT2006-14274-C02-02), and Consolider Ingenio 2010-MULTICAT. G.V. thanks the MCIINN for financial support.

Notes and references

- (a) I. Ojima, *Catalytic Asymmetric Synthesis*, 2nd edn, Wiley-VCH, New York, 2000; (b) P. J. Walsh and M. C. Kozlowski, *Fundamentals of Asymmetric Catalysis*, University Science Book, Sausalito, 2009, p. 191.
- E. M. Jacobsen, A. Pfaltz and H. Yamamoto, *Comprehensive Asymmetric Catalysis*, Springer-Verlag, Berlin, 1999.
- (a) *Dalton Trans.*, 2009(35), is a themed issue on *N*-heterocyclic carbenes which contains a total of 49 contributions; (b) S. P. Nolan, *N-Heterocyclic Carbenes in Synthesis*, Wiley-VCH, Weinheim, 2006; (c) P. L. Arnold and S. Pearson, *Coord. Chem. Rev.*, 2007, **251**, 596; (d) P. de Fremont, N. Marion and S. P. Nolan, *Coord. Chem. Rev.*, 2009, **253**, 862; (e) P. de Fremont, N. Marion and S. P. Nolan, *J. Organomet. Chem.*, 2009, **694**, 551; (f) D. Pugh and A. A. Danopoulos, *Coord. Chem. Rev.*, 2007, **251**, 610; (g) R. Corberán, E. Mas-Marzá and E. Peris, *Eur. J. Inorg. Chem.*, 2009, 1700; (h) Y. Li, X.-Q. Wang, C. Zheng and S.-L. You, *Chem. Commun.*, 2009, 5823; (i) Y.-Z. Zhang, Sh.-F. Zhu, Y. Cai, H.-X. Mao and Q.-L. Zhou, *Chem. Commun.*, 2009, 5362.
- C. J. O'Brien, E. A. B. Kantchev, G. A. Chass, N. Hadei, A. C. Hopkinson, M. G. Organ, D. H. Setiadi, T. H. Tang and D. C. Fang, *Tetrahedron*, 2005, **61**, 9723.
- R. H. Crabtree, *J. Organomet. Chem.*, 2005, **690**, 5451.
- (a) R. Dorta, E. D. Stevens, N. M. Scott, C. Costabile, L. Cavallo, C. D. Hoff and S. P. Nolan, *J. Am. Chem. Soc.*, 2005, **127**, 2485; (b) H. Jacobsen, A. Correa, C. Costabile and L. Cavallo, *J. Organomet. Chem.*, 2006, **691**, 4350; (c) W. A. Herrmann, J. Schutz, G. D. Frey and E. Herdtweck, *Organometallics*, 2006, **25**, 2437.
- (a) F. E. Hahn and M. C. Jahnke, *Angew. Chem., Int. Ed.*, 2008, **47**, 3122; (b) R. E. Douthwaite, *Coord. Chem. Rev.*, 2007, **251**, 702; (c) J. A. Mata, M. Poyatos and E. Peris, *Coord. Chem. Rev.*, 2007, **251**, 841; (d) W. A. Herrmann, *Angew. Chem., Int. Ed.*, 2002, **41**, 1290; (e) D. Bourissou, O. Guerret, F. P. Gabbaï and G. Bertrand, *Chem. Rev.*, 2000, **100**, 39; (f) F. E. Hahn, L. Wittenbecher, D. Le Van and R. Fröhlich, *Angew. Chem., Int. Ed.*, 2000, **39**, 541.
- J. P. Collman, L. S. Hegehus, J. R. Norton and R. G. Finke, *Principles and Applications of Organotransition Metal Chemistry*, University Science Books, Mill Valley, 1987.
- (a) D. Enders, H. Gielen, G. Raabe, J. Runsink and J. H. Teles, *Chem. Ber.*, 1996, **129**, 1483; (b) W. A. Herrmann, L. J. Goossen, G. R. J. Artus and C. Köcher, *Organometallics*, 1997, **16**, 2472; (c) T. J. Seiders, D. W. Ward and R. H. Grubbs, *Org. Lett.*, 2001, **3**, 3225.
- (a) C. Marshall, M. F. Ward and W. T. A. Harrison, *Tetrahedron Lett.*, 2004, **45**, 5703; (b) W. L. Duan, M. Shi and G. B. Rong, *Chem. Commun.*, 2003, 2916; (c) D. S. Clyne, J. Jin, E. Genest, J. C. Gallucci and T. V. RajanBabu, *Org. Lett.*, 2000, **2**, 1125; (d) M. C. Perry, X. Cui and K. Burgess, *Tetrahedron: Asymmetry*, 2002, **13**, 1969; (e) L. G. Bonnet, R. E. Douthwaite and R. Hodgson, *Organometallics*, 2003, **22**, 4384; (f) C. Marshall, M. F. Ward and J. M. S. Skakle, *Synthesis*, 2006, 1040.
- R. J. Lowry, M. K. Veige, O. Clément, K. A. Abboud, I. Ghiviriga and A. S. Veige, *Organometallics*, 2008, **27**, 5184.
- (a) L. G. Bonnet, R. E. Douthwaite and B. M. Kariuki, *Organometallics*, 2003, **22**, 4187; (b) L. H. Gade, V. Cesar and S. Bellemin-Lapponnaz, *Angew. Chem., Int. Ed.*, 2004, **43**, 1014; (c) J. J. Van Veldhuizen, S. B. Garber, J. S. Kingsbury and A. H. Hoveyda, *J. Am. Chem. Soc.*, 2002, **124**, 4954; (d) J. J. Van Veldhuizen, D. G. Gillingham, S. B. Garber, O. Kataoka and A. H. Hoveyda, *J. Am. Chem. Soc.*, 2003, **125**, 12502; (e) A. O. Larsen, W. Leu, C. N. Oberhuber, J. E. Campbell and A. H. Hoveyda, *J. Am. Chem. Soc.*, 2004, **126**, 11130; (f) M. S. Jeletic, M. T. Jan, I. Ghiviriga, K. A. Abboud and A. S. Veige, *Dalton Trans.*, 2009, 2764.
- M. Y. Machado and R. Dorta, *Synthesis*, 2005, 2473.
- (a) M. Carmack and C. J. Kelley, *J. Org. Chem.*, 1968, **33**, 2171; (b) K. Uchida, K. Kato and H. Akita, *Synthesis*, 1999, 1678; (c) L. J. Rubin, H. A. Lardy and H. O. L. Fischer, *J. Am. Chem. Soc.*, 1952, **74**, 425.
- J. Liu, J. Chen, J. Zhao, Y. Zhao, L. Li and H. Zhang, *Synthesis*, 2003, 2661.
- (a) C. Boehme and G. Frenking, *Organometallics*, 1998, **17**, 5801; (b) D. Nemcsok, K. Wichmann and G. Frenking, *Organometallics*, 2004, **23**, 3640.
- (a) H. M. J. Wang and I. J. B. Lin, *Organometallics*, 1998, **17**, 972; (b) I. J. B. Lin and C. S. Vasam, *Coord. Chem. Rev.*, 2007, **251**, 642; (c) J. C. Y. Lin, R. T. W. Huang, C. S. Lee, A. Bhattacharyya, W. S. Hwang and I. J. B. Lin, *Chem. Rev.*, 2009, **109**, 3561.
- (a) I. Dinares, C. García de Miguel, M. Font-Bardia, X. Solans and E. Alcalde, *Organometallics*, 2007, **26**, 5125; (b) J. Houghton, G. Dyson, R. E. Douthwaite, A. C. Whitwood and B. M. Kariuki, *Dalton Trans.*, 2007, 3065; (c) F. Hannig, G. Kehr, R. Fröhlich and G. Erker, *J. Organomet. Chem.*, 2005, **690**, 5959; (d) B. P. Morgan, G. A. Galdamez, R. J. Gilliard Jr. and R. C. Smith, *Dalton Trans.*, 2009, 2020.
- D. Baskakov, W. A. Herrmann, E. Herdtweck and S. D. Hoffmann, *Organometallics*, 2007, **26**, 626.
- Related DIOP[AuCl]₂ decomposes to Au(0) without reaction and DIOP[AuN(SO₂CF₃)₂]₂ is stable but not catalytic active and no reaction products were detected by GC.
- C. González-Arellano, A. Corma, M. Iglesias and F. Sánchez, *Chem. Commun.*, 2005, 3451.

Chiral NHC-Complexes with Dioxolane Backbone Heterogenized on MCM-41. Catalytic Activity

Gonzalo Villaverde,^[a, b] Avelino Corma,^{*,[c]} Marta Iglesias,^{*,[a]} and Félix Sánchez^{*,[b]}

Rhodium, palladium, and gold complexes of chiral (NHC)-dioxolane-amino ligands were prepared. Herein, new methods for the heterogenization of NHC-chiral complexes on porous silica supports are demonstrated for the facile recovery and recycling of these expensive catalysts. Activity, selectivity, and recyclability were investigated and compared to that of the analogous homogeneous catalysts for asymmetric hydrogenation reactions. The compounds were characterized by using a variety

of methods, including solid state cross-polarization magic-angle spinning (CP MAS) ^{13}C NMR, FT-IR spectroscopy, and elemental analysis. Heterogenized rhodium(I) and palladium(II) catalysts could be used at least four times without loss of activity or enantioselectivity. (NHC)-gold(III) complexes were easily immobilized and recycled by a treatment with benzonitrile during the washing steps between cycles. This washing maintained the activity and enantioselectivity.

Introduction

The chemistry of *N*-heterocyclic carbenes (NHCs) has developed significantly over recent years, encompassing their synthesis, reactivity, coordination chemistry, and application.^[1,2] Because of their modular structures, many modifications of the basic imidazole-based motif have been produced. Whereas one area of these studies has been directed towards the elucidation of the factors determining the stabilities of the free carbenes in terms of electronic and steric effects,^[3] another part of the investigations has focused on potential applications of NHCs, mainly as ligands for transition-metal-catalyzed reactions.^[4] In the latter context, significant recent developments include, for example, the incorporation of NHC moieties into multidentate chelate ligands^[5] and the chiral modification of NHCs with implications for their use in asymmetric catalysis.^[6] Arguably, the most significant stimulus for continued interest is the catalytic application to organo- and metal-mediated catalysis, and there is now ample evidence demonstrating that NHC systems can lead to new reactivity and improved catalytic rate, lifetime, and selectivity. Of the many reactions that have been investigated using NHC containing catalysts, hydrogenation and transfer hydrogenation have featured prominently, which is in part attributable to their wide-ranging use in synthetic chemistry and continued industrial importance. In our case, we attempted to make these efficient systems recyclable to reduce the costs in catalytic processes. In recent years, there has been an expansion in the development of immobilized catalysis in industry. The efficient separation of catalysis from the reaction mixtures is one of the key factors to decrease cost and to be environment friendly.

Previously, we have reported the synthesis of imidazolium salt as precursors to chiral NHC ligands derived from (4*R*,5*R*)-bis(iodomethyl)-2,2-dimethyl-1,3-dioxolane (Figure 1) and subsequently prepared examples of transition metal complexes.^[7] Herein, we report the synthesis of new hybrid bidentate ligands, in which a chiral dioxolane is functionalized by using a

powerful σ -donor NHC and a basic amine group. These ligands are believed to be well-suited for asymmetric catalysis, because of the closeness of the chiral information to the metal, the bulky substituents, and the electronic differentiation. One motivation was to examine if the presence of a proximal alcohol or amine group in the NHC-hybrid complexes has a positive effect on enantioselectivity.

Building on previous projects in our research group, which focused on the development of supported catalysts,^[8] alternative techniques are developed here to provide a new report of heterogenized (NHC)-dioxolane complexes covalently grafted to solid supports. The goal of this work is to develop a solid catalyst, through the immobilization of asymmetrical, chiral (NHC)-

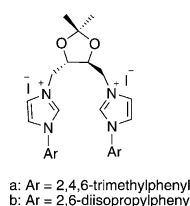


Figure 1. Chiral imidazolium salts precursors derived from (4*R*,5*R*)-bis(iodomethyl)-2,2-dimethyl-1,3-dioxolane.

- [a] G. Villaverde, Prof. M. Iglesias
Instituto de Ciencia de Materiales de Madrid, CSIC
C/Sor Juana Inés de la Cruz 3, Cantoblanco 28049 Madrid (Spain)
Fax: (+34) 913720623
E-mail: marta.iglesias@icmm.csic.es
- [b] G. Villaverde, Prof. F. Sánchez
Instituto de Química Orgánica, CSIC
C/Juan de la Cierva 3, 28006 Madrid (Spain)
Fax: (+34) 915644853
E-mail: felix-igo@iqog.csic.es
- [c] Prof. A. Corma
Instituto de Tecnología Química, CSIC
Avda los Naranjos, s/n, 46022 Valencia (Spain)
Fax: (+34) 963877809
E-mail: acorma@itq.upv.es

Supporting Information for this article is available on the WWW under <http://dx.doi.org/10.1002/cctc.201100119>.

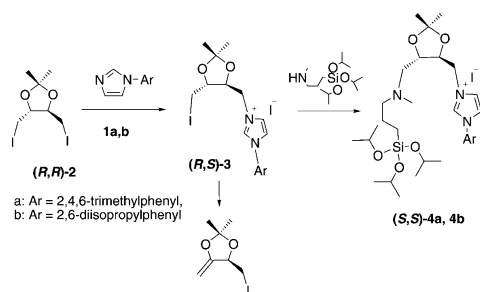
dioxolane–amine ligands on silica supports to eventually produce covalently bound, surface-grafted catalysts. These catalysts are characterized by using solid state cross-polarization magic-angle spinning (CP MAS) ^{13}C NMR, FT-IR spectroscopy, and elemental analysis. This report highlights the synthesis and characterization of these immobilized catalysts, as well as investigations into their activity, selectivity, and recyclability in the hydrogenation of olefins.

Results and Discussion

Synthesis of ligands and complexes

The synthesis of a new class of hybrid NHC ligand comprising an NHC and a tertiary amine moiety and their metal complexes derivatives are presented.

Borrowing from previous methods developed in our research group,^[7] dioxolane-modified bis-functionalized, asymmetrical, and chiral (NHC)–dioxolane–amines (**4a**, **4b**) were synthesized (Scheme 1). The manipulation of L-tartaric acid by



Scheme 1. Synthesis of chiral mono-NHC ligand precursor.

modifying described methods^[9] gave access to (4*R*,5*R*)-bis(iodomethyl)-2,2-dimethyl-1,3-dioxolane (**2**), which, if heated with one equivalent of 1-arylimidazoles **1a** or **1b**,^[10] produced quantitative yields of the respective mono-salts **3a** and **3b** as light yellow solids. These syntheses were performed by using an adaptation of a procedure described previously.^[9] The new solids **3a** and **3b** were heated in a microwave reactor with an excess of amine to afford the functionalized ligands **4a** and **4b** as light yellow oils. Notably, the use of auxiliary bases in the last step gave rise to a collection of olefinic products from the elimination reaction (Scheme 1). The imidazolium carbon (N=C=N) appeared at 138.8 (**4a**) and 138.2 ppm (**4b**).

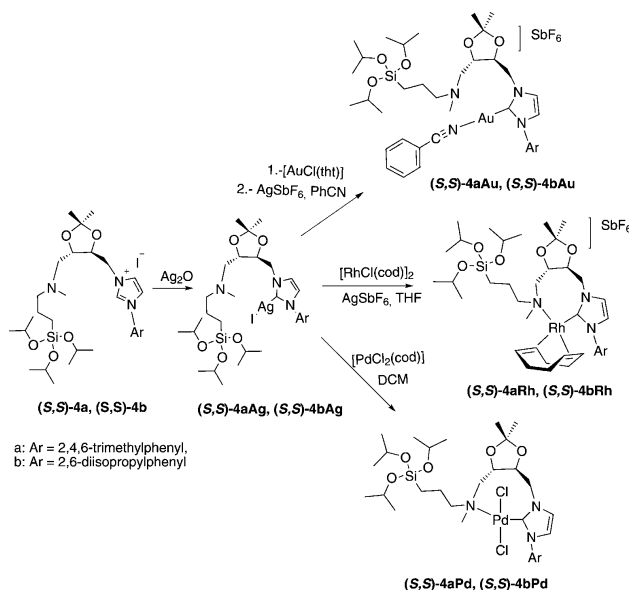
The ability of the NHCs–amine-substituted dioxolane to act as bidentate chelate ligands could be demonstrated by the preparation of silver, gold, palladium, and rhodium complexes.

The treatment of the imidazolium iodide salts (**4a**, **4b**) with Ag_2O yielded the silver complexes **4aAg** and **4bAg**. The formation of these carbene com-

plexes is consistent with a weak peak below $\delta = 174$ ppm in the ^{13}C NMR spectra, which was assigned to the C-imidazol-2-ylidene (carbene) carbon, and with the absence of the downfield peak for the H-imidazolium proton in the ^1H NMR spectra (below $\delta = 9.8$ ppm, Scheme 2).

As Ag–NHC bonds are quite weak^[11] the silver complexes could then be used as carbene transfer reagents to gold, palladium, and rhodium according to Lin et al.^[12] The reaction of the silver complexes with a solution of AgSbF_6 and $[\text{AuCl}(\text{tbt})]$ (tbt = tetrahydrothiophene), $[\text{RhCl}(\text{cod})]_2$ (cationic complexes), or $[\text{PdCl}_2(\text{cod})]$ (cod = 2,5-cyclooctadiene) yielded the respective complexes (**4S**,**5S**)–**4aAu**, **4bAu**, **4aRh**, **4bRh**, **4aPd**, and **4bPd**] (Scheme 2) in >80% yield along with the formation of AgI precipitate. Gold complexes could be obtained in benzonitrile, leading to stable species that had a benzonitrile molecule in its structure. ^{13}C NMR spectra for **4aAu** and **4bAu** show all resonances shifted as compared to the uncoordinated ligand, the diagnostic gold-bound (NCN–Au) peak at 182.5 (**4aAu**) or 179.2 ppm (**4bAu**), and the signals for the coordinating benzonitrile (see the Supporting Information). The MS spectrum for **4aAu** exhibits a peak at $m/z = 786$, which corresponds to the loss of benzonitrile and SbF_6^- . FT IR spectra for the two complexes show a strong band at 655 cm^{-1} , which was assigned to the $\nu(\text{Sb–F})$ vibration in the two gold complexes.

The transmetalation of the silver complex with $[\text{PdCl}_2(\text{cod})]$ proceeded already at room temperature in dichloromethane with a fast formation of a gray precipitate that was removed by using filtration over Celite®. The ^1H NMR spectrum shows the formation of a signal set consistent with a single diastereomer. The signals shifted to low field in comparison to the silver complex. In the ^{13}C NMR spectrum, the formation of the carbene complexes **4aPd** and **4bPd** is indicated by a carbene



Scheme 2. Synthesis of mono-NHC-complexes.

signal at 177.3 and 176.2 ppm, respectively, which is a typical value for imidazolynilidene palladium complexes, shifted high field more than 20 ppm compared to the signal of the silver carbene complex, and which is comparable to the chemical shift observed in other $[\text{PdCl}_2(\text{NHC})]$ complexes.^[13] The mass spectra confirm formation of the mononuclear complex with peaks for **4aPd** at $m/z=768$ (M^+) and 590 (L).

Under the same conditions, the Ag complex was reacted with $[\text{RhCl}(\text{cod})]\text{SbF}_6$, and complexes **4aRh** and **4bRh** were isolated (Scheme 2). The NMR spectra show the resonance attributable to the cod protons significantly broadened, because of the fluxionality of the complex, and the carbon carbene signal at 187.8 (**4aRh**) and 193.2 ppm (**4bRh**). The electrospray ionization mass spectrum (ESI-MS) shows a peak for **4aRh** at $m/z=674$ in agreement with the hydrolysis of three isopropoxyl moieties of the cationic species and for **4bRh** at $m/z=878$ that corresponds with the loss of two fluorine and the hydrolysis of $\text{SiO}i\text{Pr}$ groups of the silyloxy group.

Heterogenization on MCM-41

The complexes (**4S,5S**)-**4aAu**, **4bAu**, **4aRh**, **4bRh**, **4aPd**, **4bPd** were used for the preparation of a new family of materials based on mesoporous MCM-41 (Mobil Composition of Matter No. 41). The silyloxy-complexes were supported on MCM-41 by addition of the corresponding solution to a dispersion of MCM-41 in toluene and heating for 24 h, affording the materials **4aM-MCM-41** with metal loadings of approximately 0.4, 0.1 and 1.6 wt% Pd, Rh, and Au, corresponding to 3.8×10^{-2} , 0.97×10^{-2} , and 8.1×10^{-2} mmol g^{-1} , respectively. The amount of rhodium complex (the value given corresponds to an average of three experiments) immobilized on the support was lower than that achieved with the complexes of palladium and gold, which can only be attributed to an increased steric hindrance of the rhodium complex. The resulting solids were characterized by using FT-IR, UV/Vis, DRUV (Diffuse Reflectance UV-Vis), and solid state CP MAS ^{13}C NMR and compared with its counterpart before heterogenization (see the Supporting Information).

The powder XRD patterns of **4aAu-MCM** (before reaction) and **4aAu-MCM** (after reaction) are given in Figure 2. The pattern of the parent, calcined material MCM-41, shows four reflections in the 2θ range $2\text{--}10^\circ$, which were indexed to a hexagonal cell as (100), (110), (200), and (210). The d value of the (100) reflection is 35.2 \AA , corresponding to a lattice constant of $a=40.6^\circ$ ($=2d100/\sqrt{3}$). The positions of the peaks of **4aAu-MCM** (before reaction) remained almost unchanged after functionalizing the walls of the parent host material MCM with [complex]propyltriisopropoxysilane, suggesting the retention of the long-range hexagonal symmetry of the host material. The powder patterns also remained unchanged for material **4aAu-MCM** (after reaction). A reduction of the peak intensities is observed in this case, and becomes more relevant in the metal rich **4aAu-MCM** (before reaction). This was not interpreted as a loss of crystallinity, but rather to a reduction in the X-ray scattering contrast between the silica walls and pore-fill-

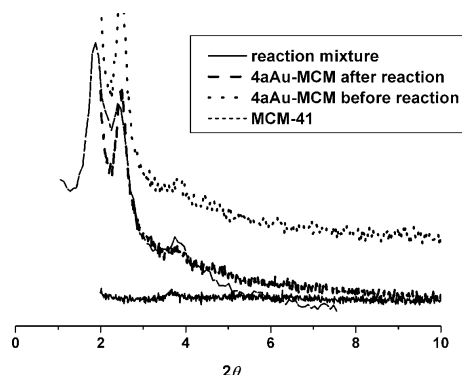


Figure 2. XRD patterns of **4aAu-MCM** (before reaction), **4aAu-MCM** (after reaction), MCM-41, and the reaction mixture.

ing material, a situation well-described in the literature,^[14] and also observed for other types of materials.^[15]

The presence of functional groups characteristic of [complex]propyltriisopropoxysilane in the materials was confirmed by using FTIR spectroscopy. The stretching vibration modes of the mesoporous framework (Si-O-Si) of the grafted materials were observed at approximately 1240 , 1070 , and 810 cm^{-1} . The introduction of the ligands **4a** and **4b** in the stepwise pathway led to the appearance of the ν (C=N) and ν (C=C) stretching modes at 1636 (in **4aAu-MCM**) and 1632 cm^{-1} (in **4aAu-MCM**) as a broad signal. The materials were also characterized by using ^{13}C CP MAS solid state NMR. The solid state ^{13}C CP MAS NMR spectra (Figure S12–S23 in the Supporting Information) of **4aPd-MCM**, **4bPd-MCM**, **4bRh-MCM**, **4aAu-MCM**, and **4bAu-MCM** materials are quite similar, as the spectra are dominated by the resonances of the aliphatic and aromatic groups. These signals appear at approximately 9.5 (Si-CH_2), 18.1 ($\text{CH}_2\text{--CH}_2\text{--CH}_2$), and 58.5 ppm (NCH_2) in **4aPd-MCM**. The metal content is small and, therefore, as the spectra are dominated by the aliphatic and aromatic signals, these signals mask any resonances from other species in lower concentrations. A similar effect has already been described previously. The peaks assigned to the $\text{SiO}i\text{Pr}$ groups appear at 24.8 (CH_3) and 61.4 ppm (OCH). A characteristic signal at 175 ppm is observed in the ^{13}C NMR spectrum for the carbene carbon atom in **4bPd-MCM**.

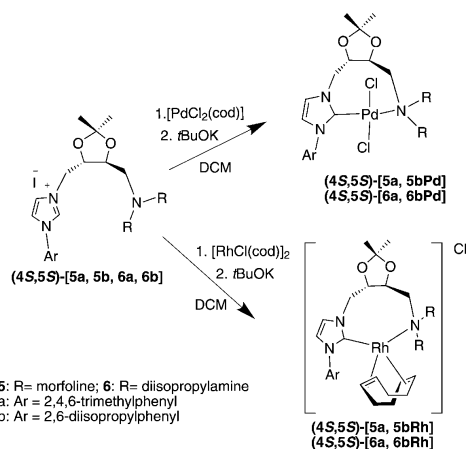
UV/Vis and DRUV spectra were similar before and after heterogenization (see the Supporting Information) and had bands at 536 , 420 , 282 , and 273 nm for **4aAu** and at 493 , 357 , 290 , 248 , and 223 nm for **4aAu-MCM**.

Reference soluble systems

At first, (NHC)–dioxolane–amines were synthesized that could be used as ligands for Rh and Pd complexes that could be used as soluble models of the heterogenized derivatives described above. The amines morpholine or diisopropylamine gave rise to the precursors **5a**, **5b** (amine = morpholine) and **6a**, **6b** (amine = diisopropylamine) in excellent yields (see the

Supporting Information, Scheme S3). However, these imidazolium precursors of NHCs with morpholine or diisopropylamine substituents failed to give NHC complexes. Hence, it was also impossible to use the ligand-transfer protocol with Ag_2O established by Lin.^[12] This discrepancy in the chemical reactivity in relation to the *N*-methyl-3-(triisopropoxysilyl)propan-1-amine-(NHC)-substituted dioxolane can be explained, in the case of morpholine, by the lower basicity of the amine, but if the amine was very basic, as was the case for diisopropylamine, the inhibition of the complex formation can be attributed more properly to steric considerations.

NHC complexes were prepared directly from the corresponding metal precursors ($[\text{RhCl}(\text{cod})]_2$, $[\text{PdCl}(\text{cod})_2]$) and subsequent deprotonation of the imidazolium salt in the presence of a base (*t*BuOK, Scheme 3). It was not possible to isolate the



Scheme 3. Synthesis of soluble mono-NHC-complexes.

complexes as pure products and they were used in subsequent reactions as obtained from the reaction mixture. Only **6aRh** was fully characterized and data can be seen in the Supporting Information. The number of signals recorded by using NMR spectroscopy is consistent with a single diastereomer, including a signal at 168.0 ppm in the ^{13}C NMR spectrum, assigned to the rhodium carbene atom, and four other rhodium-coupled doublets assigned to the coordinating cod carbon atoms.

The analogous gold(I) complexes were unstable in solution and decomposed to gold(0) if applied as catalysts.

Catalytic activity

Given the recent successful application of bidentate dioxolane-bis(NHC) ligands in asymmetric hydrogenation,^[7] a preliminary study concerning the catalytic applicability of the new soluble complexes **(4S,5S)-[5Rh, 6Rh, 5Pd, 6Pd]** in the hydrogenation of diethyl itaconate was undertaken. Initial test reactions, using Rh and Pd NHC-dioxolane-amine as soluble precatalysts for the hydrogenation of diethyl 2-R-succinates ($\text{R}=\text{H}$, benzyl-

dene) at 0.4 MPa H_2 and 40 °C, gave high activities and enantioselectivities. The reaction at 40 °C allowed differentiation of the activity between the precatalysts (Table 1). These findings are analogous to those found for the related study using bis(NHC)-dioxolane complexes.

Table 1. Hydrogenation of diethyl 2-R-succinates with soluble mono-NHC catalysts.^[a]

Entry	Catalyst	TOF [h^{-1}]		ee [%] ^[b] benzylidene
		H	benzylidene	
1	5aRh	207	17	99
2	5bRh	164	21	99
3	6aRh	492	20	99
4	6bRh	226	43	99
5	6aPd	293	29	99
6	6bPd	338	30	99
7	bis(NHC) _{Mes} Rh	258	16	99
8	bis(NHC) _{Mes} Pd	45	17	98

[a] Ethanol, 4·10⁵ Pa H_2 , 40 °C, Catalyst: 1 mol %. [b] HPLC (Chiralcel® AD-H, λ : 230 nm, Hexane:*i*PrOH = 98/2, Chiralcel® OD, λ : 250 nm, Hexane:*i*PrOH = 95/5).

The effect of modifying the *N*-substituent of NHC is shown in Table 1, Entries 1–6, indicating that the hydrogenation rate was not very sensitive to changes at this position. As it can be shown in Table 1, the best results were achieved with complexes **6aRh**, **6aRh**, **6aPd**, and **6bPd**, which contain a diisopropylamine moiety, as compared to morpholine derivatives and the corresponding bis(NHC)-dioxolane complexes (Figure 3). These results implied that to functionalize the ligand it might be better to use linear amines rather than cyclical, thus, we could support and increase the activity of the system in one step. Morpholine (Table 1, Entries 1, 2) and diisopropylamine (Table 1, Entries 3–6) substituents on the dioxolane backbone modified the yield, but not the enantioselectivity. All reactions resulted in the predominant formation of the *S*-enantiomer.

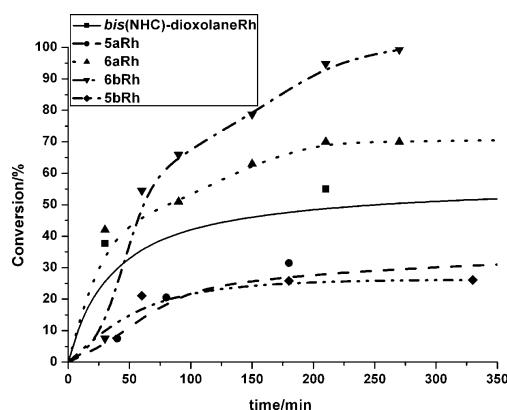


Figure 3. Kinetic profiles for the catalytic activity of Rh reference systems.

The efficiency of gold-, palladium-, and rhodium-supported complexes as catalysts for the asymmetric hydrogenation of diethyl itaconate and (*E*)-diethyl 2-benzylidene succinate was investigated and compared with that recorded using the homogeneous precatalysts (Table 2). The best results were achieved for gold and palladium complexes derived from ligand **4b** and those derived from ligand **4a** for rhodium complexes. All complexes showed significant activities for the hydrogenation of (*E*)-diethyl 2-benzylidene succinate with 99% ee.

Table 2. Hydrogenation of diethyl 2-R-succinates with supported mono-NHC catalysts.^[a]

Entry	Catalyst	R	TOF [h ⁻¹] ^[b]	ee [%] ^[c]
1	4aPd-MCM	H	67	5
2	4aRh-MCM	H	3000	5
3	4aRh-MCM	benzylidene	235	99
4	4bPd-MCM	H	28	5
5	4bPd-MCM	benzylidene	157	99
6	4bAu-MCM	H	1302	5
7	4bAu-MCM	H	17	99
8	4bAu-MCM (four cycles)	benzylidene	40	99

[a] Ethanol, 4·10⁵ Pa H₂, 40 °C, Catalyst: 1 mol%. [b] Enantioselectivity for diethyl itaconate was <10%. [c] HPLC (Chiralcel® AD-H, λ: 230 nm, Hexane/iPrOH = 98:2, Chiralcel® OD, λ: 250 nm, Hexane/iPrOH = 95:5).

Recycling studies using catalysts **4aRh**-, **4aPd**-, and **4bPd**-MCM displayed very similar activities and enantioselectivities after the initial runs, but with **4bAu**-MCM decreasing rates were observed, leading to longer reaction times (48 h). These data may suggest a fractional loss of active Au-species with each successive cycle, possibly because of leaching of gold during the washing steps between cycles or catalyst poisoning. Recycling studies by using solvents other than EtOH displayed similar losses in catalytic activity as using EtOH.

Catalyst deactivation of **4bAu**-MCM proved to be an initial problem during this study. However, it was observed that this could be minimized by treatment of the recovered material with an excess of benzonitrile at 50 °C for 2 h before the washing steps. Treatment with benzonitrile proved to have a positive effect on catalyst stability over several cycles, as seen by overlapping kinetic curves between the first and third cycles after benzonitrile treatment (Figure 4). As a result, all recycle experiments were repeated by using the benzonitrile washing step between cycles (Table 3). At slightly longer times (6 h), very high yields (≥ 97%) could be achieved for MCM catalysts over the three cycles tested, without any apparent deactivation (Figure 5). Initial runs gave similar results as shown in Table 2, and even showed marginally better activity. This increase may result from removal of any residual, non-chiral gold species that remain after the filtration steps, which followed the metallation procedure. Catalyst **4bAu**-MCM displayed very consistent yields and selectivities over four cycles.

The treatment of benzonitrile before the washing steps is thought to stabilize the gold center during the washing procedure. The gold complex must dissociate a benzonitrile ligand

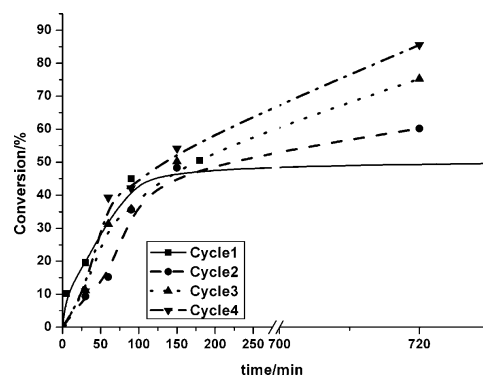


Figure 4. Kinetic profile for the recycling of **4bAu**-heterogenized complex in the hydrogenation of diethyl (*E*)-diethyl 2-benzylidenesuccinate.

Table 3. Recycling experiments for the hydrogenation of (*E*)-diethyl 2-benzylidenesuccinate with supported **4bAu**-MCM catalysts.

Run	TOF [h ⁻¹]	ee [%]
1	17	99
2 (washed with ethanol)	0	–
2 (treated with benzonitrile)	19	99
3 (washed with ethanol)	0	–
3 (treated with benzonitrile)	20	99
4 (washed with ethanol)	0	–
4 (treated with benzonitrile)	40	99

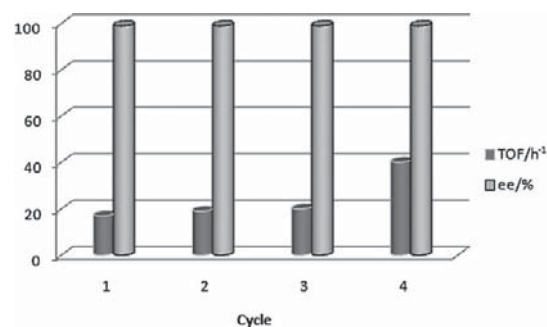


Figure 5. Recycling experiments for the hydrogenation of (*E*)-diethyl 2-benzylidenesuccinate with supported **4bAu**-MCM catalysts treated with benzonitrile after each cycle.

prior to initiation of the catalytic cycle. This vacant coordination site permits the formation of the gold intermediate prior to hydrogen addition across the carbon–carbon double bond of the olefin. After complete consumption of the olefin, a vacant coordination site remains on the gold center. Addition of excess benzonitrile shifts the equilibrium towards binding one benzonitrile ligand, thus stabilizing the Au–carbene complex, and inhibiting leaching of gold metal from the ligand. Elemental analysis data indicated that benzonitrile washing did affect the gold content in the recycled catalysts.

Attempts to assess the changes to the Au-(NHC) catalysts upon recycling through FT-IR analysis proved that a peak from benzonitrile (2229 cm^{-1}) appeared in the FT-IR spectra of complexes before heterogenization (see the Supporting Information, Figure S9, S10). No apparent differences between the fresh and recovered catalysts were observed in the IR spectra. In addition, the other frequencies were only minimally visible, attributable to the low gold loadings on the solid supports compared to the analogous studies of homogeneous complexes.

Conclusions

The immobilization of the chiral gold, palladium, and rhodium (NHC)-dioxolane-amine complexes inside MCM-41 was successfully achieved by covalent grafting. The channel structure was kept and the empty space inside the pores remained large enough to allow for catalysis to occur. Thus, we have proven that there is a simple way to immobilize and recycle chiral cationic (NHC)-gold(III) complexes with a simple washing with benzonitrile. The catalytic activity in asymmetric hydrogenation of these materials was much higher than that of the initial complexes.

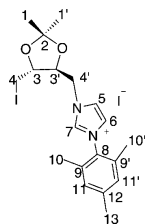
Experimental Section

General Remarks

All preparations of the metal complexes were performed under dinitrogen by using conventional Schlenk-tube techniques. Solvents were carefully degassed before use. C, H, and N analyses were performed by the analytical department of the Institute of Organic Chemistry (C.S.I.C.) by using a Lecco apparatus. Metal contents were analyzed by using atomic absorption using a Perkin-Elmer AAnalyst 300 atomic absorption apparatus and inductively coupled plasma (ICP) by using a Perkin-Elmer OPTIMA 2100 DV. IR spectra were recorded on a Bruker IFS 66v/S spectrophotometer (range $4000\text{--}200\text{ cm}^{-1}$) in KBr pellets. ^1H NMR and ^{13}C NMR spectra were recorded on Varian XR300 and Bruker 200 spectrometers. Chemical shifts were referred to tetramethylsilane (internal standard). Gas chromatography analysis was performed by using a Hewlett-Packard 5890 II. The enantiomeric excess was measured by using HPLC (Agilent 1200). $[\text{AuCl}(\text{tht})]$,^[16] $[\text{PdCl}_2(\text{cod})]$, and $[\text{RhCl}(\text{cod})_2]$ ^[17] were synthesized as described in literature. In the Supporting Information, we show complete experimental data.

Synthesis of NHC-precursors

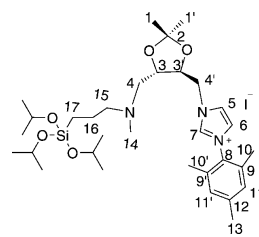
1-(((4*S*,5*R*)-5-(iodomethyl)-2,2-dimethyl-1,3-dioxolan-4-yl)methyl)-3-mesityl-1*H*-imidazol-3-ium iodide (**3a**): A mixture of (4*R*,5*R*)-bis(iodomethyl)-2,2-dimethyl-1,3-dioxolane (**2**) (3 g, 7.8 mmol) and 1-(2,4,6-trimethylphenyl)-1*H*-imidazole (**1a**) (0.96 g, 5.2 mmol) was heated in acetonitrile at 140°C for 48 h. The solvent was removed and the desired product was purified by using flash column chromatography (ethyl acetate/ketone = 2:1) to afford 1.08 g of white powder and recovering 1.71 g of the starting material (**2**).



3a: ^1H NMR (CDCl_3): δ = 9.89 (s; H_7), 7.98 (s; H_5), 7.21 (s; H_6), 7.03 (s, 2H; H_{11} , $\text{H}_{11'}$), 5.48 (dd, 1H; CH_2 , H_4), 4.83 (dd, 1H; CH_2 , H_4), 4.30 (td, 1H; CH , H_3), 3.88 (m, 1H; CH , H_3), 3.74 (dd, 1H; CH_2 , H_4), 3.59 (dd, 1H; CH_2 , H_4), 2.34 (s, 3H; CH_3 , H_{13}), 2.14 (s, 3H; CH_3 , H_{10} or $\text{H}_{10'}$), 2.07 (s, 3H; CH_3 , H_{10} or $\text{H}_{10'}$), 1.45 (s, 3H; CH_3 , H_1 or $\text{H}_{1'}$), 1.43 ppm (s, 3H; CH_3 , H_1 or $\text{H}_{1'}$); ^{13}C NMR (CDCl_3): δ = 141.6 (C_{12}), 137.6 (CH , C_7), 134.3 (C_9 or C_9'), 135.0 (C_9 or C_9'), 130.3 (C_8), 129.9 (CH , C_{11} or $\text{C}_{11'}$), 129.8 (CH , C_{11} or $\text{C}_{11'}$), 124.3 (CH , C_5), 122.8 (CH , C_6), 110.8 (C_2), 78.8 (CH , C_3), 77.3 (CH , C_3), 51.7 (CH_2 , C_4), 27.5 (CH_3 , C_1 or $\text{C}_{1'}$), 27.3 (CH_3 , C_1 or $\text{C}_{1'}$), 21.1 (CH_3 , C_{13}), 18.0 (CH_3 , C_{10} or $\text{C}_{10'}$), 17.7 (CH_3 , C_{10} or $\text{C}_{10'}$), 6.3 ppm (CH_2 , C_4); IR (KBr): $\tilde{\nu}$ = 3115–3056 (C–H), 2984–2931 (C–H), 1606 (=C), 1559–1547 (C=N), 1482–1447 (=C–N), 1204–1163 cm^{-1} (C–N); MS/ES⁺: m/z (%): 442 (34) [$M^+ + 1$], 441 (100) [M^+], 313 (34), 187 (34).

Synthesis of silyloxy precursors

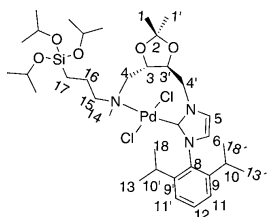
1-(((4*S*,5*S*)-2,2-dimethyl-5-((methyl(3-(triisopropoxysilyl)propyl)amino)methyl)-1,3-(dioxolan-4-yl)methyl)-3-mesityl-1*H*-imidazol-3-ium iodide (**4a**): *N*-methyl-3-(triisopropoxysilyl)propan-1-amine (63.5 mg, 0.229 mmol) and 1-(((4*S*,5*R*)-5-(iodomethyl)-2,2-dimethyl-1,3-dioxolan-4-yl)methyl)-3-mesityl-1*H*-imidazol-3-ium iodide (100 mg, 0.176 mmol) were added to a microwave reactor with 2 mL of acetonitrile and heated at 120°C , 220 W, during 3 h. As the reaction was finished, the solvent was evaporated, 120 mL of chloroform was added, and the product was washed by using aqueous ammonium hydroxide ($3 \times 1\text{ mL}$, 30%). The organic layer was dried over Na_2SO_4 and the solvent evaporated under vacuo. The crude material was washed with ethyl ether, the precipitate filtered, and the solvent was evaporated to afford 63 mg of a yellow oil.



4a: ^1H NMR (CDCl_3): δ = 9.87 (s; H_7), 7.82 (t; H_3), 7.17 (t; H_6), 7.00 (s, 2H; H_{11} , $\text{H}_{11'}$), 5.18 (dd, 1H; CH_2 , $J_{3,4} = 14.8\text{ Hz}$, $J_{4,4'} = 2.20\text{ Hz}$, H_4), 4.82 (dd, 1H; CH_2 , $J_{3,4'} = 14.20\text{ Hz}$, $J_{3,4} = 8.06\text{ Hz}$, H_4), 4.20 (sep, 3H; $J = 6.10\text{ Hz}$, 3C, H_{10}), 4.15–4.10 (m, 1H; H_3), 3.99–3.94 (m, 1H; H_3), 2.84 (dd, 1H; CH_2 , $J_{3,4} = 13.4\text{ Hz}$, $J_{4,4'} = 5.1\text{ Hz}$, H_4), 2.67 (dd, 1H; CH_2 , $J_{3,4} = 13.4\text{ Hz}$, $J_{4,4'} = 6.59\text{ Hz}$, H_4), 2.42–2.46 (m, 2H; CH_2 , H_{15}), 2.33 (s, 3H; CH_3 , H_{13}), 2.31 (s, 3H; CH_3 , H_4), 2.13 (s, 3H; CH_3 , H_{10} or $\text{H}_{10'}$), 2.05 (s, 3H; CH_3 , H_{10} or $\text{H}_{10'}$), 1.60–1.50 (m, 2H; CH_2 , H_{16}), 1.40 (s, 3H; CH_3 , H_1 or $\text{H}_{1'}$), 1.37 (s, 3H; CH_3 , H_1 or $\text{H}_{1'}$), 1.26 (d, 18H; $J = 6.10\text{ Hz}$, 6 CH_3 , H_{10}), 0.54 ppm (m, 2H; CH_2 , H_{17}); ^{13}C NMR (CDCl_3): δ = 141.4 (C_{12}), 138.8 (CH , C_7), 134.4 (C_9 or C_9'), 134.1 (C_9 or C_9'), 130.4 (C_8), 129.9 (CH , C_{11} or $\text{C}_{11'}$), 129.8 (CH , C_{11} or $\text{C}_{11'}$), 123.9 (CH , C_5), 122.6 (CH , C_6), 110.2 (C_2), 78.8 (CH , C_3), 77.2 (CH , C_3), 64.8 (3 CH_{10}), 61.6 (C_{15}), 59.1 (CH_2 , C_4), 52.1 (CH_2 , C_4), 43.0 (C_{14}), 27.2 (2 CH_3 , C_1 , $\text{C}_{1'}$), 25.5 (6 CH_3 , H_{10}), 21.0 (CH_3 , C_{13}), 20.5 (C_{16}), 18.0 (CH_3 , C_{10} or $\text{C}_{10'}$), 17.6 (CH_3 , C_{10} or $\text{C}_{10'}$), 9.5 ppm (C_{17}); IR (KBr): $\tilde{\nu}$ = 2972 (C–H), 2931 (C–H), 1667 (C=N), 1609 (C=N), 1562 (C=N), 1548 (C=N), 1370 (=C–N), 1038 (Si–O), 852 (Si–O–C), 752 (Si–C), 734 cm^{-1} (Si–C); MS/ES⁺: m/z (%): 590 (100) [M^+], 591 (50) [$M^+ + 1$].

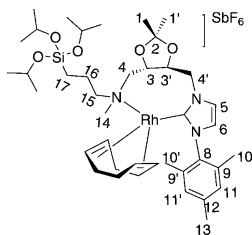
Synthesis of silyloxy-complexes

Pd complexes: Ag₂O (6 mg, 0.028 mmol) was added to a solution of **4a** (40 mg, 0.056 mmol) or **4b** (40 mg, 0.053 mmol) in dichloromethane, and the mixture was stirred at room temperature under a N₂ atmosphere for 24 h. The mixture was filtered through Celite® to remove unreacted Ag₂O and other insoluble material. [PdCl₂(cod)] (21 mg, 0.056 mmol, **4a**, or 20 mg, 0.053 mmol, **4b**) was added to the solution of the resulting silver salt in CH₂Cl₂. After 3 h at room temperature, the mixture was filtered through Celite®. The solvents were removed in vacuum, and the residue was thoroughly washed with diethyl ether and pentane. Several attempts to prepare crystals suitable for X-ray diffraction were unsuccessful.



4aPd: ¹H NMR (CDCl₃): δ = 7.89–7.62 (m; H₅), 7.58–7.44 (m, 4H; 4CH, H₁₂, H₁₁, H₁₁, H₆), 4.56–4.51 (m, 1H; CH₂, H₄), 4.34–4.09 (m, 4H, 1H; CH₂, H₄, 3CH₃, 3.49–4.44 (m, 1H; CH, H₃), 3.09–3.00 (m, 1H; CH, H₃), 2.54–2.48 (m, 1H; CH₂, H₄), 2.40–2.34 (m, 1H; CH₂, H₄), 1.61–1.67 (m, 5H; CH₃, H₁₄, CH₂, H₁₅), 1.54–1.45 (m, 4H; 2CH, H₁₀, H₁₀, CH₂, H₁₆), 1.43 (s, 3H; CH₃, H₁ or H₁), 1.42 (s, 3H; CH₃, H₁ or H₁), 1.25 (d, 18H; 6CH₃, J = 1.9 Hz, CH₃, H₁₆), 1.20 (d, 6H; 2CH₃, J = 5.42 Hz, H₁₃ or H₁₃, H₁₈ or H₁₈), 1.17 (d, 6H; 2CH₃, J = 5.42 Hz, H₁₃ or H₁₃, H₁₈ or H₁₈), 0.69–0.45 ppm (m, 2H; CH₂, H₁₇); ¹³C NMR (CDCl₃): δ = 176.2 (C–Pd, C₇), 147.5 (C₉ or C₉), 146.2 (C₉ or C₉), 132.8 (C₁₂), 132.2 (C₈), 126.3 (2CH, C₁₁, C₁₁), 124.2 (CH, C₅), 124.1 (CH, C₆), 104.1 (C₂), 77.2 (CH, C₃), 76.9 (CH, C₃), 65.8 (3CH₃, 65.4 (C₁₅), 65.2 (CH₂, C₄), 65.0 (CH₂, C₄), 52.0 (C₁₄), 30.9 (2C, C₁₀, C₁₀), 30.3 (CH₃, C₁ or C₁), 30.2 (CH₃, C₁ or C₁), 29.7 (2CH₃, H₁₃ or H₁₃, H₁₈ or H₁₈), 25.7 (2CH₃, H₁₃ or H₁₃, H₁₈ or H₁₈), 25.6 (6CH₃, H₁₆), 15.3 (C₁₆), 9.0 ppm (C₁₇); IR (KBr): ν̄ = 3133 (C–H), 2969, 2918 (C–H), 1458 (=C–N), 1375 (=C–N), 1272 (C–O), 1035 (Si–O–C), 799 (Si–C), 325 cm^{−1} (Pd–Cl); UV/Vis: λ_{max} = 476, 353, 285, 271 nm. ES/MS: m/z (%): 810 [M⁺+1], 633 [M⁺−3O₂Pr]; elemental analysis of C₃₅H₆₁Cl₂N₃O₃PdSi, calcd (%) for [Pd(**4a**)(Cl)₂·2CH₂Cl₂]: C 45.39, H 6.69, N 4.29; found: C 45.42, H 6.58, N 3.69.

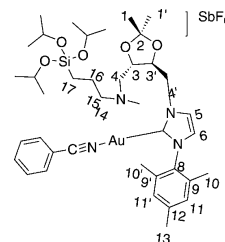
Rh complexes: Ag₂O (6 mg, 0.028 mmol) was added to a solution of **4a** (40 mg, 0.056 mmol) or **4b** (0.053 mmol, 40 mg) in dichloromethane, and the mixture was stirred at room temperature under a N₂ atmosphere for 24 h. The mixture was filtered through Celite® to remove unreacted Ag₂O and other insoluble material. A mixture of [RhCl(cod)]₂ (13.8 mg, 0.028 mmol, **4a**, or 12.8 mg, 0.026 mmol,



4b) and AgSbF₆ (19.2 mg, 0.056 mmol, **4a** or 18.2 mg, 0.053 mmol, **4b**) respectively was added to the solution of the resulting silver salt in THF. After 3 h at room temperature, the mixture was filtered through Celite®. The solvents were removed in vacuum, and the residue thoroughly washed with diethyl ether and pentane. Several attempts to prepare crystals suitable for X-ray diffraction were unsuccessful.

4aRh: ¹H NMR (CDCl₃): δ = 7.49–7.44 (m; H₅), 7.38–7.33 (m; H₆), 7.08 (s, 1H; CH, H₁₁ or H₁₁), 6.75 (s, 1H; CH, H₁₁ or H₁₁), 5.80 (d, 1H; CH₂, J = 12.2 Hz, H₄), 4.78–4.71 (m, 3H, 1H; CH₂, H₄, 2CH₃, 4.54–4.50 (m, 1H; CH, H₃), 4.49–4.36 (m; 2CH₃, 4.33–3.96 (m, 4H, 1H; 3CH₃, CH, H₃), 3.53–3.42 (m, 1H; CH₂, H₄), 3.26–3.05 (m, 1H; CH₂, H₄), 2.76–2.64 (m, 2H; CH₂, H₁₅), 2.38 (s, 3H; CH₃, H₁₃), 2.04–1.96 (m, 11H, 3H; 4CH₂, H₁₀, CH₃, H₁₄), 1.95 (s, 3H; CH₃, H₁₀ or H₁₀), 1.86 (s, 3H; CH₃, H₁₀ or H₁₀), 1.45–1.49 (m, 2H; CH₂, H₁₆), 1.42 (s, 6H; 2CH₃, H₁, H₁), 1.24–1.15 (m, 18H; 6CH₃, H₁₆), 0.60–0.51 ppm (m, 2H; CH₂, H₁₇); ¹³C NMR (CDCl₃): δ = 187.8 (C₇, C–Rh), 139.4 (C₁₂), 138.5 (C₉ or C₉), 136.7 (C₉ or C₉), 134.4 (C₈), 125.5 (2CH, C₁₁, C₁₁), 123.2 (2CH, C₅, C₆), 111.8 (C₂), 97.3 (2CH, H₁₀), 77.2 (CH, C₃), 76.7 (CH, C₃), 69.6 (2CH, H₁₀), 65.1 (C₁₅), 64.4 (3CH₃, 34.1 (CH₂, C₄), 30.78 (C₁₄), 33.7 (CH₂, C₄), 27.1 (4CH₂, H₁₀), 25.5 (2CH₃, C₁, C₁), 25.3 (6CH₃, 21.1 (CH₃, C₁₃), 19.6 (C₁₆), 17.9 (2CH₃, C₁₀, C₁₀), 9.2 (C₁₇); IR (KBr): ν̄ = 3145 (C–H), 2918 (C–H), 2876 (C–H), 1571 (C=N), 1231 (C–O), 1107 (Si–O), 861 (Si–O), 703 (Si–C), 655 (Sb–F); UV/Vis: λ_{max} = 287 nm; MS/ES: m/z (%): 674 [M⁺−3xPr], 464 ppm (L); elemental analysis of C₄₀H₆₇F₆N₃O₃RhSbSi calcd (%) for [Rh(**4a**)(cod)]SbF₆·CH₂Cl₂: C 37.18, H 5.67, N 4.15; found: C 37.60, H 5.22, N 4.59.

Au complexes: Ag₂O (6 mg, 0.028 mmol) was added to a solution of **4a** (40 mg, 0.056 mmol) or **4b** (40 mg, 0.053 mmol) in dichloromethane, and the mixture was stirred at room temperature under a N₂ atmosphere for 24 h. The mixture was filtered through Celite® to remove unreacted Ag₂O and other insoluble material. A mixture of [AuCl(tht)] (18 mg, 0.056 mmol, **4a**, or 17.0 mg, 0.053 mmol, **4b**) and AgSbF₆ (19.2 mg, 0.056 mmol, **4a**, or 18.2 mg, 0.053 mmol, **4b**) was added to the solution of the resulting silver salt in benzonitrile. After 3 h at room temperature, the mixture was filtered through Celite®. The solvents were removed in vacuum, and the residue thoroughly washed with diethyl ether and pentane. Several attempts to prepare crystals suitable for X-ray diffraction were unsuccessful.



4aAu: ¹H NMR (CDCl₃): δ = 7.66–7.55 (m, 2H; 2o-CH, BzN), 7.48–7.38 (m, 3H; p-CH, 2m-CH, BzN), 6.99–6.88 (m, 2H; H₅, H₆), 6.89 (s, 1H; CH, H₁₁ or H₁₁), 6.86 (s, 1H; CH, H₁₁ or H₁₁), 4.74–4.32 (m, 2H; CH₂, H₄), 4.26–4.03 (m, 3H; CH₂, 3.69–3.45 (m, 2H; 2CH, H₃, H₃), 2.92 (d, 1H; CH₂, J = 9.2 Hz, H₄), 2.71 (d, 1H; CH₂, J = 9.2 Hz, H₄), 2.39–2.34 (m, 2H; CH₂, H₁₅), 2.27 (s, 3H; CH₃, H₁₃), 1.98 (s, 3H; CH₃, H₁₄), 1.96 (s, 3H; CH₃, H₁₀ or H₁₀), 1.95 (s, 3H; CH₃, H₁₀ or H₁₀), 1.49–1.47 (m, 2H; CH₂, H₁₆), 1.32 (s, 3H; CH₃, H₁ or H₁), 1.30 (s, 3H; CH₃, H₁ or H₁), 1.15–1.10 (m, 18H; CH₃, H₁₆), 0.84–0.68 ppm (m, 2H; CH₂, H₁₇); ¹³C NMR (CDCl₃): δ = 182.5 (C–Au, C₇), 139.7 (C₁₂), 134.9 (C₉ or C₉), 134.8 (C₉ or C₉), 134.4 (p-CH, BzN), 132.8 (2o-CH, BzN), 132.6 (C₈), 132.2 (2CH, C₁₁, C₁₁), 129.4 (CH, C₅), 129.3 (CH, C₆), 129.1 (2m-CH, BzN), 121.2 (CN, BzN), 112.3 (C–CN, BzN), 111.2 (C₂), 77.80 (CH, C₃), 77.1 (CH, C₃), 68.1 (C₁₅), 66.6 (2CH₂, C₄, C₄), 65.0 (3CH₃, 53.4 (C₁₄), 29.7 (2CH₃, C₁, C₁), 25.6 (6CH₃, H₁₆), 21.2 (CH₃, C₁₃), 21.1 (C₁₆), 17.1 (CH₃, C₁₀ or C₁₀), 14.1 (CH₃, C₁₀ or C₁₀),

10.9 ppm (C_{17}); IR (KBr): $\tilde{\nu}$ = 3155 (C_{Ar} -H), 2979 (C-H), 2918 (C-H), 2229 (CN), 1244, 1216 (C-O-C), 1035 (Si-O), 889 (Si-O-C), 853 (Si-C), 756 (Si-C), 655 cm^{-1} (Sb-F); UV/Vis: λ_{max} = 536, 420, 282, 273 nm; ES/MS: m/z (%): 786 [M^+ -BzN], 972 [M^+ -1+Na].

Synthesis of Heterogenized Complexes

A solution of 10 mg of the corresponding triisopropoxy-complex in CH_2Cl_2 (5 mL) was added to a suspension of the mesoporous solids MCM-41 (100 mg) in toluene (25 mL). The slurry was heated at 110 °C for 16 h. The mixture was cooled, and the solid filtered off and washed thoroughly with ethanol, dichloromethane and diethyl ether.

4a Pd-MCM: Stable white solid. ^{13}C NMR (300 MHz, solid phase, 25 °C, ppm, partial): δ = 140.1 (C_{12}), 135.4 (2C; C_9 , C_9), 132.0–125 (C_8 , 4CH, C_{11} , C_{11} , C_5 , C_6), 112.2 (C_2), 77.4 (CH, C_3), 72.2 (CH, C_3), 61.4 (CH_{ipr}), 58.4 (C_{13}), 55.3 (CH_2 , C_4), 54.0 (CH_2 , C_4), 48.4 (CH_3 , C_{14}), 30.0 ($2CH_3$, C_1 , C_1), 24.8 (CH_3 , H_{ipr}), 18.1–17.0 (5C; CH_3 , C_{13} , C_{16} , CH_3 , C_{10} or C_{10}), 13.3 (CH_3 , C_{10} or C_{10}), 9.5 ppm (C_{17}); IR (KBr): $\tilde{\nu}$ = 1629 (C=C) and (C=N), 1223 (Si-O-Si), 1087 (Si-O-Si), 808 (Si-O-C), 812 (Si-C), 566 cm^{-1} (Pd-C); UV/Vis (solid): λ_{max} = 576, 521, 362, 336, 286, 258, 225 nm; elemental analysis (%): found: C 6.35, H 7.23, N 5.48, Pd 0.37.

4b Rh-MCM: ^{13}C NMR (300 MHz, solid phase, 25 °C): δ = 197.0 (C_7 , C-Rh), 160.0 (C_9 , C_9), 136.0 (br, CH, C_{12} , C_8), 129.9 (2CH, C_{11} , C_{11}), 124.9 (2CH, C_5 , C_6), 110.2 (C_2), 103 (2CH, H_{cod}), 75.6 (CH, C_3), 73.5 (CH, C_3), 70.0 (2CH, H_{cod}), 60.8 (3CH, H_{ipr}), 58.5 (CH_2 , C_{15}), 41.8 (CH_2 , C_4), 37.9 (CH_3 , C_{14}), 32.0 (CH_2 , C_4), 30.0–23.0 (br, $2CH_3$, C_1 , C_1 , 6CH $_3$, H_{ipr} , $2CH_3$, C_{13} or C_{13} , C_{18} or C_{18} , 2CH, C_{10} , C_{10} , 4CH $_2$, H_{cod}), 22.9–8 ppm (br, $2CH_3$, C_{13} or C_{13} , C_{18} or C_{18} , CH_2 , C_{16} , CH_2 , C_{17}). IR (KBr): $\tilde{\nu}$ = 1624 (C=C), 1372 (C=N), 1213 (Si-O-Si), 1091 (Si-O), 799 (Si-O-C), 555 cm^{-1} (Rh-C); UV/Vis (solid): λ_{max} = 512, 363, 337, 288, 257, 219 nm; elemental analysis (%): found: C 4.83, H 2.42, N 0.19, Rh 0.01.

4a Au-MCM: Stable white solid. ^{13}C NMR (300 MHz, solid phase, 25 °C): δ = 179.0 (C-Au, C_7), 137.0 (C_{12}), 135.0 (br, C_9 , C_9 , p -CH, 2O-CH, BzN, C_8 , 2CH; 2C, C_{11} , C_{11}), 129.6 (br, 2CH, C_5 , C_6 , 2m-CH, BzN), 122.5 (CN, BzN), 111.3 (br, C-CN, BzN, C_3), 78.3 (br, 2CH, C_3 , C_3), 72.0 (CH_2 , C_{13}), 59.9 ($2CH_2$, C_4 , C_4), 58.2 (CH_{ipr}), 58.8 (CH_3 , C_{14}), 25.3 (br, $2CH_3$, C_1 , C_1 and CH_3 , H_{ipr}), 18.7 (br, CH_3 , C_{13} , CH_2 , C_{16} , CH_3 , C_{10} or C_{10}), 13.4 (CH_3 , C_{10} or C_{10}), 8.0 ppm (C_{17}); IR (KBr): $\tilde{\nu}$ = 1632 (C=C) and (C=N), 1209 (C-O-C), 1086 (Si-O), 802 cm^{-1} (Si-C); UV/Vis (solid): λ_{max} = 493, 357, 290, 248, 223 nm; elemental analysis (%): found: C 4.59, H 5.37, N 0.48, Au 1.6.

Catalytic activity

The catalytic properties, in hydrogenation reactions of alkenes, of the complexes were examined under conventional conditions for batch reactions in a reactor (Autoclave Engineers) of 100 mL capacity at 40 °C temperature, 4×10^5 Pa dihydrogen pressure and a 1/1000 metal:substrate molar ratio. The evolution of the reaction of hydrogenated product was monitored by using gas-chromatography. The enantiomeric excess was measured by using HPLC equipped with chiral columns Chiralcel® OD [diethyl 2-benzylidene succinate], λ : 250 nm, Hexane: i PrOH = 95/5, 0.5 mL min^{-1} flow rate, and Chiralcel® AD-H [diethyl itaconate], λ : 230 nm, Hexane: i PrOH = 98/2, 0.4 mL min^{-1} flow rate.

Acknowledgements

The authors thank the Dirección General de Investigación Científica y Técnica of Spain (Project MAT2006-14274-C02-02) and Con-

solider Ingenio 2010-MULTICAT. G.V.C. thanks MCINN for financial support.

Keywords: carbene ligands • hydrogenation • heterogeneous catalysis • immobilization • supported catalysts

- [1] For monographs, see a) F. Glorius in *N-Heterocyclic Carbenes (NHC) in Transition Metal Catalysis (Topics in Organometallic Chemistry)*, (Ed.: F. Glorius) Springer, Berlin, **2006**; b) S. P. Nolan in *N-Heterocyclic Carbenes in Synthesis*, (Ed.: S. P. Nolan) Wiley-VCH, Weinheim, **2006**.
- [2] For general reviews on NHCs, see: a) D. Bourissou, O. Guerret, F. P. Gabbaï, G. Bertrand, *Chem. Rev.* **2000**, *100*, 39–92; b) F. E. Hahn, M. C. Jahnke, *Angew. Chem.* **2008**, *120*, 3166–3216, *Angew. Chem. Int. Ed.* **2008**, *47*, 3122–3172; c) V. Nair, V. Sreekumar, *Angew. Chem.* **2004**, *116*, 5240–5245; *Angew. Chem. Int. Ed.* **2004**, *43*, 5130–5135; d) N. Marion, S. Díez-González, S. P. Nolan, *Angew. Chem.* **2007**, *119*, 3046–3058, *Angew. Chem. Int. Ed.* **2007**, *46*, 2988–3000; e) P. de Frémont, N. Marion, S. P. Nolan, *Coord. Chem. Rev.* **2009**, *253*, 862–892; f) O. Schuster, L. Yang, H. G. Raubenheimer, M. Albrecht, *Chem. Rev.* **2009**, *109*, 3445–3478.
- [3] L. Cavallo, A. Correa, C. Costabile, H. Jacobsen, *J. Organomet. Chem.* **2005**, *690*, 5407–5413.
- [4] a) W. A. Herrmann, *Angew. Chem.* **2002**, *114*, 1342–1363, *Angew. Chem. Int. Ed.* **2002**, *41*, 1290–1309; application of NHCs in olefin metathesis: b) Y. Schrodi, R. L. Pederson, *Aldrichimica Acta* **2007**, *40*, 45–52.
- [5] For phosphine-functionalized NHCs see, for example: a) A. A. Danopoulos, N. Tsoureas, S. A. Macgregor, C. Smith, *Organometallics* **2007**, *26*, 253–263, and references therein; b) N. Stylianides, A. A. Danopoulos, N. Tsoureas, *J. Organomet. Chem.* **2005**, *690*, 5948–5958; c) A. A. Danopoulos, S. Winston, T. Gelbrich, M. B. Hursthouse, R. P. Toozee, *Chem. Commun.* **2002**, 482–483; d) C. C. Lee, W. C. Ke, K. T. Chan, C. L. Lai, C. H. Hu, H. M. Lee, *Chem. Eur. J.* **2007**, *13*, 582–591, and references therein; e) F. E. Hahn, M. C. Jahnke, T. Pape, *Organometallics* **2006**, *25*, 5927–5936, and references therein; f) O. Kaufhold, A. Stasch, P. G. Edwards, F. E. Hahn, *Chem. Commun.* **2007**, 1822–1824; g) S. Nanchen, A. Pfaltz, *Helv. Chim. Acta* **2006**, *89*, 1559–1573; h) J. Zhong, J. H. Xie, A. E. Wang, W. Zhang, Q. L. Zhou, *Synlett* **2006**, 1193–1196 and references therein; i) L. D. Field, B. A. Messerle, K. Q. Vuong, P. Turner, *Organometallics* **2005**, *24*, 4241–4250; j) E. Bappert, G. Helmchen, *Synlett* **2004**, 1789–1793; k) T. Focken, G. Raabe, C. Bolm, *Tetrahedron: Asymmetry* **2004**, *15*, 1693–1706; l) H. Lang, J. J. Vittal, P. H. Leung, *J. Chem. Soc. Dalton Trans.* **1998**, 2109–2110; m) W. A. Herrmann, C. Kocher, L. J. Goßboen, G. R. J. Artus, *Chem. Eur. J.* **1996**, *2*, 1627–1636; other donor functions: n) H. V. Huynh, C. H. Yeo, G. K. Tan, *Chem. Commun.* **2006**, 3833–3835; o) M. Poyatos, A. Maise-Francois, S. Bellemin-Lapponnaz, L. H. Gade, *Organometallics* **2006**, *25*, 2634–2641; p) P. L. Arnold, M. Rodden, C. Wilson, *Chem. Commun.* **2005**, 1743–1745.
- [6] a) M. C. Perry, K. Burgess, *Tetrahedron: Asymmetry* **2003**, *14*, 951–961; b) V. César, S. Bellemin-Lapponnaz, L. H. Gade, *Chem. Soc. Rev.* **2004**, *33*, 619–636.
- [7] A. Aranz, C. González-Arellano, A. Juan, G. Villaverde, A. Corma, M. Iglesias, F. Sánchez, *Chem. Commun.* **2010**, 46, 3001–3003.
- [8] a) A. Corma, M. Iglesias, C. del Pino, F. Sánchez, *Chem. Commun.* **1991**, 1253–1255; b) A. Corma, M. Iglesias, M. V. Martín, J. Rubio, F. Sánchez, *Tetrahedron: Asymmetry* **1992**, *3*, 845–848; c) A. Corma, A. Fuerte, M. Iglesias, F. Sánchez, *J. Mol. Catal. A: Chem.* **1996**, *107*, 225–234, and references therein; d) M. J. Alcón, A. Corma, M. Iglesias, F. Sánchez, *J. Mol. Catal. A: Chem.* **2003**, *194*, 137–152; e) A. Corma, E. Gutiérrez-Puebla, M. Iglesias, A. Monge, S. Pérez-Ferreras, F. Sánchez, *Adv. Synth. Catal.* **2006**, *348*, 1899–1907; f) A. Corma, C. González-Arellano, M. Iglesias, S. Pérez-Ferreras, F. Sánchez, *Synlett* **2007**, 1771–1774; g) C. González-Arellano, A. Corma, M. Iglesias, F. Sánchez, *Adv. Synth. Catal.* **2004**, *346*, 1316–1328.
- [9] a) M. Carmack, C. J. Kelley, *J. Org. Chem.* **1968**, *33*, 2171–2173; b) K. Uchida, K. Kato, H. Akita, *Synthesis* **1999**, 1678–1686; c) L. J. Rubin, H. A. Lardy, H. O. L. Fischer, *J. Am. Chem. Soc.* **1952**, *74*, 425–428.
- [10] J. Liu, J. Chen, J. Zhao, Y. Zhao, L. Li, H. Zhang, *Synthesis* **2003**, *17*, 2661–2666.

- [11] a) C. Boehme, G. Frenking, *Organometallics* **1998**, *17*, 5801–5809; b) D. Nemcsok, K. Wichmann, G. Frenking, *Organometallics* **2004**, *23*, 3640–3646.
- [12] a) H. M. J. Wang, I. J. B. Lin, *Organometallics* **1998**, *17*, 972–975; b) I. J. B. Lin, C. S. Vasam, *Coord. Chem. Rev.* **2007**, *251*, 642–670; c) J. C. Y. Lin, R. T. W. Huang, C. S. Lee, A. Bhattacharyya, W. S. Hwang, I. J. B. Lin, *Chem. Rev.* **2009**, *109*, 3561–3598.
- [13] a) I. Dinarès, C. García de Miguel, M. Font-Bardia, X. Solans, E. Alcalde, *Organometallics* **2007**, *26*, 5125–5128; b) J. Houghton, G. Dyson, R. E. Douthwaite, A. C. Whitwood, B. M. Kariuki, *Dalton Trans.* **2007**, 3065–3073; c) F. Hannig, G. Kehr, R. Fröhlich, G. Erker, *J. Organomet. Chem.* **2005**, *690*, 5959–5972; d) B. P. Morgan, G. A. Galdamez, R. J. Gilliard Jr., R. C. Smith, *Dalton Trans.* **2009**, 2020–2028.
- [14] a) B. Marler, U. Oberhagemann, S. Vortmann, H. Gies, *Microporous Mater.* **1996**, *6*, 375–383; b) W. Hammond, E. Prouzet, S. D. Mahanti, T. J. Pinna-vaia, *Microporous Mesoporous Mater.* **1999**, *27*, 19–25.
- [15] M. Vasconcellos-Dias, C. D. Nunes, P. D. Vaz, P. Ferreira, M. J. Calhorda, *Eur. J. Inorg. Chem.* **2007**, 2917–2925.
- [16] D. Drew, J. R. Doyle, A. G. Shaver, *Inorg. Synth.* **1972**, *13*, 47–55.
- [17] G. Giordano, R. H. Crabtree, *Inorg. Synth.* **1990**, *28*, 88–90.

Received: April 4, 2011

Published online on June 20, 2011

Cite this: DOI: 10.1039/c1dt10597c

www.rsc.org/dalton

PAPER

Development of homogeneous and heterogenized rhodium(I) and palladium(II) complexes with ligands based on a chiral proton sponge building block and their application as catalysts†

Gonzalo Villaverde,^{a,b} Avelina Arnanz,^a Marta Iglesias,^{**a} Angeles Monge,^a Félix Sánchez^{*b} and Natalia Snejko^a

Received 7th April 2011, Accepted 9th June 2011

DOI: 10.1039/c1dt10597c

Chiral compounds prepared from proton sponge building block

8-((2*R*,5*R*)-2,5-dimethylpyrrolidin-1-yl)naphthalen-1-amine were found to be effective chiral ligands for obtaining complexes of rhodium(I) and palladium(II) by reaction with [RhCl(cod)]₂, PdCl₂(cod) or Pd(OAc)₂. The complexes bearing triethoxysilane groups were immobilized on mesoporous MCM-41 in order to obtain new heterogeneous catalysts. Both materials are active in the hydrogenation of alkenes and could be recycled without loss of activity or enantioselectivity.

Introduction

Heterogenization of homogeneous single-site catalysts on solid support materials allows combination of the superior activity and selectivity of homogeneous with the simple recovery of heterogeneous catalyst. Heterogenized catalysts can also be used in fixed- or flow-bed reactors, which additionally simplify process development. Therefore, such systems have been extensively studied during the past two decades.¹

Active centers may be immobilized in several ways, depending on the binding between active center and support. The family of the silicon based porous MCM materials,² led to new paths for the reaction between suitable precursors with the Si–OH groups in the internal walls of the large surface of the hexagonally ordered parallel channels. The applications of the resulting inorganic materials containing active sites are important in different fields, ranging from catalysis to optoelectronics.^{1,3} Typical approaches for such reactions include direct grafting, where a functionalized complex reacts with the OH groups, or tethering where a step by step route is followed, starting by reaction between the walls and a functionalized organic molecule (ligand) which then binds the metal center.⁴

1,8-bis(dimethylamino)naphthalene (**1**) introduced by Alder⁵ and sold by Aldrich as “Proton Sponge®” it is not only the best-known compound of its type but is inexpensive and straight-

forward to derivatise. While **1** has a high affinity towards H⁺, it is indifferent to other electrophiles, which is in contrast to usual nitrogen bases. Some examples of reactivity of **1** apart from routine protonation include, somewhat surprisingly, its role as a hydride donor in its reaction with *mer*-RhCl₃(dmo)₃ or [RuCl(dppb)]₂(**1**-Cl)₃,⁶ with fluoroalkyl complexes of iridium,⁷ or with B(C₆F₅)₃,⁸ to form the 1,1,3-trimethyl-2,3-dihydroperimidinium cation (TMP⁺). There is also a single example of a metal complex coordinating (directly) to **1**, (*via* the amino groups); the reaction with Pd(hfac)₂ (hfac: hexafluoroacetylacetonate) immediately generates a poorly-characterized charge-transfer product, which after standing for a week forms the cationic complex [Pd(hfac)(**1**)]⁺.⁹ The hfac ligand may be substituted for β-diketones and one of these complexes was structurally characterized; coordination causes severe distortion of the proton sponge, the N⋯N distance opening to 2.94 Å from 2.51 Å. The proton sponge ligand is easily displaced in this complex, even by water. **1** can also act as a weak carbon nucleophile, but only in the presence of exceptionally reactive electrophiles.¹⁰ Other examples for proton sponges include 4,9-dichloroquinoline[7,8-*h*]quinoline (**2**),¹¹ 1,8-bis(*N,N,N*-tetramethylguanidino)naphthalene (**3**)¹² and chiral, atropisomeric, binaphthyl substituted 1,8-bis(dimethylamino)naphthalene derivatives (**4**) in the racemic as well as enantiopure states.¹³ Recently, the transition metal complexes of the proton sponge **2**¹⁴ and **3**¹⁵ were reported.

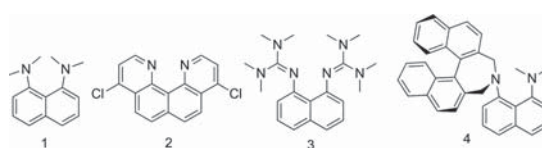


Chart 1

^aInstituto de Ciencia de Materiales de Madrid, CSIC, C/Sor Juana Inés de la Cruz 3, Cantoblanco, 28049, Madrid, Spain. E-mail: marta.iglesias@icmm.csic.es; Fax: (+)34(91)3720623; Tel: (+)34(91)3349000

^bInstituto de Química Orgánica General, CSIC, C/Juan de la Cierva, 3, 28006, Madrid, Spain. E-mail: felix-igo@iqog.csic.es; Fax: (+)34(91)5644853; Tel: 34(91)2587590

† Electronic supplementary information (ESI) available: Compound characterization data, including images of ¹³C NMR spectra, kinetic curves, HPLC traces and crystallographic data (CIF). CCDC reference numbers 805292–805293. For ESI and crystallographic data in CIF or other electronic format see DOI: 10.1039/c1dt10597c

Several years ago, the formation of a diaminoacetal was reported by condensation of 1,8-diaminonaphthalene with the chromium tricarbonyl complex of benzaldehyde¹⁶ and the synthesis of a Pd complex with a pincer ligand obtained *via* a condensation of isophthalic dicarboxaldehyde and 2 equiv. of 1,8-diaminonaphthalene.¹⁷ The aim of this study is to gain insight into the effects of the ligand properties such as the rigidity or flexibility of chiral chelating ligands and the influence of donor atoms in determining the asymmetric induction in the catalytic process. Specifically, to establish the relation between regioselectivity, induced by chiral chelate ligands in the catalytic process to involve each conformational isomer in the solution, and the enantiomeric excess of the product. We believe that the potential of this chiral building block to influence asymmetric transformations should be investigated. As part of an ongoing project on the design and synthesis of ligands for asymmetric catalytic reactions, we developed a modular synthetic strategy for preparing new ligands based on 8-((*2R,5R*)-2,5-dimethylpyrrolidin-1-yl)naphthalen-1-amine (type (*R,R*)-A or type (*R,R*)-B in Fig. 1). Nitrogen atoms from pyridine, amine or imine moieties are different electronically and are assumed to provide different binding properties to transition metals. Although pyridine is a strong electron-donating ligand, the delocalized π -system provides a tool for tuning the electronic nature of this moiety with substituents. While the different donor abilities of the pyridine, phenol, amine or imine groups can serve as an electronic differentiator for transition metal-catalyzed asymmetric reactions, the *trans*-2,5-disubstituted pyrrolidine moiety can provide a chiral influence for asymmetric discrimination on prochiral substrates.

Recently, we have shown that complexes with anionic linear Schiff ligands (Chart 2, (a)) have excellent catalytic activity in several reactions.¹⁸ On the other hand, we have also developed a series of novel conformationally restricted ONN-Pincer-type ligands (Chart 2, (b)) resembling coordination environments present in Schiff-base ligands.¹⁹ To study the scope and efficiency of these systems, we modified the substituents on the pyridine ring or on the imine group to create different electronic properties. Herein we report the syntheses, characterization and reactivity of rhodium and palladium complexes with chiral perimidine (*R,R*)-5, (*R,R*)-6 (Fig. 1, type A), and imino derivatives (*R,R*)-7, and (*R,R*)-8 (Fig. 1, type B). These compounds were obtained *via* condensation of an aldehyde and the chiral building block (proton sponge precursor) 8-((*2R,5R*)-2,5-dimethylpyrrolidin-1-yl)naphthalen-1-amine that exhibit unusual structures and interesting reactivity. These complexes and their respective heterogenized complexes on MCM-41 were shown to be effective catalysts for enantioselective hydrogenation.

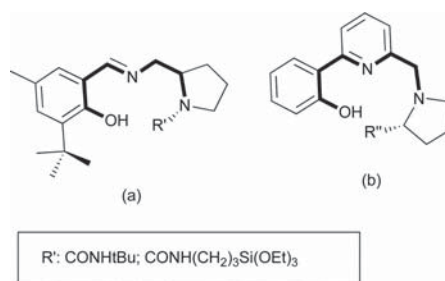


Chart 2

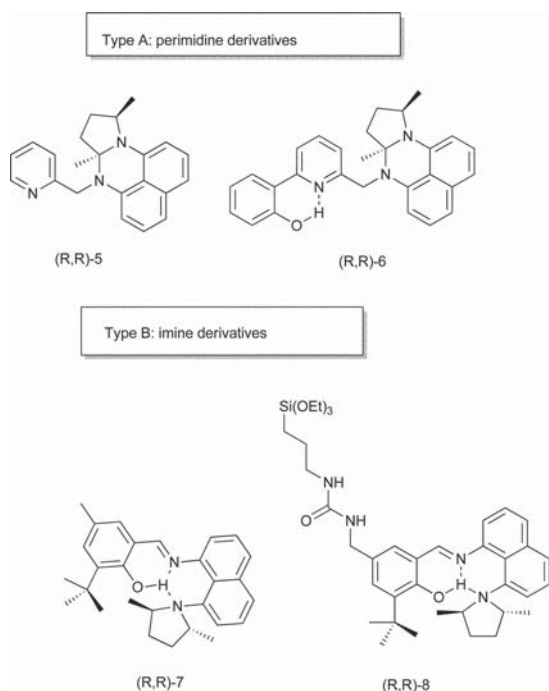


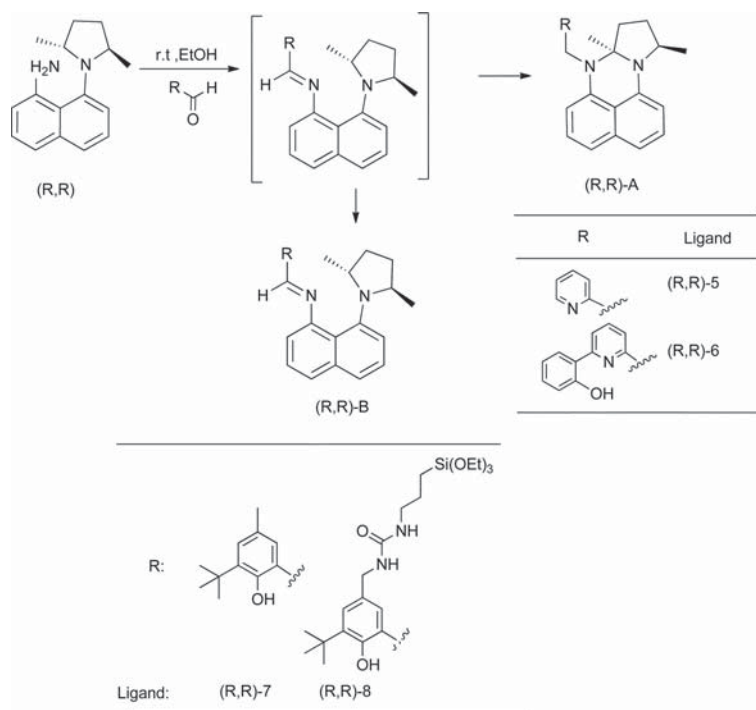
Fig. 1 Chiral perimidine and imine ligands.

Results and discussion

Synthesis of ligands from 8-((*2R,5R*)-2,5-dimethylpyrrolidin-1-yl)naphthalen-1-amine

Several groups²⁰ including those of Alder,²¹ Staab,²² Pozharskii²³ and Lloyd-Jones²⁴ have investigated and derivatized the proton sponge 1,8-bis(dimethylamino)naphthalene. We have used 8-((*2R,5R*)-2,5-dimethylpyrrolidin-1-yl)naphthalen-1-amine as a precursor to obtain new chiral ligands. This precursor has been derivatized by reaction with different aldehydes in order to obtain pincer-type ligands containing such functionality. Treatment of different aldehydes (depicted in Scheme 1) with 8-((*2R,5R*)-2,5-dimethylpyrrolidin-1-yl)naphthalen-1-amine, in ethanol at room temperature in the presence of molecular sieves (4 Å), gave compounds of type (*R,R*)-A or (*R,R*)-B (Scheme 1) in moderate to good yield (40–70%). All new compounds have been characterized by ¹H NMR, ¹³C NMR, FTIR spectroscopy and ESI mass spectrometry (see experimental).

Initially, we expected an imino compound as a product in all cases. However, the ¹H-NMR spectra of type (*R,R*)-A compounds obtained from pyridine-2-carbaldehyde and 6-(2-hydroxyphenyl)pyridine-2-carbaldehyde did not match with the NMR spectra of the expected imino compounds, as we could see the signals of diastereotopic CH₂-N groups as ABXY system at δ 4.82, 4.57 ((*R,R*)-5), and 4.70, 4.45 ((*R,R*)-6) ppm. Thus, we suspected that the products type (*R,R*)-A were not imino compounds.



Scheme 1 Condensation products of 8-((2*R*,5*R*)-2,5-dimethylpyrrolidin-1-yl)naphthalen-1-amine with different aldehydes.

Single crystal X-ray diffraction studies have been performed on **(R,R)-6**. Fig. 2 shows the molecular structure with the atomic numbering. Crystal data and structure refinement details of **(R,R)-6** are given in Table S1.[†] Each structure consists of a central pyridine ring that is substituted at its 2-position by a phenol group and at its 6-position by an amine-containing CH₂-(7*aR*,10*R*)-7*a*,10-dimethyl-7*a*,8,9,10-tetrahydro-7*H*-pyrrolo[1,2-*a*]perimidine unit. The amine group is inclined essentially orthogonal to the plane of the adjacent pyridyl unit. The phenol moieties are almost co-planar with respect to the pyridine unit [tors.: C(17)–C(16)–C(15)–N(3) –4.7 (3)] and are disposed mutually *cis* as a result of a hydrogen bonding interaction between the phenol hydrogen atom and the neighboring pyridine nitrogen [N(3)–H(1) 1.852(2)

Å; O(1)–N(3) 2.576(2) Å]. The *ipso* carbons, C(1) and C(7), deviate slightly from the naphthalene plane 0.032(6) and 0.081(6) Å, respectively. The torsion angle between C(7)–N(2) and C(1)–N(4) is 7.0 (2)°. The N(1)–N(2) distance (2.378(3) Å) is shorter than an idealized value, 2.51 Å. This distortion of N::N could come from the stress caused by the cyclisation. When we use **5** and **6** as chiral chelate ligands, the nitrogen atom N(1) is not in the direction of metal atom and the metal is far away. Thus, **5** and **6** act as chiral N,N or N,N,O ligands, not as N,N,N- or N,N,N,O ligand. The mass spectra of **6** reveal protonated molecular ion peak.

Treatment of 3-*tert*-butyl-2-hydroxy-5-methylbenzaldehyde or *N*-(3-*tert*-butyl-5-formyl-4-hydroxyphenyl)carbamoyl-4-(triethoxysilyl)butanamide and 8-[(2*R*,5*R*)-2,5-dimethylpyrrolidin-1-yl]naphthalen-1-amine in ethanol gave **(R,R)-7** and, **(R,R)-8**, imino ligands (type **(R,R)-B**), as yellow oils in good yields. Mass spectrum of **(R,R)-7** reveals protonated molecular ion peak while in their IR spectra absorption bands characteristic for their imino functionalities (*ca.* 1618 cm^{−1}) are evident. In their ¹H NMR spectra, the imine compounds gave a singlet at δ 8.26 (**(R,R)-7**), 8.32 (**(R,R)-8**) consistent with the presence of CH=N protons, phenol hydrogen atom appears at low field, as a broad singlet at δ 13.86 ppm (**(R,R)-7**), 14.11 ppm (**(R,R)-8**), these values suggest that the proton is coordinate between the two nitrogen atoms and the oxygen atom is inside the structure, stabilizing the imino compounds and prevent the cyclization.

To support the spectroscopic data, crystals of **(R,R)-7** have been the subject of single crystal X-ray diffraction studies. A perspective view is depicted in Fig. 3; crystal data and structure refinement

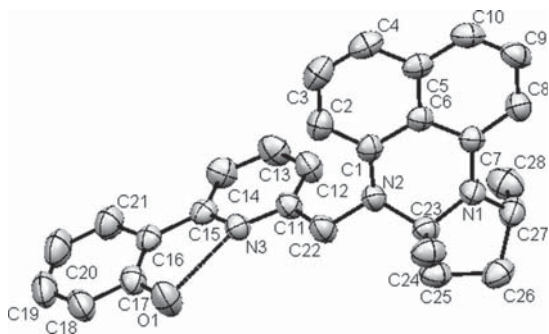
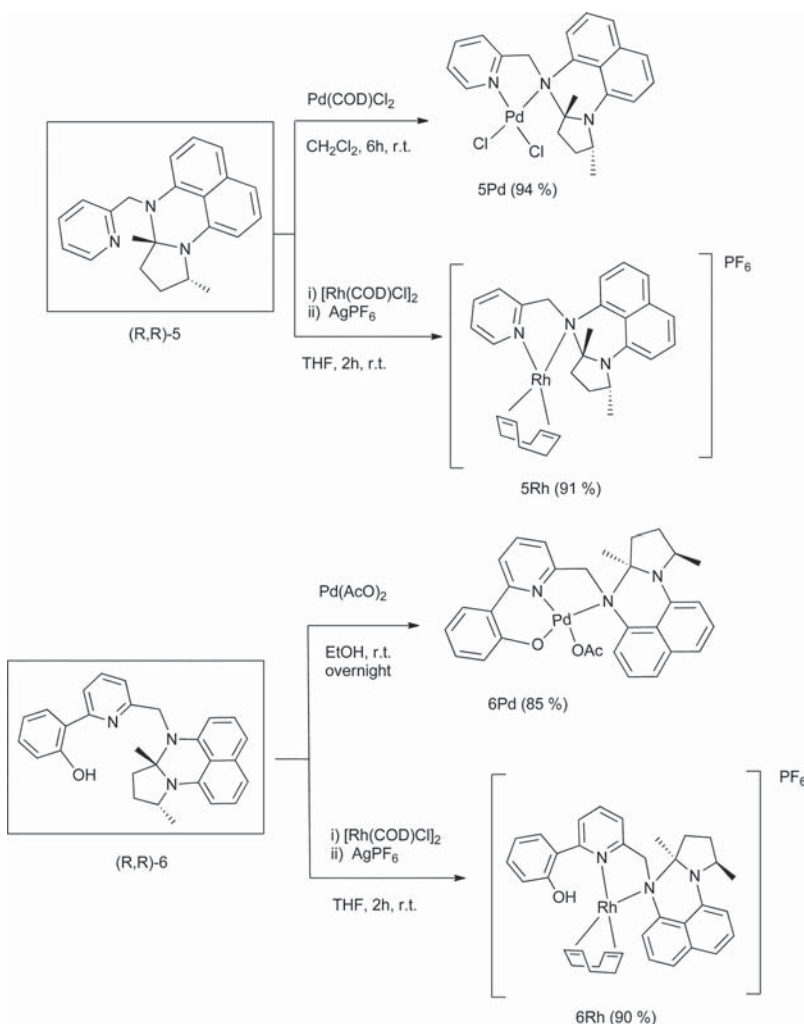


Fig. 2 Molecular structure of **(R,R)-6**.



Scheme 2 Synthesis of perimidine-complexes.

details of **(R,R)-7** are given in Table S2.† The di amine group is inclined essentially orthogonal to the plane of the phenol unit (46.80°). There is a hydrogen bonding interaction between the phenol hydrogen atom, the neighboring imine nitrogen [N(2)–H(1) 1.850(3) Å; O(1)–N(2) 2.591(3) Å] and the amine group [N(1)–N(2) 2.756 Å; N(1)–H(1) 2.940(3) Å]. The *ipso* carbons, C(1) and C(3), deviate slightly from the naphthalene plane 0.110 and 0.021 Å, respectively. The torsion angle between C(1)–N(1) and C(3)–N(2) is $-13.4(2)^\circ$. In this case the N(1)–N(2) distance (2.756(4) Å) is larger than an idealized value, 2.51 Å. The stereochemistry of **(R,R)-7** is the same as that of 8-((2*R*,5*R*)-2,5-dimethylpyrrolidin-1-yl)naphthalen-1-amine, as expected, **(R,R)-7** and **(R,R)-8** act as tridentate ligands when coordinated to metals.

In both families, the absolute configuration of asymmetric carbons is maintained throughout the process; starting from a configuration *R* we obtain a configuration *R*.

Synthesis of rhodium and palladium complexes

Several complexes incorporating **(R,R)-5**, **(R,R)-6**, **(R,R)-7**, and **(R,R)-8** as ligands were prepared by standard methods (Schemes 2, 3).

The reactions of **(R,R)-5** and **(R,R)-6** with [Pd(cod)Cl₂] or Pd(OAc)₂ were carried out at room temperature in CH₂Cl₂ or EtOH solution in a 1 : 1 complex : ligand ratio. The products, [Pd(L*)X], **5Pd**, **6Pd** (L* = **(R,R)-5**, X = Cl₂; **(R,R)-6**, X = OAc), were obtained in almost quantitative yields as stable brown solids by careful precipitation from pentane; which later underwent elemental analysis, ESI-MS and ¹H-¹³C NMR spectroscopy. Thus, the ESI-MS spectra of **5Pd** and **6Pd** show the peaks from the fragments due to elimination of the ion chloride [M⁺ - Cl] (471.3 for **5Pd**) or acetate [M⁺ - OAc] (585.5 for **6Pd**). All assignments were confirmed by good agreement between the observed and calculated isotopic distributions. The absence of the ν(OH) band

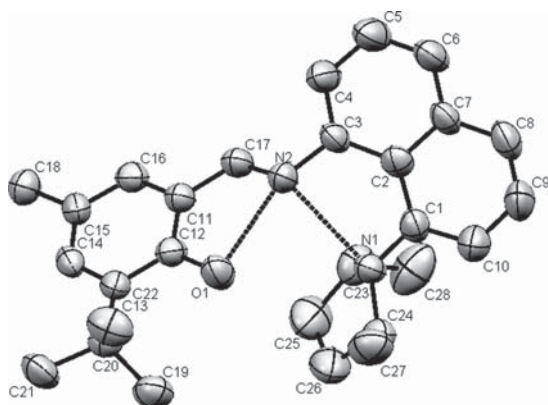
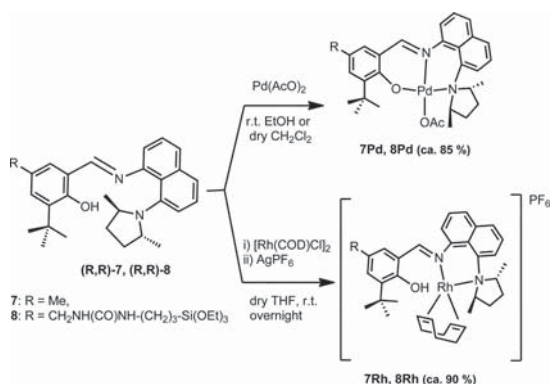


Fig. 3 Molecular structure of (R,R)-7.



Scheme 3 Synthesis of imino-complexes.

(present in the spectra of the free ligand **6** at $\sim 3430\text{ cm}^{-1}$) is in accordance with loss of the -OH proton. The IR spectrum of **6Pd** also shows strong bands at 1290 and $\sim 1600\text{ cm}^{-1}$ assigned to the symmetric and asymmetric $\nu(\text{COO})$ vibrations, respectively, in agreement with those expected for monocoordinate acetate ligands.²⁵ New bands at 555 cm^{-1} are ascribed to $\nu(\text{Pd-O})$ (**6Pd**).

Diamagnetic palladium complexes have been characterized by ^1H and ^{13}C NMR spectroscopies. All assignments are based on several correlations in the 2D spectra. They are fully consistent with the structures depicted in Scheme 2. In all cases, the spectra show the simultaneous occurrence of two sets of signals which are attributable on the one hand to the substituted pyridine entity and on the other hand to the amine sponge derivative part of the ligand. In the ^1H NMR spectra all the resonances were high field shifted as compared to the uncoordinated ligand and they were in agreement with metallation of the ligand with coordination of the metal atom *via* the pyridine nitrogen atom. Deprotonation of the -OH group was confirmed by the absence of OH resonance in the ^1H spectrum. The ^1H NMR spectrum shows the signal of the MeCOO protons as a singlet at $\delta = 1.88\text{ ppm}$ (**6Pd**). The ^{13}C NMR spectrum of **6Pd** showed the signals assigned to the OAc group.

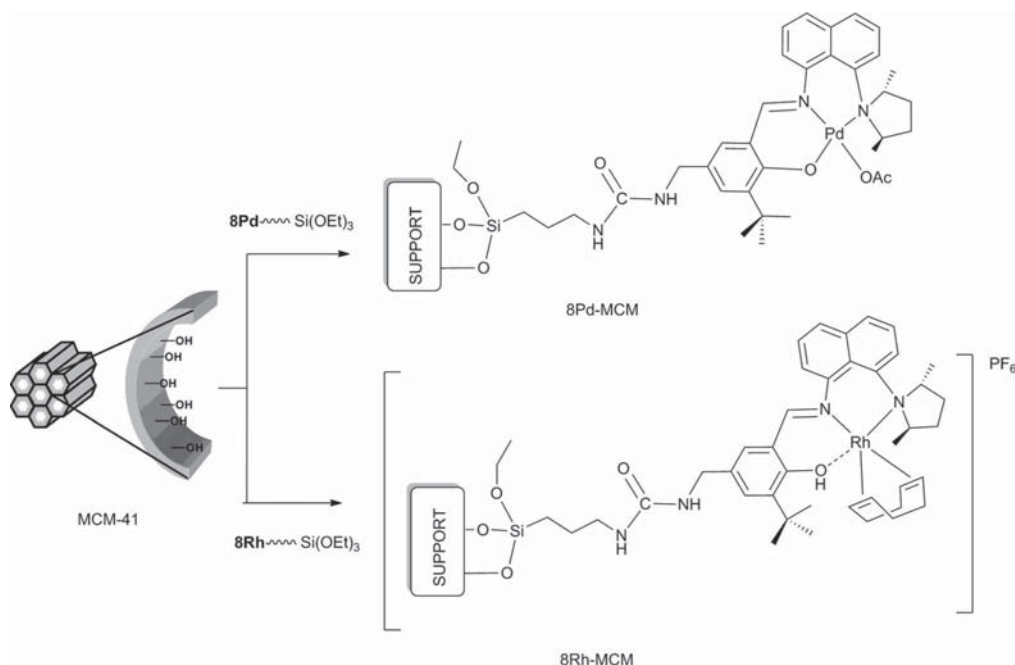
The cationic complexes, $[\text{Rh}(\text{cod})(\text{L}^*)]\text{PF}_6$, (**5Rh**, **6Rh**) ($\text{L}^* = (\text{R},\text{R})\text{-5}$, $(\text{R},\text{R})\text{-6}$), were synthesized by the reaction of $[\text{RhCl}(\text{cod})]_2$ with a stoichiometric amount of solid AgPF_6 and, subsequently

after 1 h the corresponding L^* -chiral ligand, in THF solution. Filtration through Celite and evaporation of the solvent yielded a solid product, which was recrystallized by careful addition of diethyl ether. The experimental data allowed us to establish that both $(\text{R},\text{R})\text{-5}$ and $(\text{R},\text{R})\text{-6}$ ligand act, in the formation of complexes, as chelating ligands. In the ^1H NMR spectra the cyclooctadiene resonances are observed as four broad lines between 1.8 and 4.8 ppm due to fluxionality in the conformation of the cyclooctadiene chelate. Complexes exhibit four signals in their ^{13}C spectra attributable to the carbon atoms of the cod ligand. Elemental analysis and the ESI-MS spectra (540.3 for **5Rh** and 632.3 for **6Rh** corresponding to $[\text{M}^+ - \text{PF}_6]$) are consistent with the proposed formulation shown in Scheme 2, but a single crystal structure has not yet to be obtained. The -OH group deprotonation was not observed for rhodium complex with ligand **6**, the infrared spectrum presents a signal corresponding to $\nu(\text{OH})$ at 3443 cm^{-1} .

The reactions between the imino compounds $(\text{R},\text{R})\text{-7}$ or $(\text{R},\text{R})\text{-8}$ with $\text{Pd}(\text{OAc})_2$ were carried out at room temperature in EtOH solution, respectively, in a $1:1$ complex : ligand ratio. The products, $[\text{Pd}(\text{L}^*)(\text{OAc})]$, **7Pd**, **8Pd** ($\text{L}^* = (\text{R},\text{R})\text{-7}$, $(\text{R},\text{R})\text{-8}$) were obtained in almost quantitative yields as stable solids (Scheme 3). These complexes were characterized by electro-spray mass spectrometry. Thus, the ESI-MS spectrum of **7Pd** shows the peak from the fragment due to elimination of the acetate at m/z 519.3 $[\text{M}^+ - \text{OAc}]$. All assignments were confirmed by good agreement between the observed and calculated isotopic distributions. In **7Pd**, the absence of the $\nu(\text{OH})$ band (present in the IR spectrum of the free ligand $(\text{R},\text{R})\text{-7}$ at $\sim 3430\text{ cm}^{-1}$) is in accordance with loss of the -OH proton. The IR spectrum showed a band at 1585 cm^{-1} assigned to coordinated $\text{C}=\text{N}$, about 30 cm^{-1} less than the free ligand, as expected for coordination of the imine. The IR spectrum also shows strong bands at 1320 and 1650 cm^{-1} assigned to the symmetric and asymmetric $\nu(\text{COO})$ vibrations, respectively, in agreement with those expected for monocoordinate acetate ligands.²⁵ A new band at 541 cm^{-1} is ascribed to $\nu(\text{Pd-O})$ for **7Pd**.

Diamagnetic palladium complexes have been characterized by ^1H and ^{13}C NMR spectroscopy. All assignments are based on several correlations in the 2D spectra. They are fully consistent with the structures depicted in Scheme 3. In all cases, the spectra show the simultaneous occurrence of two sets of signals which are attributable on the one hand to the substituted pyridine entity and on the other hand to the amine sponge derivative part of the ligand. In the ^1H NMR spectra all the resonances were high field shifted as compared to the uncoordinated ligand and they were in agreement with metallation of the ligand with coordination of the metal atom *via* the pyridine nitrogen atom. In the ^1H NMR of both **7Pd** and **8Pd**, the absence of the OH resonance indicates the deprotonation of the -OH group. The ^1H NMR spectrum of **7Pd** showed a singlet at 7.99 due to imine proton shifted upfield 0.27 ppm compared with the free ligand. Also, the acetate group was observed as a singlet at 1.34 ppm . The ^{13}C NMR spectrum of **7Pd** showed the imine carbon at δ 153.7 ppm (160.4 ppm for **8Pd**) and two signals for acetate at δ 29.7 and 197.1 .

Cationic complexes, $[\text{Rh}(\text{cod})(\text{L}^*)]\text{PF}_6$, (**7Rh**, **8Rh**) ($\text{L}^* = (\text{R},\text{R})\text{-7}$ and $(\text{R},\text{R})\text{-8}$), were synthesized by the reaction of $[\text{RhCl}(\text{cod})]_2$ with a stoichiometric amount of solid AgPF_6 and, subsequently after 30 min the corresponding L^* -chiral ligand, in THF solution.



Scheme 4 Heterogenization of imino complexes.

Filtration through Celite and evaporation of the solvent yielded a solid product, which was recrystallized using Et₂O. The ¹H NMR spectrum of the isolated product **7Rh** showed four broad lines between 1.8 and 4.8 ppm, due to fluxionality in the conformation of the cod chelate, a singlet at δ 5.96 due to the imine (**5.93** **8Rh**), and a broad singlet at δ 12.41 (9.82 for **8Rh**) assigned to the uncoordinated OH group. Complexes exhibit four signals in the ¹³C spectrum attributable to the carbon atoms of the cod ligand. ESI-MS spectrum show the mass for the molecular peak at 625.5 for **7Rh** [$M^+ - PF_6$]), but a single crystal structure has yet to be obtained. IR spectra show the corresponding to $\nu(OH)$ at 3408 cm⁻¹. The $\nu(C=N)$ stretch was observed at 1619 cm⁻¹.

When the chiral ligands are coordinated to the metal, this introduces a new chiral centre in the complex at the coordinated N atom and metal centre. We can deduce from NMR data, the coordination of the metal ion is completely stereospecific and gives rise to a single diastereoisomer.

Heterogenization of complexes containing pendant alkoxy silane groups to MCM-41

In the last years we have developed a modular system combining functionalized ligands with different supports and linkers in order to have a systematic access to a variety of immobilized chiral catalysts.⁴ The pure siliceous MCM-41 (MCM) parent material was derivatized following the strategy depicted in Scheme 4. This consisted of the grafting of a spacer, CH₂NHCONH(CH₂)₃Si(OEt)₃, on the walls of the MCM material. MCM-41 is short range materials containing a large number of silanol groups available for grafting. MCM-41 however, presents a long range ordering with hexagonal symmetry with regular monodirectional channels of 3.5 nm diameter.

Supported complexes were obtained by refluxing a mixture of the precursor **8Pd** or **8Rh** and the support, in toluene, with metal loadings of approximately 0.20–0.30 mmol-metal g⁻¹ support. These materials were characterized by elemental content analysis, FT IR, DFTR and CP-MAS solid state, ¹³C NMR spectroscopy. Complexation reactions yielded materials with the expected ratios of metal to nitrogen loadings. In general these results showed us that little other than the expected reactions are occurring on the functionalized silica surface.

The presence of functional groups characteristic of **8Pd** or **8Rh** in the materials was checked by FTIR spectroscopy. The stretching vibrations modes of the mesoporous framework (Si–O–Si) of the grafted material **8Pd**- or **8Rh**-MCM are observed at around 1240, 1070, and 810 cm⁻¹, as in the parent MCM, while new bands appear at ca. 2950 and 2850 cm⁻¹, assigned to the $\nu(C-H)$ stretching of the aliphatic linear chain in MCM-Pr and pyrrolidine ring. The presence of ligands leads to the appearance of the $\nu(C=N, C=O, C=C)$ stretching modes at 1640–1570 cm⁻¹. A new band at ca. 550 cm⁻¹ is ascribed to $\nu(Pd-O)$. The complexes immobilized on supports have been characterized by diffuse reflectance spectroscopy. The complexes show several band maxima in the UV region agreeing with the assignment of the bands as intraligand transitions in the aromatic ring, and charge-transfer transition. The diffuse reflectance spectra of complexes are almost identical before and after the heterogenization process, indicating that the complexes maintain their geometry and their electronic surrounding even after heterogenization without significant distortion.

The materials were also characterized by cross-polarization magic-angle spinning ¹³C CP MAS solid state NMR. The solid state ¹³C CP MAS NMR spectra (Supporting Information) of

Table 1 Catalytic hydrogenation of prochiral olefins with palladium and rhodium-complexes^a

Entry	Cat.	Diethyl itaconate		(E)-Diethyl 2-benzylidenesuccinate	
		ee (%) ^c	TOF ^b	ee (%) ^d	TOF ^b
1	5Pd	≤ 5	588	50	118
2	5Rh	≤ 5	600	97	36
3	6Pd	≤ 5	582	10	109
4	6Rh	≤ 5	590	60	92
5	7Pd	≤ 5	600	85	158
6	8Pd-MCM	≤ 5	1176	80	210
7	7Rh	≤ 5	602	95	108
8	8Rh-MCM	≤ 5	1164	90	300
9	3Pd (ref. 14a)	6	3368	12	640
10	3Pd-MCM (ref. 14a)	≤ 10	4980	≤ 10	900
11	6bPd (ref. 15a)	≤ 5	2800	15	565
12	13Pd-MCM (ref. 15b)	10	234	30	78

^a Conditions: 4 atm, 40 °C, S/C ratio 1000:1, diethyl itaconate; S/C ratio 100:1, (E)-diethyl 2-benzylidenesuccinate. ^b TOF: h⁻¹. ^c Measured by HPLC (λ: 230 nm, hexane/iPrOH: 98:2, column chiralcel AD-H), (S) isomer. ^d Measured by HPLC (λ: 254 nm, hexane/iPrOH: 95:5, column chiralcel OD), (S) isomer.

8Pd-MCM, **8Rh-MCM** materials are quite similar, since the spectra are dominated by the resonances of the aliphatic and aromatic groups. These signals appear at 8.6 and 8.3 ppm (Si-CH₂), 28.6 (CH₂-CH₂-CH₂), 44.0–43.6 ppm (N-CH₂); aromatic region δ = 130.3–156.4 ppm, δ = 160.5, 160.1 ppm (N=CH) and δ = 198 ppm (OAc). The majority of peaks corresponding to the ¹³C NMR spectrum of homogeneous complexes were present in the ¹³C spectrum of their heterogenized counterparts.

Catalytic activity

In order to evaluate the catalytic performances of these new Rh(II), Pd(II) complexes we have tested them in hydrogenation reactions. The following paragraphs show the results obtained in experimental conditions that allow us to make a comparative study of different catalysts and substrates. Obviously for preparative application a tuning of conditions has to be done for each case. Certainly for preparative applications it is necessary to adjust the experimental conditions for each case.

We chose two substrates with different steric hindrance, as a model, to make a comparative study between the soluble and systems to check the recyclability heterogenised and later we will study the full catalytic activity by varying the substrates and reactions.

The structurally well defined supported rhodium and palladium catalytic materials were tested in the asymmetric hydrogenation of several substrates. The hydrogenation of (E)-diethyl 2-benzylidenesuccinate or diethyl itaconate with Rh- and Pd-complexes were carried out under standard conditions (EtOH as the solvent, 4 atm hydrogen pressure, 40 °C). In all cases, with all catalysts, complete conversion of substrate was observed. Results were summarized in Table 1. Heterogenized catalysts show higher enantioselectivity than the homogeneous catalysts. High enantiomeric excess (98% ee) was observed in the asymmetric hydrogenation of diethyl (E)-diethyl 2-benzylidenesuccinate.

Table 2 Recycling experiments of **8Rh-MCM** in the catalytic hydrogenation of (E)-diethyl 2-benzylidenesuccinate

Cycle	TOF (h ⁻¹) ^a	ee (%) ^b
1	300	90
2	285	88
3	290	85

^a TOF: mmol subs./mmol cat.h. ^b Measured by HPLC (λ: 254 nm, hexane/iPrOH: 95:5, column chiralcel OD), (S) isomer.

Table 1 shows the effect of ligand substituents have on activity and enantioselectivity, if we compare the catalytic activity of complex **6Pd**, in this work, with that of previously reported for [(S)-N-(tert-butyl)-1-((6-(2-hydroxyphenyl)pyridine-2-yl)methyl)pyrrolidine-2-carboxamide]Pd (ligand type (**a**) in Chart 1, complex **6bPd** in reference 19a) and with **13Pd-MCM-41** (described in reference 19b), which have the prolinamide as chiral group, it appears that although the latter has a better catalytic activity (TOF: 565 h⁻¹ entry 11 vs. 109 h⁻¹, entry 3), the enantiomeric excess is comparable in both cases (15% vs. 10%).^{19a} Similarly in this case the enantioselectivity increases considerably when the catalyst is heterogenized (entry 12).^{19b} If we now compare the results obtained with the complexes derived from (**R,R**)-**7** (this work) with those previously reported for catalysts with the phenol-imino-amino ligand, 2-(((1-benzylpyrrolidin-2-yl)methylene)amino)-6-(tert-butyl)-4-methylphenol as ligand, (ligand type (**b**) in Chart 1, complexes **3Pd**, **3Pd-MCM-41** in reference 18a) we found that the most active catalysts are those with the Schiff base system derived with a proline derivative group (entries 9, 10 in Table 1). However, the highest enantioselectivity is obtained with the catalyst reported in this paper (entries 5, 7).

Catalyst recycling

From an environmental point of view, it is desirable to minimize the amount of waste for each organic transformation. Reusability is an important feature to be monitored for application of heterogenized single-site catalysts. Before reuse, the catalyst was separated from the reaction mixture by filtration and washed with ethanol. After the first run, the reaction reached >99% after 3 h and this remained steady up to the 4th run, proving that the catalyst is highly stable and simple to recycle. Because the homogeneous catalyst shows lower activity than the heterogenized, we confirmed that the presence of site-isolated metal complexes grafted onto MCM-41 was responsible for enhanced conversion and that the reaction is truly heterogeneous.

The catalytic materials were easily separated from the substrate/product solution by simple filtration subsequent washing, and then added fresh substrate, and solvent without further addition of catalyst. The recycling process could be repeated four times with no significant loss in selectivity, and minimal losses in activity (Table 2 and Fig. 4). Furthermore, the filtrate, which was colorless, was placed in a catalyst free autoclave and fresh substrate was added. Dihydrogen pressure was applied, however no further conversion was observed. This demonstrates that no metal leaching from the silica surface is occurring. The metal content (loading) of the recycled catalytic material was the same as the starting catalytic material suggesting little, if any, metal

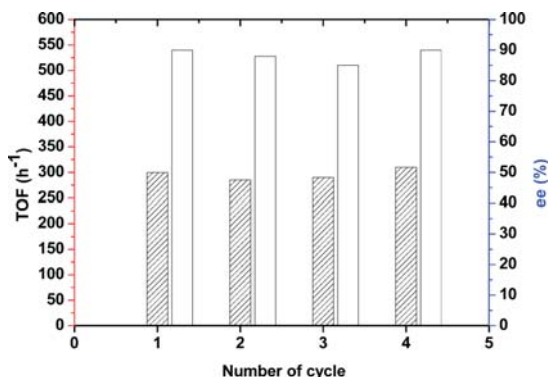


Fig. 4 Recycling of 8Rh-MCM.

leaching. Hot filtration experiments and ICP measurements were independently carried out to rule out the possibility of leaching.

In order to check the stability of metal complexes supported on the solid matrix, we have characterized the solid before and after reaction. As can be deduced from IR, ¹³C NMR and UV-vis spectra the nature of supported species is very similar and the most important signals for ligands appear in the same position after reaction.

Conclusions

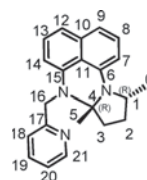
In this work we report the synthesis of the first pincer type complexes derived from a chiral proton sponge precursor, as well as a surprising cyclisation transformation that takes place under mild conditions to afford perimidine derivatives from several aldehydes and 8-((2*R*,5*R*)-2,5-dimethylpyrrolidin-1-yl)naphthalen-1-amine with good yields. The complexes derived from both types of ligands present high activity and enantioselectivity in hydrogenation of prochiral olefins. The supported complexes in MCM-41 show better activity than the homogeneous counterpart, and they could be recycled for subsequent cycles without loss of any material's features.

Experimental section

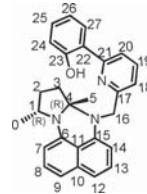
General remarks

All manipulations were carried out by using standard Schlenk vacuum-line techniques under an atmosphere of oxygen-free argon. All solvents for synthetic use were dried and distilled, under an argon atmosphere, by standard procedures.²⁶ ¹³C MAS or CP/MAS NMR spectra of powdered samples, in some cases also with a Toss sequence, in order to eliminate the spinning side bands, were recorded at 100.63 MHz, 6 μs 90° pulse width, 2 ms contact time and 5–10 recycle delay, using a Bruker MSL 400 spectrometer equipped with an FT unit. The spinning frequency at the magic angle (54°44') was 4 KHz. The reaction was monitored by gas chromatography with helium as carrier gas, 10 psi; injector temperature: 230 °C; detector temperature: 250 °C.

Synthesis of ligands



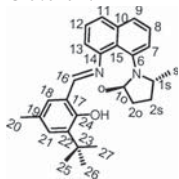
(*7aR*,10*R*)-*7a*,10-dimethyl-7-(pyridin-2-ylmethyl)-*7a*,8,9,10-tetrahydro-7*H*-pyrrolo[1,2-*a*]perimidine ((*R,R*)-**5**). To a solution of 8-((2*R*,5*R*)-2,5-dimethylpyrrolidin-1-yl)naphthalen-1-amine (300 mg, 1.25 mmol) in absolute ethanol (20 mL) and in the presence of molecular sieves (2 g, 4 Å) was added an ethanolic solution (10 mL) of 3 pyridine-2-carbaldehyde (133 mg, 1.25 mmol). The reaction mixture was stirred overnight at room temperature and filtered. The residue was dried under reduced pressure and purified by flash chromatography, *R_f* 0.25 (5:1 heptane/ethyl acetate) to obtain a pale pink solid Yield = 290 mg, 71%. M.p.: 58–60 °C. IR (KBr, cm⁻¹): ν_{CHarom} 3048 (w); ν_{CHalip} 2970 (m), 2922 (m); $\nu_{\text{C}\equiv\text{C}}$, $\nu_{\text{C}\equiv\text{N}}$ 1582 (s), 1435 (s), 1418 (s); δ_{CH} 1374 (m), 1337 (s); $\delta_{\text{CHout plane}}$ 810 (s), 756 (s); ρ_{CH} 639 (m), 607 (w), 517 (m). ¹H NMR (300 MHz, CDCl₃): δ 8.75 (ddd, 1H, H₂₁, J_{HH} = 0.9, 1.6, 4.8 Hz); 7.70 (dt, 1H, H₁₉, J_{HH} = 1.7, 7.5 Hz); 7.58 (d, 1H, H₁₈, J_{HH} = 7.3 Hz); 7.45 (t, 1H, H₁₃, J_{HH} = 7.7 Hz); 7.33–7.22 (m, 4H, H₈, H₉, H₁₂, H₂₀); 6.56 (d, 1H, H₁₄, J_{HH} = 7.3 Hz); 6.25 (dd, 1H, H₇, J_{HH} = 3.0, 5.2 Hz); 4.82 (d, 1H, H₁₆, -CH₂-, ABXY, J_{HH} = 17.6 Hz); 4.57 (d, 1H, H₁₆, -CH₂-, ABXY, J_{HH} = 17.6 Hz); 4.29 (m, 1H, H₁, -CH_{2pyrr}); 2.55–2.47 (m, 2H, 2 -CH_{2pyrr}); 2.34 (m, 1H, -CH_{2pyrr}); 1.95 (m, 1H, -CH_{2pyrr}); 1.49 (d, 3H, H₀, -CH₃, J_{HH} = 6.6 Hz); 1.37 (s, 3H, H₅, -CH₃). ¹³C NMR (125 MHz, CDCl₃): δ 159.6 (C₁₇); 149.1 (C₂₁); 141.9 (C₁₅); 138.9 (C₆); 137.0 (C₁₉); 134.8 (C₁₀); 127.0 (C₁₃); 126.8 (C₉); 121.8 (C₂₀); 120.8 (C₁₈); 117.1 (C₈); 115.3 (C₁₂); 114.9 (C₁₁); 104.5 (C₇); 103.9 (C₁₄); 78.5 (C₄); 53.8 (C₁₆, -CH₂-); 52.6 (C₁); 36.8 (C₃); 29.5 (C₂); 20.0 (C₀, -CH₃); 18.5 (C₅, -CH₃). Anal. Calc. for C₂₂H₂₃N₃ (329.4): C, 80.2; H, 7.0; N, 12.8. Found: C, 80.2; H, 7.2; N, 12.5%. ESI-MS *m/z* (%): 329.0 [M⁺], 314.0 [M⁺-CH₃], 252.0 [M⁺-Py].



2-(6-([(*7aR*,10*R*)-*7a*,10-dimethyl-*7a*,8,9,10-tetrahydro-7*H*-pyrrolo[1,2-*a*]perimidin-7-yl)methyl} pyridin-2-yl)phenol ((*R,R*)-**6**). To a solution of 8-((2*R*,5*R*)-2,5-dimethylpyrrolidin-1-yl)naphthalen-1-amine (50 mg, 0.208 mmol) in absolute ethanol (2 mL) and in the presence of molecular sieves (2 g, 4 Å) was added an ethanolic solution (4 mL) of 6-(2-hydroxyphenyl)pyridine-2-carbaldehyde (41.4 mg, 0.208 mmol). The reaction mixture was stirred overnight at room temperature and filtered. The residue was dried under reduced pressure and purified by flash chromatography (15:1 heptane/ethyl acetate) to afford a pale pink solid. Yield = 33 mg, 38%. M.p.: 90–93 °C. IR (KBr, cm⁻¹): ν_{OH} 3435 (m); ν_{CHarom} 3194 (w), 3051 (w); ν_{CHalip} 2963 (m), 2925 (m), 2867 (m); $\nu_{\text{C}\equiv\text{C}}$, $\nu_{\text{C}\equiv\text{N}}$ 1596 (s), 1578 (vs), 1458 (s), 1430 (s); δ_{CH}

1374 (m), 1335 (m), 1299 (s); $\delta_{\text{CHout plane}}$ 818 (s), 756 (s); ρ_{CH} 633 (w). ^1H NMR (300 MHz, CDCl_3): δ 13.60 (s br, 1H, OH); 7.84 (dd, 1H, H_{27} , $J_{\text{HH}} = 1.5$, 8.0 Hz); 7.79 (s br, 1H, H_{30}); 7.71 (t, 1H, H_{19} , $J_{\text{HH}} = 7.7$ Hz); 7.39–7.31 (m, 3H, H_9 , H_{13} , H_{25}); 7.15 (s br, 1H, H_{18}); 7.13 (d, 1H, H_8 , $J_{\text{HH}} = 4.4$ Hz); 7.08 (d, 1H, $J_{\text{HH}} = 3.7$ Hz) and 7.04 (d, 1H, $J_{\text{HH}} = 4.4$ Hz) (H_{12} and H_{24}); 6.95 (dt, 1H, H_{26} , $J_{\text{HH}} = 1.5$, 7.3 Hz); 6.44 (d, 1H, H_{14} , $J_{\text{HH}} = 7.3$ Hz); 6.11 (t, 1H, H_7 , $J_{\text{HH}} = 4.4$ Hz); 4.70 (d, 1H, H_{16} , $-\text{CH}_2-$, ABXY, $J_{\text{HH}} = 17.6$ Hz); 4.45 (d, 1H, H_{16} , $-\text{CH}_2-$, ABXY, $J_{\text{HH}} = 17.6$ Hz); 4.16 (m, 1H, H_{11} , $-\text{CH}_{\text{pyrr}}$); 2.42–2.32 (m, 2H, $-\text{CH}_{2\text{pyrr}}$); 2.25–2.18 (m, 1H, $-\text{CH}_{2\text{pyrr}}$); 1.84–1.81 (m, 1H, $-\text{CH}_{2\text{pyrr}}$); 1.37 (d, 3H, H_0 , $-\text{CH}_3$, $J_{\text{HH}} = 5.9$ Hz); 1.25 (s, 3H, H_5 , $-\text{CH}_3$). ^{13}C NMR (125 MHz, CDCl_3): δ 159.9 (C_{22}); 157.5 (C_{23}); 156.7 (C_{17}); 141.7 (C_{15}); 138.8 (C_6); 138.7 (C_{19}); 134.9 (C_{10}); 131.5 (C_9); 127.1 (C_{13}); 126.4 (C_{27}); 126.3 (C_{18}); 124.7 (C_{21}); 119.2 (C_{24}); 118.9 (C_{25}); 118.6 (C_{26}); 117.5 (C_8); 117.4 (C_{20}); 115.4 (C_{12}); 114.9 (C_{11}); 104.5 (C_7); 104.1 (C_{14}); 78.5 (C_4); 53.2 (C_{16} , $-\text{CH}_2-$); 52.7 (C_1); 36.9 (C_3); 29.5 (C_2); 20.0 (C_0 , $-\text{CH}_3$); 18.6 (C_5 , $-\text{CH}_3$). Anal. Calc. for $\text{C}_{28}\text{H}_{27}\text{N}_3\text{O}$ (421.5): C, 79.8; H, 6.5; N, 10.0. Found: C, 79.6; H, 6.8; N, 10.2%. ESI-MS m/z (%): 421.0 [M^+], 406.0 [$\text{M}^+ - \text{CH}_3$].

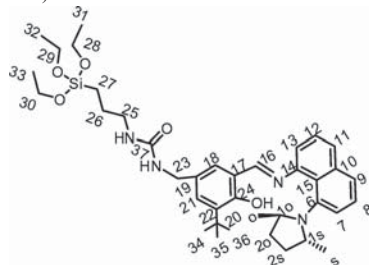
Crystal data for **RR-6**: $\text{C}_{28}\text{H}_{27}\text{N}_3\text{O}$, $M = 421.53$, orthorhombic, $a = 10.414(3)$ Å, $b = 13.565(3)$ Å, $c = 15.401(4)$ Å, $\alpha = 90.00^\circ$, $\beta = 90.00^\circ$, $\gamma = 90.00^\circ$, $V = 2175.6(9)$ Å³, $T = 296(2)$ K, space group $P2_12_12_1$, $Z = 4$, 15489 reflections measured, 2280 independent reflections ($R_{\text{int}} = 0.0750$). The final R_1 values were 0.0376 ($I > 2\sigma(I)$). The final $wR(F^2)$ values were 0.0812 ($I > 2\sigma(I)$). The final R_1 values were 0.0475 (all data). The final $wR(F^2)$ values were 0.0846 (all data). CCDC 805292.



2-tert-butyl-6-((E)-(8-((2R,5R)-2,5-dimethylpyrrolidin-1-yl)naphthalen-1-ylimino)methyl)-4-methylphenol ((R,R)-7). To a solution of 3-tert-butyl-2-hydroxy-5-methylbenzaldehyde (176 mg, 0.915 mmol) in absolute ethanol (20 mL) was added 8-[(2R,5R)-2,5-dimethylpyrrolidin-1-yl]naphthalen-1-amine (200 mg, 0.915 mmol). After stirring at room temperature for 24 h, the reaction mixture was filtered and washed with ethanol. The residue was dried under reduced pressure and purified by flash chromatography (10:1 heptane/ethyl acetate) to obtain a microcrystalline orange solid. Yield = 199 mg, 58%. M.p.: 73–75 °C. IR (KBr, cm^{-1}): ν_{OH} 3445 (m); ν_{CHarom} 3049 (w); ν_{CHalip} 2961 (m), 2920 (m), 2870 (m); $\nu_{\text{C=N}}$, $\nu_{\text{C=C}}$ 1618 (s), 1564 (vs), 1439 (s); $\delta_{\text{CHout plane}}$ 1370 (m), 1330 (s). UV-Vis: λ_{max} = 302 nm, 343 nm. ^1H NMR (300 MHz, CDCl_3): δ 13.86 (s br, 1H, OH); 8.26 (s, 1H, H_{16} , N=CH); 7.67 (dd, 1H, H_9 , $J_{\text{HH}} = 1.3$, 8.4 Hz); 7.50 (d, 1H, H_{11} , $J_{\text{HH}} = 8.0$ Hz); 7.43–7.37 (m, 2H, H_8 , H_{12}); 7.18 (d, 1H, $J_{\text{HH}} = 1.8$ Hz) and 6.99 (d, 1H, $J_{\text{HH}} = 1.8$ Hz) (H_{18} and H_{21}); 7.05 (d, 1H, H_{13} , $J_{\text{HH}} = 7.5$ Hz); 6.94 (dd, 1H, H_7 , $J_{\text{HH}} = 1.3$, 7.1 Hz); 3.75–3.66 (m, 1H) and 3.51–3.46 (m, 1H) (H_{15} and H_{10} , $-\text{CH}_{\text{pyrr}}$); 2.30 (s, 3H, H_{20} , $-\text{CH}_3$); 1.96–1.86 (m, 1H) and 1.80–1.70 (m, 1H) (H_{25} and H_{20} , $-\text{CH}_{2\text{pyrr}}$); 1.46 (s, 9H, $H_{25,26,27}$); 1.39–1.33 (m, 1H) and 1.18–1.09 (m, 1H) (H_{25} and H_{20} , $-\text{CH}_{2\text{pyrr}}$); 1.25 (d, 3H, $-\text{CH}_3$, $J_{\text{HH}} = 6.2$ Hz) and 0.36 (d, 3H, $-\text{CH}_3$, $J_{\text{HH}} = 6.2$ Hz) (H_0 and H_5). ^{13}C NMR (125 MHz, CDCl_3): δ 161.0 (C_{16} , N=CH); 158.2 (C_{24}); 147.2 (C_{14}); 143.7 (C_6); 137.2 (C_{22}); 136.9 (C_{10}); 131.0 (C_{19}); 130.8 (C_{18}); 130.1 (C_{21}); 128.1 (C_{15});

126.5 (C_9); 125.7 (C_{12}); 125.4 (C_8); 122.4 (C_{11}); 119.1 (C_{17}); 118.5 (C_{13}); 118.0 (C_7); 58.8 (C_{18}); 51.4 (C_{10}); 34.7 (C_{23}); 31.6 (C_{20}); 29.4 (3C, $C_{25,26,27}$); 29.2 (C_{28}); 20.7 (C_{20} , CH_3 -Ph); 18.3 (C_0 , $\text{CH}_{3\text{pyrr}}$); 17.5 (C_5 , $\text{CH}_{3\text{pyrr}}$). Anal. Calc. for $\text{C}_{28}\text{H}_{34}\text{N}_2\text{O}$ (414.6): C, 81.1; H, 8.3; N, 6.8. Found: C, 81.0; H, 8.5; N, 6.5%. ESI-MS m/z (%): 414.0 [M^+], 399.0 [$\text{M}^+ - \text{CH}_3$], 223.0 [$\text{M}^+ - \text{CH}_3 - \text{Bu} - \text{Ar} - \text{OH} - \text{imine}$].

Crystal data for **RR-7**: $\text{C}_{28}\text{H}_{34}\text{N}_2\text{O}$, $M = 414.57$, monoclinic, $a = 9.8047(8)$ Å, $b = 8.8134(8)$ Å, $c = 14.0070(12)$ Å, $\alpha = 90.00^\circ$, $\beta = 91.3630(10)^\circ$, $\gamma = 90.00^\circ$, $V = 1210.04(18)$ Å³, $T = 296(2)$ K, space group $P2_1$, $Z = 2$, 8037 reflections measured, 4000 independent reflections ($R_{\text{int}} = 0.0324$). The final R_1 values were 0.0636 ($I > 2\sigma(I)$). The final $wR(F^2)$ values were 0.1125 ($I > 2\sigma(I)$). The final R_1 values were 0.1082 (all data). The final $wR(F^2)$ values were 0.1281 (all data). CCDC 805293.



N-(3-tert-butyl-5-((E)-(8-((2R,5R)-2,5-dimethylpyrrolidin-1-yl)naphthalen-1-ylimino)methyl)-4-hydroxybenzylcarbamoyl)-4-(triethoxysilyl)butanamide ((R,R)-8). Using a similar procedure to that described for (R,R)-7, from *N*-(3-tert-butyl-5-formyl-4-hydroxyphenylcarbamoyl)-4-(triethoxysilyl)butanamide (0.378 g, 0.832 mmol) and 8-[(2R,5R)-2,5-dimethylpyrrolidin-1-yl]naphthalen-1-amine (200 mg, 0.832 mmol) in absolute ethanol (3 mL). After purification by flash chromatography (4:1 heptane/ethyl acetate) an orange oil was obtained. Yield = 405 mg, 72%. ^1H NMR (300 MHz, CDCl_3): δ 14.11 (s br, 1H, OH); 8.32 (s, 1H, H_{16} , N=CH); 7.65 (dd, 1H, H_9 , $J_{\text{HH}} = 1.1$, 7.9 Hz); 7.50 (d, 1H, H_{11} , $J_{\text{HH}} = 7.9$ Hz); 7.44–7.37 (m, 2H, H_8 , H_{12}); 7.27 (d, 1H, H_{18} , $J_{\text{HH}} = 2.7$ Hz); 7.16 (d, 1H, H_{21} , $J_{\text{HH}} = 2.7$ Hz); 7.05 (d, 1H, H_{13} , $J_{\text{HH}} = 7.7$ Hz); 6.93 (dd, 1H, H_7 , $J_{\text{HH}} = 1.0$, 7.2 Hz); 4.34 (s, 2H, H_{23} , $-\text{CH}_2-$); 3.80 (q, 6H, $H_{28,29,30}$, $J_{\text{HH}} = 7.0$ Hz); 3.75–3.69 (m, 1H, H_{10} , $-\text{CH}_{\text{pyrr}}$); 3.54–3.48 (m, 1H, H_{15} , $-\text{CH}_{\text{pyrr}}$); 3.23–3.16 (m, 2H, H_{25} , $-\text{CH}_2-$); 1.98–1.87 (m, 1H, H_{20} , $-\text{CH}_{2\text{pyrr}}$); 1.75–1.70 (m, 1H, H_{25} , $-\text{CH}_{2\text{pyrr}}$); 1.69–1.61 (m, 2H, H_{26} , $-\text{CH}_2-$); 1.46 (s, 9H, $H_{34,35,36}$); 1.42–1.30 (m, 1H, H_{20} , $-\text{CH}_{2\text{pyrr}}$); 1.26 (d, 3H, H_0 , $-\text{CH}_3$, $J_{\text{HH}} = 5.6$ Hz); 1.20 (t, 9H, $H_{31,32,33}$, $J_{\text{HH}} = 7.0$ Hz); 1.13–1.10 (m, 1H, H_{25} , $-\text{CH}_{2\text{pyrr}}$); 0.65 (m, 2H, H_{27} , $-\text{CH}_2$ -Si); 0.39 (d, 3H, H_5 , $-\text{CH}_3$, $J_{\text{HH}} = 5.6$ Hz). ^{13}C NMR (125 MHz, CDCl_3): δ 160.5 (C_{16} , N=CH); 159.9 (C_{37} , C=O); 158.0 (C_{24}); 146.9 (C_{14}); 143.7 (C_6); 138.0 (C_{22}); 136.9 (C_{10}); 130.5 (C_{19}); 129.4 (C_{18}); 129.2 (C_{21}); 128.1 (C_{15}); 126.9 (C_9); 125.8 (2C, C_{12} , C_8); 122.5 (C_{11}); 119.2 (C_{17}); 118.7 (C_{13}); 118.0 (C_7); 58.9 (C_{18}); 58.5 (3C, $C_{28,29,30}$); 51.5 (C_{10}); 44.6 (C_{23} , $-\text{HN-CH}_2$ -Ph); 43.0 (C_{25} , $-\text{CH}_2-$); 34.9 (C_{20}); 31.6 (C_{20}); 29.4 (3C, $C_{34,35,36}$); 29.2 (C_{28}); 23.6 (C_{26} , $-\text{CH}_2-$); 18.4 (C_0 , CH_3); 18.3 (3C, $C_{31,32,33}$); 17.5 (C_5 , CH_3); 7.6 (C_{27} , $-\text{CH}_2$ -Si).

Synthesis of complexes

(R,R)-5Pd. $\text{Pd}(\text{cod})\text{Cl}_2$ (43 mg, 0.152 mmol) in CH_2Cl_2 (10 mL) was added to a solution of (R,R)-5 (50 mg, 0.152 mmol) in the same solvent and the mixture was stirred at room temperature

for 6 h. After the solvent had been removed under vacuum to 0.5 mL, the product was precipitated by careful addition of pentane and collected by filtration, to afford a stable light brown solid. Yield = 73 mg, 94%. IR (KBr, cm^{-1}): ν_{CHarom} 3049 (w); ν_{CHalip} 2965 (m), 2925 (m) 2875 (m); $\nu_{\text{C}=\text{C}}$, $\nu_{\text{C}=\text{N}}$ 1609 (s) 1587 (vs), 1420 (s); δ_{CH} 1373 (m), 1338 (m); $\delta_{\text{CHout of plane}}$ 811 (s), 758 (s); ρ_{CH} 638 (w), 603 (w), 514 (w). ^1H NMR (300 MHz, CDCl_3): δ 9.04 (m, 1H_{Py}); 7.63 (m, 1H_{Py}); 7.56 (m, 1H_{Py}); 7.28 (m, 1H_{Py}); 7.13 (d, 2H_{Nph}, $J_{\text{HH}} = 8.0$ Hz); 7.05 (d, 2H_{Nph}, $J_{\text{HH}} = 7.3$ Hz); 6.38 (dd, 2H_{Nph}, $J_{\text{HH}} = 1.0$, 6.4 Hz); 5.97 (d, 1H, -CH₂-, ABXY, $J_{\text{HH}} = 18.1$ Hz); 5.61 (d, 1H, -CH₂-, ABXY, $J_{\text{HH}} = 18.1$ Hz); 4.03 (m, 1H, -CH_{pyrr}); 2.89–2.56 (m, 2H, -CH_{2pyrr}); 2.37–2.17 (m, 2H, -CH_{2pyrr}); 1.25 (d, 3H, -CH₃, $J_{\text{HH}} = 10.2$ Hz); 0.89 (s, 3H, -CH₃). ^{13}C NMR (125 MHz, CDCl_3): δ 161.7 (C_{Py}); 152.1 (C_{Py}); 141.2 (C_{Nph}); 139.0 (C_{Py}); 134.8 (C_{Nph}); 127.1 (C_{Py}); 124.0 (2C_{Nph}); 123.7 (C_{Py}); 118.0 (2C_{Nph}); 116.7 (2C_{Nph}); 105.1 (2C_{Nph}); 79.2 (-CN-CH_{3pyrr}); 55.6 (-CH₂-); 52.7 (-CH-CH_{3pyrr}); 36.6 (-CH_{2pyrr}); 31.0 (-CH_{2pyrr}); 20.0 (-CH₃); 18.1 (-CH₃). Anal. Calcd. for $\text{C}_{22}\text{H}_{23}\text{Cl}_3\text{N}_3\text{Pd}$ (506.8): C, 52.1; H, 4.6; N, 8.3. Found: C, 52.4; H, 4.8; N, 7.8%. ESI-MS m/z (%): 471.3 [M^+ -Cl], 435.3 [M^+ -2Cl], 329.3 [M^+ -2Cl-Pd].

(*R,R*)-5Rh. AgPF₆ (38.5 mg, 0.152 mmol) in THF (10 mL) was added to a solution of [Rh(cod)Cl]₂ (37 mg, 0.076 mmol) in THF (10 mL) and the mixture was stirred vigorously at room temperature for 30 min. The resulting AgCl was filtered off and the yellow solution was treated with (*R,R*)-5 (50 mg, 0.152 mmol) in the same solvent. The mixture was stirred at room temperature for 2 h. After the solvent had been removed under vacuum to 0.5 mL, the product was precipitated by careful addition of Et₂O and collected by filtration, to afford a stable dark green solid. Yield = 95 mg, 91%. IR (KBr, cm^{-1}): ν_{CHalip} 2962 (m), 2924 (m) 2886 (m), 2839 (m); $\nu_{\text{C}=\text{C}}$, $\nu_{\text{C}=\text{N}}$ 1614 (s), 1587 (s), 1413 (m); δ_{CH} 1378 (m), 1335 (m); ν_{PF} 842 (vs); $\delta_{\text{CHout of plane}}$ 762 (m); ρ_{CH} 558 (s). ^1H NMR (300 MHz, CDCl_3): δ 8.00 (m, 1H_{Py}); 7.85 (m, 1H_{Py}); 7.73 (m, 1H_{Py}); 7.50 (m, 1H_{Py}); 7.40 (dd, 2H_{Nph}, $J_{\text{HH}} = 1.0$, 7.9 Hz); 7.24 (d, 2H_{Nph}, $J_{\text{HH}} = 7.9$ Hz); 6.53 (d, 2H_{Nph}, $J_{\text{HH}} = 7.4$ Hz); 5.82 (d, 1H, -CH₂-, ABXY, $J_{\text{HH}} = 16.2$ Hz); 4.41 (d, 1H, -CH₂-, ABXY, $J_{\text{HH}} = 16.0$ Hz); 4.05 (m, 2H, -CH=C_{cod}); 3.87 (m, 1H, -CH_{pyrr}); 3.58 (m, 2H, -CH=C_{cod}); 2.58 (m, 2H, -CH_{2cod}); 2.33 (m, 2H, -CH_{2cod}); 2.21 (m, 2H, -CH_{2cod}); 1.87 (m, 2H, -CH_{2cod}); 1.68 (d, 3H, -CH₃, $J_{\text{HH}} = 6.0$ Hz); 1.58 (m, 2H, -CH_{2pyrr}); 1.32 (m, 2H, -CH_{2pyrr}); 1.15 (s, 3H, -CH₃). ^{13}C NMR (125 MHz, CDCl_3): δ 160.7 (C_{Py}); 146.2 (C_{Py}); 141.0 (C_{Py}); 138.5 (C_{Nph}); 134.5 (C_{Nph}); 128.0 (2C_{Nph}); 126.4 (C_{Py}); 123.7 (C_{Py}); 117.5 (2C_{Nph}); 115.8 (2C_{Nph}); 105.7 (2C_{Nph}); 87.0 (2C, -CH=CH_{cod}); 83.0 (2C, -CH=CH_{cod}); 77.2 (-CN-CH_{3pyrr}); 57.9 (-CH₂-); 51.6 (-CH-CH_{3pyrr}); 39.6 (-CH_{2pyrr}); 30.3 (2C, 2-CH_{2cod}); 29.9 (2C, 2-CH_{2cod}); 29.4 (-CH_{2pyrr}); 20.3 (-CH₃); 15.6 (-CH₃). Anal. Calcd. for $\text{C}_{30}\text{H}_{35}\text{F}_6\text{N}_3\text{PRh}$ (685.5): C, 52.6; H, 5.1; N, 6.1. Found: C, 52.3; H, 5.0; N, 5.8%. ESI-MS m/z (%): 540.3 [M^+ -PF₆], 432.3 [M^+ -PF₆-cod], 330.3 [M^+ -cod-Rh].

(*R,R*)-6Pd. Pd(AcO)₂ (26.7 mg, 0.119 mmol) in CH₂Cl₂ (10 mL) was added to a solution of (*R,R*)-6 (50.1 mg, 0.152 mmol) in the same solvent and the mixture was stirred at room temperature overnight. After the solvent had been removed under vacuum to 0.5 mL, the product was precipitated by careful addition of pentane and collected by filtration, to afford a stable brown solid. Yield = 65 mg, 85%. IR (KBr, cm^{-1}): ν_{CHarom} 3055 (w); ν_{CHalip} 2964 (m), 2924 (w), 2891 (vw); $\nu_{\text{C}=\text{O}}$ 1624 (s); $\nu_{\text{C}=\text{C}}$, $\nu_{\text{C}=\text{N}}$ 1596 (vs), 1573 (s), 1467 (s); δ_{CH} 1406 (s), 1378 (m), 1360 (m); $\nu_{\text{C-O}}$ 1317 (s);

$\delta_{\text{CHout of plane}}$ 821 (m), 755 (m); δ_{OCO} 686 (w); $\nu_{\text{Pd-O}}$ 555 (vw). ^1H NMR (300 MHz, CDCl_3): δ 9.35 (dd, 1H_{Py}, $J_{\text{HH}} = 1.1$, 7.5 Hz); 7.80 (m, 1H_{Nph}); 7.79 (m, 1H_{Nph}); 7.73 (d, 1H_{Py}, $J_{\text{HH}} = 7.8$ Hz); 7.61 (dd, 1H_{Py}, $J_{\text{HH}} = 1.0$, 7.9 Hz); 7.55 (d, 1H_{Py}, $J_{\text{HH}} = 8.1$ Hz); 7.40 (dd, 1H_{Nph}, $J_{\text{HH}} = 1.0$, 7.9 Hz); 7.30 (d, 1H_{Nph}, $J_{\text{HH}} = 7.9$ Hz); 7.20 (m, 1H_{Ph}); 7.19 (m, 1H_{Ph}); 6.85 (m, 1H_{Nph}); 6.68 (m, 1H_{Ph}); 6.57 (d, 1H_{Nph}, $J_{\text{HH}} = 7.5$ Hz); 4.57 (d, 1H, -CH₂-, ABXY, $J_{\text{HH}} = 17.2$ Hz); 4.22 (d, 1H, -CH₂-, ABXY, $J_{\text{HH}} = 17.1$ Hz); 4.05 (m, 1H, -CH_{pyrr}); 2.68 (dd, 1H, -CH_{2pyrr}, $J_{\text{HH}} = 6.8$, 12.1 Hz); 2.37 (m, 1H, -CH_{2pyrr}); 1.91 (m, 1H, -CH_{2pyrr}); 1.88 (s, 3H, CH₃CO₂-); 1.65 (s, 3H, -CH₃); 1.62 (m, 1H, -CH_{2pyrr}); 1.35 (d, 3H, -CH₃, $J_{\text{HH}} = 6.2$ Hz). ^{13}C NMR (125 MHz, CDCl_3): δ 197.0 (CH₃CO₂-); 164.4 (C-O, C_{Ph}); 161.0 (C_{Nph}); 153.2 (C_{Nph}); 142.4 (C_{Py}); 138.8 (C_{Nph}); 136.5 (C_{Nph}); 134.3 (C_{Py}); 132.1 (C_{Ph}); 128.5 (C_{Ph}); 127.6 (C_{Py}); 127.1 (C_{Nph}); 126.9 (C_{Py}); 123.6 (C_{Py}); 122.6 (C_{Ph}); 121.8 (C_{Ph}); 120.1 (C_{Nph}); 117.0 (C_{Nph}); 116.2 (C_{Nph}); 116.0 (C_{Ph}); 113.7 (C_{Nph}); 105.4 (C_{Nph}); 86.2 (-CN-CH_{3pyrr}); 66.5 (-CH₂-); 51.7 (-CH-CH_{3pyrr}); 34.9 (-CH_{2pyrr}); 28.7 (-CH_{2pyrr}); 24.3 (CH₃CO₂-); 22.2 (-CH₃); 20.0 (-CH₃). Anal. Calcd. for $\text{C}_{30}\text{H}_{29}\text{N}_3\text{O}_3\text{Pd}$ (586.0): C, 61.5; H, 5.0; N, 7.2. Found C, 61.8; H, 4.9; N, 7.7%. ESI-MS m/z (%): 585.5 [M^+], 526.5 [M -CH₃CO₂], 421.5 [M -CH₃CO₂-Pd].

(*R,R*)-6Rh. AgPF₆ (48 mg, 0.190 mmol) in THF (10 mL) was added to a solution of [Rh(cod)Cl]₂ (46.4 mg, 0.095 mmol) in THF (10 mL) and the mixture was stirred vigorously at room temperature for 30 min. The resulting AgCl was filtered off and the yellow solution was treated with (*R,R*)-6 (80 mg, 0.190 mmol) in the same solvent. The mixture was stirred at room temperature for 2 h. After the solvent had been removed under vacuum to 0.5 mL, the product was precipitated by careful addition of Et₂O and collected by filtration, to afford a stable (in solid state) dark yellow solid. Yield = 133 mg, 90%. This compound decomposes in solution (the compound turns red) and the NMR spectrum cannot be collected in common solvents, only ^{13}C MAS solid was used for characterization; ^1H NMR solid proton spectrum does not provide information because the signals are broad. IR (KBr, cm^{-1}): ν_{OH} 3443 (m); ν_{CHarom} 3101 (vw), 3058 (vw); ν_{CHalip} 2964 (m), 2926 (m), 2880 (m), 2837 (m); $\nu_{\text{C}=\text{C}}$, $\nu_{\text{C}=\text{N}}$ 1596 (s), 1578 (s), 1537 (s), 1461 (s); δ_{CH} 1378 (m), 1335 (m), 1299 (m); ν_{PF} 843 (vs); $\delta_{\text{CHout of plane}}$ 760 (m); ρ_{CH} 557 (s). ^{13}C NMR (300 MHz, solid): δ 158.3 (C_{Ph}); 154.5 (C_{Ph}); 152.0 (C_{Py}); 140.2 (C_{Nph}); 138.5 (2C, C_{Nph}, C_{Py}); 135.4 (C_{Nph}); 133.5 (C_{Nph}); 127.6 (2C, C_{Nph}, C_{Ph}); 126.3 (2C_{Py}); 119.1 (5C, 3C_{Ph}, C_{Nph}, C_{Py}); 115.3 (2C_{Nph}); 104.6 (2C_{Nph}); 80.9 (5C, 2-CH=CH_{cod}-, -CN-CH_{3pyrr}); 53.4 (-CH₂-); 53.3 (-CH-CH_{3pyrr}); 39.0 (-CH_{2pyrr}); 30.6 (5C, 4-CH_{2cod}-, -CH_{2pyrr}); 19.7 (-CH₃); 19.5 (-CH₃). Anal. Calcd. for $\text{C}_{36}\text{H}_{39}\text{F}_6\text{N}_3\text{OPRh}$ (777.6): C, 55.6; H, 5.1; N, 5.4; found C, 50.8; H, 4.5; N, 4.4%. (*R,R*)-6Rh + 3/2 CH₂Cl₂: C, 50.2; H, 4.5; N, 4.6). ESI-MS m/z (%): 632.3 [M^+], 523.3 [M^+ -H⁺-cod].

(*R,R*)-7Pd. Pd(AcO)₂ (21.6 mg, 0.096 mmol) in EtOH (10 mL) was added to a solution of (*R,R*)-8 (40 mg, 0.096 mmol) in the same solvent and the mixture was stirred at room temperature overnight. After the solvent had been removed under vacuum to 0.5 mL, the product was precipitated by careful addition of pentane and collected by filtration, to afford a stable light brown solid. Yield = 48 mg, 85%. IR (KBr, cm^{-1}): ν_{CHarom} 3053 (w); ν_{CHalip} 2960 (vs), 2921 (vs), 2867 (s); $\nu_{\text{C}=\text{O}}$ 1650 (s); $\nu_{\text{C}=\text{C}}$, $\nu_{\text{C}=\text{N}}$ 1585 (vs), 1572 (vs), 1529 (s); δ_{CH} 1457 (s), 1426 (s), 1373 (s), $\nu_{\text{C-O}}$ 1320 (s); $\delta_{\text{CHout of plane}}$ 819 (m), 765 (m); δ_{OCO} 710 (w); $\nu_{\text{Pd-O}}$ 541 (vw). ^1H NMR (300 MHz, CDCl_3): δ 7.99 (s, 1H, N=CH); 7.30 (d, 1H_{Nph}, $J_{\text{HH}} = 6.4$ Hz); 7.28

(m, 1H_{Nph}); 7.27 (d, 1H_{Nph}, $J_{\text{HH}} = 6.4$ Hz); 7.26 (d, 1H_{Nph}, $J_{\text{HH}} = 5.9$ Hz); 7.10 (d, 1H_{Ph}, $J_{\text{HH}} = 2.2$ Hz); 7.05 (d, 1H_{Ph}, $J_{\text{HH}} = 2.2$ Hz); 6.41 (d, 1H_{Nph}, $J_{\text{HH}} = 7.5$ Hz); 6.31 (d, 1H_{Nph}, $J_{\text{HH}} = 7.5$ Hz); 4.00 (dc, 1H, -CH_{2pyrr}, $J_{\text{HH}} = 1.3$, 6.4 Hz); 2.37–2.30 (m, 1H, -CH_{2pyrr}); 2.15–2.11 (m, 1H, -CH_{2pyrr}); 2.10–2.00 (m, 1H, -CH_{2pyrr}); 1.82–1.76 (m, 1H, -CH_{2pyrr}); 1.40 (s, 3H, -CH_{3Ph}); 1.34 (d, 3H, -CH_{3pyrr}, $J_{\text{HH}} = 7.0$ Hz); 1.34 (s, 3H, CH_{3CO₂-}); 1.32 (d, 3H, -CH_{3pyrr}, $J_{\text{HH}} = 6.0$ Hz); 1.29–1.27 (m, 1H, -CH_{pyrr}); 1.09 (s, 9H, 3 -CH_{3*t*-Bu}). ¹³C NMR (125 MHz, CDCl₃): δ 197.1 (CH_{3CO₂-}); 153.7 (N=CH); 142.0 (C_{Nph}); 141.1 (C_{Ph}); 139.2 (C_{Nph}); 136.9 (C_{Ph}); 136.4 (C_{Ph}); 135.1 (C_{Ph}); 134.3 (C_{Nph}); 130.2 (C_{Nph}); 130.3 (C_{Nph}); 127.8 (C_{Nph}); 126.9 (C_{Nph}); 116.1 (C_{Ph}); 115.2 (C_{Ph}); 114.9 (C_{Nph}); 103.3 (C_{Nph}); 102.7 (C_{Nph}); 52.2 (-CH-CH_{3pyrr}); 36.4 (-CH_{2pyrr}); 29.7 (CH_{3CO₂-}); 29.7 (-CH-CH_{3pyrr}); 29.6 (-CH_{3Ph}); 29.4 (-CH_{2pyrr}); 22.7 (C-*t*-Bu); 20.1 (-CH_{3pyrr}); 18.1 (3C, 3 -CH_{3*t*-Bu}); 14.9 (-CH_{3pyrr}). Anal. Calcd. for C₃₀H₃₆N₂O₃Pd (579.0): C, 62.2; H, 6.3; N, 4.8; found: C, 62.6; H, 6.3; N, 4.7%. ESI-MS m/z (%): 519.3 [M⁺-OAc], 415.5 [L].

(*R,R*)-7Rh. AgPF₆ (24.4 mg, 0.096 mmol) in THF (10 mL) was added to a solution of [Rh(cod)Cl]₂ (23.5 mg, 0.048 mmol) in THF (10 mL) and the mixture was stirred vigorously at room temperature for 30 min. The resulting AgCl precipitated was filtered off and the yellow solution was treated with (*R,R*)-8 (40 mg, 0.096 mmol) in the same solvent. The mixture was stirred at room temperature for 2 h. After the solvent had been removed under vacuum to 0.5 mL, the product was precipitated by careful addition of Et₂O and collected by filtration, to afford a stable dark beige solid. Yield = 67 mg, 90%. IR (KBr, cm⁻¹): ν_{OH} 3408 (m); ν_{CHarom} 3054 (vw); ν_{CHalip} 2962 (m), 2921 (m), 2882 (m), 2838 (m); $\nu_{\text{C=C}}$, $\nu_{\text{C=N}}$ 1619 (m), 1591 (s), 1467 (m), 1432 (m); δ_{CH} 1375 (m), 1300 (s), 1231 (m); ν_{PF} 843 (vs); $\delta_{\text{CHout plane}}$ 755 (w), 731 (w); ρ_{CH} 558 (m), 500 (m). ¹H NMR (300 MHz, CDCl₃): δ 12.41 (s br, OH); 7.44–7.34 (m, 3H_{Nph}); 7.26–7.16 (m, 3H_{Nph}); 6.53 (m, 1H_{Ph}); 6.51 (m, 1H_{Ph}); 5.96 (s, 1H, N=CH); 4.79–4.69 (m, 1H, -CH_{2pyrr}); 4.41–4.39 (m, 2H, -CH=C_{cod}); 4.24–4.19 (m, 1H, -CH_{2pyrr}); 4.11–4.07 (m, 2H, -CH=C_{cod}); 3.29–3.20 (m, 1H, -CH_{pyrr}); 2.66–2.55 (m, 2H, -CH_{2cod}); 2.52–2.38 (m, 2H, -CH_{2cod}); 2.31–2.28 (m, 1H, -CH_{2pyrr}); 2.22 (s, 3H, -CH_{3Ph}); 2.08–1.96 (m, 2H, -CH_{2cod}); 1.95–1.84 (m, 2H, -CH_{2cod}); 1.46 (d, 3H, -CH_{3pyrr}, $J_{\text{HH}} = 8.8$ Hz); 1.40 (s, 9H, -CH_{3*t*-Bu}); 1.28 (d, 3H, -CH_{3pyrr}, $J_{\text{HH}} = 11.5$ Hz); 0.91–0.86 (m, 1H, -CH_{2pyrr}). ¹³C NMR (125 MHz, CDCl₃): δ 171.2 (N=CH); 158.3 (C_{Ph}); 148.4 (C_{Nph}); 143.6 (C_{Nph}); 138.0 (C_{Ph}); 134.6 (C_{Nph}); 131.7 (C_{Ph}); 130.9 (C_{Ph}); 127.8 (C_{Ph}); 127.6 (C_{Nph}); 126.3 (C_{Nph}); 126.3 (2C_{Nph}); 122.7 (C_{Nph}); 120.1 (C_{Ph}); 116.1 (C_{Nph}); 115.3 (C_{Nph}); 83.0 (2C, -CH=CH_{cod}); 80.8 (2C, -CH=CH_{cod}); 52.5 (-CH-CH_{3pyrr}); 52.3 (-CH-CH_{3pyrr}); 35.1 (C-*t*-Bu); 32.7 (-CH_{2pyrr}); 30.3 (2C, 2 -CH_{2cod}); 29.8 (3C, 3 -CH_{3*t*-Bu}); 29.7 (2C, 2 -CH_{2cod}); 29.5 (-CH_{2pyrr}); 20.0 (-CH_{3Ph}); 18.5 (-CH_{3pyrr}); 8.8 (-CH_{3pyrr}). Anal. Calcd. for C₃₆H₄₆F₆N₂OPRh (770.6): C, 56.1; H, 6.0; N, 3.6; found: C, 51.8; H, 6.0; N, 3.1%. **7Rh-CH₂Cl₂**: C, 51.9; H, 5.6; N, 3.3%. ESI-MS m/z (%): 625.5 [M⁺ - PF₆], 415.5 [L].

(*R,R*)-8Pd. Pd(AcO)₂ (10.11 mg, 0.045 mmol) in dry CH₂Cl₂ (10 mL) was added to a solution of (*R,R*)-8 (30.5 mg, 0.045 mmol) in the same solvent and the mixture was stirred at room temperature overnight. After the solution was purified through celite and subsequent the solvent was removed under vacuum to 0.5 mL, the product was precipitated by careful addition of pentane and collected by filtration, to afford a stable dark red solid. Yield = 33 mg, 87%. UV-Vis: λ_{max} (nm) = 531, 434, 376,

296. ¹H NMR (300 MHz, CDCl₃): δ 8.32 (s, 1H, N=CH); 7.68 (d, 1H_{Nph}, $J_{\text{HH}} = 8.0$ Hz); 7.50 (t, 1H_{Nph}, $J_{\text{HH}} = 7.3$ Hz); 7.44–7.40 (m, 2H_{Nph}); 7.36 (d, 1H_{Ph}, $J_{\text{HH}} = 2.2$ Hz); 7.17 (d, 1H_{Ph}, $J_{\text{HH}} = 2.2$ Hz); 7.06 (d, 1H_{Nph}, $J_{\text{HH}} = 6.6$ Hz); 6.94 (d, 1H_{Nph}, $J_{\text{HH}} = 7.3$ Hz); 4.34 (d, 2H, -CH₂-Ph, $J_{\text{HH}} = 4.4$ Hz); 3.78 (c, 6H, -O-CH₂-CH₃, $J_{\text{HH}} = 7.3$ Hz); 3.53–3.42 (m, 1H, -CH_{pyrr}); 3.24–3.15 (m, 3H, 1H, -CH_{pyrr}, 2H, -CH₂₋); 1.97–1.85 (m, 2H, -CH_{2pyrr}); 1.71–1.58 (m, 1H, -CH_{2pyrr}); 1.67–1.60 (m, 2H, -CH₂₋); 1.47 (s, 9H, -CH_{3*t*-Bu}); 1.30–1.28 (m, 4H) (1H, -CH_{2pyrr}) (3H, CH_{3CO₂-}); 1.25–1.23 (m, 6H, -CH_{3pyrr}); 1.21 (t, 9H, -O-CH₂-CH₃, $J_{\text{HH}} = 7.3$ Hz); 0.68–0.60 (m, 2H, -CH₂-Si). ¹³C NMR (125 MHz, CDCl₃): δ 197.2 (CH_{3CO₂-}); 160.4 (N=CH); 159.8 (C=O); 158.2 (C_{Ph}); 146.9 (C_{Nph}); 138.5 (C_{Nph}); 137.9 (C_{Ph}); 133.7 (C_{Nph}); 130.1 (C_{Ph}); 129.4 (C_{Ph}); 129.1 (C_{Ph}); 128.1 (C_{Nph}); 126.8 (C_{Nph}); 125.4 (2C_{Nph}); 122.4 (C_{Nph}); 119.1 (C_{Ph}); 118.6 (C_{Nph}); 117.9 (C_{Nph}); 58.9 (-CH-CH_{3pyrr}); 58.4 (3C, 3 -O-CH₂-CH₃); 51.3 (-CH-CH_{3pyrr}); 44.5 (-CH₂₋); 42.9 (-CH₂₋); 34.8 (C-*t*-Bu); 31.5 (-CH_{2pyrr}); 29.7 (CH_{3CO₂-}); 29.3 (3C, 3 -CH_{3*t*-Bu}); 29.1 (-CH_{2pyrr}); 25.6 (-CH_{3pyrr}); 23.5 (-CH₂₋); 18.2 (3C, 3 -O-CH₂-CH₃); 17.4 (-CH_{3pyrr}); 7.5 (-CH₂-Si).

(*R,R*)-8Rh. AgPF₆ (8.21 mg, 0.0325 mmol) in dry THF (10 mL) was added to a solution of [Rh(cod)Cl]₂ (7.93 mg, 0.0162 mmol) in the same solvent and the mixture was stirred vigorously at room temperature for 30 min. The resulting AgCl precipitated was filtered off and the yellow solution was treated with (*R,R*)-9 (22 mg, 0.0325 mmol) in dry THF. The mixture was stirred at room temperature overnight. After the solution was purified through celite and subsequent the solvent was removed under vacuum to 0.5 mL, the product was precipitated by careful addition of Et₂O : pentane (1 : 1) and collected by filtration, to afford a stable dark green solid. Yield = 27.5 mg, 82%. UV-Vis: λ_{max} (nm) = 512, 356, 287. ¹H NMR (300 MHz, CDCl₃): δ 9.82 (s br, OH); 7.37–7.18 (m, 3H_{Nph}); 7.12–6.98 (m, 3H, 2H_{Ph}, 1H_{Nph}); 6.65 (d, 1H_{Nph}, $J_{\text{HH}} = 6.6$ Hz); 6.43 (d, 1H_{Nph}, $J_{\text{HH}} = 6.6$ Hz); 5.93 (s, 1H, N=CH); 4.73–4.65 (m, 1H, -CH_{2pyrr}); 4.44–4.37 (m, 2H, -CH=C_{cod}); 4.31–4.05 (m, 5H) (1H, -CH_{2pyrr}, 2H, -CH=C_{cod}, 2H, -CH_{2Ph}); 3.76 (m, 6H, -O-CH₂-CH₃); 3.25 (m, 3H) (1H, -CH_{pyrr}, 2H, -CH₂₋); 2.66–2.54 (m, 2H, -CH_{2cod}); 2.45–2.31 (m, 2H, -CH_{2cod}); 2.28–2.24 (m, 1H, -CH_{2pyrr}); 2.24–2.04 (m, 4H, -CH_{2cod}); 1.89–1.83 (m, 2H, -CH₂₋); 1.51–1.49 (m, 3H, -CH_{3pyrr}); 1.37 (m, 9H, 3 -CH_{3*t*-Bu}); 1.25–1.22 (m, 12H, CH_{3pyrr}, -O-CH₂-CH₃); 1.12–1.00 (m, 1H, -CH_{2pyrr}); 0.89–0.74 (m, 2H, -CH₂-Si). ¹³C NMR (125 MHz, CDCl₃): δ 166.4 (N=CH); 155.8 (br, 2C, C_{Ph}, C₃₇, C=O); 148.9 (C_{Nph}); 141.6 (C_{Nph}); 138.5 (C_{Ph}); 136.6 (C_{Nph}); 134.7 (C_{Ph}); 128.9 (C_{Ph}); 127.0 (C_{Ph}); 126.7 (C_{Nph}); 125.5 (C_{Nph}); 124.9 (C_{Nph}); 124.4 (C_{Nph}); 122.0 (C_{Nph}); 120.3 (C_{Ph}); 115.9 (C_{Nph}); 115.4 (C_{Nph}); 80.4 (2C, -CH=CH_{cod}); 79.6 (2C, -CH=CH_{cod}); 65.8 (3C, -O-CH₂-CH₃); 53.4 (-CH-CH_{3pyrr}); 52.4 (-CH-CH_{3pyrr}); 43.0 (-CH₂₋); 42.5 (-CH₂₋); 34.7 (C-*t*-Bu); 30.3 (2C, -CH_{2cod}); 30.0 (-CH_{2pyrr}); 29.7 (2C, -CH_{2cod}); 29.4 (3C, -CH_{3*t*-Bu}); 29.1 (-CH_{2pyrr}); 22.7 (-CH₂-Si); 19.9 (3C, 3 -O-CH₂-CH₃); 16.2 (-CH_{3pyrr}); 7.9 (2C, -CH_{3pyrr}, -CH₂-Si).

Synthesis of heterogenized complexes

A solution of metal complex (*R,R*)-8Pd or (*R,R*)-8Rh (0.022 mmol), bearing a triethoxysilyl group, in CH₂Cl₂ (5 mL) was added to a well-stirred toluene suspension (25 mL) of the mesoporous solid (MCM-41, 150 mg). The slurry was heated at 110 °C for 16 h. After the mixture was cooled, the solid was filtered off, washed thoroughly with ethanol and diethyl ether and dried

under vacuum, to afford the respective heterogenized complexes in almost quantitative yields.

(R,R)-8Pd-MCM. Stable dark brown-reddish solid. Elemental analysis indicated 1.4 mass% Pd. Found C, 5.4; H, 1.4; N, 0.73%. IR (KBr, cm^{-1}): $\nu_{\text{C=O}}$, $\nu_{\text{C=N}}$, $\nu_{\text{C=C}}$ 1641 (s), 1575 (s), $\nu_{\text{Si-O}}$ 1085, $\nu_{\text{Pd-O}}$ 544 (vw). DFTR: λ_{max} (nm) = 675, 619, 488, 363, 329, 287, 263, 231. ^{13}C NMR (300 MHz, Solid): δ 198.0 (CH_3CO_2^-); 160.5 (N=CH); 158.0 (C=O); 140.4–121.0 (15C, 5C_{Ph} and 10C_{Nph}); 120.7 (C_{Ph}); 59.5 (*-O-CH₂-CH₃*); 59.0 (*-CH₂-pyrr*); 51.3 (*-CH₂-pyrr*); 44.0 (*-CH₂-*); 43.00 (*-CH₂-*); 34.6 (C_{*i*-Bu}); 28.0 (6C, 3-*-CH₂-3_i-Bu*, 2-*-CH₂-pyrr*, *CH₃CO₂-*); 23.6 (*-CH₂-*); 16.0 (4C, 3-*-O-CH₂-CH₃*, *-CH₃-pyrr*); 13.3 (*-CH₃-pyrr*); 8.6 (*-CH₂-Si*).

(R,R)-8Rh-MCM. Stable dark green solid. Elemental analysis indicated 1.4 mass% Rh. Found C, 5.1; H, 1.4; N, 0.6%. IR (KBr, cm^{-1}): $\nu_{\text{C=O}}$ 1638 (s), $\nu_{\text{C=N}}$, $\nu_{\text{C=C}}$ 1580; $\nu_{\text{Si-O}}$ 1085, $\nu_{\text{P-F}}$ 803 (vs). DFTR: λ_{max} (nm) = 666, 561, 362, 331, 287, 255, 226. ^{13}C NMR (300 MHz, Solid): δ 160.1 (N=CH); 152.0 (C=O); 140.4–115.0 (16C_{arom}, 6C_{Ph} and 10C_{Nph}); 80.0 (4C, 2-*-CH=CH_{cood}*); 59.5 (*-O-CH₂-CH₃*); 53.00 (2C, 2-*-CH₂-pyrr*); 43.6 (2C, 2-*-CH₂-*); 34.3 (C_{*i*-Bu}); 28.6 (9C, 4-*-CH₂-cood*, 3-*-CH₂-3_i-Bu*, 2-*-CH₂-pyrr*); 21.5 (*-O-CH₂-CH₃*, *-CH₂-*); 15.6 (*-CH₃-pyrr*); 8.3 (2C, *-CH₃-pyrr*, *-CH₂-Si*).

Catalytic activity

Hydrogenation of alkenes. The catalytic properties, in the hydrogenation of (*E*)-diethyl 2-benzylidenesuccinate and diethyl itaconate, of rhodium and palladium complexes were examined under conventional conditions for batch reactions in a reactor (Autoclave Engineers) of 100 mL capacity at 40 °C temperature, 4 atm dihydrogen pressure and 1/100 or 1/1000 metal/substrate molar ratio. The evolution of the hydrogenated reaction product was monitored by gas chromatography.

Specifically: To a suspension of the catalyst, **8Rh-MCM** (15 mg, 2.0×10^{-3} mmol of Rh) in ethanol (40 mL), was added a solution of 52.4 mg (0.2 mmol) of (*E*)-diethyl 2-benzylidene succinate and the mixture stirred at 40 °C, 1000 rpm. The evolution of the reaction was monitored by gas chromatography.

Recycling experiments. At the end of the process the reaction mixture was centrifuged, and the catalyst residue washed to completely remove any remaining products and/or reactants. The solid was used again and any change in the catalytic activity was observed. In each of the four runs, up to 95% conversion was reached after 220 min and ee (%) was maintained after 4 cycles.

Acknowledgements

The authors thank the Dirección General de Investigación Científica y Técnica of Spain (Project MAT2006-14274-C02-02), and Consolider Ingenio 2010-MULTICAT. G.V. thanks MCIINN for financial support.

Notes and references

- (a) M. H. Valkenberg and W. F. Hölderich, *Catal. Rev.*, 2002, **44**, 321–374; (b) A. Taguchi and F. Schüth, *Microporous Mesoporous Mater.*, 2005, **77**, 1–45; (c) D. De Vos, M. Dams, B. Sels and P. Jacobs, *Chem. Rev.*, 2002, **102**, 3615–3640; (d) F. Hoffmann, M. Cornelius and J. Morell, *Angew. Chem.*, 2006, **118**, 3290–3328; F. Hoffmann, M. Cornelius, J. Morell and M. Froba, *Angew. Chem., Int. Ed.*, 2006, **45**, 3216–3251.
- (a) C. T. Kresge, M. E. Leonowicz, W. J. Roth, J. C. Vartuli and J. S. Beck, *Nature*, 1992, **359**, 710–712; (b) J. S. Beck, J. C. Vartuli, W. J. Roth, M. E. Leonowicz, C. T. Kresge, K. D. Schmitt, C. T. W. Chu, D. H. Olson, E. W. Sheppard, S. B. McCullen, J. B. Higgins and J. L. Schlenker, *J. Am. Chem. Soc.*, 1992, **114**, 10834–10843.
- (a) D. M. Ford, E. E. Simanek and D. F. Shantz, *Nanotechnology*, 2005, **16**, S458–S475; (b) C. D. Nunes, M. Pillinger, A. A. Valente, I. S. Gonçalves, J. Rocha, P. Ferreira and F. E. Kühn, *Eur. J. Inorg. Chem.*, 2002, **5**, 1100–1107.
- (a) A. Corma, C. del Pino, M. Iglesias and F. Sánchez, *Chem. Commun.*, 1991, **18**, 1253–1255; (b) A. Corma, M. Iglesias, M. V. Martín, J. Rubio and F. Sánchez, *Tetrahedron: Asymmetry*, 1992, **3**, 845–848; (c) A. Corma, A. Fuerte, M. Iglesias and F. Sánchez, *J. Mol. Catal. A: Chem.*, 1996, **107**, 225–234 and references therein; (d) M. J. Alcón, A. Corma, M. Iglesias and F. Sánchez, *J. Mol. Catal. A: Chem.*, 2003, **194**, 137–152.
- R. W. Alder, P. S. Bowman, W. R. S. Steele and D. R. Winterman, *Chem. Commun.*, 1968, **13**, 723–724.
- S. N. Gamage, R. H. Morris, S. J. Rettig, D. C. Thackeray, I. S. Thorburn and B. R. J. James, *J. Chem. Soc., Chem. Commun.*, 1987, **12**(12), 894–895.
- R. P. Hughes, I. Kovacic, D. C. Lindner, J. M. Smith, S. Willemsen, D. Zhang, I. A. Guzei and L. R. Arnold, *Organometallics*, 2001, **20**, 3190–3197.
- A. Di Saverio, F. Focante, I. Camurati, L. Resconi, T. Beringhelli, G. D'Alfonso, D. Donghi, D. Maggioni, P. Mercandelli and A. Sironi, *Inorg. Chem.*, 2005, **44**, 5030–5041.
- T. Yamasaki, N. Ozaki, Y. Saika, K. Ohta, K. Goboh, F. Nakamura, M. Hashimoto and S. Okeya, *Chem. Lett.*, 2004, **33**, 928–929.
- F. Terrier, J. C. Halle, M. J. Pouet and M. P. J. Simonin, *J. Org. Chem.*, 1986, **51**, 409–411.
- M. A. Zirnstein and H. A. Staab, *Angew. Chem.*, 1987, **99**, 460–461; M. A. Zirnstein and H. A. Staab, *Angew. Chem., Int. Ed. Engl.*, 1987, **26**, 460–461.
- V. Raab, J. Kipke, R. M. Gschwind and J. Sundermeyer, *Chem. Eur. J.*, 2002, **8**, 1682–1693.
- (a) J. P. Mazaleyrat and K. Wright, *Tetrahedron Lett.*, 2008, **49**, 4537–4541; (b) G. Brancatelli, D. Drommi, G. Femino, M. Saporita, G. Bottari and F. Faraone, *New J. Chem.*, 2010, **34**, 2853–2860.
- H. U. Wüstefeld, W. C. Kaska, F. Schüth, G. D. Stucky, X. Bu and B. Krebs, *Angew. Chem.*, 2001, **113**, 3280–3282; H. U. Wüstefeld, W. C. Kaska, F. Schüth, G. D. Stucky, X. Bu and B. Krebs, *Angew. Chem., Int. Ed.*, 2001, **40**, 3182–3184.
- U. Wild, O. Hübner, A. Maronna, M. Enders, E. Kaifer, H. Wadepohl and H. J. Himmel, *Eur. J. Inorg. Chem.*, 2008, 4440–4447.
- S. U. Son, H. Y. Jang, I. S. Lee and Y. K. Chung, *Organometallics*, 1998, **17**, 3236–3239.
- I. G. Jung, S. U. Son, K. H. Park, K. C. Chung, J. W. Lee and Y. K. Chung, *Organometallics*, 2003, **22**, 4715–4720.
- (a) C. González-Arellano, A. Corma, M. Iglesias and F. Sánchez, *Adv. Synth. Catal.*, 2004, **346**, 1316–1328; (b) C. González-Arellano, E. Gutiérrez-Puebla, M. Iglesias and F. Sánchez, *Eur. J. Inorg. Chem.*, 2004, **9**, 1955–1962.
- (a) N. Debono, M. Iglesias and F. Sánchez, *Adv. Synth. Catal.*, 2007, **349**, 2470–2476; (b) C. del Pozo, N. Debono, A. Corma, M. Iglesias and F. Sánchez, *ChemSusChem*, 2009, **2**, 650–657.
- N. J. Farrer, R. McDonald and J. S. McIndoe, *Dalton Trans.*, 2006, **38**, 4570–4579.
- R. W. Alder, M. R. Bryce, N. C. Goode, N. Miller and J. Owen, *J. Chem. Soc., Perkin Trans.*, 1981, **1**, 2840–2847.
- H. A. Staab, C. Krieger, G. Hieber and K. Oberdorf, *Angew. Chem., Int. Ed. Engl.*, 1997, **36**, 1884–1884.
- (a) A. F. Pozharskii, O. V. Ryabtsova, V. A. Ozeryanskii, A. V. Degtyarev, O. N. Kazheva, G. G. Alexandrov and O. A. Dyachenko, *J. Org. Chem.*, 2003, **68**, 10109–10122; (b) A. V. Degtyarev and A. F. Pozharskii, *Chem. Heterocycl. Compd.*, 2008, **44**, 1138–1145; (c) V. A. Ozeryanskii, D. A. Shevchuk, A. F. Pozharskii, O. N. Kazheva, A. N. Chekhlov and O. A. Dyachenko, *J. Mol. Struct.*, 2008, **892**, 63–67.
- J. P. H. Charmant, G. C. Lloyd-Jones, T. M. Peakman and R. L. Woodward, *Eur. J. Org. Chem.*, 1999, **10**, 2501–2510.
- K. Nakamoto, in *IR and Raman Spectra of Inorganic and Coordination Compounds*, 5th ed., WILEY & SONS, New York, 1997.
- D. D. Perrin, S. L. F. Armarego, D. R. Perrin, in *Purification of Laboratory Chemicals*, PERGAMON PRESS, New York, 1980.

